

**Chemical Synthesis and Biological
Evaluation of Potential Anti-Cancer
Agents Based on the Azinomycins.**

By

Maxwell Aku Casely-Hayford

**A thesis submitted to The University of London in partial fulfilment of the
requirement for the degree of Doctor of Philosophy**

May 2004

**The School of Pharmacy
University of London
29/39 Brunswick Square
London WC1N 1AX**



ProQuest Number: 10104311

All rights reserved

INFORMATION TO ALL USERS

The quality of this reproduction is dependent upon the quality of the copy submitted.

In the unlikely event that the author did not send a complete manuscript and there are missing pages, these will be noted. Also, if material had to be removed, a note will indicate the deletion.



ProQuest 10104311

Published by ProQuest LLC(2016). Copyright of the Dissertation is held by the Author.

All rights reserved.

This work is protected against unauthorized copying under Title 17, United States Code.
Microform Edition © ProQuest LLC.

ProQuest LLC
789 East Eisenhower Parkway
P.O. Box 1346
Ann Arbor, MI 48106-1346

Abstract

Azinomycins A **1** and B **2** isolated from the culture broths of *Streptomyces griseofuscus* S42227, exhibit potent in vitro cytotoxic activity and significant in vivo antitumour activity. The compounds contain two electrophilic functional groups – an epoxide and an aziridine residue – that react with nucleophilic sites in duplex DNA to form cross-links at 5'-dGNT and 5'-dGNC sequences. Although the aziridine functionality is required for cross-linking, the azinomycin metabolite (2*S*, 3*S*)-3,4-epoxy-2-(3-methoxy-5-methyl-1-naphthoyloxy)-3-methylbutanamide containing an intact epoxide but devoid of the 1-aza-bicyclo[3.1.0]hexane ring system retains significant biological activity (IC₅₀ in P388 murine leukaemia = 0.0012 µg/ml) comparable to agents such as cisplatin and mitomycin C. The natural product possesses (2*S*, 3*S*) stereochemistry. All the four diastereoisomers of 3,4-epoxy-2-(3-methoxy-5-methyl-1-naphthoyloxy)-3-methylbutanamide were synthesised to evaluate how the nature of stereochemistry influences cytotoxicity and DNA binding ability. The synthesis involved Sharpless asymmetric dihydroxylation of benzyl 3-methylbut-2-enoate using AD-mix- α or AD-mix- β to give a diol with (*R*) or (*S*) stereochemistry respectively. The (*R*) and (*S*) diols were converted into the four stereoisomers of benzyl 3,4-epoxy-2-hydroxy-3-methylbutanoate, coupled to the chromophore ethyl 3-methoxy-5-methyl-1-naphthoic acid and further converted to the azinomycin analogue (2*S*, 3*S*)-**3** and its isomers. These compounds together with other analogues containing modifications to the chromophore were investigated for cytotoxic activity. Their mode of action was investigated by studying their effect on the electrophoretic mobility of supercoiled plasmid DNA. Analogues with DNA cross-linking ability were designed and synthesised from 1-(2-aminoethyl)-piperidin-3-ol and 3,4-epoxy-2-(3-methoxy-5-methyl-1-naphthoyloxy)-3-methylbutanoic acid involving Boc-protection of the terminal primary amine, mesylation of the secondary hydroxyl group and transformation of this functionality to the chloro compound. Subsequent deprotection of the Boc-group and coupling to the left hand portion gave a series of piperidine-based analogues. These compounds were tested in the NCI 60 cell line panel and their mode of binding investigated using agarose gel DNA cross-linking and unwinding assays. Totally synthetic analogues with properties useful in the design of bioreductive and biooxidative prodrugs were synthesised by coupling the piperidine analogue **124** or the allylic alcohol **29** to the naphthoic acid chloride **94**.

Abstract	i
Contents	ii
Acknowledgements	v
List of Figures, Schemes and Tables	vi
Abbreviations	xvi

Chapter 1 - INTRODUCTION

1.0	Introduction	1
1.1	Cancer Chemotherapy: The Role of Natural Products	5
1.2	The Azinomycins:	6
1.2.1	Isolation	6
1.2.2	Biological Activity of The Natural Products	8
1.2.3	The Physicochemical Properties of The Azinomycins	9
1.3	Stereoselective Chemical Synthesis of The Azinomycin Metabolite	10
1.4	Synthesis of The 1-Azabicyclo[3.1.0]hex-2-ylidene Dehydroamino Acid Subunit	16
1.5	The Total Synthesis of Azinomycin A	21
1.6	Molecular Modelling Studies of The Azinomycin Antitumour Antibiotics	26
1.7	The Mechanism of Action of The Natural Products And Their Synthetic Counterparts	27
1.8	Aims of The Study	31

Chapter 2 – Synthesis and Biological Studies of Azinomycin Analogues

2.0	Introduction	33
2.1	Synthesis of Four Diastereoisomers and Analogues	35
2.1.1	Synthesis of The Epoxide Unit	35
2.1.2	Synthesis of The Chromophore, The Metabolite and its Analogues	41
2.2	Biological Studies. DNA Intercalation and Cytotoxicity Studies.	50
2.2.1	DNA Intercalation	50
2.2.2	DNA Unwinding Assay	52
2.2.3	DNA Unwinding Assay Results and Discussion	53
2.2.4	Discussion	59
2.2.5	Cytotoxicity Studies of The Diastereoisomers	60
2.2.6	Antitumour Activity In the U2-OS Cell Line	61
2.2.7	Cytotoxicity Results and Discussion: The Effect of Stereochemistry on Azinomycin Cytotoxicity	62
2.3	Discussion	66
2.4	Conclusions	69

Chapter 3 – Design and Synthesis of DNA Cross-linking Analogues of the Azinomycins

3.0	Introduction	72
3.1	Synthesis of the cross-linking compounds and analogues	78
3.2.1	DNA Interstrand Cross-Linking	81
3.2.2	DNA Cross-Linking Agarose Gel Assay	81
3.2.3	DNA Cross-linking Results	83
3.2.4	Effect of Piperidine Based Analogues on Unwinding of	

Supercoiled Φ F174 Plasmid DNA	89
3.2.5 Cytotoxicity Studies of Piperidine Based Analogues of Azinomycins	92
3.3 Discussion	95
3.4 Conclusions	98
 Chapter 4 – Development of a Prodrug Based on the Azinomycins	
4.0 Introduction	100
4.0.1 Design of a Prototype Bioreductive Prodrug Based Upon The Azinomycin analogue 3	100
4.1 Synthesis of the Bioreductive Prodrug precursor	104
4.2 DNA Unwinding Studies of Piperidine Based Analogues	105
4.3 The Bio-Oxidative Prodrug Activation Pathway	108
4.4 Synthesis of the Biooxidative Prodrug Precursor	109
4.5 Preliminary Biological Investigations of Potential Bio-Oxidative Prodrugs	110
4.6 Discussion	112
 Chapter 5 - Eperimental	
5.1 Biology Experimental	115
5.3 Chemistry Experimental	120
 References	
 Appendices	

Acknowledgements

I would like to thank The School of Pharmacy, University of London for providing resources and funding throughout my PhD. I am indebted to my supervisors: Dr Mark Searcey whose enthusiastic interrogation – “anything interesting happening?” always kick-started my imagination! Thank you for your excellent supervision and for sharing my disappointment when experiments did not work and my excitement when they finally worked, Professor Laurence Patterson for his unflinching support, encouragement and valuable comments on my thesis.

I would also like to thank the following people who have helped in the quest to understand the biological mode of action of the azinomycins.

Dr Andy Wilderspin for help with molecular biology experiments and for allowing me to work in lab 435. Dr Colin James for molecular modelling.

Samantha Kneller and the NCI for cytotoxicity studies, Professor Paul Smith for cytotoxicity studies in U2-OS and HoeR cell lines, Dr Samantha Orr and Shaun at de Montford University for the CHO work. Professor John Hartley for allowing me to undertake DNA cross-linking studies in his lab at the Department of Oncology, UCL. Dr. Mire Zloh for help and training on the NMR instrument, the late Mike Cocksedge and Emmanuelle for providing mass spectra. Kersti Karu for CHN analysis. All other technical staff at the School of Pharmacy and the Department of Oncology UCL for their help.

Dede Emahi thank you for not banging on the door (sometimes) when I lock myself up to write!

My colleagues Dr John Paul Malkinson (HPLC training), Dr Klaus Pors (for donating 1-(2-Amino-ethyl)-piperidine-3-ol and giving advice on side chain synthesis), Dr Robert Falconer (advice on the Mitsunobu reaction), Natalia Ortuzar-Kerr and Sukwant Grewel, thank you all for your help and for your company in the “dungeon”.

Last but not the least I would like to thank my parents Mr and Mrs Adormey Casely-Hayford, Grace and the entire family for their support and encouraging words; to Vanessa and Jeff, no my research is not about purifying water!!

List of Figures**CHAPTER 1**

Figure 1.1	Metabolic activation of cyclophosphamide	4
Figure 1.2	Structure of some anticancer drugs	6
Figure 1.3	Structure of the azinomycins	7
Figure 1.4	Proposed structures of carzinophilin	8
Figure 1.5	Azinomycin A and B showing bond <i>a</i> and <i>b</i>	16
Figure 1.6	Retrosynthetic analysis of the aziridine segment	17
Figure 1.7	Bromination with <i>N</i> -bromosuccinamide or Bromine	18
Figure 1.8	Structure of azinomycins showing disconnections	24
Figure 1.9	N-7 alkylation by the azinomycin analogue 3	28
Figure 1.10	Effect of intercalator structure on cytotoxicity	28
Figure 1.11	Structure of dimeric epoxy amides	29

CHAPTER 2

Figure 2.1	Structure of duocarmycin SA showing sites of modifications	33
Figure 2.2	Azinomycin metabolite indicating changes	34
Figure 2.3	Catalytic Cycle of the Asymmetric Dihydroxylation reaction	37
Figure 2.4	NMR spectrum for racemic mixture of compound 30	39
Figure 2.5	NMR spectrum for (2 <i>S</i> , 3 <i>S</i>)- 30	40
Figure 2.6	NMR spectrum for (2 <i>S</i> , 3 <i>R</i>)- 30	40
Figure 2.7	NMR spectrum for (2 <i>S</i> , 3 <i>S</i>)- 105	46
Figure 2.8	NMR spectrum for (2 <i>S</i> , 3 <i>R</i>)- 106	47
Figure 2.9	Sketches depicting the secondary structure of normal DNA and DNA containing intercalated proflavin molecules	51

Figure 2.10	The structures of some representative intercalating molecules	52
Figure 2.11	Effect of echinomycin on the electrophoretic mobility of ϕ F174 plasma DNA	54
Figure 2.12	Effect of 117 on the electrophoretic mobility of ϕ F174 plasma DNA	55
Figure 2.13	Effect of 113 on the electrophoretic mobility of ϕ F174 plasma DNA	55
Figure 2.14	Effect of 3 on the electrophoretic mobility of ϕ F174 plasma DNA	56
Figure 2.15	Effect of melphalan on the electrophoretic mobility of ϕ F174 plasma DNA	57
Figure 2.16	Effect of (2 <i>S</i> , 3 <i>S</i>)- 3 on the electrophoretic mobility of ϕ F174 plasma DNA in the presence and absence of ethidium bromide	57
Figure 2.17	Effect of (2 <i>R</i> , 3 <i>R</i>)- 3 on the electrophoretic mobility of ϕ F174 plasma DNA in the presence and absence of ethidium bromide	58
Figure 2.18	Effect of (2 <i>R</i> , 3 <i>S</i>)- 3 on the electrophoretic mobility of ϕ F174 plasma DNA	58
Figure 2.19	Effect of bromide (2 <i>S</i> , 3 <i>S</i>)- 105 and 109 on the electrophoretic mobility of ϕ F174 plasma	59
Figure 2.20	Computer model of (2 <i>S</i> , 3 <i>S</i>)- 3 bound and intercalated into DNA	59
Figure 2.21	Anomalous base pairing of guanine with thymine	66
Figure 2.22	Proposed mechanism of action of the azinomycin metabolite	67
Figure 2.23	Graph of IC ₅₀ plotted against diastereomers	68
Figure 2.24	Computer modelled energy-minimised structure of (2 <i>S</i> , 3 <i>S</i>)- 3 and (2 <i>S</i> , 3 <i>R</i>)- 3	69

CHAPTER 3

Figure 3.1	Structure of mustard gas, the major nitrogen mustards in clinical use and an isolated guanine lesion I	73
Figure 3.2	Structures of mitomycin C, azinomycin A and B, and the analogue (2 <i>S</i> , 3 <i>S</i>)-3	75
Figure 3.3	HPLC profile of azinomycin cross-linking reaction	76
Figure 3.4	Structures of the azinomycins and the piperidine based analogues	77
Figure 3.5	Schematic representation of the response to denaturation and renaturation of crosslinked DNA	81
Figure 3.6	Summary of crosslink assay conditions	82
Figure 3.7	Structures of azinomycin derivatives used to explore DNA cross-linking	83
Figure 3.8	DNA crosslink assay autoradiograph of 129	84
Figure 3.9	DNA crosslink assay autoradiograph of 130 and 125	84
Figure 3.10	Concentration response curve (a) and autoradiograph (b) of agarose gel after 1 h incubation of pUC 18 and 126 .	86
Figure 3.11	Concentration response curve (a) and autoradiograph (b) of agarose gel after 2 h incubation of pUC 18 and 126 .	87
Figure 3.12	Concentration response curve (a) and autoradiograph (b) of agarose gel after 3 h incubation of pUC 18 and 126 .	88
Figure 3.13	Effect of 129 on the electrophoretic mobility of ϕ F174 plasma DNA	89
Figure 3.14	Effect of 125 , 126 , 130 on the electrophoretic mobility of ϕ F174 plasma DNA	90

Figure 3.15	Mechanism of aziridine ion formation	96
Figure 3.16	Proposed mechanism of interstrand cross-link formation by the piperidine analogue	97

CHAPTER 4

Figure 4.1	A. <i>N</i> -oxides of DNA anthraquinone intercalators. B. AQ4N and its reductive metabolites	102
Figure 4.2	Structures of A. 2,6-disubstituted <i>N</i> -methyl derivative, B. <i>N</i> -oxide analogue, 131 azinomycin analogue with prodrug potential, 132 control analogue	103
Figure 4.3	Effect of 131 on the electrophoretic mobility of ϕ F174 plasma DNA	105
Figure 4.4	Effect of 132 on the electrophoretic mobility of ϕ F174 plasma DNA	106
Figure 4.5	Effect of 133 on the electrophoretic mobility of ϕ F174 plasma DNA	106
Figure 4.6	Effect of 133 on the electrophoretic mobility of ϕ F174 plasma DNA (heated sample)	107
Figure 4.7	Effect of 117 on the electrophoretic mobility of ϕ F174 plasma DNA	111
Figure 4.8	(a) Cytotoxicity of 117 on CHO cells (with or without CYP3A4) (b) Cytotoxicity of ((2S , 3S)- 3) on CHO cells (with or without CYP3A4)	112

List of Schemes**CHAPTER 1**

Scheme 1.1	Route to the naphthalene ring system	11
Scheme 1.2	Shibuya method for the synthesis of 3	12
Scheme 1.3	Armstrong synthesis of 3	13
Scheme 1.4	Shishido synthesis of the azinomycin analogue 3	14
Scheme 1.5	Konda route to the (2 <i>S</i> , 3 <i>S</i>) epoxide unit	14
Scheme 1.6	Shipman synthesis of the (2 <i>S</i> , 3 <i>S</i>) epoxide unit	15
Scheme 1.7	Armstrong's Passerini three-component condensation	16
Scheme 1.8	Armstrong's synthesis of the 1-azabicyclo[3.1.0]hex-2-ylidene dehydroamino acid unit	18
Scheme 1.9	Coleman's synthesis of the selectively protected aldehyde unit	20
Scheme 1.10	Synthesis of the 1-azabicyclo[3.1.0]hexane ring system	20
Scheme 1.11	Terashima synthesis of 4- <i>O</i> -methyl-13-desacetyl-12,13- dihydroazinomycin	22
Scheme 1.12	Terashima synthesis of azinomycin B analogue	23
Scheme 1.13	Coleman total synthesis of azinomycin A	25

CHAPTER 2

Scheme 2.1	Synthesis of allylic alcohols	36
Scheme 2.2	Epoxidation of allylic alcohols	38
Scheme 2.3	Synthesis of 3-methoxy naphthoic acid chloride	42
Scheme 2.4	Proposed mechanism of enol formation	42
Scheme 2.5	Synthesis of 3-benzyloxy-5-methyl-naphthalene-1-carbonyl	

	chloride	43
Scheme 2.6	Synthesis of the naphthoic acid chloride	43
Scheme 2.7	Synthesis of benzyl 3,4-epoxy-2-(3-methoxy-5-methyl-1-naphthoyloxy)-3-methylbutanoate	45
Scheme 2.8	Synthesis of (2 <i>S</i> , 3 <i>S</i>)-3,4-epoxy-2-(3-methoxy-5-methyl-1-naphthoyloxy)-3-methylbutanamide	48
Scheme 2.9	Synthesis of 3-benzyloxy-5-methyl-naphthalene-1-carboxylic acid benzyloxycarbonyl-(2-methyloxiranyl)methyl ester and 3-methoxy-5-methyl-naphthalene-1-carboxylic acid benzyloxycarbonyl-(2-methyloxiranyl)methyl ester	49
Scheme 2.10	Synthesis of 3-methoxy-5-methyl-naphthalene-1-carboxylic acid 1-carbamoyl 2-methyl-propyl ester	49

CHAPTER 3

Scheme 3.1	Proposed mechanism of DNA-DNA interstrand cross-link formation by mechlorethamine	74
Scheme 3.2	Synthesis of 2-(3-chloro-piperidin-1-yl)ethylammonium chloride	78
Scheme 3.3	Synthesis of 3-methoxy-5-methyl-naphthalene-1-carboxylic acid [2-(3-hydroxy-piperidin-1-yl)-ethyl carbamoyl]- (2-methyloxiranyl)-methyl ester and 3-methoxy-5-methyl-naphthalene-1-carboxylic acid [2-(3-chloro-piperidin-1-yl)-ethyl carbamoyl]- (2-methyloxiranyl)-methyl ester	79
Scheme 3.4	Alternate synthesis of 3-methoxy-5-methyl-naphthalene-1-	

	carboxylic acid [2-(3-chloro-piperidin-1-yl)-ethyl carbamoyl]- (2-methyloxiranyl)-methyl ester	80
Scheme 3.5	Synthesis of 3-methoxy-5-methyl-naphthalene-1-carboxylic acid [2-(3-hydroxy-piperidine-1-yl)-ethyl carbamoyl]- (2-methyloxiranyl)methylallyl ester and 3-methoxy-5-methyl-naphthalene-1-carboxylic acid [2-(3-chloro-piperidine-1-yl)-ethyl carbamoyl]-(2-methyloxiranyl)methylallyl ester	80
CHAPTER 4		
Scheme 4.1	Synthesis of 3-methoxy-5-methyl-naphthalene-1-carboxylic acid [2-(3-chloro-piperidin-1-yl)-ethyl] amide and 3-methoxy-5-methyl-naphthalene-1-carboxylic acid [2-(3-chloro-piperidine-1-yl)-ethyl] amide	104
Scheme 4.2	Synthesis of <i>N</i> -[2-(3-chloro-piperidin-1-yl)ethyl]-benzamide	105
Scheme 4.3	Mode of formation of the azinomycin metabolite analogue and the proposed route of possible biotransformation	107
Scheme 4.4	The epoxidation of isoprene, styrene and secobarbital by cytochrome P-450	108
Scheme 4.5	Synthesis of (<i>S</i>)-3-methoxy-5-methyl-1-naphthalene carboxylic acid 1-carbamoyl-2-methyl-allyl ester	109
Scheme 4.6	Synthesis of (<i>R</i>)-3-methoxy-5-methyl-1-naphthalene carboxylic acid 1-carbamoyl-2-methyl-allyl ester	110

List of Tables**Chapter 2**

Table 2.1	IC ₅₀ values for stereoisomers of the azinomycin metabolite in U2 OS and HoeR cell lines	61
Table 2.2	IC ₅₀ for stereoisomers of the azinomycin analogue in the NCI 60 cell line panel	63

Chapter 3

Table 3.1	Table showing mode of action of selected compounds	91
Table 3.2	Antitumour activity (GI ₅₀) of compounds 3 , 125 , 126 and 130	94

Chapter 4

Table 2.1	IC ₅₀ values in U2-OS and HoeR cell lines	110
-----------	--	-----

Abbreviations

ATP	Adenosine Triphosphate
γ ³² P-ATP	Radiolabelled Adenosine Triphosphate
Anhyd.	Anhydrous
Br	Broad
BAP	Bacterial Alkaline Phosphate
Boc	<i>tert</i> -Butyl carbonate
Boc ₂ O	di <i>tert</i> -butyl dicarbonate
°C	Degrees Celsius
CHO	Chinese Hamster Ovary Cell Lines
CYP	Cytochrome P-450 Enzymes
cm	Centimetre, centimetres
d	doublet
dd	doublet of doublets
DCM	Dichloromethane
dH ₂ O	Distilled water
ddH ₂ O	Double distilled water
DMF	<i>N,N</i> -Dimethylformamide
DMSO	Dimethylsulfoxide
DNA	Deoxy ribonucleic acid
EtBr	Ethidium bromide
equiv.	Equivalent
EDTA	Ethylenediamine tetraacetic acid
FAB MS	Fast Atom Bombardment Mass Spectroscopy
GI	Growth Inhibition
h	Hour, hours
Hz	Hertz
IR	Infrared spectroscopy
<i>J</i>	Scalar coupling
lit.	Literature
m	Multiplet
<i>m</i> -CPBA	<i>meta</i> -Chloroperoxybenzoic acid
mp	Melting point

M	Molar
μ M	Micro molar
min.	Minute, minutes
nM	Nano molar
NCI	National Cancer Institute
NMR	Nuclear Magnetic Resonance Spectroscopy
q	Quartet
RNA	Ribonucleic acid
RT	Room Temperature
s	Singlet
tRNA	Transfer ribonucleic acid
t	Triplet
TAE	Buffer containing Tris base, Acetic acid and EDTA
TeoA	Triethanolamine
THF	Tetrahydrofuran
TLC	Thin Layer Chromatography
Tris	Tris(hydroxymethyl)aminomethane

Chapter 1

Introduction

1.0 Introduction

*Whatever seemed ruthless, implacable, predatory could be analogised to cancer
cancer was never viewed other than a scourge; it was metaphorically, the barbarian within.*

Susan Sontag, *Illness as Metaphor* (1978)

Cancer can manifest itself in the brain, throat, lungs, stomach and colon, pancreas, liver, bones, muscles, joints, and in principal, any tissue site where cells divide.¹ This malignant condition is characterised by uncontrolled proliferation, loss of function of affected organs and tissues, invasiveness and metastasis to distant sites in the body.² Carcinogenesis, is a multistep mechanism resulting from the accumulation of errors in cellular DNA and vital regulatory pathways that may lead to inactivation of tumour suppressor genes and the induction of oncogenes from proto-oncogenes.² The gene damage is often caused by environmental and lifestyle factors like smoking and diet. It is initiated in a single cell, which then multiplies and acquires additional changes that give it survival advantage over its neighbours.³ The cells must then proliferate to generate billions of cells that constitute a cancer. As it takes a long time to generate these errors and cell numbers, it follows that the longer one lives, the more likely one is to get cancer.³ The success of the fight against childhood and infectious diseases have meant that more people now survive into older age when they are more likely to get cancer, with 65 per cent of cases occurring in those over 65.⁴

The difficulty in treating cancer lies in the fact that cancer cells are biochemically not very different from the normal cells they have originated from. This makes the ultimate task of selectively killing the cancerous cells rather a difficult one. Cancer therapy varies according to the type of neoplasia and the extent of invasion. Surgery, radiotherapy, and chemotherapy are all effective treatments of cancer and have been used alone and in combination. Surgery and radiotherapy are local treatments that can often eradicate primary or localised tumours but may ultimately fail because the tumour has metastasised to other areas of the body.⁵ In this case, chemotherapy which is a systemic therapy, is used to control or eliminate metastatic disease and reduce mortality.⁵ Chemotherapy now provides a cure for a significant number of patients with childhood leukaemia, Hodgkin's disease and testicular cancer.

Most cytotoxic drugs are highly reactive compounds and react with dividing cells in tumours as well as in some normal tissues, such as the bone marrow and GI tract. The behaviour of covalent DNA-binding anticancer drugs leads to serious and sometimes life threatening side effects, and can include the production of second malignancies. In some unusual cases, the rapid reactivity* of the alkylating agent mechlorethamine has been exploited in therapy by delivering the drug directly into arteries supplying the area in which the tumour is localised.⁶ This technique has only been marginally successful when the tumour is localised in an extremity where higher local drug concentrations can be achieved by limb perfusion resulting in lower drug concentration in bone marrow, yielding increased selective toxicity.⁶ It is therefore desirable to have anticancer drugs that possess a degree of discrimination between cancerous and normal cells. Many attempts have been made to exploit the imbalance of enzyme distribution in normal and tumour cells.

Cyclophosphamide is a modified mustard and was developed in the hope that it might be preferentially activated in tumour cells. Tumours have been found to have relatively high phosphatase and phosphoramidase activities.⁵ It was therefore postulated that the phosphoramidate ring cleavage would produce an active compound within the tumour cells. The prodrug cyclophosphamide is not cytotoxic to cells in vitro but cultured cells are killed when they are incubated with the drug in the presence of a liver homogenate. In vivo, it undergoes a microsomal cytochrome P-450-dependent metabolic activation in the liver.⁷ The compound is initially converted to 4-hydroxycyclophosphamide, which equilibrates with its acyclic tautomeric form, aldophosphamide (Figure 1.1).⁸ Further enzymatic oxidation produces the two inactive major metabolites 4-ketocyclophosphamide and carboxyphosphamide.⁹ Apart from aldehyde dehydrogenation, aldophosphamide is transformed via a β -elimination reaction to give phosphoramidate mustard and acrolein. Phosphoramidate mustard is a potent cytotoxic alkylating agent which can itself decompose to normitrogen mustard, another cytotoxic agent. Although tumour selectivity was not achieved, the drug is clinically useful and the concept of its development is still relevant in the field of anticancer prodrug research today.

* Animal experiments have shown that over 90% of the mechlorethamine administered disappears from the plasma within 4 minutes.⁶

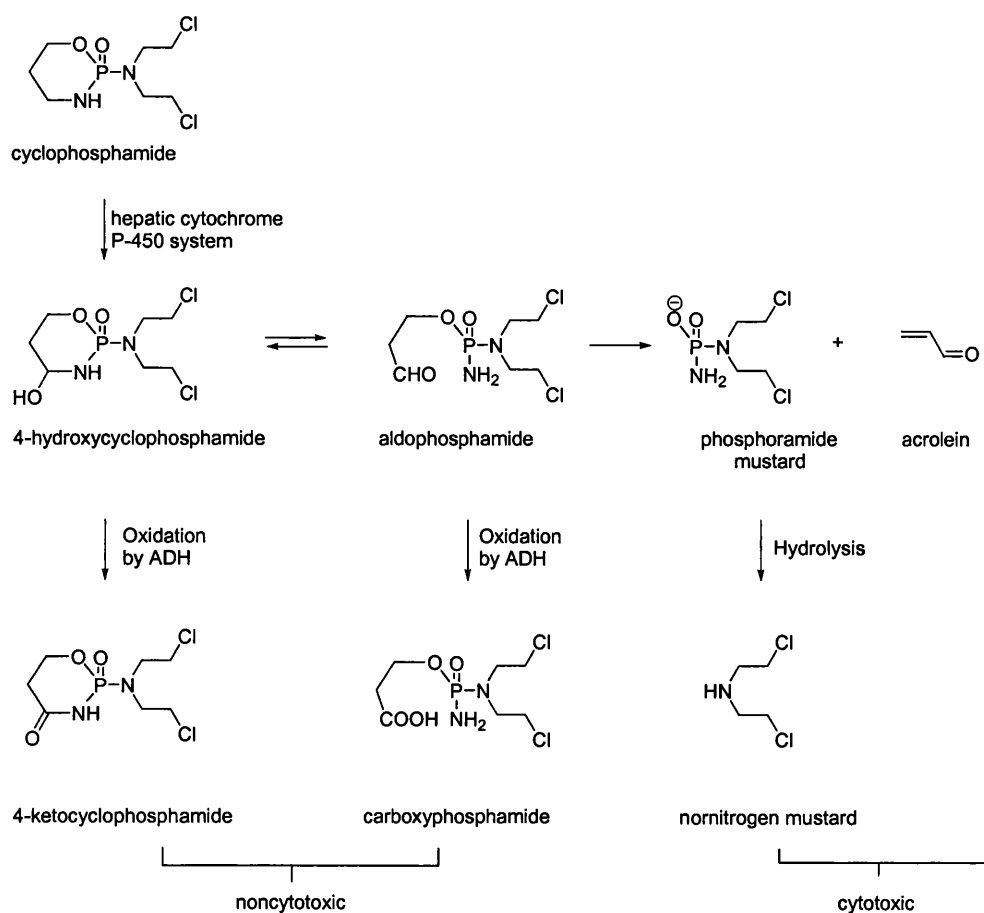


Figure 1.1 Proposed route for the metabolic activation of cyclophosphamide.

Cancer chemotherapy is replete with cytotoxic compounds. Indeed there is a huge array of compounds which are cytotoxic but have not made it into the clinic due their indiscriminate activity leading to toxicity to normal cells. The duocarmycins for example are among the most cytotoxic agents discovered to date ($IC_{50} = 10$ pM, L1210 cells) and have been found to undergo a binding-driven covalent bond formation to their biological target DNA. Duocarmycin SA and its analogues have been described as “nature’s prodrugs” due to their inactivity towards other biological nucleophiles apart from DNA.^{10,11} They only become reactive when bound to the minor groove of DNA. This selectivity for DNA is however not exclusive to cancer cells making the duocarmycins too toxic to be employed as chemotherapeutic drugs in their natural form. A pre-requisite of drug design in the development of antitumour agents based on the duocarmycins therefore appears to be a methodology of targeting them to their site of action by exploiting the biochemical differences between cancer cells and normal ones. This development can only be possible by

disseminating the molecules and thoroughly understanding the basis of their activity through synthetic, biochemical and structural investigations. Such a combination has led to the development of the pro-drug AQ4N based upon the extensive knowledge of the biological activity of the anthracycline antibiotics.¹²

1.1 Cancer Chemotherapy: The Role of Natural Products

The concept of treating cancer with drugs goes back at least 500 years when preparations of silver, zinc and mercury were used. The usefulness of drugs in the systemic treatment of cancer was first documented in 1865 when Lissauer gave potassium arsenite (Fowler's solution) to a patient with leukaemia and noted a positive effect.¹³ Synthetic alkylating agents were the first effective clinically employed anticancer drugs and originate from sulphur and nitrogen mustards developed for chemical attacks in the First and Second World Wars.⁵ The serendipitous discovery of bone marrow suppression and, subsequently, antitumour activity formed the basis for the synthesis of a large series of clinically useful derivatives, including melphalan and cyclophosphamide, all found to derive their biological effects from an ability to alkylate and crosslink DNA.⁵

Natural products have dominated cancer chemotherapy for the past 30 years but the use of nature's chemical catalogue for cancer treatment goes back much further. The American Indians used extracts from the roots of mayapple, *podophylum peltatum* as an effective treatment for skin cancers.¹⁴ Of the clinically employed drugs teniposide and etoposide were later developed from the main constituent of the mayapple, podophylotoxin. This class of compounds act by inhibiting DNA type II topoisomerase.^{5,14} Similarly, the microtubule inhibitor drugs vinblastine and vincristine were developed from *Catharanthus rosea* (also called *Vinca rosea*) which was used as a hypoglycaemic agent in many parts of Asia.¹⁴ Vinblastine and vincristine were first introduced in the late 1960s and have contributed to long-term remissions and cures with childhood leukaemia, testicular cancer, Hodgkin's disease and many other cancers.¹⁵ These folk medicine inspired discoveries encouraged the National Cancer Institute (NCI) to begin a large-scale screening program for antitumour agents.¹⁶ This effort yielded paclitaxel (Taxol), obtained from the bark of the Pacific yew tree. Taxol is highly efficacious in breast and ovarian cancers and is the drug of choice for treating a number of otherwise refractory cancers.^{5,14}

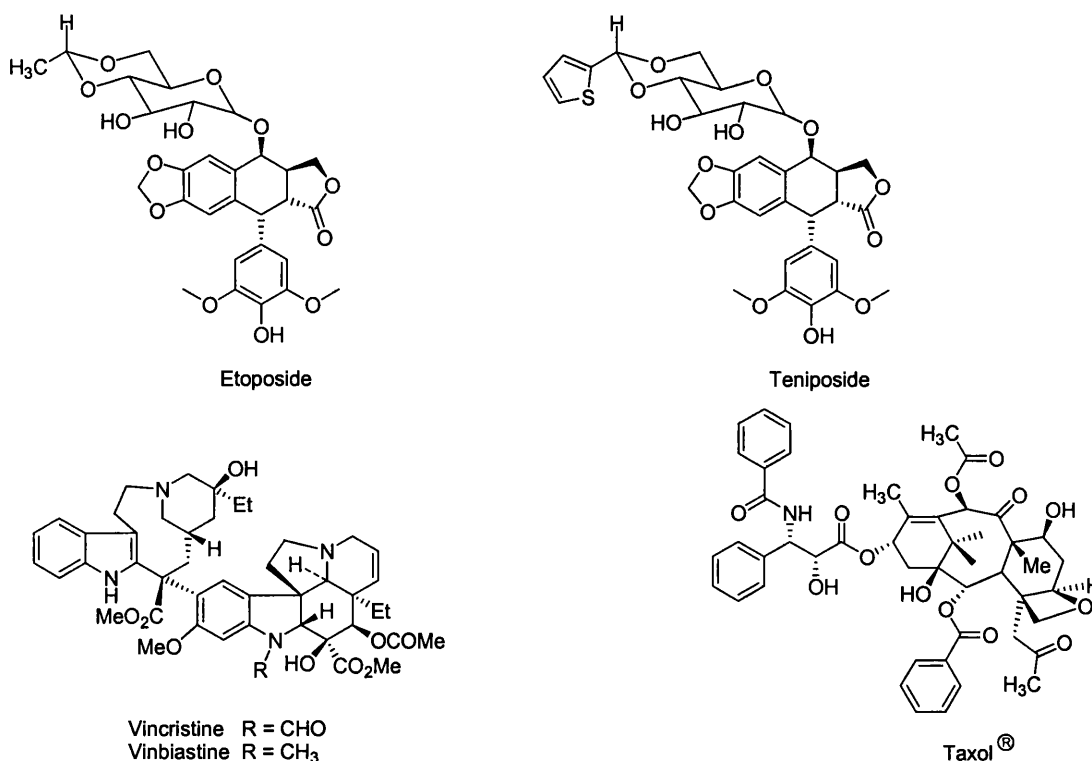


Figure 1.2 Structures of some anticancer drugs

Microorganisms have been the principal source of antibacterial agents but have also provided the antitumour antibiotics class of the anticancer drugs. Most notable being the clinically used bleomycins,¹⁷ mitomycin C and the anthracyclines,¹⁸ while agents under investigation include CC-1065 and the duocarmycins,¹⁰ ecteinascidin 743 and the azinomycins.¹⁹

1.2 The Azinomycins:

1.2.1 Isolation

In the course of screening for new antitumour substances by researchers of the SS Pharmaceutical company in Japan, azinomycins A (**1**) and B (**2**) were discovered.²⁰ They were isolated from the culture broth of the soil bacterium *Streptomyces griseofuscus* and found to have potent *in vitro* cytotoxic activity in L5178Y cell lines.²⁰ They were later examined for *in vivo* cytotoxic activity in a range of tumours

in mice including P388 leukemia and were found to elicit significant antitumour activity similar to mitomycin C which is used in the clinic.²¹ Azinomycin A was somewhat less effective than azinomycin B in the tumour systems employed.²¹ At the time of their discovery, the truncated analogue **3**, which comprises of the naphthalene and the epoxide fragments was also isolated and was thought to be inactive in initial cytotoxic and antitumour experiments.^{20,21} However it was later found to possess potent cytotoxic activity. The structure of the compounds was ascertained by analysis of ^1H and ^{13}C NMR, mass and IR spectra.²² It was then noted that their spectral data was similar to that of carzinophilin which was discovered three decades earlier, but the difference in molecular formulas convinced the group erroneously that the azinomycins were new antitumour antibiotics.²² This assumption was later proven to be false by Armstrong et al., who disclosed that the ^1H and ^{13}C NMR of carzinophilin and azinomycin B were superimposable and that the two are in fact the same molecule.^{23,48}

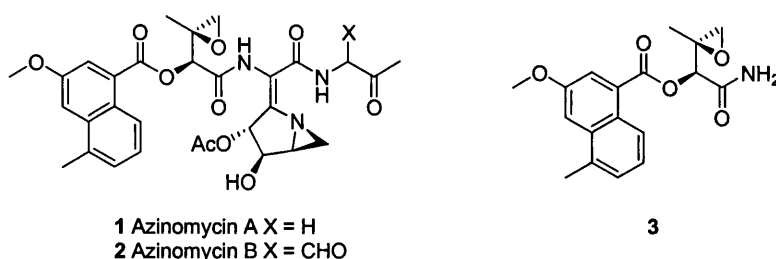


Figure 1.3 Structure of the azinomycins

Carzinophilin was isolated from a streptomyces species and was found to be potent against Erlich sarcoma in mice.²⁴ Its structure was elusive until the independent discovery of the azinomycins.²⁵⁻²⁸ Lown and collaborators initially proposed carzinophilin to be a bisintercalating bisalkylator with the structure **4** (Figure 1.4) based on the molecular formula $\text{C}_{50}\text{H}_{58}\text{N}_5\text{O}_{18}$.²⁷ However Onda²⁸ obtained the molecular formula $\text{C}_{31}\text{H}_{33}\text{N}_3\text{O}_{12}$ by secondary ion mass spectrometry (SIMS) and consequently revised the structure to an *N*-acetylaziridine intercalator possessing a highly oxygenated structure **5** (Figure 1.4).

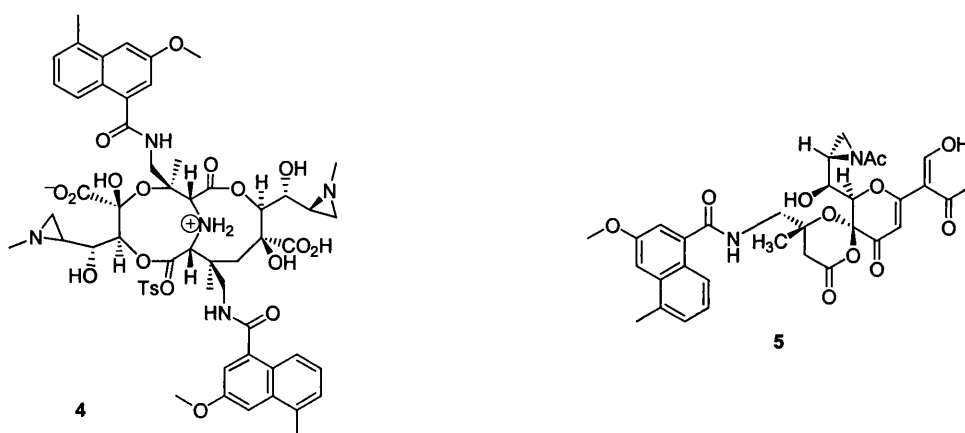


Figure 1.4 Proposed structures of carzinophilin

These early structural revelations led to an effort by Shibuya²⁹ to complete the total synthesis of carzinophilin as reported by Lown et al.

1.2.2 Biological Activity of The Natural Products

The azinomycins have promising in vitro cytotoxicity against the L5178Y tumour cell line.²⁰ In this cell line the concentrations at which 50 % of cell growth is inhibited (IC₅₀) were 0.07 $\mu\text{g/ml}$ and 0.11 $\mu\text{g/ml}$ for azinomycin A and B respectively.²⁰ They were also shown to be active against Gram-positive and Gram-negative bacteria but inactive against yeast and fungi.²⁰ The information gleaned from the initial in vitro antibacterial and cytotoxic experiments encouraged the Japanese SS Pharmaceutical company to undertake in vivo testing in mice to ascertain the antitumour activities of the azinomycins against various murine tumours including: P388 leukemia, P815 mastocytoma, B-16 melanoma and Erlich sarcoma.²¹ Solid tumours such as lung carcinoma and Meth A fibrosarcoma were also used. The mice were inoculated with 1×10^6 cells and the drugs were administered daily for 10 days, 24 h after inoculation.²¹ Administration of azinomycin B (32 $\mu\text{g/kg/day}$) to mice inoculated with P388 leukemia, produced 4/7 (57%) survivors at 45 days and a 193 % increase in life span (ILS, relative to untreated mice), compared to 4/7 survivors at 45 days and an ILS of 204 % for mitomycin C although this was at a much higher dose of 1g/kg/day. In the same tumour model azinomycin A gave an ILS of 76 % and 0/7 survivors after 45 days.² In the Erlich sarcoma tumour model azinomycin B gave an ILS of 161 % and 63 %

survivors.²¹ In B-16 melanoma, azinomycin B also produced a marked prolongation of lifespan, whereas no effect was observed in solid tumours such as Lewis lung carcinoma and Meth A fibrosarcoma. Azinomycin A was more cytotoxic than Azinomycin B in vitro against L5178Y and various bacteria²⁰ however, the antitumour potency of azinomycin A was somewhat less than azinomycin B and the tumour spectrum was also narrower.²¹ The activity of azinomycin B was dose dependent and the LD₅₀ by a single administration was found to be 190 µg/kg. Earlier, Hata²⁴ and co-workers had reported that carzinophilin (azinomycin B)* was cytotoxic in vitro and also prolonged mice survival period when administered to animals inoculated with Yoshida sarcoma, Erlich carcinoma and ascitic hepatoma of 7974 strain. In 1954, a clinical study of azinomycin B was performed and was shown to have remarkable efficacy in malignant neoplasm of the connective tissue, namely sarcoma, Hodgkins disease or skin cancer.³⁰ In one case of skin cancer, the patient did not respond to an adequate amount of intravenous azinomycin B, but on local application of gauze soaked in azinomycin B solution prepared as for intravenous injection, responded very favourably with rapid reduction of the ulcer surface and eventual disappearance of the tumour cells.³⁰ Consequently, oral, rectal, intra-arterial and local routes of administration were developed. This highlights the need for targeting of these promising antitumour antibiotics to their site of action, a development that can only be made possible by an ardent study of the chemistry and the mechanism of action of these novel potential drugs.

1.2.3 The Physicochemical Properties of The Azinomycins

The azinomycins, especially azinomycin A are quite unstable. They are especially labile in acidic media^{20,24} and DNA interstrand cross-link formation by azinomycin B have been shown to be pH dependent with more rapid cross-link formation occurring at lower pH.³¹ This suggests that acidic environments have an activating effect on the reactive centres of the molecule, probably the aziridine moiety. It has been proposed that this acid lability property of the agents may explain in part, the selectivity of these compounds since the tumour cell environment is characterised by having a slightly lower pH than normal cell environment.¹⁹ However the pH window of

* In this dissertation the name azinomycin B will be used to refer to both azinomycin B and carzinophilin.

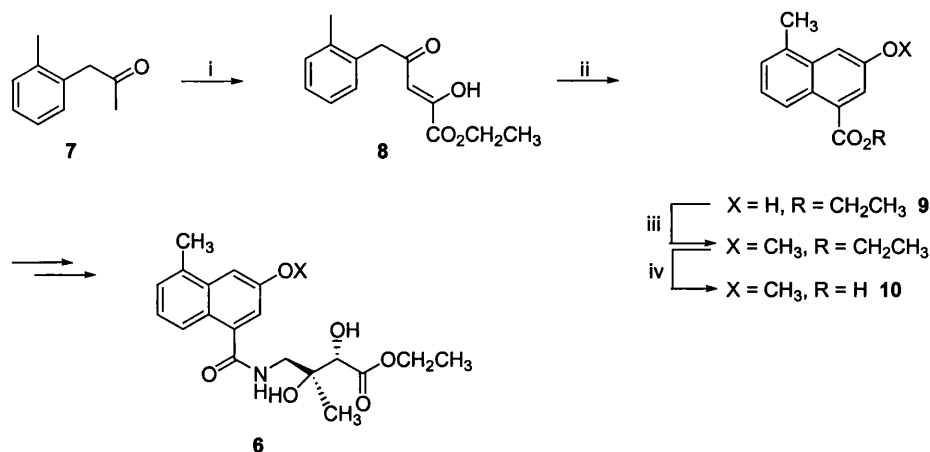
opportunity is between 6~7 as the activity of azinomycin B is influenced by the change of pH, being most stable at pH 7.0, relatively stable at pH 8~9 and pH 6 but loses its biological activity when pH is reduced to less than 5.0.²⁴ In the in vitro activity against *S. lutea*, the antibacterial activity is highest at pH 6~7 and vanishes promptly when the pH falls lower than 5.0. Also activity is lost with the increase of alkalinity.²⁴ It is not clear whether the loss of activity at higher pH is due to a remarkable stability or the ring opening of the aziridine by nucleophiles. The latter is more plausible as the compounds contain a highly strained 1-azabicyclo[3.1.0]hexane ring which is prone to opening at C10 by nucleophiles.^{32,33} It has been proposed that the C12 hydroxyl group may contribute to the observed instability of the natural products.^{34,35}

The azinomycins A (1) and B (2) (Figure 1.2) represent novel structures, which possess a unique structural motif in the form of the 1-azabicyclo[3.1.0]hex-2-ylidene dehydroamino acid fragment. Only one other natural product, ficellomycin, is known to contain a 1-azabicyclo[3.1.0]hexane ring system.^{36,37} The complex, functionally rich structures have made them attractive targets for synthetic chemists. The high activity in this field culminated in unravelling of the total synthesis of these natural products.³⁸ The natural products are unstable, therefore in spite of the vigorous synthetic studies of these compounds, studies of structure-activity relationships from a DNA-binding point of view have been scarce. Even the final product in the total synthesis reaction was characterised in situ due to this instability.³⁸ To date, little progress has been made in developing these compounds into a clinical setting although they possess biological potency similar to mitomycin C which is clinically employed in the treatment of colon and bladder carcinomas.

1.3 Stereoselective Chemical Synthesis of The Azinomycin Metabolite

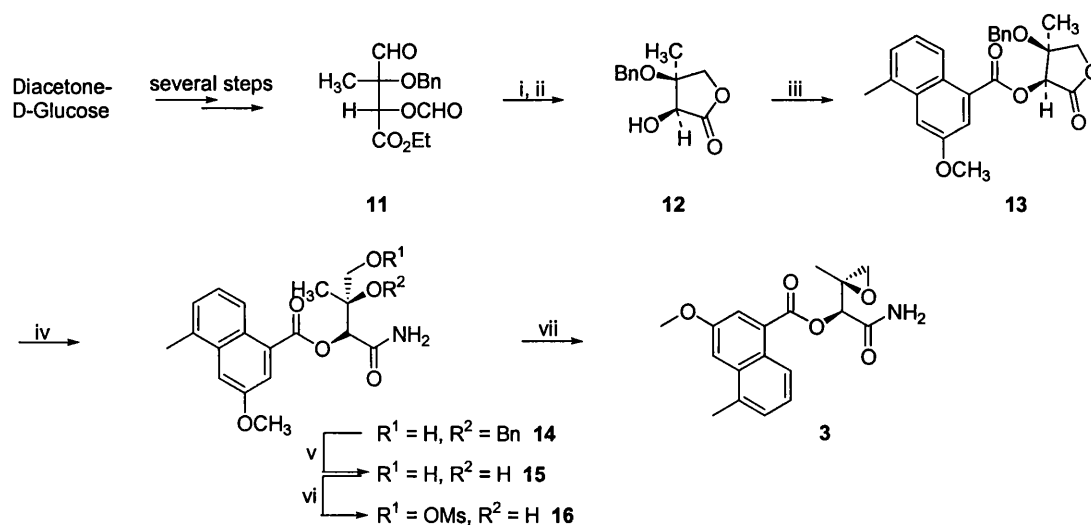
Shibuya's synthetic studies of the azinomycins based on the erroneous structure of azinomycin B 4 were the first synthetic effort made into these compounds.²⁹ This initial work formed the basis of the synthesis of the azinomycin chromophore that has been used by all workers since this time. Although based on a wrong target, Shibuya synthesised one of the degradation products 6 of azinomycin A that formed the C1-C18 segment of the structure 4.²⁹ 3-Methoxy-5-methylnaphthalene-1-carboxylic acid 10 was synthesised via a condensation reaction of 1-(2-

methylphenyl)-2-propanone **7** with diethyl oxalate to furnish the enol **8**, which was cyclised to the naphthol **9** under acidic conditions. Subsequent methylation and base catalysed hydrolysis then gave **10** in high yield, which was coupled to the side chain synthesised from D-glucose to give the azinomycin degradation product **6**.²⁹



Scheme 1.1 Route into the naphthalene ring system. *Reagents and conditions:* (i) $(\text{CO}_2\text{CH}_2\text{CH}_3)_2$, NaOEt, RT, 82 %. (ii) conc. H_2SO_4 , CHCl_3 , -78 to 0°C , 70 %. (iii, iv) dimethyl sulfate aq NaOH, 0°C to reflux 92 %.

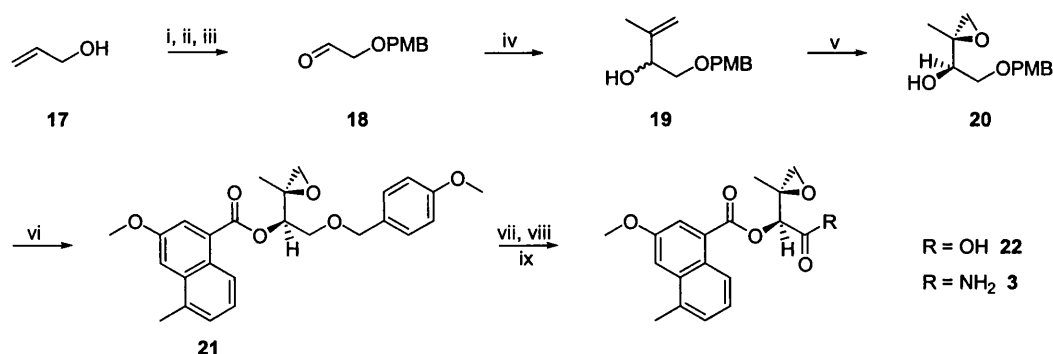
Five years after this work, Shibuya and Terauchi disclosed the first approach to the epoxide subunit of the azinomycins.³⁹ Previously they had synthesised the intermediate **11** from D-glucose in nine steps. In this work³⁹ **11** was derived from commercially available diacetone-D-glucose in more than 70 % overall yield over a five step linear reaction. Reduction of the aldehyde **11** and reflux of the resultant diol with catalytic amount of TsOH then generated the γ -lactone **12** (Scheme 1.2). Acylation of the free hydroxy group of **12** with 3-methoxy-5-methyl-1-naphthoyl chloride and subsequent aminolysis of the lactone with methanolic ammonia provided the amide in excellent yield and without cleavage of the naphthoate ester bond.³⁹



Scheme 1.2 Shibuya method for the synthesis of **3**. *Reagents and conditions.* (i) NaBH_4 , EtOH-THF (1:1), 0°C . (ii) TsOH (cat.), benzene, reflux 92 %. (iii) **10** acid chloride, $(i\text{-Pr})_2\text{EtN}$, DMAP, CH_2Cl_2 , 0°C . (iv) 15 % $\text{NH}_3/\text{CH}_3\text{OH}$, 91 %. (v) 10 % Pd-C/AcOH, H_2 . (vi) MsCl, $(i\text{-Pr})_2\text{EtN}$, CH_2Cl_2 , RT, 73 %. (vii) K_2CO_3 , acetone, reflux.

Hydrogenolysis to remove the benzyl group gave the diol **15**, selective mesylation using MsCl resulted in the monomesylate **16**, which was then heated with K_2CO_3 to form the epoxyamide **3**. This stereospecific synthesis, although lengthy and impractical (17 linear steps from D-glucose) was important because it established the stereochemistry of the natural products as (18*S*, 19*S*). This was made possible by comparison of the optical rotation of the synthetic and natural epoxyamide **3** $\{[\alpha]_{\text{D}}^{25} = +47.5$ (c 0.32, MeOH) (synthetic); $[\alpha]_{\text{D}}^{25} = +48$ (c 0.33, MeOH) (natural). A second route to the epoxide has also been developed by Shibuya et al starting from D-fructose.⁴⁰

Most other groups working on the synthesis of the azinomycins and their metabolite **3** have focused on the use of the Sharpless asymmetric epoxidation to introduce the epoxide functionality. First reports of the use of this reaction were by Armstrong *et al.* and Shishido and co-workers. Armstrong's group utilised allyl alcohol **17** which was protected as its 4-methoxy benzyl ether (PMB) and subjected to ozone/dimethylsulfide to afford aldehyde **18** (Scheme 1.3).²³ Addition of the freshly prepared vinyl Grignard reagent afforded allylic alcohol (\pm)-**19**. Treatment of (\pm)-**19** under SAE conditions using D-(-)-diisopropyl tartrate facilitated kinetic resolution of the substrate and resulted in the formation of the desired (*R*) alcohol **20**.



Scheme 1.3 *Reagents and conditions:* (i) PMBCl, NaH, DMF, 80 %; (ii) O_3 , CH_2Cl_2 , -78°C ; (iii) DMS 45 %; (iv) $\text{H}_2\text{C}=\text{CCH}_3\text{MgBr}$, THF, -20°C 66 %; (v) (-)-DIPT, $\text{Ti}(\text{O}^i\text{Pr})_4$, $t\text{BuOOH}$, CH_2Cl_2 , 45 %; (vi) **10**, DCC, DMAP, CH_2Cl_2 , 73 %; (vii) DDQ, $\text{CH}_2\text{Cl}_2/\text{H}_2\text{O}$, 94 %; (viii) Swern ox. (ix) NaClO_2 , NaH_2PO_4 , THF/ $t\text{BuOH}$, 44 %.

Dicyclohexyl carbodiimide coupling of the alcohol **20** (Scheme 1.3) with 3-methoxy-5-methyl-1-naphthoic acid **10** resulted in formation of the desired ester **21**. Oxidative deprotection of the PMB protecting group followed by a two step oxidation gave the carboxylic acid **22**.

With the aim of developing a more practical route to **3**, Shishido and co-workers⁴¹ embarked on an efficient synthesis of these compounds starting from the Schreiber's epoxy alcohol⁴² **24** (Scheme 1.4). Diisopropenyl carbinol was subjected to the Sharpless asymmetric epoxidation according to the protocol of Schreiber⁴² using D-(-)-diisopropyl tartrate to give the epoxy alcohol **24** in 69 % yield (Scheme 1.4). Esterification with naphthoic acid **10** using DCC chemistry and subsequent oxidative cleavage of the alkene double bond gave methyl ketone **26**. The ketone was further transformed into the enol carbonate **27**, which was then exposed to the conditions of Lemieux-Johnson oxidation to provide the required carboxylic acid **22**. The conversion of **27** into **22** took a prolonged reaction time (10 days) as opposed to the conversion of **25** into **26** (42 h) probably due to steric hindrance of the carbonate group.

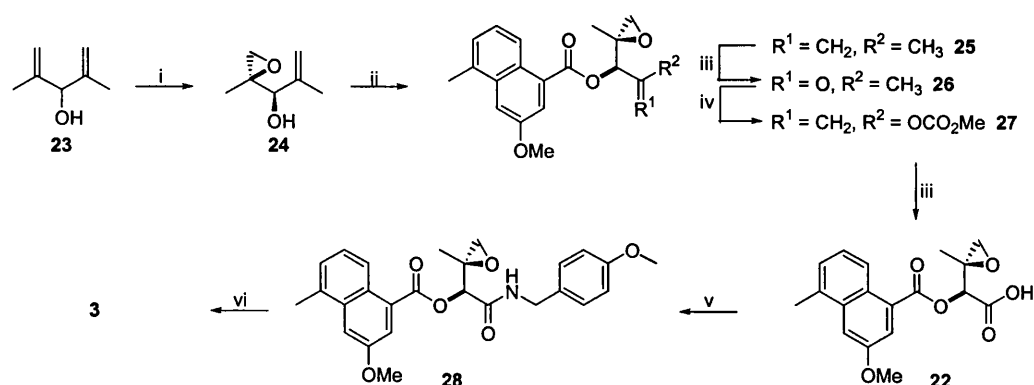


Figure 1.4 *Reagents and conditions:* (i) D-(-)-diisopropyl tartrate, Ti(OⁱPr)₄, ^tBuOOH, CH₂Cl₂, -20 °C, 16 h, 69 %; (ii) **10**, DCC, DMAP, CH₂Cl₂, RT, 94 %; (iii) NaIO₄, OsO₄, Et₂O-H₂O (1:1), for **25** RT, 42 h, 92 %, for **27** RT, 255 h, 62 %; (iv) LiHMDS, HMPA, MeOCOC(=O)Cl, THF, -78 °C – RT, 1 h, 100 %; (v) *p*-methoxybenzylamine, PyBOP[®], HOBt, Et₃N, DMF, RT, 0.5 h, 69 %; (vi) DDQ, CH₂Cl₂-H₂O, (18:1), 0 °C, 4 h, 81 %.

Treatment of the resulting acid with 4-methoxybenzylamine in the presence of the coupling reagents PyBOP and HOBt gave **28**. Oxidative cleavage of the PMB group of the resultant benzamide using DDQ provided the epoxy amide **3**.⁴¹ A few years after the revelations of Armstrong and Shishido, Konda et al provided a more direct route to the (2*S*, 3*S*) epoxide unit based on the precursor (±)-**29**, which was synthesised from acetone in two steps.⁴³

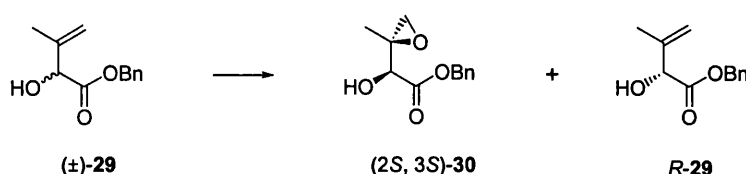
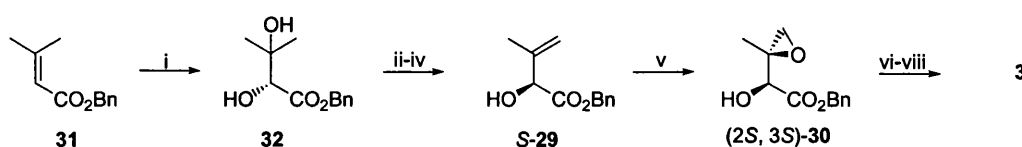


Figure 1.5 *Reagents and conditions:* (i) D-(-)-Diisopropyl tartrate acid, Ti(OⁱPr)₄, ^tBuOH, -20 °C

Kinetic resolution of racemic **29** under SAE conditions using D-(-)-diisopropyl tartrate gave a 48 % isolated yield and 98 % ee of (2*S*, 3*S*)-**30**, along with recovered (*R*)-**29** (Scheme 1.5).⁴³ Coleman's group provided further refinements⁴⁴ to Konda's original work and also described several routes⁴⁵ to the allylic alcohol (±)-**29**. This route was one of the most practical to the epoxy alcohol motif of the azinomycins until Shipman's development of an alternative route to the left-hand portion of the azinomycins based on the Sharpless asymmetric dihydroxylation/ asymmetric

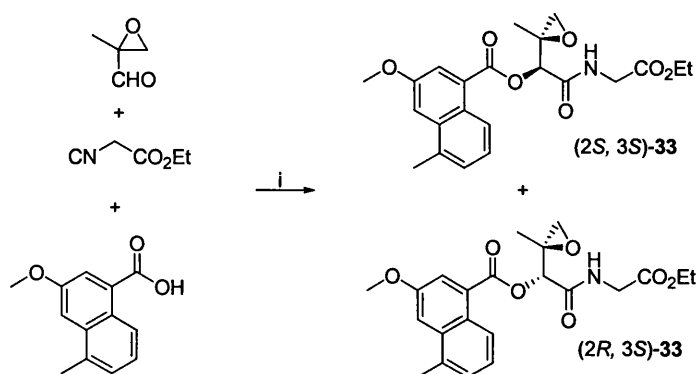
epoxidation methodology.^{46,47} Shipman's route is unique in that it maintained stereochemistry throughout the synthesis. This was achieved by using AD-mix- α in the dihydroxylation reaction of benzyl protected dimethyl acrylic acid **31** to give the diol (*R*)-**32** in 80 % yield and >95 % ee (Scheme 1.6). Selective mesylation, epoxide formation and subsequent acid catalysed epoxide ring opening gave the intermediate (*S*)-**29**. At this stage, a number of different oxidation methods were examined for the stereocontrolled epoxidation of homochiral allylic alcohol (*S*)-**29** and the best method to (*2S*, *3S*)-**30** was found to be a Sharpless AE reaction employing *D*-(-)-diethyl tartrate.^{46,47}



Scheme 1.6 *Reagents and conditions:* (i) AD-mix- α , NaHCO₃, MeSO₂NH₂, ^tBuOH, H₂O; (ii) MsCl, CH₂Cl₂, Et₃N; (iii) Na₂CO₃, MeCN; (iv) CSA, toluene; (v) Ti(OⁱPr)₄, *D*-(-)-DET, ^tBuOH CH₂Cl₂ (vi) 10-Cl, Et₃N, DMAP, CH₂Cl₂; (vii) Pd-C, H₂, MeOH; (viii) NH₄OH, Et₃N, HOBT, PyBOP, DMF.

Single crystal X-ray crystallographic studies unambiguously established the stereochemistry of **30**. Epoxide **30** was transformed into epoxy amide **3** in three steps involving coupling of the epoxy alcohol with the acid chloride of **10**, hydrogenolysis of the resultant ester provided the carboxylic acid **22** which was then subjected to PyBOP, HOBT coupling conditions to afford epoxy amide **3**.

In the quest for the rapid synthesis of structural analogues of the azinomycins for structure–activity relationship (SAR) studies, Armstrong et al developed a highly convergent synthesis of the left hand portion of the molecule involving the Passerini three-component condensation (Scheme 1.7).⁴⁸ In this strategy, each of the components contained one of the postulated functionalities involved in binding to DNA.



Scheme 1.7 Reagents and conditions: (i) EtOAc, 25 °C.

In this reaction, the three components 2-methylglycidal, ethyl isocyanoacetate and 1-naphthoic acid were simply stirred in ethyl acetate to give the epoxy amide **33** in good yield as 3.6:1 mixture of diastereomers. Importantly, the (*S*, *S*)-stereochemistry found in the natural products was found to be the major diastereomer in this reaction. Armstrong et al have used this methodology to rapidly generate libraries of azinomycin analogues.^{49,50}

1.4 Synthesis of The 1-Azabicyclo[3.1.0]hex-2-ylidene Dehydroamino Acid Subunit

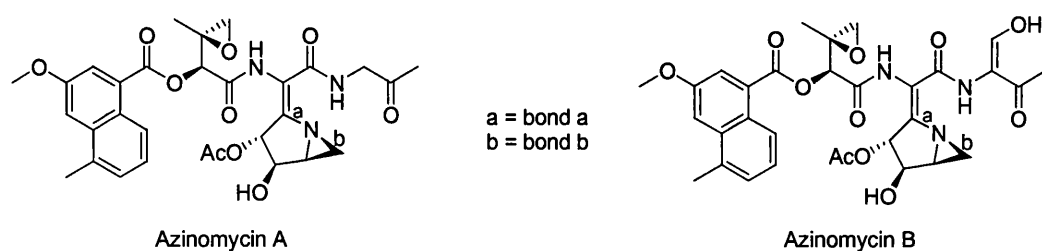


Figure 1.5

The synthesis of the densely functionalised 1-azabicyclo[3.1.0]hex-2-ylidene dehydroamino acid subunit presents a challenge due to its inherent ring strain, instability in acidic media,^{20,24} reactivity towards nucleophiles^{32,33} and the control of the geometry around the tetrasubstituted alkene. In the quest for the total synthesis of the azinomycins, this unit has attracted interest from several research groups, as a successful synthesis, could provide a route for the realisation of the total synthesis of this class of promising antitumour antibiotics. Coleman and Armstrong⁵¹⁻⁵⁴ have independently devised a strategy for the synthesis of this ring system, which involves

an intramolecular addition-elimination reaction for the formation of bond a. Terashima provided an alternative route, which involved formation of bond b to form the aziridine ring. Further retrosynthetic analysis led to the disconnection of the alkene from the backbone to provide a glycine phosphonate synthon and a functionalised aldehyde synthon.

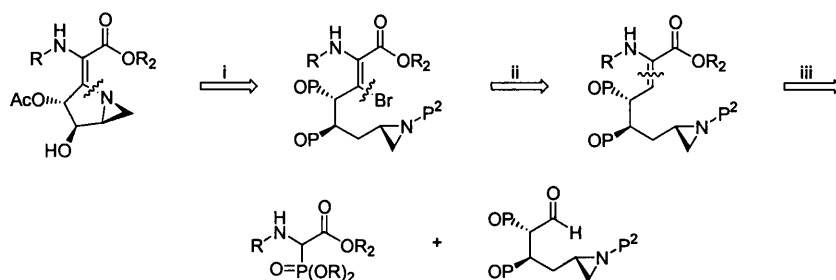
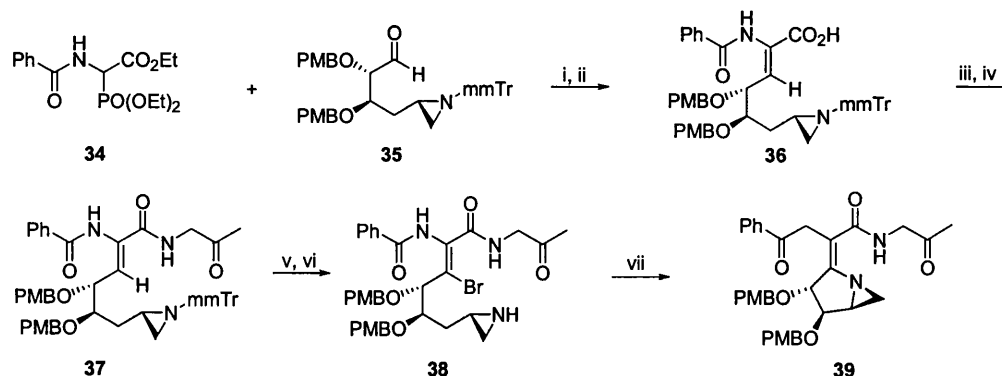


Figure 1.6 Retrosynthetic analysis of the aziridine segment by Armstrong and Coleman: (i) alkylation with Michael addition-elimination; (ii) stereoselective bromination; (iii) stereoselective Wadsworth-Horner-Emmons

In the forward reaction this requires the reaction of a glycine phosphonate with a functionalised aldehyde containing the intact aziridine, a stereoselective bromination and a Michael addition–elimination reaction to complete the synthesis.

Armstrong et al provided the first approach into this ring system. The synthesis began with the Wadsworth-Horner-Emmons condensation of glycine phosphonate **34** and aldehyde **35** (made from D-arabinose or L-serine)⁵³ in the presence of LDA to provide a 4:1 *Z/E* mixture of isomers.⁵⁴ Hydrolysis of this mixture provided the carboxylic acid with the *Z* geometry **36**. The left-hand ketone of the azinomycin was introduced by condensation of **36** with (–)-1-amino-2-propanol under DCC/HOBt conditions. The reaction mixture was then directly subjected to Swern oxidation conditions, due to instability of the product to afford the ketone **37**.⁵⁴



Scheme 1.8 *Reagents and conditions:* (i) LDA, THF, $-78 \rightarrow 0$ °C; (ii) LiOH, THF, H_2O , 50 °C; (iii) $\text{H}_2\text{NCHCH}(\text{OH})\text{CH}_3$, DCC, HOBT; (iv) $(\text{COCl})_2$, DMSO, Et_3N , CH_2Cl_2 , -78 °C \rightarrow RT (vi) $\text{Cl}_3\text{CCO}_2\text{H}$, CH_2Cl_2 then Et_3N , RT (vii) Et_3N , CDCl_3 , 50 °C, 8h.

Introduction of bromine at the β position was achieved by addition of 1.1 equiv. of bromine at low temperature (-78 °C) followed by DABCO to afford the isomerically pure vinyl bromide. Addition of trichloroacetic acid followed by quenching with triethylamine readily removed the monomethoxytrityl protecting group to obtain the aziridine **38**. The cyclisation of vinyl bromide **38** was monitored by ^1H NMR spectroscopy using CDCl_3 as a solvent. The reaction did not proceed after an initial addition of triethylamine and stirring at room temperature for 30 min. However, warming to 50 °C afforded the [3.1.0] bicyclic aziridine with the *Z* geometry.⁵⁴ This synthesis produced the cyclic compound with wrong stereochemistry. It was later discovered that the conditions of the bromination were key to which stereoisomer is produced.⁵¹ Thus, bromination of the (*Z*)-isomer with bromine at -78 °C gives the cyclic compound with the (*Z*)-geometry, while treatment with NBS in dichloromethane gives the (*E*)-isomer exclusively (Scheme 1.9).⁵¹

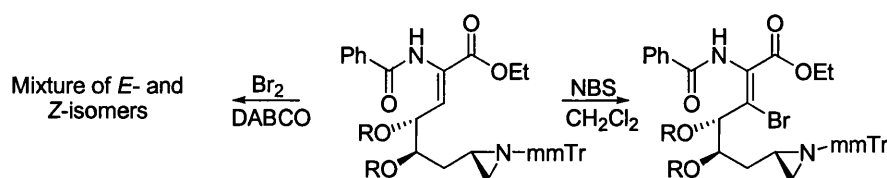
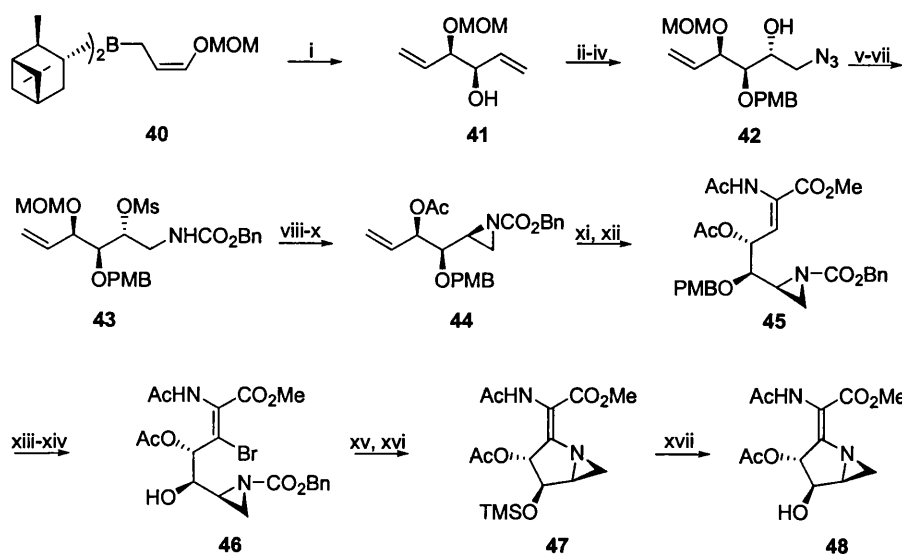


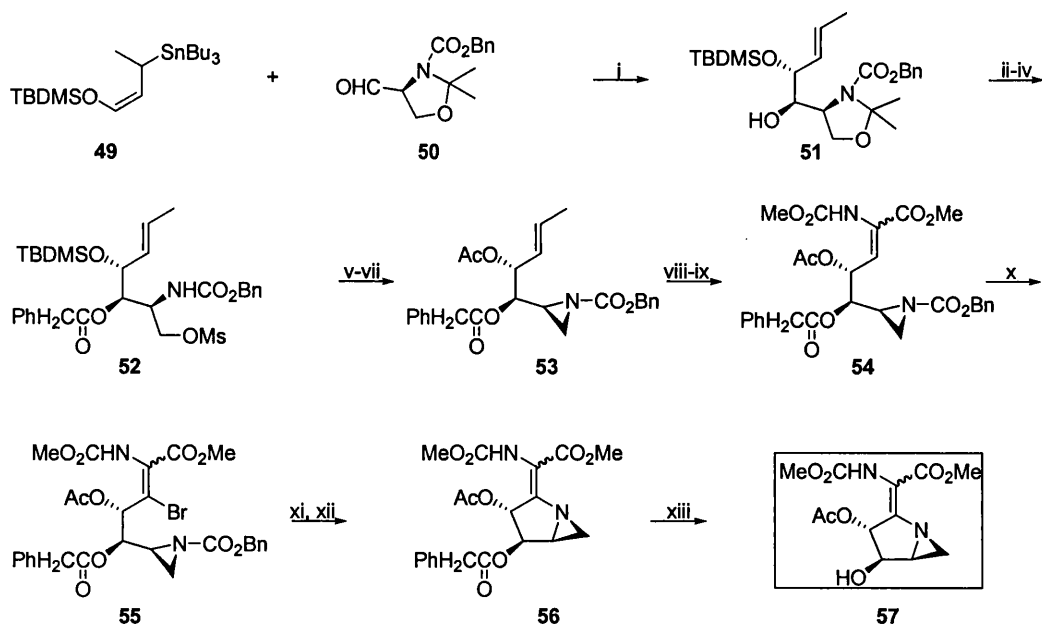
Figure 1.7 Bromination with NBS or bromine

Coleman's group in a similar fashion utilised *D*-glucose to access the aldehyde providing for the first time the selectively protected aldehyde unit although

deprotection of the C12 oxygen could not be achieved to give a free hydroxy group found in the natural products.⁵⁵⁻⁵⁷ Recently, the same group devised a strategy to the 1-azabicyclo[3.1.0]hexanes carrying differentially protected hydroxy groups. More importantly, the C-12 deprotection of the oxygen could be achieved to give a bicyclic ring with the free hydroxy group.^{35,57-59} The synthesis began with asymmetric allylation of acrolein using organoborane **40** to give diene **41**. Sharpless asymmetric epoxidation resulted in epoxidation of the double bond next to the free hydroxy group.⁵⁸ After protection of this group, the epoxide ring was opened with sodium azide to give azide **42**. Reduction of the azide of **42**, *N*-acylation, *O*-acylation of the secondary hydroxy group, cleavage of the acetal and subsequent introduction of the azinomycin C13 acetate afforded **44** via **43**.⁵⁸ Ozonolysis of **44** effected oxidative cleavage of the double bond in this compound and paved the way for a Wadsworth-Horner-Emmons olefination with the phosphonate (reagent xii) to give the dihydroamino acid **45** with a *Z/E* ratio of 4:1. Treatment of **45** with NBS and then (2,2,6,6-tetramethylpiperidine) gave the corresponding vinyl bromide which was transformed into alcohol by oxidative deprotection of the PMB ether. However acetate migration from the C13 to C12 hydroxy group during the aziridine deprotection led to the protection of this hydroxy group as the labile triethsilyl ether. Transformation of the aziridine to the free amine followed by treatment with piperidine, effected the cyclisation to 1-azabicyclo[3.1.0]hexane **47** which was then deprotected at C12 to afford the target compound **48**.⁵⁸



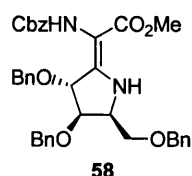
Scheme 1.9 Reagents and conditions: (i) acrolein, $\text{BF}_3 \cdot \text{Et}_2\text{O}$; (ii) L-(+)-DIPT, $t\text{-BuOOH}$, $\text{Ti}(\text{O}^i\text{Pr})_4$, -10°C ; (iii) NaH , PMBBr ; (iv) NaN_3 , NH_4Cl , H_2O , $\text{CH}_3\text{OCH}_2\text{CH}_2\text{OH}$; (v) PPh_3 , toluene, H_2O ; (vi) ClCO_2Bn , Et_3N ; (vii) MsCl , Et_3N ; (viii) HCl , MeOH ; (ix) Ac_2O , pyridine; (x) KO^tBu , THF ; (xi) O_3 then Me_2S ; (xii) $\text{AcHNCH}[\text{PO}(\text{OMe})_2]\text{CO}_2\text{Me}$, KO^tBu , -65°C ; (xiii) NBS , CHCl_3 then TMP ; (xiv) DDQ , H_2O , CHCl_3 ; (xv) N,O -bis(trimethylsilyl)acetamide, 90°C , THF ; (xvi) Et_3SiH , PdCl_2 , Et_3N then piperidine, CDCl_3 ; (xvii) HF , piperidine.



Scheme 1.10 Reagents and conditions: $\text{MgBr}_2 \cdot \text{Et}_2\text{O}$, CH_2Cl_2 ; (ii) ethylene glycol, CSA , THF , 50°C ; (iii) MsCl , Et_3N , CH_2Cl_2 ; (iv) $\text{PhCH}_2\text{CO}_2\text{H}$, DCC , DMAP ; (v) HF , MeCN ; (vi) Ac_2O , DMAP ; (vii) KO^tBu , THF , -78°C ; (viii) O_3 then Me_2S ; (ix) $\text{MeO}_2\text{CHNCH}[\text{PO}(\text{OMe})_2]\text{CO}_2\text{Me}$, LiCl , $i\text{-Pr}_2\text{NH}$; (x) NBS , CHCl_3 then KO^tBu ; (xi) Et_3SiH , $\text{Pd}(\text{OAc})_2$; (xii) Dowex 1X8-400, CHCl_3 ; (xiii) penicillin G acylase, $\text{pH } 7.5$, D_2O , D_3CCN .

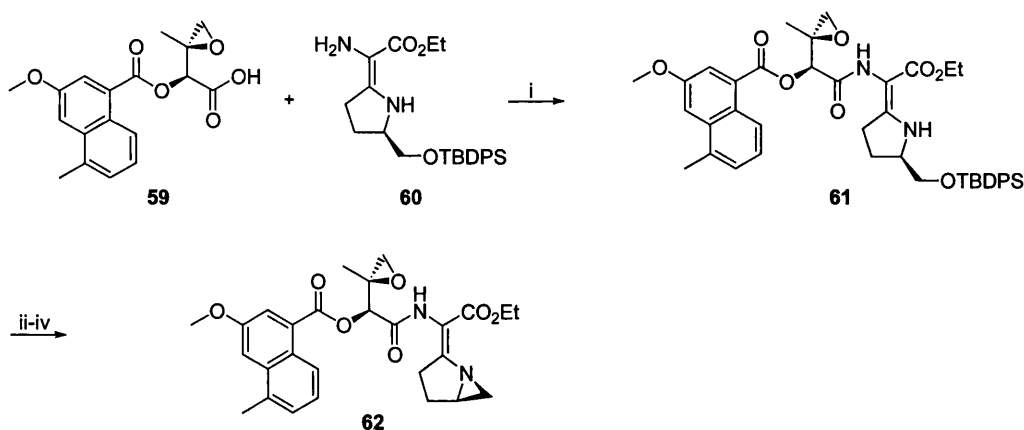
The Coleman group later developed a route involving an enzyme cleavable protecting group, namely a phenylacetyl ester at the C12 position (Scheme 1.9).⁵⁹ In this study, the serine aldehyde **50** was treated with a Lewis acid and the stannane added at room temperature to produce the compound **51**. Cleavage of the oxazolidine ring of **51** resulted in a diol, which was selectively acylated at the primary alcohol with methanesulfonyl chloride (Scheme 1.9). Esterification of the remaining alcohol with phenylacetic acid then provided **52**.⁵⁹ Interchange of C13 hydroxy protecting groups to afford **53** was achieved by HF removal of the silyl group and acylation of the resulting alcohol with acetic anhydride and base. Ozonolysis of the double bond of **53** followed by olefination of the resulting aldehyde with the glycine phosphonate (reagent ix Scheme 1.10) produced dehydroamino acid **54** as a mixture of stereoisomers. The vinyl bromide was introduced by treatment of **54** with NBS⁶⁰ and the aziridine *N*-protecting group was cleaved to afford the free aziridine, which underwent cyclisation upon warming in the presence of Dowex anion-exchange resin to afford the pyrrolidine **56**. Using 5 – 10 mol % polymer-supported penicillin G acylase in a mixed solvent system of acetonitrile/aqueous buffer the C12 phenylacetate ester of **56** was deprotected to give the azinomycin right-hand portion intermediate **57**.⁵⁹ Unfortunately, the bicyclic ring systems containing a free hydroxy group at C12 proved to be unstable and therefore compounds **48** and **57** could only be characterised in situ. The source of instability is believed to be the unprotected hydroxy group since the penultimate C12 ester **56** and the corresponding *p*-methoxybenzyl ether are sufficiently stable to permit isolation and storage. It is believed that this hydroxy group is the cause of instability in the natural products.³⁴

Terashima and co-workers used strategies involving the formation of bond a (Figure 1.5) to access the bicyclic moiety of the azinomycins,^{61,62} an effort which ultimately led to the first reported synthesis of a compound containing the left and right-hand portions of the azinomycins.^{32,33,63,64} In 1999 Konda reported a novel route to the dihydroamino acid **58**⁶⁵ which involved an intramolecular 1,3-dipolar cycloaddition of an azide and an olefin functionality. Although they did not proceed to make the 1-azabicyclo[3.1.0]hexane ring system, this compound could in principle, be converted into the bicyclic ring system.



1.5 The Total Synthesis of Azinomycin A

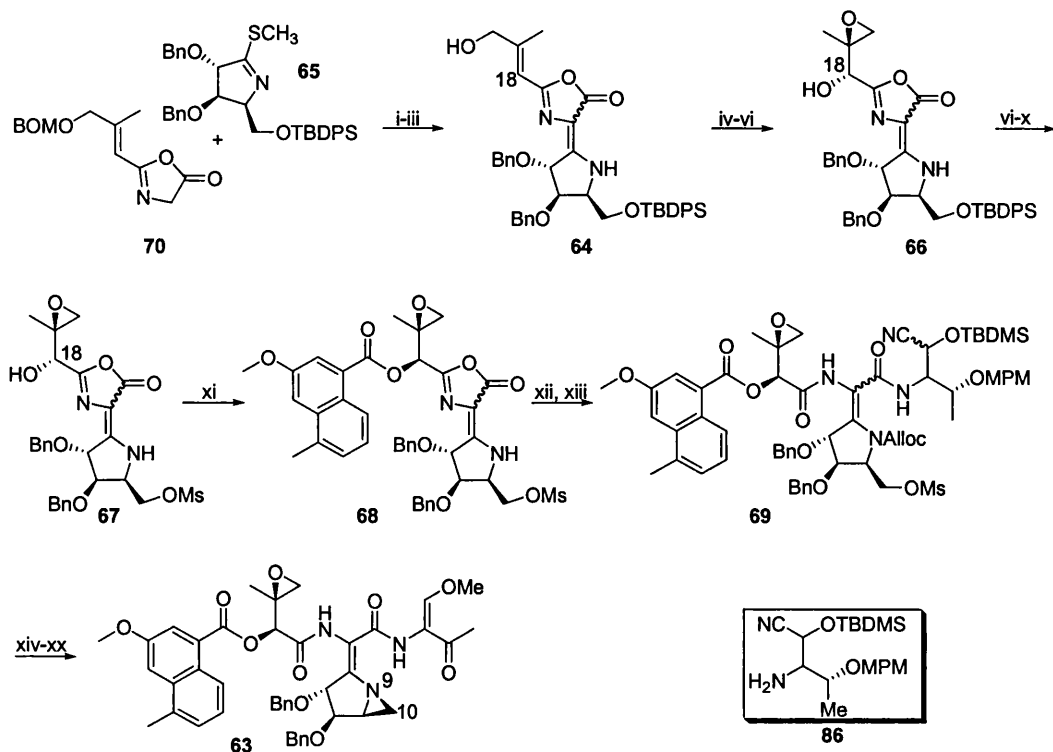
In spite of the wealth and quality of research into the various constituents of the densely functionalised azinomycin structure, the total synthesis of these compounds proved elusive until the recent report of the synthesis of azinomycin A by Coleman *et al.*³⁸ Terashima *et al.* spearheaded research in this area and were the first to describe the synthesis of a compound containing all the proposed DNA binding units (epoxide, aziridine and naphthoyl ester) of the azinomycins (Scheme 1.11).^{32,33,63}



Scheme 1.11 Terashima synthesis of 4-*O*-methyl-13-desacetyl-12,13-dihydroazinomycin. *Reagents and conditions:* (i) DCC, HOBT, THF; (ii) TBAF, THF; (iii) MsCl, Et₃N, -78 °C; (iv) KHMDS, THF.

Enamine **60** which they had earlier developed,^{33,61,62} was coupled with carboxylic acid **59**, prepared using the methodology developed by Shibuya *et al.* to give **61** as a tautomeric mixture. Deprotection to give the free C11 hydroxy group and subsequent mesylation followed by base-induced ring cyclisation then effected epoxy aziridine **62**. In a similar, recent synthesis, Shipman and co-workers^{65,66} made the same epoxy aziridine **62** (which does not contain the problematic substituents on the pyrrolidine ring) via a different route to demonstrate its DNA-crosslinking ability.⁶⁸ Terashima

later described an advanced structure en route to the synthesis of the complex azinomycin B (Scheme 1.12).



Scheme 1.12 Terashima synthesis of azinomycin B analogue: *Reagents and conditions:* (i) toluene, 60 °C; (ii) DDQ; (iii) NaBH₄; (iv) (DHQ)₂PHAL, OsO₄ then H₂S; (v) MsCl, γ-collidine; (vi) DBU; (viii) Dess-Martin reagent; (viii) TBAF; (ix) MsCl, γ-collidine; (x) NaBH₄, CeCl₃·7H₂O, 80 % de; (xi) naphthoic acid, WSCI·HCl, DMAP; (xii) Alloc₂O, cat. DMAP; (xiii) **86**, toluene, then concentration at 50 °C; (xiv) DDQ; (xv) Dess–Martin reagent; (xvi) Pd(PPh₃)₄, AcOH; (xvii) TBAF, AcOH; (xviii) aq. NaHCO₃; (xix) CH₂N₂; (xx) 4 Å MS.

This route made use of a cleverly designed synthon **64**, which is actually a masked fragment that corresponds to the epoxide and aziridine amino acids.³² It started with the treatment of **70**, which was developed from hydroxymethyl-2-butenate, with excess thioimide **65** to give the condensation product as a 78:22 inseparable mixture of (*E*)- and (*Z*)-isomers in 58 % yield. Deprotection of the BOM group by sequential oxidation with DDQ and reduction of the resultant aldehyde to give the allylic alcohol **64**. Modified Sharpless AD of this allyl alcohol using stoichiometric amounts of osmium tetroxide and the ligand (DHQ)₂PHAL followed by decomposition of the osmate with H₂S produced the corresponding triol with >95 % de. After selectively mesylating the primary alcohol, treatment of the mesylate with

DBU then gave epoxide **66**. For the epimerisation of the C18 secondary hydroxyl group a sequential oxidation and reduction protocol was utilised.³² To accomplish this, **66** was first oxidised with Dess-Martin reagent to the corresponding ketone. The TBDPS protecting group was removed and the resulting hydroxyl protected as the mesyl ester. Reduction of the C18 ketone was achieved stereoselectively with a combination of $\text{CeCl}_3 \cdot 7\text{H}_2\text{O}$ and NaBH_4 in MeOH to give the desired (*S*)-C18 alcohol **67**. Condensation of **67** with the naphthoic acid chromophore furnished ester **68**. Treatment of **68** with Alloc_2O and catalytic DMAP followed by the addition of **86** and concentration in vacuo was found to successfully produce the desired (*E*)-amide **69** as a major product in 78 % yield. A series of reactions involving MPM group deprotection, oxidation of the resultant hydroxy group to give the *O*-silylated β -ketocyanohydrin whose N-alloc group was removed. Desilylation, alkaline treatment, methylation of the resulting enol and finally closure of the aziridine ring using TBAF gave the target compound **63**. Although this compound is structurally similar to azinomycin B, with exception of the protected hydroxyl groups, all attempts to transform it into the natural products failed as attempts to effect reductive debenzoylation at C12 and C13 resulted in cleavage of the aziridine ring via breakage of the N9–C10 bond.

Recently Coleman et al reported the total synthesis of azinomycin A **1**.³⁸ Five disconnections at ester, amide, olefin and C–N bonds arrived retrosynthetically at the five crucial synthons: 1) naphthoic acid, 2) epoxyalcohol, 3) glycine phosphonate, 4) aziridine, and 5) 1-amino-2-propanol. Due to the observation that the C12 hydroxyl group on the aziridine moiety presented a problem, the route was adjusted to allow a late stage introduction of this group.

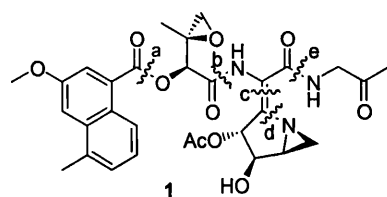
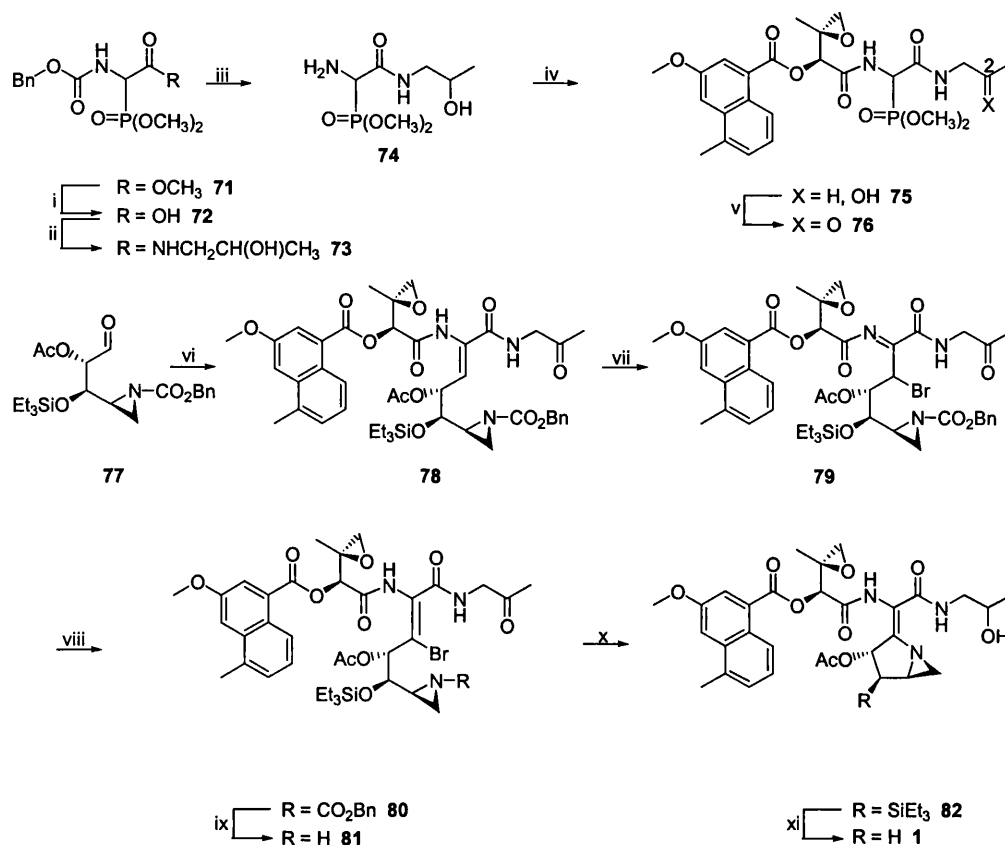


Figure 1.8 Structure of azinomycin showing disconnections.



Scheme 1.13 *Reagents and conditions:* (i) LiOH, then Dowex H^+ (ii) $\text{NH}_2\text{CH}_2\text{CH}(\text{OH})\text{CH}_3$, DCC, HOBT; (iii) H_2 , Pd-C; (iv) **22**, EDC, CH_2Cl_2 ; (v) Swern oxidation; (vi) $^t\text{BuOK}$, CH_2Cl_2 , $-50\text{ }^\circ\text{C}$; (vii) NBS, CH_2Cl_2 , (viii) $^t\text{BuOK}$, CH_2Cl_2 , $40\text{ }^\circ\text{C}$; (ix) Et_3SiH , PdCl_2 , CH_2Cl_2 ; (x) Dowex (CO_3^{2-}), CH_2Cl_2 , $45\text{ }^\circ\text{C}$.

Phosphonate **75** containing the backbone of the azinomycins was constructed in a convergent manner by a series of esterifications and amide bond formations (Scheme 1.13).³⁸ The aminophosphonate **74** was made from glycine phosphonate **73** by saponification to afford the crude acid in quantitative yield after acidification with Dowex H^+ . The acid was then coupled with (\pm)-1-amino-2-propanol using dicyclohexylcarbodiimide to afford **73**, which was then treated under hydrogenolysis conditions to remove the benzyl carbamate and give the amide **74** in 99% yield. Coupling of the previously discussed epoxy acid **22** (Scheme 1.3) with amino phosphonate **74** afforded the fully elaborated top-half phosphonate **75** in good yield (79 %). Swern oxidation conditions were used to oxidise the C2 hydroxy group at this point to avoid synthetic manipulations subsequent to dehydroamino acid introduction. This avoidance policy outweighed the potential problems with a competing intramolecular olefination between the C2 carbonyl and the phosphonate

group. Wadsworth–Horner–Emmons olefination of aldehyde **77** with phosphonate **76** was achieved using potassium *tert*-butoxide at low temperature and gave a mixture of (*Z*)/(*E*) dihydroamino acid **78** in 40 % yield which thereby completed the construction of the entire azinomycin skeleton. Intramolecular olefination of the phosphonate anion onto the C2 carbonyl group of **76** proved to be a minor reaction pathway which yielded < 5 % of the corresponding cyclic product. Bromination of **78** with NBS using silica gel catalyst proceeded to afford the α -bromoimine **79** in 75 % yield, which was tautomerised under basic conditions and provided the vinyl bromide with the desired (*E*) configuration. Selective removal of the aziridine *N*-benzyl carbamate using a palladium-catalysed, process produced the corresponding free aziridine amine without reduction of other functional groups in the molecule. Cyclisation was then effected upon warming in the presence of Dowex anion exchange resin to afford 12-*O*-triethylsilyl azinomycin A **82**. Finally, removal of the C12 hydroxy protecting group afforded azinomycin A **1**. This free hydroxyl product was found to be unstable and was therefore characterised in situ. Again the instability was thought to be due to the free C12 hydroxyl since the penultimate intermediate 12-*O*-triethylsilyl azinomycin A **82** possessed a greater degree of stability.³⁸

1.6 Molecular Modelling Studies of The Azinomycin Antitumour Antibiotics

To date, understanding of the site and mechanism of action of these agents remains unclear, this fact coupled with the unavailability of the natural products for DNA interaction studies urged Coleman and co-workers to carry out a number of computational studies of the binding of the natural product to DNA, the biological target. To accomplish this, they developed force-field parameters for the natural products⁶⁹ and a model was subsequently developed for formation of covalent interstrand DNA cross-links by azinomycin B.⁷⁰ Two models were considered as the initial non-covalent association of the agent with DNA can occur by two different pathways: first, simple association of the agent with the surface of the major groove and secondly, association of the agent with the major groove accompanied and, or facilitated by intercalation. The study suggested that DNA cross-linking by azinomycin B occurs through an initial alkylation of the N7 of adenine by the aziridine C10 followed by alkylation of the N7 of guanine on the opposite strand by the epoxide group to effect covalent cross-link formation. Both experimental models

had the same outcome which is consistent with experimental observations made by Fujiwara and Saito⁴² but does not address the role of the naphthalene moiety in the binding reaction.

1.7 The Mechanism of Action of The Natural Products And Their Synthetic Counterparts.

The left hand-hand portion of the azinomycins, itself a natural product initially thought to be inactive, actually possesses potent cytotoxic activity which rivals that of the natural products with a more elaborate chemical composition. This structure, **3**, represents a useful tool since it is more chemically robust, more easily accessible and a thorough understanding of this molecule can help gain insight into the molecular mechanism of DNA cross-linking by the intact natural products. Zang and Gates have disclosed the most comprehensive characterisation of non-covalent DNA binding and DNA alkylation by this naphthalene epoxide.⁷² Using 5'-³²P-labeled 145 base pair restriction fragment DNA they showed that **3** generates base-labile lesions selectively at guanosine residues in double stranded DNA. This result strongly suggests that **3** alkylates DNA at the N7 position of guanine to produce an alkylguanine lesion as previously proposed by other groups for intact azinomycin. The alkylation event proceeded with low, if any, sequence selectivity; alkylation occurs at every guanosine residue in the DNA fragment but at much lower concentration than a simple epoxide alkylating agent **83**. About 50 000 times higher concentrations of **83** were needed to produce alkylation yields similar to that generated by the epoxy amide **3**.⁷² This evidence strongly supports the theory the **3** may bind non-covalently to DNA and that the naphthalene chromophore plays a role in this respect. Their preliminary results for UV-Vis, fluorescence, T4 ligase DNA-unwinding assay, and viscometry experiments show the naphthalene residue binds to DNA by intercalation. This mode has been suggested for the azinomycinns in spite of generally held belief that naphthalene derivatives are poor DNA intercalators. Recently, Coleman and co-workers⁷³ contradicted these findings by proposing that the naphthalene moiety does not associate intercalatively with DNA although their findings were based largely on non-alkylating structures such as **84** and **85** (Figure 1.9).

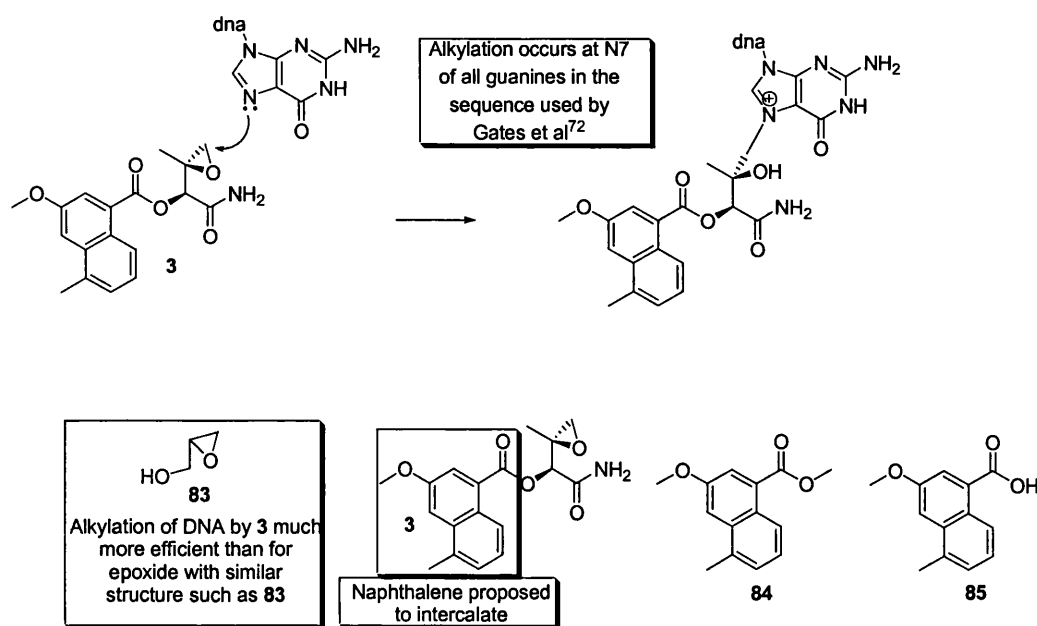


Figure 1.9 Zang and Gates results propose intercalation and guanine alkylation by **3**. Coleman proposed a non intercalative binding largely based on results based on **84** and **85**.

		Cytotoxicity IC ₅₀ values				
		A270	A2780cisR	CH1	SKOV-3	HT29
3		<0.05	0.076	<0.05	1.25	0.33
a		1.8	3.5	1.4	12.0	4.3
b		0.44	1.1	0.55	5.1	2.15
c		0.39	1.35	0.17	13.0	2.6
d		>25	>25	>25	>25	>25
e		>25	>25	>25	>25	>25

Figure 1.10 Effect of intercalator structure on cytotoxicity

After completing the stereoselective synthesis of **3**, Shipman and co-workers began investigations on how the nature of the aromatic group influences cytotoxicity in order to generate more potent analogues.⁷⁴ In the process, they synthesised the series of compounds in Figure 1.10. Even a very subtle change from the methyl to ethyl at the C3 of the naphthalene residue results in a substantial loss of potency. When the aromatic group in the epoxide was changed to the 2-quinoxaline group, an established intercalator, activity was lost.⁷⁴ This finding is interesting since the

quinoxaline chromophore does intercalate and was expected to potentiate the activity of the analogue through a stronger binding for DNA than the naphthalene chromophore. This suggests that the 3-D orientation of the compound at the target site is equally as important as the ability to interact intercalatively with DNA and that the naphthalene core may be better placed to satisfy this criterion. Although the quinoxaline intercalates, it might place the epoxide unit in an unfavourable position for attack by the N-7 of guanine. Likewise, a change to a phenyl group was detrimental for the activity of the compound. Both the 1- and 2-naphthalene-carboxylic acid analogues lost up to 20-fold activity but remained reasonably potent, perhaps due to an unsatisfactory orientation of the naphthalene, which consequently places the epoxide moiety in an unfavourable position.

Further effort directed towards gaining insight in the mechanism of action of the azinomycins led to the design, synthesis and DNA cross-linking studies of the epoxide dimers **85a – c**.⁷⁵

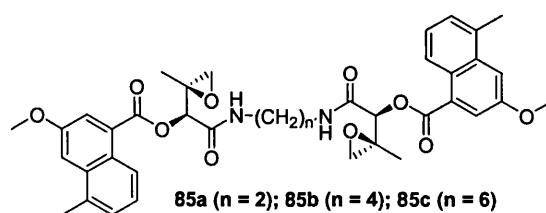
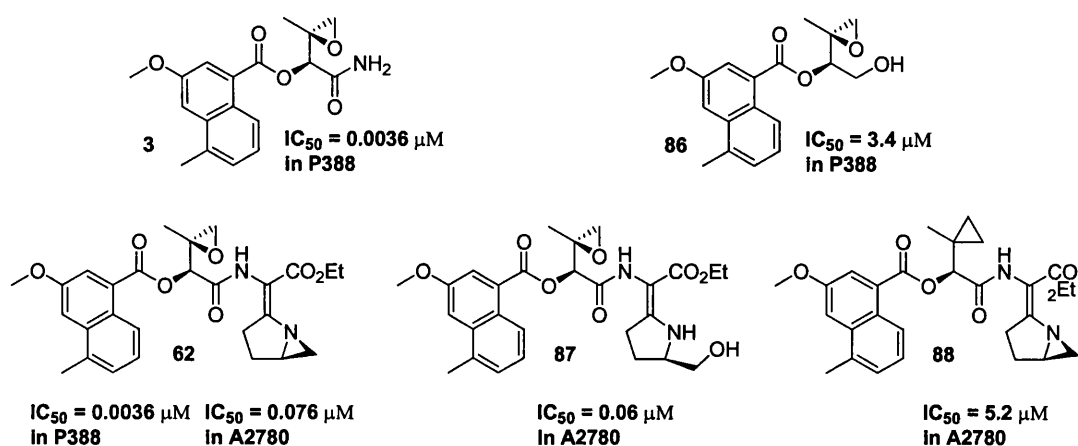


Figure 1.11 Structure of dimeric epoxy amides

In the cross-linking studies, mono epoxide **3** produced no interstrand cross-link (ISC) activity at concentrations up to 50 μM . In contrast, the bisepoxides induce DNA cross-linking at concentrations as low as 0.1 μM .⁷⁵ These studies suggested that a spacer consisting of about four methylene groups is optimal for cross-linking ability. The six carbon linker compound **85c** induces ISCs but at a much higher concentration. The sequence selectivity for the bisepoxides was investigated using the Taq DNA polymerase assay and this showed that all three bisepoxides and epoxide **3** induce Taq stops preferentially at G residues indicating alkylation at these bases,⁷⁵ which is consistent with earlier findings.⁷² Further more, the bisepoxides block polymerase at fewer bases than the corresponding monoepoxide **3**, suggesting enhanced sequence specificity. Interestingly, the monoepoxide demonstrates similar

cytotoxicity as the bisepoxides raising the interesting question as to whether cross-linking is necessary for activity.⁷⁵

Compound **62**, developed both by Terashima and Shipman and co-workers,⁷⁶ has been shown to cross-link DNA, producing 100 % cross-link formation after 1.5 h, whereas **87** and **88**, devoid of the aziridine or epoxide, respectively, show no detectable DNA ISC activity.⁶⁸



Since **62** cross-links DNA, it was expected to be more cytotoxic, however the mono epoxide compound **3** and the analogue **87** devoid of the aziridine moiety have similar cytotoxicity (in P388^{77,78} and A2780⁶⁸ cell lines) as the cross-linking agent **62**. The aziridine **88** devoid of the epoxide moiety however is less cytotoxic than the cross-linking agent.

Considering all the material available on the azinomycins and their derivatives today, a principal question arises of the requirement of interstrand cross-linking for biological activity. Armstrong, Lown, Saito and recently Coleman have demonstrated cross-linking for the natural products. Whatever the order of adduct formation, it has been suggested that this is required for antitumour activity. All the results to date however suggest that the truncated azinomycin analogue **3** has potent antitumour activity in a variety of cell lines that matches and in some cases even surpasses the activity of a cross-linking derivative^{68, 78}

1.8 Aims of The Study

The azinomycin antitumour antibiotics are potent cytotoxins targeting cell division and growth processes present in all dividing cells. Their high potency and low molecular weight makes them ideal cancer chemotherapeutic drug candidates. However, their chances of entering the clinic in their current form are poor due to the instability and nonselective activity of the parent compound. In order to develop potent, clinically relevant analogues and to find mechanisms by which these agents may be targeted to tumours through prodrug approaches, (including ADEPT and GDEPT), it is crucial to understand the ligand–target interactions that contribute to the biological activity of the natural product. The study of antitumour antibiotics through the design and synthesis of analogues containing systematic structural modifications, leads to an understanding of the mechanistic detail of the interaction of the natural products with their target and ultimately to the design of potent analogues with therapeutic applications. With this in mind, the specific aims are:

- i) To design and synthesise analogues of the azinomycins containing subtle structural modifications.
- ii) To investigate the mechanism underlying the biological activity of the compounds using molecular biology techniques including DNA cross-linking and unwinding.
- iii) To develop a prodrug strategy for targeting the azinomycins to their biological target, DNA.

Chapter 2

Synthesis and biological studies of azinomycin analogues: Effect of Stereochemistry on Biological Activity.

2.0 Introduction

The biological activity of drugs depends on their interaction with biological targets, such as proteins (receptors, enzymes), nucleic acids (DNA and RNA) and biomembranes (phospholipids and glycolipids). All these targets have complex three-dimensional structures, which are capable of specifically recognising (binding) the ligand molecule in only one in many possible arrangements in three-dimensional space. It is the three-dimensional structure of the drug target that determines which of the potential drug candidate molecules is bound within its cavity and with what affinity. Therefore changes that affect the three-dimensional structure of drug molecules, such as a change in stereochemistry and substitution pattern can affect the mode of interaction and consequently the biological activity of these compounds.

For example the duocarmycins, which were isolated from a streptomyces species, are extremely potent cytotoxic agents, which derive their activity from sequence selective alkylation at the N3 of adenine in the DNA minor groove.⁷⁹ Vital to the unravelling of the mechanism of action of these agents in particular and indeed many other natural products in general is the design and synthesis of analogues of the natural products that allowed the introduction of subtle structural changes (**Figure 2.1**).¹⁰

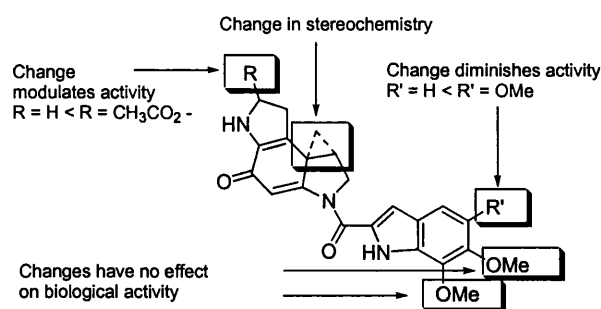


Figure 2.1 Structure of duocarmycin SA showing sites of modifications

This technique led to the discovery that analogues possessing the unnatural stereochemistry (i.e. (–)-duocarmycin SA) underwent a change in DNA alkylation sequence selectivity and as a result displayed a concomitant decrease in biological activity.¹⁰ Other key observations were that the 5-MeO substituent of the right hand indole was required for biological potency⁸⁰ and that removal of the 6- and 7-MeO

groups led to no perceivable decrease in biological activity. Further investigations revealed that removal of the left hand alkylation unit C6-methyl ester functionality diminished activity and both the ester and methoxy groups led to similar and cumulative decreases in activity and DNA alkylation efficacy.⁸¹ These and other observations led to a suggestion for the mechanism of action of the duocarmycins, involving a binding-induced conformational change. This mechanism could not have been suggested without the synthesis of analogues of the natural products containing deep-seated structural modifications.

The azinomycin metabolite **3**, isolated from *streptomyces griseofuscus* S42227 is thought to stem from the hydrolysis of the parent antibiotic.²⁰ Compound **3** has been extensively explored from a synthetic point of view¹⁹ but very little has been disclosed in the study of structure-activity relationships from a DNA binding, biological and mechanistic point of view.⁸² This molecule being small and more easily accessible through readily available and relatively inexpensive starting materials presents good prospects for development as a drug candidate. Vital to the development of this compound into a clinically useful entity is the deconvolution of its mechanism of action. In this chapter, I aim to use the “substituent directed mutagenesis” approach (**Fig. 2.2**) as a tool to investigate what role the various substituents play in the mode of binding of the compounds to their biological target DNA. In this approach, the design and synthesis of structural analogues is used to define the factors that contribute to binding and biological activity of the compounds.¹⁰

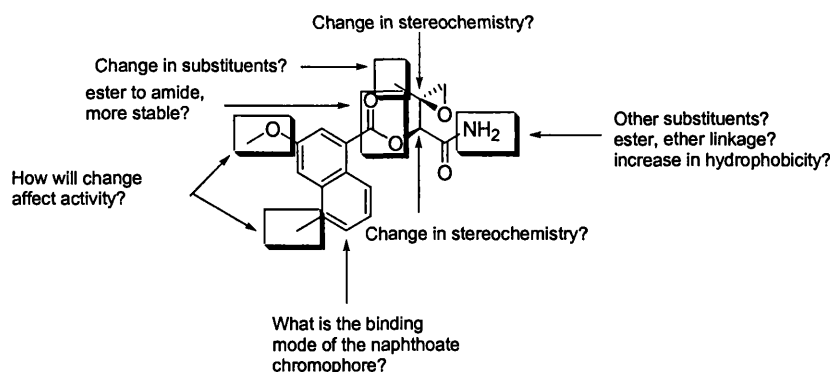


Figure 2.2 Structure of the azinomycin metabolite **3** indicating changes that can be made.

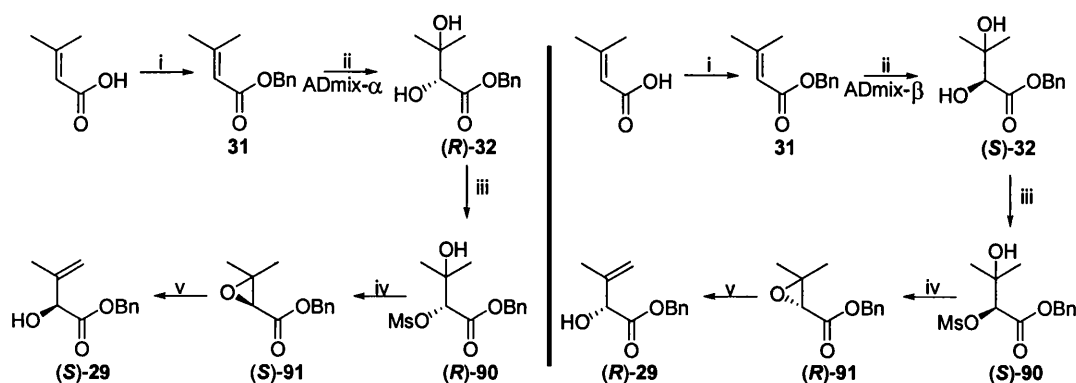
Many groups investigating the azinomycin metabolite **3** have focused on the natural (*S, S*) stereoisomer and the question as to whether the unnatural (*2S, 3R*), (*2R, 3R*) and (*2S, 3R*) stereoisomers have the same DNA binding and biological activity is still unanswered. The exception is a brief investigation of the (*2R, 3R*) isomer which suggested a decrease in activity.⁷⁴ The functionally rich azinomycins and their metabolite present many opportunities for structural modifications for the medicinal chemist. The epoxide group could be removed and replaced with an alkane, alkene or a mustard functionality. The methoxy and methyl group on the chromophore could also be extended to increase the hydrophobicity of the compound to probe their role in the biological efficacy of the compounds.

2.1 Chemistry Results

2.1.1 Synthesis of the epoxide unit.

Studies of the azinomycin analogue **3** were initiated by investigating the effects of stereochemistry of the epoxide moiety on biological activity. These compounds were synthesised using the route developed by Shipman⁴⁷ and co-workers to the left-hand portion of the azinomycins based upon the Sharpless⁸³ asymmetric dihydroxylation reaction incorporating the modification introduced by Casely-Hayford and Searcey.⁸² Commercially available 3,3-dimethylacrylic acid was refluxed under phase transfer conditions⁴⁷ in a solution of aqueous KOH and tetra-*n*-butylammonium iodide in chloroform to afford the benzyl ester **31** in high yield (81 %) [FAB MS *m/z* 191 (*M* + *H*)⁺]. The ¹H NMR of compound **31** showed the aromatic protons at 7.31 ppm with the methylene protons of the benzyl group appearing as a singlet at 5.15 and the H-2 proton singlet at 5.75 ppm. The methyl groups were found at 2.19 and 1.90 ppm. Enantioselective *cis*-dihydroxylation of this *trans*-disubstituted α,β -unsaturated ester was achieved by making a solution of AD-mix- α , methanesulphonamide and NaHCO₃ in *t*-BuOH and H₂O at room temperature. The reaction mixture was cooled to 0 °C and the ester **31** added in one portion and the heterogenous slurry stirred at 4 °C for 60 h to give the diol (*R*)-**32** in 83 % yield [FAB MS *m/z* 225 (*M* + *H*)⁺, 247 (*M* + *Na*)⁺]. The corresponding (*S*)- isomer (*S*)-**32** was synthesised by employing AD-mix- β in the enantioselective *cis*-dihydroxylation reaction (Scheme 2.1).^{47,84} The

NMR spectra of the ester **31** and the dihydroxy compound differ in the shift of the methylene protons which occur as doublet of doublets at δ 5.27 (1H, d, $J = 12.0$ Hz) and δ 5.21 (1H, d, $J = 12.4$ Hz). The H-2 protons, two hydroxy groups, and the two methyl group protons occurred at δ 3.99 (1H, d, $J = 6.8$ Hz), δ 3.18 (1H, br d, $J = 6.8$ Hz), δ 2.57 (1H, br s), 1.26 and 1.17 ppm respectively.



Scheme 2.1 Synthesis of allylic alcohols. Reagents and Conditions: (i) BnBr, KOH, Buⁿ₄NI, CHCl₃, H₂O, 81 %; (ii) NaHCO₃, MeSO₂NH₂, Bu^tOH, H₂O, 83 %; (iii) MsCl, CH₂Cl₂, Et₃N, 0 °C, 80 %; (iv) Na₂CO₃, MeCN, 80 °C, 86 %; (v) (+/-)-camphor-10-sulfonic acid (CSA), toluene, 110 °C, 79 %.

The Sharpless asymmetric dihydroxylation (AD) reaction proceeds with enantiofacial selectivity with the alkene attacked on the top (β)-face in the case of AD-mix- β which employs dihydroquinidine ligand,⁸⁴ or from the bottom α -face in the case of AD-mix- α which employs dihydroquinine derived ligands.⁸⁵ Terminal, 1,1-disubstituted and *trans*-disubstituted as well as trisubstituted olefins are regarded as the “standard” substrates for the AD reaction⁸⁵ and reactions employing these substrates and the AD-mixes proceeded smoothly to give the diols (*R*)-**32** [α]_D²² -8.5 (*c* 1.06 CH₂Cl₂) and (*S*)-**32** [α]_D²² 6.1 (*c* 1.0 CH₂Cl₂); [lit. for (*R*)-**32** [α]_D²⁰ -10.8 (*c* 1.0, EtOH)⁴⁷]. Buffering of the reaction mixture by addition of NaHCO₃ was required to prevent ester hydrolysis. Figure 2.3 shows the catalytic cycle of the AD reaction with K₃Fe(CN)₆ as the co-oxidant.⁸⁶

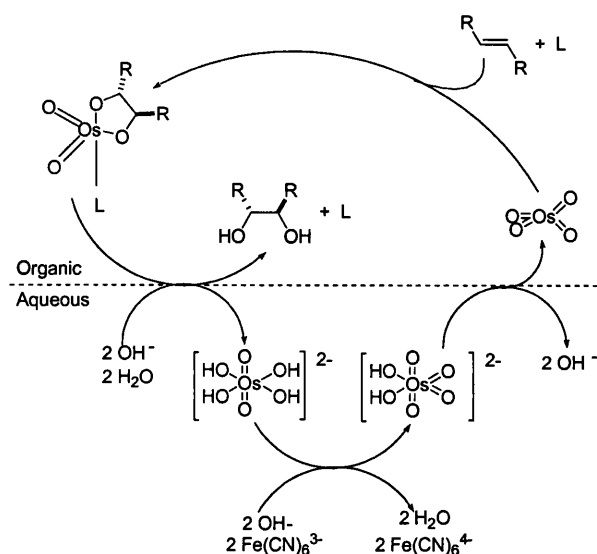
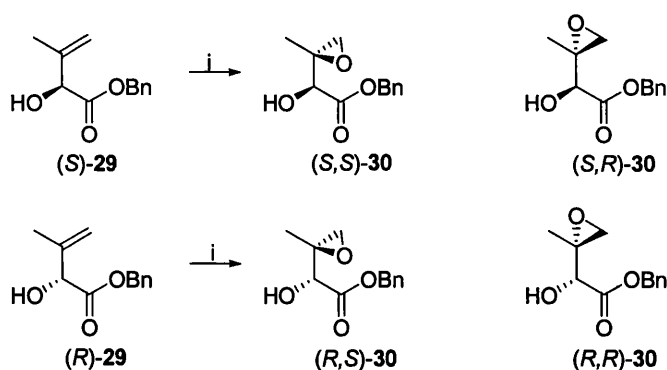


Figure 2.3 Catalytic cycle of the AD reaction. Addition of MeSO_2NH_2 accelerates the hydrolysis of the osmium(IV) glycolate product.

To stirred solutions of the diols (2*R*)- and (2*S*)-benzyl 2,3-dihydroxy-3-methylbutanoate (*R*)-**32** and (*S*)-**32** and Et₃N in dry dichloromethane was added methane sulfonyl chloride dropwise to give the secondary mesylates (*S*)-**90** [α]_D²² – 37 (*c* 1.1 CH₂Cl₂) and (*R*)-**90** [α]_D²² 26.2 (*c* 1.1 CH₂Cl₂); lit. [α]_D²⁰ 21.5 (*c* 1.0 EtOH)⁴⁷, [FAB MS *m/z* 303 (M + H)⁺, 325 (M + Na)⁺]. This oxirane precursor was then exposed to dry K₂CO₃ in acetonitrile and then heated at reflux under N₂ for 48 h to effect facile cyclisation through nucleophilic attack by the tertiary hydroxyl group to give the (2*R*)- and (2*S*)-benzyl 2,3-epoxy-3-methylbutanoate (*R*)-**91** [α]_D²² – 2.9 (*c* 2.1 CH₂Cl₂) and (*S*)-**91** [α]_D²² 5.7 (*c* 0.4 CH₂Cl₂); lit. [α]_D²⁰ 3.5 (*c* 1.2 EtOH)⁴⁷ (**Scheme 2.1**). This cyclisation although facially selective, occurs with inversion of stereochemistry since the OH group can only attack C-2 on the opposite face of the molecule to the mesylate group in an S_N2 type of attack. In the ¹H NMR of the 2,3-epoxide, the H-2 proton occurred as a singlet at 3.37 ppm whereas the two doublets of the methylene group showed up at δ 5.24 (1H, d, *J* = 12.0 Hz, 1H), δ 5.18 (1H, d, *J* = 12.0 Hz, 1H) and the methyl protons at 1.41 and 1.36 ppm. Subsequent acid catalysed ring opening of the epoxide was performed using catalytic amounts of (±)-camphor-10-sulfonic acid in dry toluene which proceeded smoothly to afford the allylic alcohols (*S*)-**29** [α]_D²² 61.8 (*c* 0.8 CH₂Cl₂); lit. [α]_D²⁰ – 71.7 (*c* 1.1 EtOH)⁴⁷

and (*R*)-**29** [α]_D²² – 66.4 (*c* 2.1 CH₂Cl₂), [FAB MS *m/z* 207 (*M*+H)⁺, 229 (*M*+Na)⁺]. For the allylic alcohol, the characteristic =CH₂ groups gave two multiplet peaks at 5.13 and 5.02 ppm, the H-2 and OH protons gave a singlet at 4.62 and 3.10 ppm respectively. The Sharpless asymmetric epoxidation method⁸⁷ was not employed here for the synthesis of the two components of each enantiomer since this kinetic resolution method only produces the (*2S*, *3S*) and (*2R*, *3R*) stereoisomers. Therefore the allylic alcohol (*S*)-**29** was epoxidised with mCPBA (**Scheme 2.2**), without stereochemical control to give a 33:67 mixture of the (*2S*, *3S*):(*2S*, *3R*) diastereomers by ¹H NMR spectroscopy taken on a 400 MHz machine (**Figure 2.4**) [FAB MS *m/z* 421 (*M*+H), 443 (*M*+Na⁺)]. The H-2 proton for the diastereoisomers was resolved to 0.03 Hz and appeared at 4.04 and 4.01 ppm. This could be due to the shielding or deshielding of one of the H-2 protons. Also in the mixture, the H-4 proton gives rise to three doublets at 2.97, 2.85 and 2.63 ppm with *J* = 4.8 Hz. The CH₂ of the benzyl group appears as a multiplet in the mixture but as a doublet of doublets in the pure isomers. The methyl and benzyl group appearing at 1.31 and 7.35 ppm are largely unaffected in the different stereoisomers.



Scheme 2.2 Epoxidation of allylic alcohols. Reagents and conditions: (i) mCPBA, C₂H₂, 0 °C – RT.

Column chromatography in 0-30 % ethyl acetate/hexane allowed separation of the diastereoisomers. The NMR of (*2S*, *3S*)-**30** showed the characteristic H-2 proton as a singlet at 4.01 ppm (**Figure 2.5**) identical to the literature value of (4.01 ppm), which corresponds to the (*2S*, *3S*) diastereomer and the H-4 proton gave two doublets at 2.85 ppm and 2.64 ppm with *J* = 4.8 Hz (lit. 2.83 ppm and 2.59 ppm, *J* = 4.8 Hz). For the corresponding diastereoisomer (*2S*, *3R*)-**30**, the H-2 singlet signal appeared at 4.05 ppm (**Figure 2.6**) whereas the H-4 proton gave two doublet signals at 2.99 ppm

and 2.63 ppm with $J = 4.8$ Hz. It appears that the H-4 signal at 2.63 ppm is common to both stereoisomers whereas the doublets at 2.85 ppm and 2.99 ppm are specific to the (2*S*, 3*S*) and (2*S*, 3*R*) diastereoisomers respectively.

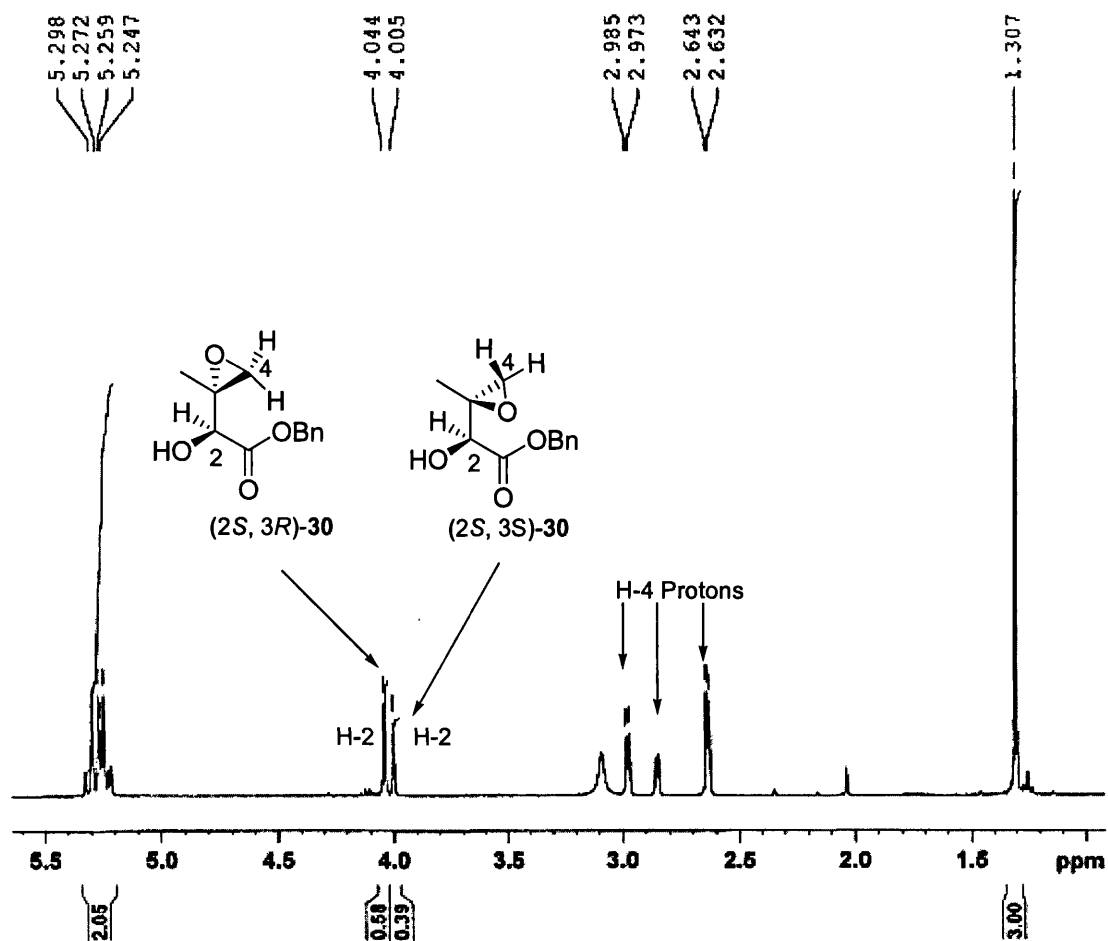


Figure 2.4 NMR data for the diastereomeric mixture showing the H-2 proton for the (2*S*, 3*S*) and (2*S*, 3*R*) diastereoisomers 4.005 and 4.044 ppm respectively. The CH₂ of the benzyl group appears as a multiplet at 5.30- 5.25 ppm

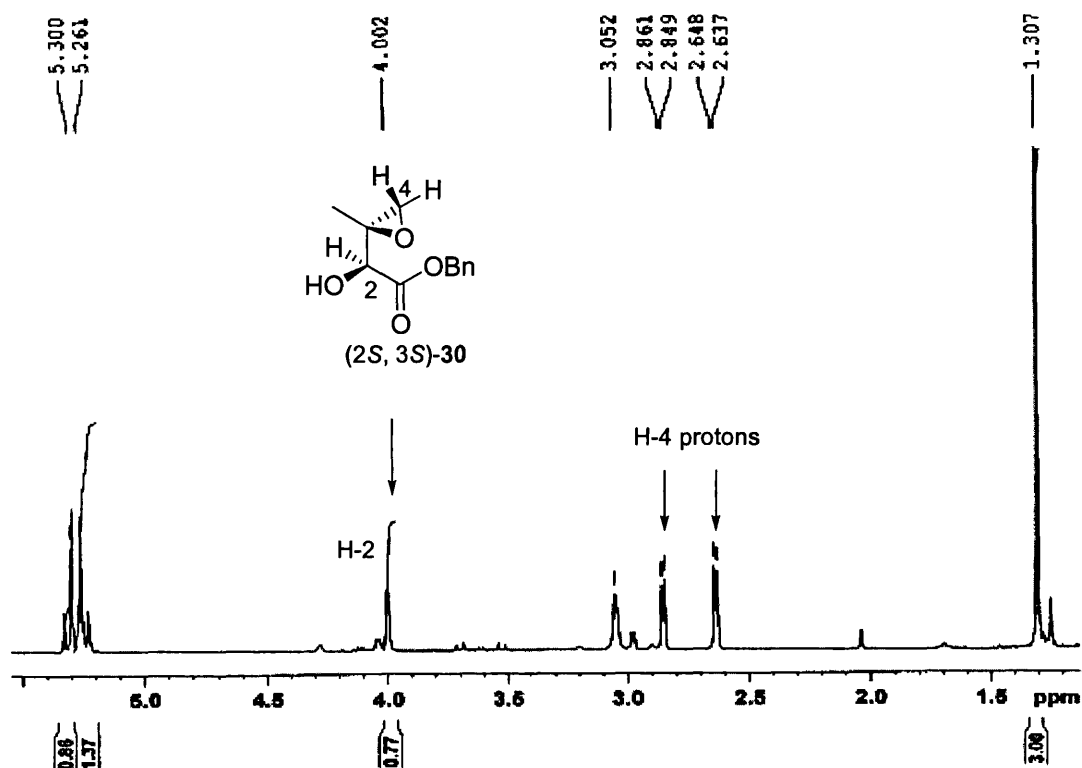


Figure 2.5 NMR data for (2*S*, 3*S*)-30 showing the H-2 proton at 4.00 and the two H-4 doublets at 2.64 and 2.85 ppm. There is a minor contamination with the (2*S*, 3*S*) isomer, which disappears in the purification steps before the final product.

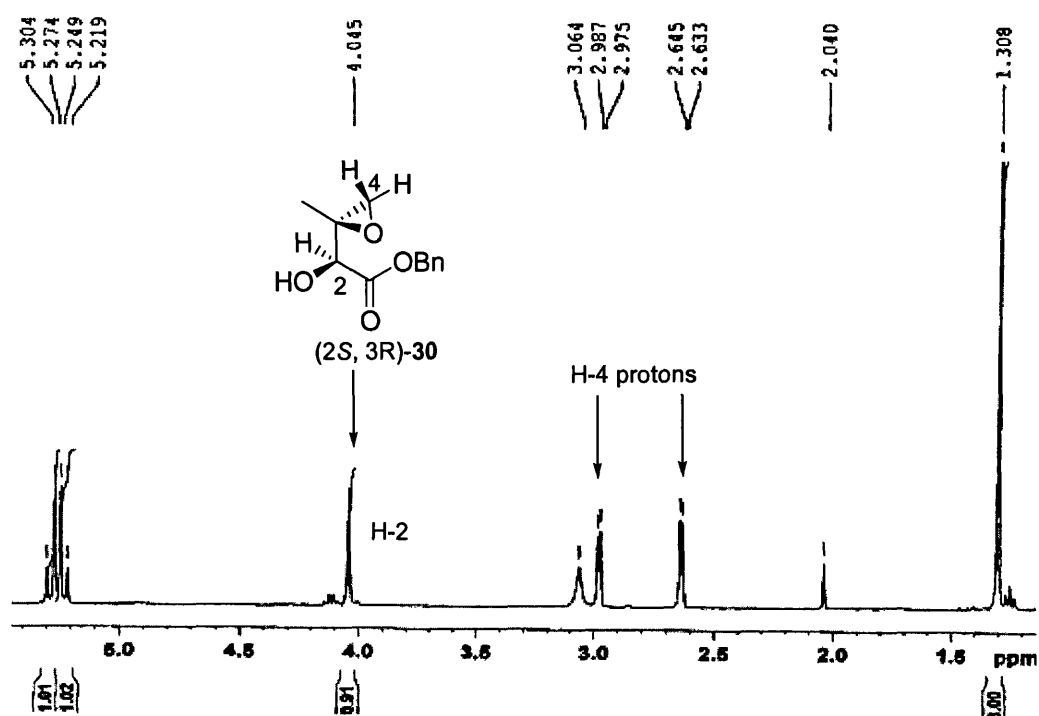
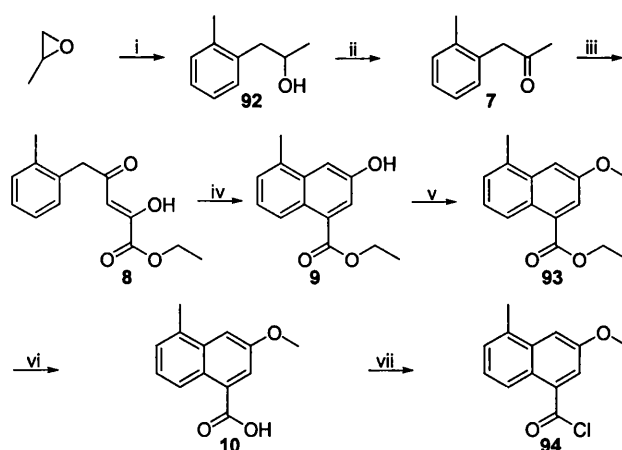


Figure 2.6 NMR data for (2*S*, 3*R*)-30 showing the H-2 proton at 4.05 and the two H-4 doublets at 2.63 Hz and 2.99 ppm.

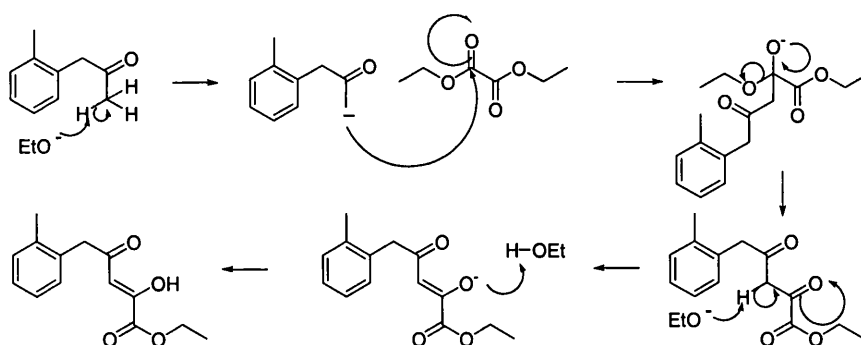
2.1.2 Synthesis of the chromophore, the natural product and its analogues

Shibuya *et al*'s (1983) reported synthesis of the naphthoic acid remains the sole entry into this system (**Scheme 2.3**).²⁹ The preparation of these naphthalene derivatives involves conversion of the Grignard reagent *o*-tolyl magnesium bromide into the secondary alcohol **92** by treatment with propylene oxide under a nitrogen atmosphere to give 1-(2-methylphenyl)propanol in 69 % yield [FAB MS m/z 151 (M+H), 173 (M+Na)⁺]. The unsymmetrical epoxide is attacked predominantly on the less substituted carbon atom but a small percentage of the product arising from attack on the sterically hindered carbon was also obtained giving a ratio of (–CH₂–):(–CHCH₃) alkylation as 1:20. The ketone 1-(2-methylphenyl)acetone **7** was synthesised by treating a solution of the secondary alcohol 1-(2-methylphenyl)propanol **92** with chromic acid⁸⁸ and the reaction followed by TLC.

Base-promoted condensation⁸⁹ was achieved by stirring the ketone **7** in 2 M NaOEt over 5 min after which diethyl oxalate was added and further stirred for 2 h. This gave the enol via the proposed mechanism in Scheme 2.4. The resulting derivative was cyclised to the ethyl-3-hydroxy-5-methyl-1-naphthoate **9** [FAB MS m/z 231 (M+H)⁺, 253 (M+Na)⁺]. Contrary to the report that the cyclisation of the keto allyl derivative **8** to the naphthol **9** will proceed using catalytic amounts of concentrated H₂SO₄ at –70 °C,²⁹ in our hands the reaction did not proceed under these conditions. Different conditions were investigated at this stage including variation of the ratio of enol to conc. H₂SO₄ from 1:1 to 1:10 and carrying out the reaction at 0 °C and –70 °C. (**Scheme 2.3**). After this investigation, it appeared that the optimal conditions for cyclisation involved 1:10 ratio of starting material to H₂SO₄ in CHCl₃ at 0 °C for 1 h. A longer reaction time resulted in acid catalysed hydrolysis of the ethyl ester **93**, which is undesirable at this stage of the synthesis.



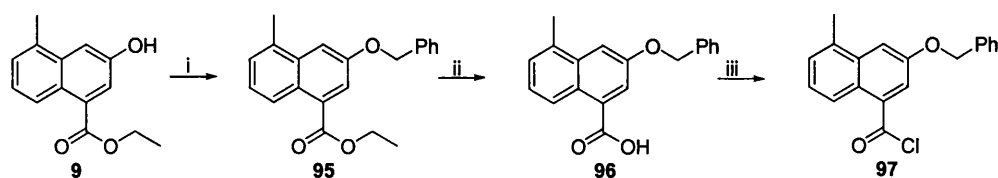
Scheme 2.3 Synthesis of naphthoic acid chloride chromophore. Reagents and conditions: (i) o-tolyl magnesium bromide, Et₂O, N₂ atm. 0 °C-RT, then NH₄Cl (aq) 69 %; (ii) Jones' reagent, Et₂O, 45 %; (iii) (CO₂Et)₂, NaOEt; (iv) conc. H₂SO₄, CHCl₃, 0 °C, 40 % from 7; (v) NaH, MeI, DMF, 90 %; (vi) LiOH in H₂O:MeOH:THF in a 1:2:3 ratio, 94 %; (vii) SOCl₂, reflux.



Scheme 2.4 Proposed mechanism of enol formation.

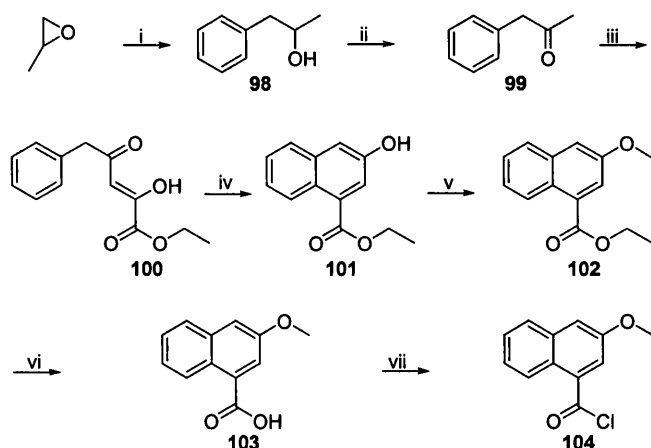
The ethyl 3-hydroxy-5-methyl-1-naphthoate **9** was then added with stirring to NaH in dry DMF and stirred for 30 min after which iodomethane was added. After stirring for a further 30 min the reaction was quenched with H₂O and the mixture extracted with EtOAc to provide ethyl 3-methoxy-5-methyl-1-naphthoate **93** in 90 % yield [FAB MS *m/z* 245 (M+H), 267 (M+Na⁺)]. Ester hydrolysis of **93** employing LiOH in H₂O/MeOH/THF in a ratio 1:2:3 produced carboxylic acid **10** in 94 % yield [FAB MS *m/z* 217 (M+H)⁺, 239 (M+Na)⁺]. Due to the instability of the acid chloride, this intermediate was freshly prepared prior to any coupling by refluxing in excess thionyl chloride for 2 h after which the reaction mixture was concentrated in vacuo to remove the excess reagent and provide the acid chloride **94**.

The chromophore in which the methoxy group was replaced by benzyl ether functionality in order to investigate the effect of increase in bulk at this position was synthesised from the naphthol **9** (Scheme 2.5). Here the naphthol was stirred together with sodium hydride in dry DMF and benzyl bromide added. After quenching the reaction mixture with H₂O, the product was extracted, purified and exposed to base-catalysed ester hydrolysis conditions to give the acid **96**. This was then refluxed in SOCl₂ to obtain the corresponding acid chloride **97**, which was used without further purification.



Scheme 2.5 (i) NaH, MeI, DMF, 88 %; (ii) LiOH, H₂O, MeOH, THF in a 1:2:3 ratio, 90 %; (iii) SOCl₂, reflux.

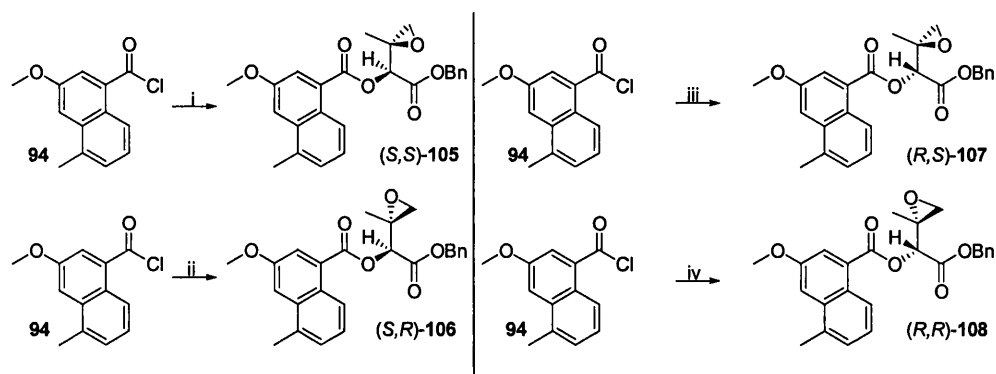
To synthesise the chromophore devoid of the methyl group, phenylmagnesium bromide was employed (Scheme 2.6). Propylene oxide was treated with the Grignard reagent to obtain phenylpropanol **98**, which was then oxidised to phenyl acetone in the presence of Jones' reagent. Condensation of the ketone with diethyl oxalate was effected in a 2 M solution of NaOEt to give the α,β -unsaturated ethyl ester **100** and the crude product treated with excess (1:10) concentrated H₂SO₄ in CHCl₃ at 0 °C for 1 hr to give the naphthol lacking the methyl group.



Scheme 2.6 *Synthesis of naphthoic acid chloride chromophore. Reagents and conditions:* (i) phenylmagnesium bromide, Et₂O, N₂ atm. 0 °C-RT, then NH₄Cl (aq) 71 %; (ii) Jones' reagent, Et₂O, 45 %; (iii) (CO₂Et)₂, NaOEt; (iv) conc. H₂SO₄, CHCl₃, 0 °C, 35 % from **99**; (v) NaH, MeI, DMF, 90 %; (vi) LiOH, H₂O, MeOH, THF in a 1:2:3 ratio, 90 %; (vii) SOCl₂, reflux.

Methylation of the OH group and subsequent hydrolysis of the ethyl ester gave the naphthoic acid **103**, which is then converted into the acid chloride intermediate **104**.

Epoxy alcohol (2*S*, 3*S*)-**30**, Et₃N and catalytic DMAP were stirred in dry dichloromethane for 20 min and the freshly prepared acid chloride in dry dichloromethane was added dropwise and the mixture stirred for 4 h to give (2*S*, 3*S*)-benzyl 3,4-epoxy-2-(3-methoxy-5-methyl-1-naphthoyloxy)-3-methylbutanoate (2*S*, 3*S*)-**105** in 86 % yield [FAB MS *m/z* 421 (*M*+*H*), 443 (*M*+Na⁺)]. The epoxy alcohols (2*S*, 3*R*)-**30**, (2*R*, 3*R*)-**30** and (2*R*, 3*S*)-**30** were used to synthesise their corresponding ester as depicted in Scheme 2.7.



Scheme 2.7 Synthesis of epoxy amide. Reagents and conditions: (i) (2*S*, 3*S*)-**30**, Et₃N, cat. DMAP, CH₂Cl₂, 0 °C, 79 %; (ii) (2*S*, 3*R*)-**30**, Et₃N, cat. DMAP, CH₂Cl₂, 0 °C; (iii) (2*R*, 3*S*)-**30**, Et₃N, cat. DMAP, CH₂Cl₂, 0 °C; (iv) (2*R*, 3*R*)-**30**, Et₃N, cat. DMAP, CH₂Cl₂, 0 °C;

The proton NMR for (2*S*, 3*S*)-**105** showed H-2 at 5.25 ppm and the two doublets for H-4 at 2.99 ppm and 2.69 ppm (**Figure 2.7**) and again corresponding to the literature value of the (2*S*, 3*S*) ester which registers the H-2 proton at 5.24 ppm and H-4 at 2.98 and 2.69 ppm.⁴⁷ Other signals include the two hydrogen atoms of the (CO₂CH₂Ph) group which appear as a doublet of doublets at 5.33 and 5.25 ppm *J* = 12.4 Hz (lit. 5.33, 5.25 ppm *J* = 12.3 Hz).⁴⁷ For the corresponding diastereoisomer (2*S*, 3*R*)-**106**, the H-2 proton is found at 5.07 ppm whereas the H-4 doublets occur at 3.08 and 2.78 ppm (**Figure 2.8**). In this isomer, the (CO₂CH₂Ph) signal is found slightly upfield to the (2*S*, 3*S*) isomer at 5.30 and 5.23 ppm *J* = 12.0 Hz. The methyl and aromatic protons are largely unaffected by the change in stereochemistry and therefore have identical chemical shifts in both isomers.

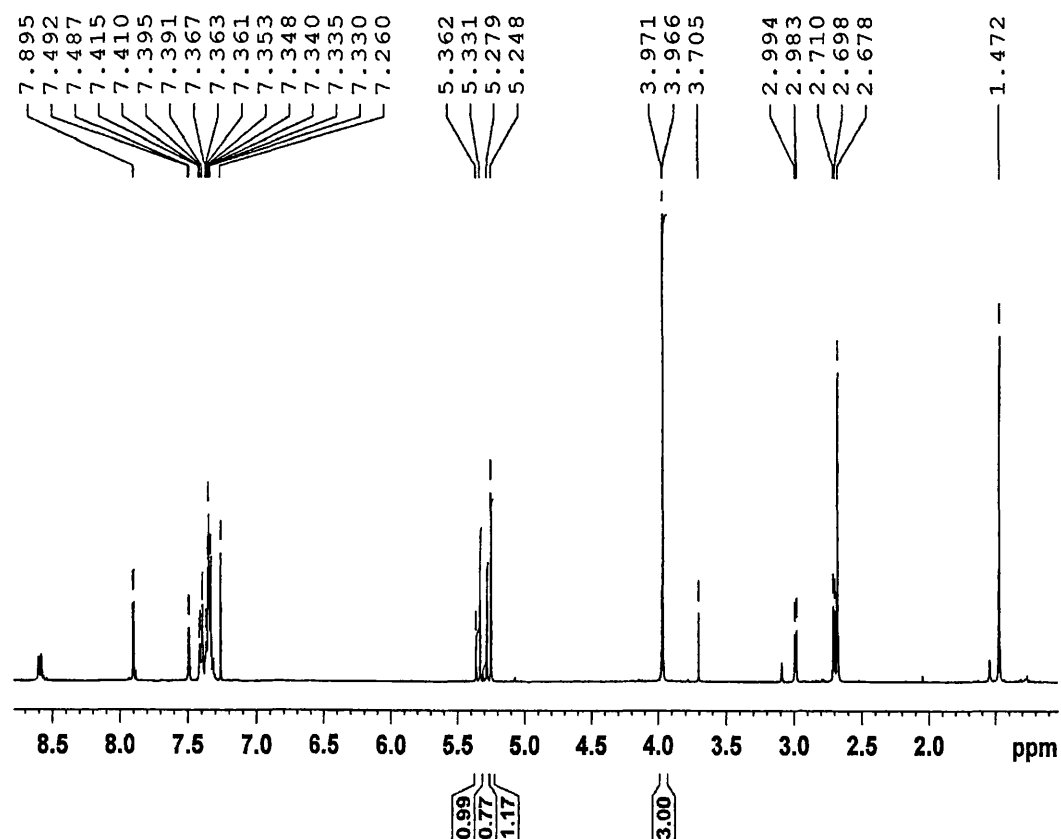
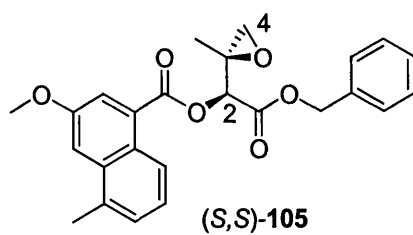


Figure 2.7 NMR data on (2*S*, 3*S*)-105 showing the H-2 and H-4 protons at 5.25, 2.98 and 2.70 ppm respectively



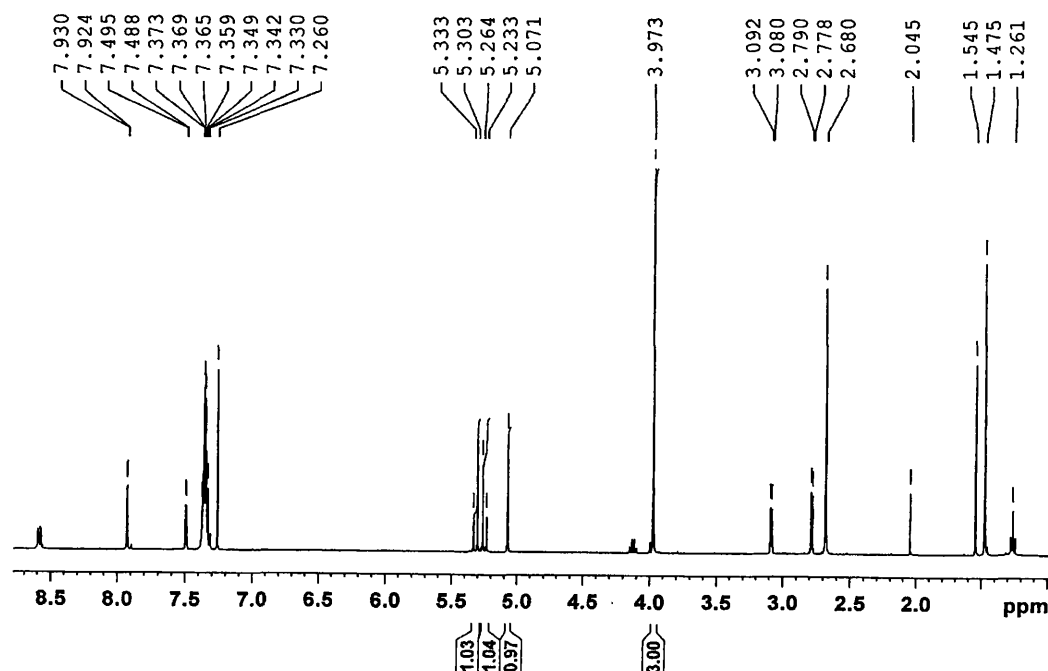
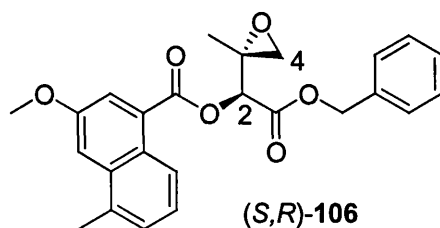
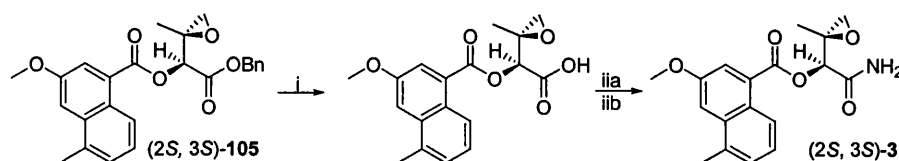


Figure 2.8 NMR data on (2*S*, 3*R*)-106 showing the H-2 and H-4 protons 5.07, 3.08 and 2.78 ppm respectively



Hydrogenation of the benzyl esters to their carboxylic acid intermediates was achieved by stirring the esters with Pd-C in dry methanol under hydrogen atmosphere. The reaction suspension was then filtered through a pad of celite and the resulting solution concentrated in vacuo and used directly in the coupling reaction. Formation of the terminal amide was performed by re-dissolving the freshly made acid in dry DMF, cooling to 0 °C and successively adding 35 % aqueous ammonia, Et₃N, HOBt and PyBOP after which the reaction mixture was warmed to room temperature and stirred for 18 h to afford the 3,4-epoxybutanamides (2*S*, 3*S*)-3, (2*S*, 3*R*)-3, (2*R*, 3*S*)-3, and (2*R*, 3*R*)-3 [FAB MS *m/z* 217 (M+H)⁺, 239 (M+Na)⁺], the yields were between 41-46 %. Due to the low yield of the coupling reaction,

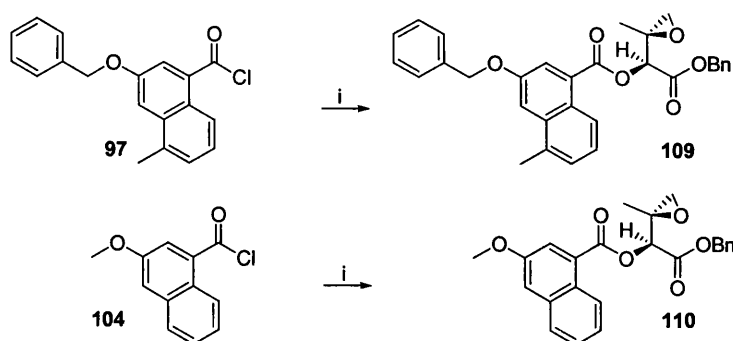
Coleman's route to the synthesis of the amide (2*S*, 3*S*)-**3** using ethyl chloroformate and Et₃N to form the mixed anhydride in THF which was then treated with 35 % ammonia to form the amide was investigated, but proved to be less successful than the PyBOP/HOBt route. Although the epoxide functionality is chemically robust, the low yield could be due to the epoxide ring opening reaction progressing in parallel to the amide formation reaction. The characteristic H-2 proton occurred as a singlet at 5.22 ppm and the two doublets for the H-4 oxiranyl protons at 3.03 and 2.80 ppm for the (2*S*, 3*S*)-**3** isomer whereas the H-2 and two H-4 protons occurred at 5.32, 3.14 and 2.84 ppm respectively for the corresponding (2*S*, 3*R*)-**3** diastereoisomer. In this molecule, the methyl, primary amine and aromatic protons were unaffected by change in stereochemistry. The optical rotations for (2*S*, 3*S*)-**3** and (2*S*, 3*R*)-**3** were $[\alpha]_D^{26}$ 41.2 (*c* 0.3 CH₂Cl₂); lit. $[\alpha]_D^{20}$ 54.3 (*c* 0.4 EtOH)⁴⁷ and $[\alpha]_D^{26}$ 30.1 (*c* 0.3 CH₂Cl₂) respectively.



Scheme 2.8 Synthesis of (2*S*, 3*S*)-3,4-epoxy-2-(3-methoxy-5-methyl-1-naphthoyloxy)-3-methylbutanamide (i) Pd-C, H₂, MeOH; (iia) 35 % NH₄, HOBT, Et₃N, PyBOP, DMF, 0 °C-RT, 46 %; (iib) Et₃N, C₃H₅ClO₂, 35 % NH₃

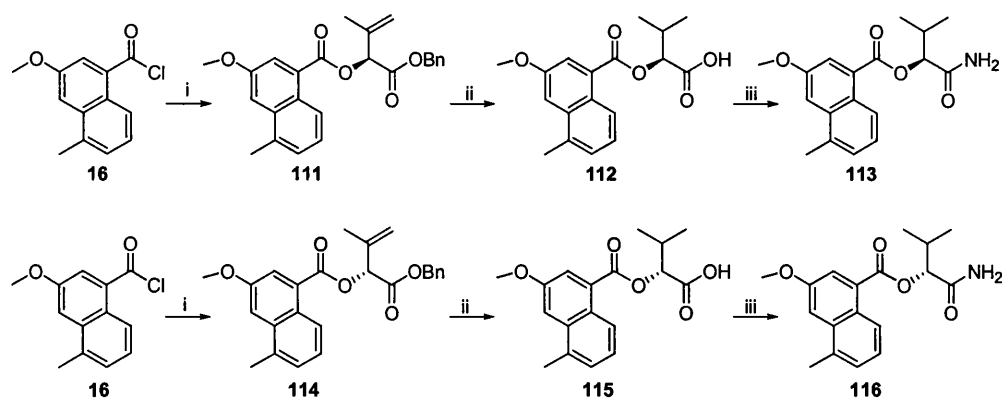
The epoxy amides were also successfully synthesised by coupling (*S*)- or (*R*)-diastereomeric epoxy alcohols to the acid chloride chromophore and progressing with the diastereomeric mixture until the final epoxy amide product after which the diastereoisomers were successfully separated by column chromatography, the ¹H NMR and mass spectra of these compounds were identical to the ones synthesised through the stereoselective route.

The benzyl ester analogues of the azinomycin metabolite containing modifications on the chromophore were synthesised following the route used for the synthesis of the stereoisomers (Scheme 2.9).

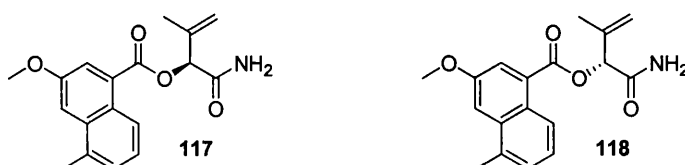


Scheme 2.9 Synthesis of ester analogues. Reagents and conditions: (i) (2*S*, 3*S*)-**30**, Et₃N, cat. DMAP, CH₂Cl₂, 0 °C, 79 %;

To investigate the contribution of the alkylating functionality to the overall activity of these azinomycins, compounds **113** and **116** devoid of the epoxide were prepared from **16** by coupling the allyl alcohols (*S*)- and (*R*)-**29**, to the acid chloride chromophore. Hydrogenation of **111** simultaneously reduced the double bond and the benzyl group to give the alkane carboxylic acid **112**, which was then treated with Et₃N, HOBT/PyBoP in the presence of ammonia to afford the amide **113**. Other non-alkylating analogues (**117** and **118**) in which the alkene is preserved by selective deprotection of the benzyl group were also prepared. (Scheme 4.5 and 4.6, chapter 4).



Scheme 2.10 Reagents and conditions: (i) (*S*) or (*R*)-**29**, Et₃N, DMAP, CH₂Cl₂; (ii) 10 % Pd/C, MeOH; (iii) 35 % NH₄OH, Et₃N, HOBT, PyBOP, DMF



Compound **117**, which is a novel functional analogue of the azinomycins and developed as a prodrug alternative to the active azinomycins and the azinomycin analogues based on **3** (see chapter 4), is anticipated to have a significant difference in its mechanism of interaction with DNA. Although **117** is not predicted to bind covalently to DNA, the planar naphthoate chromophore could bind to DNA through intercalation. The binding mode of the naphthoate chromophore is likely to be significant in elucidating the mechanism of antitumour action of these compounds and has implications for the development of other azinomycin-based drug candidates. This is because analogues without the naphthoate chromophore have a marked reduction in antitumour activity. There is some debate as to the contribution of DNA intercalation to the binding of the azinomycin to DNA. While one group⁷² has suggested DNA intercalation of the naphthoate through investigations of viscometric and unwinding effects, Coleman et al used non-covalently binding analogues of (2*S*, 3*S*)-**3** and, with similar assays, found that intercalation did not occur. They also used fluorescent resonance energy transfer with (2*S*, 3*S*)-**3** to support the lack of intercalation of the chromophore. Significantly Coleman et al did not use (2*S*, 3*S*)-**3** in their unwinding assay but extrapolated the fluorescent resonance energy transfer experiment to include this. The naphthalene chromophore of neocarzinostatin, an enediyne antitumour antibiotic, is structurally similar to that of the azinomycins. Neocarzinostatin naphthoate has been shown to associate intercalatively with duplex DNA.⁹⁰ In view of these conflicting accounts of the role of the naphthoate in the mechanism of action of the azinomycins and its congeners we sought to investigate the mode of association of the novel alkenylamide **117** with duplex DNA.

2.2 DNA Intercalation Studies Using The Unwinding Assay.

2.2.1 DNA Intercalation

Compounds that bind intercalatively to DNA are characterised by a planar aromatic chromophore. A large number of antibacterial and antitumour drugs exert their biological effect through an intercalation mechanism. The intercalation hypothesis was first described in the work of Lerman⁹¹, who observed that a 3,6 disubstituted acridine (proflavin) intercalated into DNA by a process in which the planar

chromophore of the drug was inserted between adjacent base pairs in the DNA double helix (**Figure 2.9**).⁹¹ The driving force for intercalation was proposed to originate from one or more of several interactions ranging from electrostatic, entropic, hydrogen bonding to Van der Waals and hydrophobic interactions between the planar chromophore and the base pairs surrounding it.⁹² Generally these interactions vary depending on the chemical and physical nature of the intercalators.

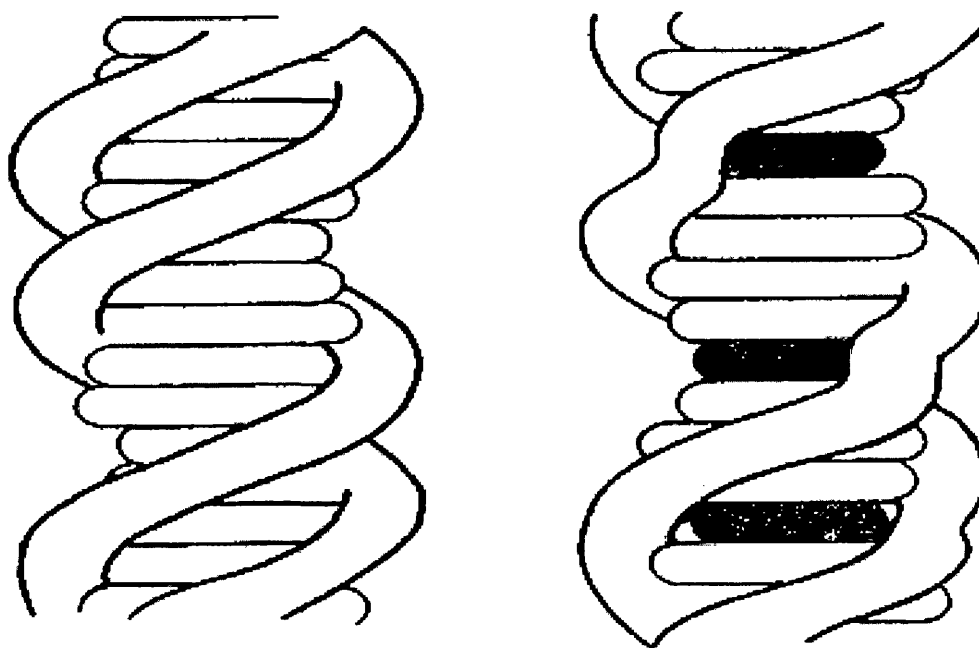


Figure 2.9 Cartoon depicting the secondary structure of B DNA (left) and DNA containing intercalated proflavin molecules (right)⁹¹

Intercalative binding of drugs to DNA involves drug-induced local uncoiling of the double helix to provide the space needed for the drug molecule to be inserted.^{91,93} Such uncoiling results in removal and reversal of the supercoils of closed circular DNA an event which changes the sedimentation coefficient, viscosity and electrophoretic mobility of the supercoiled DNA. The complex formation is freely reversible. Waring and co-workers⁹³ confirmed the intercalation hypothesis first proposed by Lerman for proflavin and have extended and developed the model further to include ethidium, daunomycin and nogalamycin.

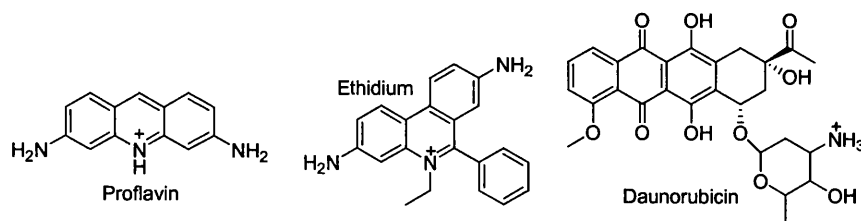


Figure 2.10 The structures of some representative intercalating molecules

Intercalation studies are usually done by using either linear or closed circular DNA. Intercalating agents of several kinds can be studied by using techniques that can monitor the hydrodynamic properties that are altered in DNA upon intercalation. The ligands can range from simple agents such as proflavin and ethidium to more complex agents like the anthracyclines, e.g., doxorubicin, nogalamycin and the quinoline bisintercalators like echinomycin and ditercalinium. Together with the changes in DNA properties, several changes in the physicochemical properties of the intercalators are also observed on binding to DNA.⁹⁴ For fluorescent intercalators, changes can also occur in its fluorescence spectrum. In the case of ethidium and propidium, the intensity of emission of fluorescence is enhanced.⁹⁵ However in the case of anthracyclines such as doxorubicin and daunomycin, fluorescence intensity is quenched.⁹⁵ For some acridines, like quinacrine, the fluorescence emission may be quenched or enhanced depending on basic composition and DNA sequence. The intercalators can also induce changes in the absorption and circular dichroic spectral properties of DNA.⁹⁶

2.2.2 DNA Unwinding Assay

High resolution structural studies using either X-ray diffraction or NMR are the most convincing methods of establishing the mode of binding of compounds to DNA. Should such high resolution data not be available, the binding mode can be inferred from the results of biophysical studies. Upon intercalation the planar chromophore is in close contact with the DNA base pairs, and can be positioned perpendicular or parallel to the DNA helix axis. Viscometric and fluorescence resonance energy transfer techniques are among the definitive solution assays for detecting

intercalation.⁹⁷ The fluorescence contact energy transfer experiment measures fluorescence resonance energy transfer that occurs between an acceptor and donor pair when there is spectral overlap between donor and acceptor, and when their mutual distances and dipole orientation are right. Le PecQ et al have demonstrated that intercalators fulfil this criteria.⁹⁸ Viscosity, which is proportional to L^3 for rod-like DNA of length L , can be used to measure the length changes that occur during intercalation.⁹¹

The DNA unwinding assay, whilst not a definitive assay, has been used extensively to show DNA binding by intercalation for a number of bisintercalators. ϕ F174 or a suitable circular supercoiled plasmid DNA is incubated with different drug : DNA ratios and the product electrophoresed on a neutral agarose gel at 50 V for three hours. The gel is then stained with ethidium bromide and viewed with a uv trans-illuminator. Isolated DNA exists mainly in the supercoiled state with a small fraction in the relaxed state. Upon interaction of the drug with DNA via intercalation, unwinding of the duplex occurs and this gives rise to an increase in length of the DNA fragments.⁹⁹ This unwinding and subsequent increase in length, in turn, causes a characteristic decrease in electrophoretic mobility in agarose gel. The electrophoretic mobility decreases until it reaches the equivalence point when the coiling in DNA is completely removed and the DNA duplex assumes the shape of a relaxed circular form. As more ligand intercalates, the DNA circle becomes strained in the opposite direction and causes left-handed coiling. These changes are currently accepted as evidence for the intercalative mode of binding to DNA.⁹⁵

2.2.3 Unwinding Assay Results and Discussion

Echinomycin is a well characterised DNA bis-intercalator¹⁰⁰ and was chosen as a positive control in the DNA unwinding assay employed. The experiment was performed according to the procedure outlined in the biology experimental section and figure 6 shows the unwinding gels for echinomycin. Lane 1 in gel **a** and **b** (Figure 2.11) is ϕ F174 supercoiled DNA alone with no added drug and lanes 2 to 8 show supercoiled DNA with increasing concentrations of drug.

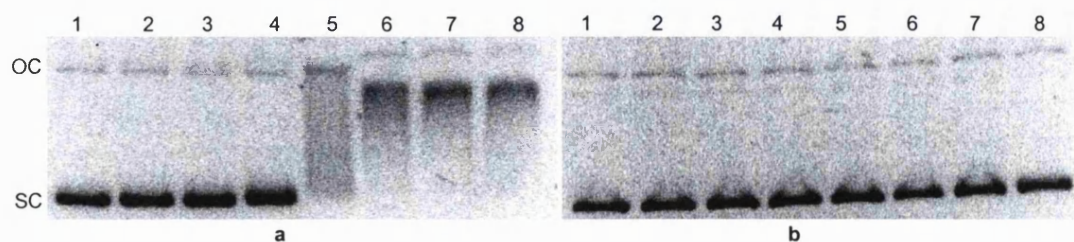


Figure 2.11 Effect of echinomycin on the electrophoretic mobility of $\phi F174$ plasmid DNA. Lane 1 DNA only, lanes 2-8 10^{-3} , 10^{-2} , 10^{-1} , 1.0, 10, 20, 30 drug/bp ratio. DNA ($3.84 \mu\text{M}$). Gel **a** was electrophoresed in the absence of ethidium bromide whereas gel **b** was electrophoresed in the presence of ethidium bromide. SC = Supercoiled DNA, OC = Open Circular DNA.

At a drug/bp ratio of 0.1 (Figure 2.11a, lane 5) there is complete loss of supercoiling with evidence of unwinding. A further increase in concentration of drug to 1.0 drug/bp ratio and above is manifest by an increase in DNA mobility consistent with formation of negative supercoiling (Figure 2.11a, lanes 6-8). Figure 2.11b shows that in the presence of ethidium bromide the echinomycin has no effect on the mobility of supercoiled DNA. This further supports our interpretation that echinomycin does unwind DNA by intercalation. The presence of ethidium, a well characterised DNA intercalator displaces the echinomycin thereby preventing unwinding. This inhibition of intercalation of one intercalator by a stronger intercalator is suggestive of intercalative binding in an unwinding assay, as another intercalator cannot reverse DNA relaxation and unwinding if this interaction has been caused through a different mechanism such as DNA nicking. The DNA binding properties of **117** and the closely related analogue **113** were subsequently investigated (Figures 2.12 and 2.13). These results show that **117** and **113** do not relax supercoiled DNA even at very high concentrations (drug/bp ratios of 30.0) and therefore did appear not to associate with DNA through intercalative binding.

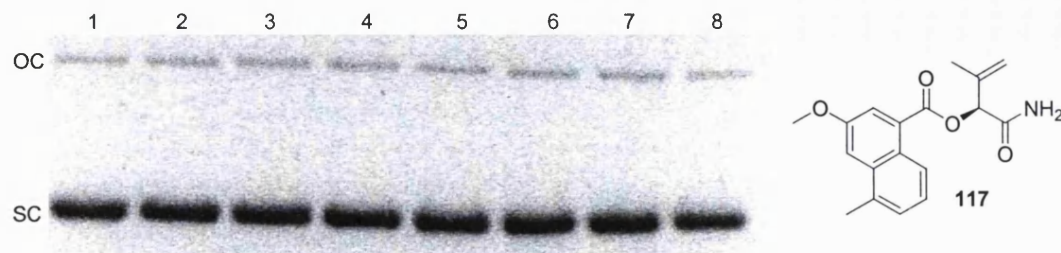


Figure 2.12 Effect of compound **117** on the electrophoretic mobility of ϕ F174 plasmid DNA. Lane 1 DNA only, lanes 2-8 10^{-3} , 10^{-2} , 10^{-1} , 1, 10, 20, 30 drug/bp ratio. DNA ($3.84 \mu\text{M}$). SC = Supercoiled DNA, OC = Open Circular DNA.

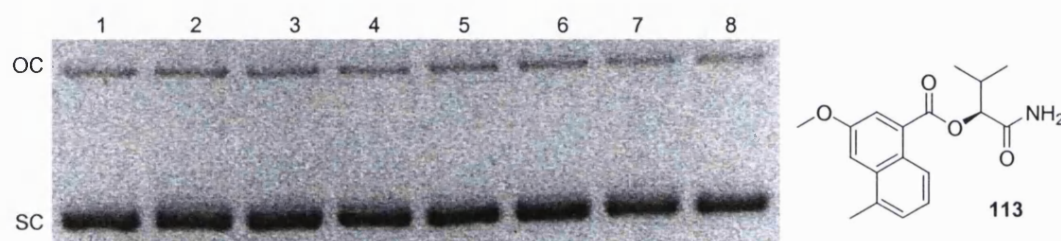


Figure 2.13 Effect of **113** on the electrophoretic mobility of ϕ F174 plasmid DNA. Lane 1 DNA only, lanes 2-8 10^{-3} , 10^{-2} , 10^{-1} , 1, 10, 20, 30 drug/bp ratio. DNA ($3.84 \mu\text{M}$). SC = Supercoiled DNA, OC = Open Circular DNA.

The analogues **113** and **117**, which were synthesised from the allyl alcohol, lack the electrophilic epoxide moiety and did not show any cytotoxic activity in osteosarcoma cell lines. When the synthetic and biologically active natural isomer (2*S*, 3*S*)-**3** was used in the unwinding assay it was revealed that this DNA alkylator does unwind and relax supercoiled ϕ F174 plasmid DNA (**Figure 2.14**), with unwinding starting at a drug/bp ratio of 0.01 (lane 3) and total relaxation occurring at a drug/bp ratio of 0.1 (lane 4). At concentrations of (2*S*, 3*S*)-**3** above 1 mol ratio the relaxed DNA appears to continue to undergo negative supercoiling (**Figure 2.14**).

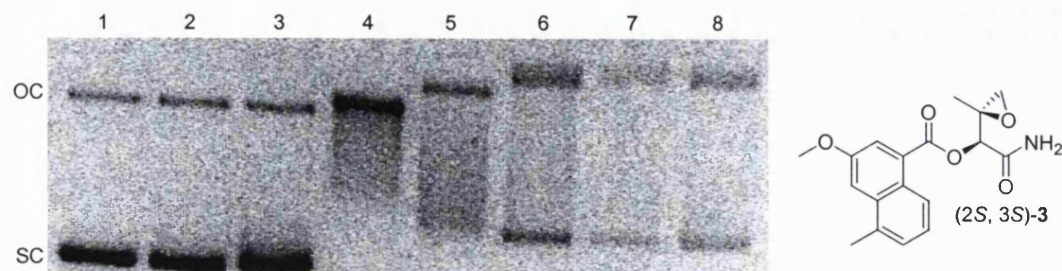


Figure 2.14 Effect of (2S, 3S)-3 on the electrophoretic mobility of ϕ F174 plasmid DNA. Lane 1 DNA only, lanes 2-8 10^{-3} , 10^{-2} , 10^{-1} , 10^0 , 10, 20, 30 drug/bp ratio. DNA ($3.84 \mu\text{M}$). SC = Supercoiled DNA, OC = Open Circular DNA.

These results are consistent with that shown previously.⁷² Since these compounds alkylate duplex DNA, one further possibility is that DNA strand breakage rather than intercalation is the mechanism for the relaxation of the supercoiled DNA. Melphalan and other clinically important antitumour agents are able to convert supercoiled DNA to open circular (single strand cleavage) and linear (double strand cleavage) forms. In the present study DNA relaxation is induced by melphalan (**Figure 2.15a**). However in the presence of EtBr* (ethidium bromide), relaxation of DNA is not inhibited because melphalan induces relaxation through DNA cleavage. With a nicked DNA duplex, the reaction is irreversible as nicking occurs prior to the electrophoresis and this nicking (bond cleavage) cannot be reformed under the conditions of the experiment. Figure 2.15 shows the effect of melphalan on the electrophoretic mobility of plasmid DNA. Gel **a** in figure 2.15 was electrophoresed in the absence of EtBr whereas gel **b** in figure 2.15 was electrophoresed in the presence of EtBr. Unlike the echinomycin unwinding gel in figure 2.11b, figure 2.15b shows that EtBr does not inhibit DNA relaxation due to DNA strand cleavage by melphalan.

* EtBr is abbreviation for ethidium bromide

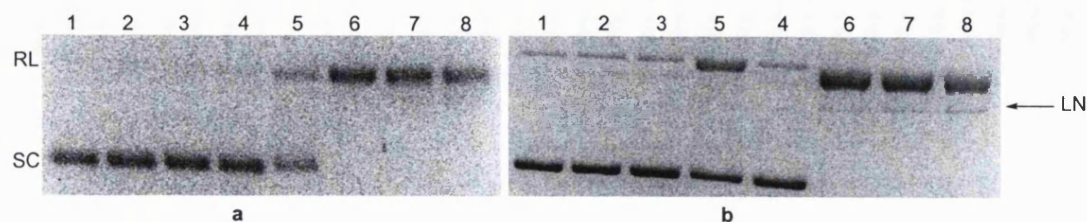


Figure 2.15 Effect of melphalan on the electrophoretic mobility of $\phi F174$ plasmid DNA. Lane 1 DNA only, lanes 2-8 10^{-3} , 10^{-2} , 10^{-1} , 1, 10, 20, 30 drug/bp ratio. DNA ($3.84 \mu\text{M}$). Gel **a** was electrophoresed in the absence of ethidium bromide whereas gel **b** was electrophoresed in the presence of ethidium bromide. SC = Supercoiled DNA, OC = Open Circular DNA. lanes 4 and 5 were interchanged in the loading process.

A similar study using (2*S*, 3*S*)-**3** shows that the electrophoretic mobility of supercoiled DNA duplex is not affected when electrophoresis was performed in the presence of EtBr (**Figure 2.16b**).

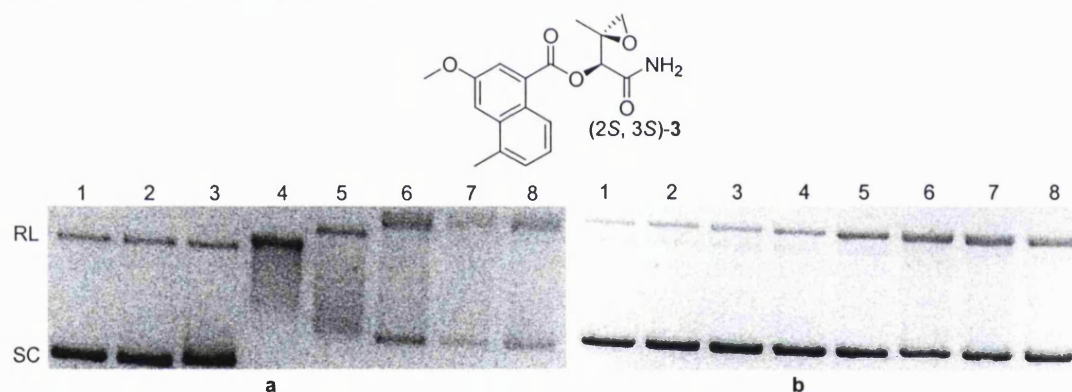


Figure 2.16 Effect of (2*S*, 3*S*)-**3** on the electrophoretic mobility of $\phi F174$ plasmid DNA. Lane 1 DNA only, lanes 2-8 10^{-3} , 10^{-2} , 10^{-1} , 1, 10, 20, 30 drug/bp ratio. DNA ($3.84 \mu\text{M}$). Gel **a** was electrophoresed in the absence of ethidium bromide (same as **Figure 2.14**) whereas gel **b** was electrophoresed in the presence of ethidium bromide. SC = Supercoiled DNA, OC = Open Circular DNA.

This inhibition of unwinding/relaxation of supercoiled DNA suggests that the unwinding process does not involve DNA cleavage and further strengthens the evidence that this compound binds to DNA intercalatively.

The effect of stereochemistry on DNA unwinding was studied by comparison of (2*S*, 3*S*)-**3** with (2*R*, 3*R*)-**3** and (2*S*, 3*R*)-**3**. In figure 2.17 gel **a**, the assay result show that the unnatural enantiomer, (2*R*, 3*R*)-**3**, unwinds DNA at a similar concentration as the natural isomer (2*S*, 3*S*)-**3** suggesting that the changes in

stereochemistry at both the 2 and 3 positions to give the enantiomer of (2*S*, 3*S*)-**3** do not affect the association of these compounds with DNA.

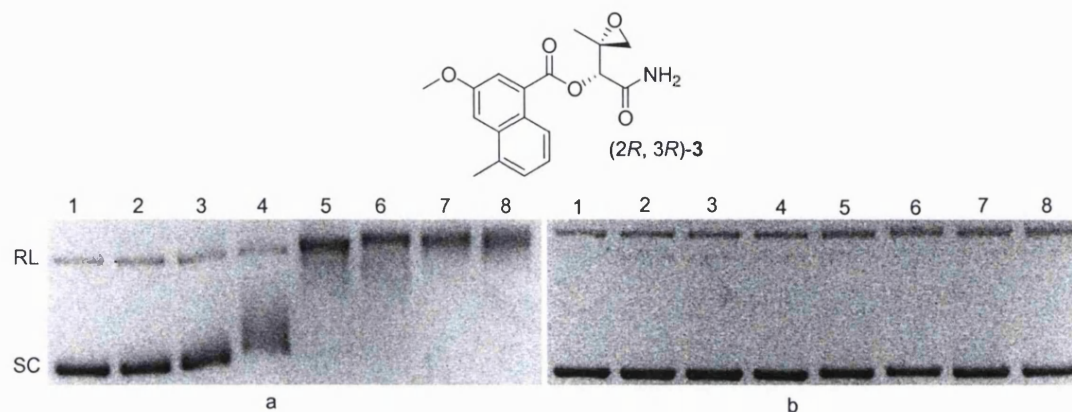


Figure 2.17 Effect of (2R, 3R)-3 on the electrophoretic mobility of ϕ F174 plasmid DNA. Lane 1 DNA only, lanes 2-8 10^{-3} , 10^{-2} , 10^{-1} , 1, 10, 20, 30 drug/bp ratio. DNA (3.84 μ M). Gel **a** was post-stained with ethidium bromide whereas gel **b** was electrophoresed in the presence of ethidium bromide. SC = Supercoiled DNA, OC = Open Circular DNA.

The inhibition of unwinding in the presence of EtBr indicates that the binding of (2*R*, 3*R*)-**3** is reversible (**Figures** 2.16b, 2.17b). Both isomers of azinomycins initiate unwinding at a drug base pair ratio of 0.01 and at 0.1 complete unwinding is achieved. The (2*S*, 3*R*) diastereoisomer (2*S*, 3*R*)-**3** unlike (2*S*, 3*S*)-**3** and (2*R*, 3*R*)-**3** enantiomers has a weaker affinity for DNA with unwinding observed at a drug/bp of 0.1 and complete unwinding only being attained at a drug/bp of 1 (**Figure** 2.18). This represents a ten-fold decrease in DNA affinity due to a change in stereochemistry from *S* to *R* at carbon atom 3.

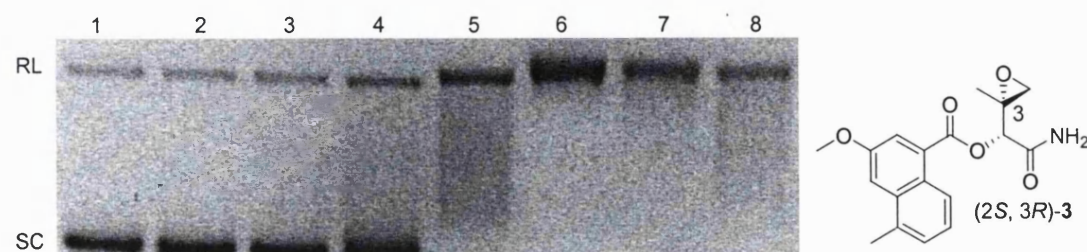


Figure 2.18 Effect of compound (2*S*, 3*R*)-**3** on the electrophoretic mobility of ϕ F174 plasmid DNA. Lane 1 DNA only, lanes 2-8 10^{-3} , 10^{-2} , 10^{-1} , 1, 10.0, 20, 30 drug/bp ratio. DNA (3.84 μ M). SC = Supercoiled DNA, OC = Open Circular DNA.

Compound (2*S*, 3*S*)-**105** the benzyl ester containing the epoxide moiety, was also subjected to the same conditions for the DNA unwinding assay, as were the compounds **109** and **110**, containing changes to the chromophore. None of these compounds displayed any DNA unwinding ability (Figures 2.19a, 2.19b). This is not entirely surprising, as other works have shown that the benzyl ester is inactive as an antitumour agent.⁷⁴ Presumably the amide function is important in making an interaction with the target DNA and this is inhibited by the presence of the bulky benzyl ester.

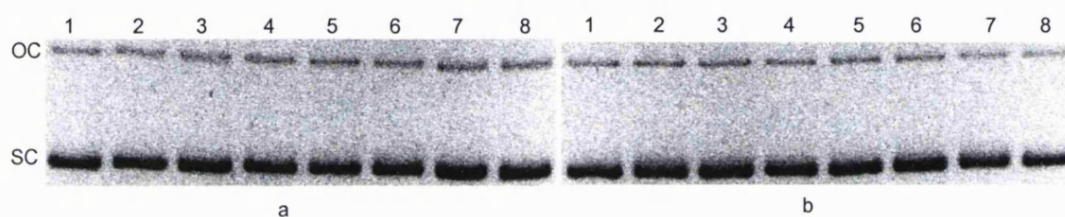


Figure 2.19 Effect of compounds (2*S*, 3*S*)-**105** and **109** on the electrophoretic mobility of ϕ F174 plasmid DNA. Lane 1 DNA only, lanes 2-8 10^{-3} , 10^{-2} , 10.0, 1, 10.0, 20, 30 drug/bp ratio. DNA (3.84 μ M). SC = Supercoiled DNA, OC = Open Circular DNA.

When (2*S*, 3*S*)-**3** was modelled with DNA using the software program ‘NAMOT – Nucleic Acid Modelling Tool’ it was revealed that the model attains lowest energy when the naphthoate chromophore binds intercalatively (**Figure 2.20**) instead of when left unassociated on the periphery of the duplex.

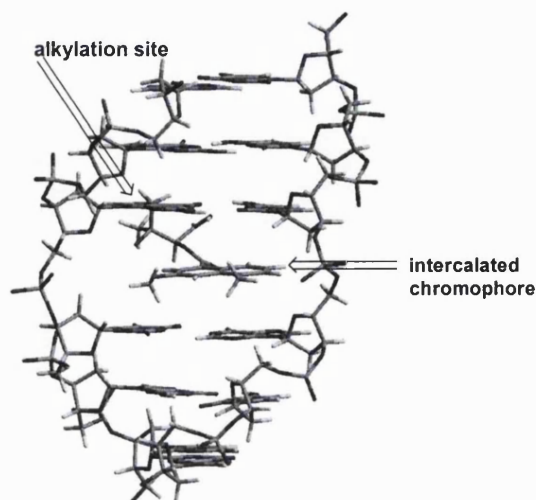


Figure 2.20 Computer model of **3** bound and intercalated into DNA

2.2.4 Discussions

This study shows that the stereochemistry of the compounds is a vital component of the interaction with DNA, with the (2*S*, 3*S*) and (2*R*, 3*R*) being the most favoured structures for DNA recognition as seen in the unwinding profiles for (2*S*, 3*S*)-**3**, (2*S*, 3*R*)-**3**, and (2*R*, 3*R*)-**3**. Although alkylation through the epoxide functionality is vital for stabilising the intercalated drug, the ester analogue (2*S*, 3*S*)-**105**, which is endowed with this functionality, has no affinity for DNA, as observed by the lack of unwinding ability of (2*S*, 3*S*)-**105**. This finding is consistent with the azinomycin analogue **3** undergoing rapid association/dissociation with DNA, a process that precedes the alkylation of DNA. Hence functionality which shifts this equilibrium towards drug/DNA association, facilitates alkylation which in turn stabilises the intercalated agent/DNA adduct. The amide moiety could hydrogen bond with DNA base pairs and stabilise the agent/DNA complex for alkylation to occur. The energy-minimised structure of the agent/DNA adduct shows the amide NH₂ directed towards a base pair on the opposite strand, indicating a possible interaction between these two groups. The ester analogue however, lacks such hydrogen bonding and as such may be only weakly associated with the DNA duplex. It appears that a prerequisite for intercalation of the azinomycin analogue **3** is the presence of an alkylating functionality and groups that facilitate hydrogen bonding since analogues devoid of alkylating units or the secondary amide do not show any intercalation characteristics. This conclusion is in agreement with an earlier proposal that the azinomycin analogue (2*S*, 3*S*)-**3** does have an intrinsic affinity to DNA and that this analogue have an intercalative mode of binding.⁷²

2.2.5 Cytotoxicity Studies of The Diastereoisomers

DNA interstrand cross-linking agents (ISCs) often display chemotherapeutic, or cytotoxic properties.¹⁰¹ Most clinically used agents for the treatment of cancer such as the nitrogen mustards, cisplatin and mitomycin C are known to induce ISC formation. While the aziridine group of the azinomycin is undoubtedly important for the formation of DNA cross-links, azinomycin analogues containing an intact epoxide group but no aziridine residue retain significant biological activity. The epoxyamide (2*S*, 3*S*)-3, which is the hydrolysis product of the azinomycins, is a monoalkylator of DNA and has been shown to possess similar activity to its parent compound. Analogues of this left-hand subunit, which do not incorporate the epoxide, lose the ability to form DNA monoadducts and are not cytotoxic. Due to the chemical instability of the parent azinomycins, the more chemically robust left-hand subunit with its potent biological activity presents a highly attractive option as a lead compound to probe the mechanism of action of the azinomycins and to develop low molecular weight anticancer drug candidates. Despite this potential, work in this area is focused on the natural isomer of the azinomycin metabolites leaving the question unanswered as to whether other unnatural isomers will present more attractive anticancer agents. This section seeks to determine the influence of stereochemistry on cytotoxicity of the diastereoisomers utilising the results obtained from U2-OS cells and the NCI 60 cell line panel.

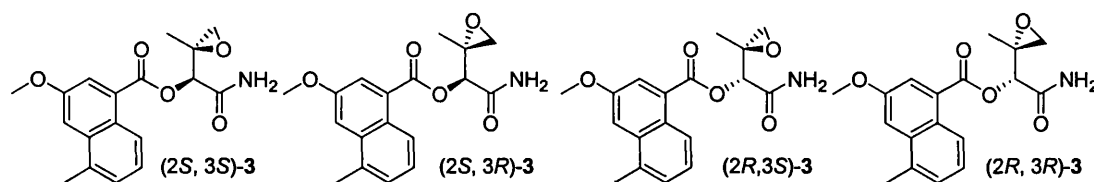
2.2.6 Initial Antitumour Activity In The U2-OS Cell Line

Panel/ Cell line	IC ₅₀ (nM) of compound						
	(2 <i>S</i> , 3 <i>S</i>)-3	(2 <i>S</i> , 3 <i>R</i>)-3	(2 <i>R</i> , 3 <i>R</i>)-3	(2 <i>R</i> , 3 <i>S</i>)-3	117	118	113
U2-OS	15	120	40	40	>10 000	>10 000	>10 000
HoeR	14	121	40	45	>10 000	>10 000	>10 000

Table 2.1 Cytotoxicity of 113, 117 and 118 and the four diastereoisomers of (2*R*, 3*R*)-3 in U2-OS and HoeR. U2 OS is a human osteosarcoma cell line, HoeR is a Hoechst 415 resistant version of U2-OS.

The preliminary cytotoxicity studies in the osteosarcoma cell lines U2-OS show that the natural product (2*S*, 3*S*)-**3** and its unnatural stereoisomers have biological activity in the (nM) range and suggests there is some difference in biological potency between isomers. The natural (2*S*, 3*S*) isomer seems to be optimal in terms of cytotoxic potency. This result also demonstrates that compounds devoid of the epoxide functionality have no biological activity. In concert with the DNA interacting studies it suggests a link between DNA unwinding ability and bioactivity. The inactivity of the alkene amide is of interest since this class of compounds has been designed and synthesised from a pro-drug perspective (see chapter 4).

2.2.7 Cytotoxicity Results using the NCI Cell Line Panel: The Effect of Stereochemistry on Agent Cytotoxicity



The (2*S*, 3*S*)-**3**, (2*S*, 3*R*)-**3**, (2*R*, 3*S*)-**3** and the (2*R*, 3*R*)-**3** stereoisomers were tested in the NCI 60 cell line panel, which includes different human tumour cell lines, of leukaemia, melanoma and cancers of the lung, colon, brain, breast, ovary, prostate and kidney. All compounds were found to exhibit potent cytotoxic activity and showed IC₅₀s in the low μ M region (Table 2.2). The IC₅₀ values for (2*S*, 3*S*)-**3** are very similar to the values for (2*R*, 3*R*)-**3**, which range from 0.010 μ M in some leukaemia cell lines to 2.29 μ M in selected melanoma cell lines. In some of the cell lines, for example the melanoma cell line MALME-3M, the enantiomer of the natural products i.e the (2*R*, 3*R*)-**3** showed significantly higher activity than the corresponding natural isomer (2*S*, 3*S*)-**3**. The mean IC₅₀s across all cell lines for (2*S*, 3*S*)-**3** and (2*R*, 3*R*)-**3** are 0.29 μ M and 0.20 μ M respectively suggesting slightly higher cell sensitivity to (2*R*, 3*R*)-**3** than (2*S*, 3*S*)-**3**.

Cell line	(2S, 3S)-3	(2S, 3R)-3	(2R, 3S)-3	(2R, 3R)-3
leukemia				
CCRF-CEM	<0.011	0.828	0.062	<0.010
HL-60(TB)			<0.010	<0.010
K562	0.028	1.03	0.524	0.54
MOLT-4	<0.010	0.119	0.024	<0.010
RPMI-8226	0.254	0.455	2.51	0.0723
SR		0.715		
NSCLC				
A549/ATCC	1.41	2.29	2.93	0.577
EKVX	2.78	9.29	7.44	3.15
HOP-62	0.045	0.431	0.927	0.019
HOP-92	0.212	0.32	2.61	0.029
NCI-H226	1.13		2.72	1.36
NCI-H23	0.067	0.792	1.46	0.103
NCI-H322M	2.59	1.98	3.56	0.368
NCI-H460	0.737	2.56	2.16	0.446
NCI-H522	1.56	3.48	4.81	1.79
COLON				
COLO 205	0.43	1.68	2.38	0.283
HCT-116	0.017	0.522	0.416	0.027
HT29	0.22	1.68	1.78	0.176
KM12	1.48	2.28	1.11	0.089
SW-620	<0.01	0.422	0.152	<0.01
CNS				
SF-268	0.0196	1.84	0.262	0.0249
SF-295	0.434	1.73	2	0.523
SF-539	0.549	1.39	1.99	0.453
SNB-19	1.76	2.25	3.35	0.331
SNB-75	1.91	1.82	3.02	0.757
U251	0.0234	0.218		<0.010
MELAN				
MALME-3M	4.14	1.91	1.69	0.921
M14	0.15	2.01	1.58	0.218
SK-MEL-2	1.18	3.24	3.26	2.29
SK-MEL-28	1.8	2.38	1.89	0.651
SK-MEL-5	0.193	1.19	1.51	0.178
UACC-257	1.11	2.3	2.21	0.458
UCC-62	0.151	1.16	1.4	0.15
OVAR				
IGROV1	0.773	2.48	2.37	0.651
OVCAR-3	0.336	2	2	0.482
OVCAR-4	4.55	3.49	4.95	1.85
OVCAR-5	0.45	2.46	2.34	0.417
OVCAR-8	0.133	0.716	0.594	0.021
SK-OV-3	1.97	4.15	3.45	0.833
PROST				

PC-3	0.137	1.13	1.69	0.071
DU-145	0.319	2.33	1.73	0.615
BREAST				
MCF7	<0.010	0.449	0.069	<0.010
NCI/ADR-RES	0.0151	0.426	0.233	<0.010
MDA-MB-		100	7.73	8.29
HS 578T	1.56	3.13	4.52	1.34
MDA-MB-	0.152	1.6	1.54	0.393
BT-549	1.16	2.05	2.03	1.53
T-47D	1.73	1.4	2.14	0.556
RENAL				
786-0	0.031	0.112	1.19	0.029
A498	2.45	<0.010	17.3	1.57
ACHN	<0.010	0.257	0.133	<0.010
CAKI-1	0.306	1.37	1.88	0.39
RXF 393	0.604	1.62	1.65	1.2
SN12C	0.261	1.74	0.967	0.031
TK10	0.671	2.27	2	0.664
UO-31	0.311	2.46	3.1	0.7

Table 2.2 IC₅₀ values (μM) for (2*S*, 3*S*)-3, (2*S*, 3*R*)-3, (2*R*, 3*S*)-3, and (2*R*, 3*R*)-3

A change in stereochemistry from (2*S*, 3*S*)-3 to (2*S*, 3*R*)-3 results in a 4-10 fold decrease in activity in the majority of cell lines. The (2*S*, 3*S*)-3 isomer has a mean IC₅₀ of 0.29 μM whilst the diastereoisomer (2*S*, 3*R*)-3 has a mean IC₅₀ of 1.26 μM, indicating some degree of chiral recognition. The IC₅₀ for (2*S*, 3*R*)-3 is comparable to enantiomer (2*R*, 3*S*)-3; a marked decrease in activity, compared to the naturally occurring azinomycin analogue. These compounds have a mean IC₅₀ of 1.26 μM and 1.31 μM respectively making them 10 fold less active than the (2*S*, 3*S*), (2*R*, 3*R*) isomers. The graphs showing patterns of cytotoxicity for (2*S*, 3*S*)-3, (2*S*, 3*R*)-3, (2*R*, 3*S*)-3 and (2*R*, 3*R*)-3 are presented in Appendix I, Tables 1-4. (2*S*, 3*S*)-3 and (2*R*, 3*R*)-3 have a mean IC₅₀ of 0.29 μM and 0.20 μM and the data shows these enantiomers have very similar activity patterns and are highly active in certain leukaemia, colon, CNS, renal and breast cancer cell lines. In particular the leukaemia cell line CCRF-CEM and MOLT-4, the colon cancer cell line SW-60, the renal cancer cell line ACHN, and the breast cancer cell line MCF7, (2*S*, 3*S*)-3 and (2*R*, 3*R*)-3 have growth inhibition activity more than 100 times that of the mean for all cell lines indicating that these cell lines are particularly susceptible to azinomycins. Melanoma, ovarian and prostate cancer cell lines are least susceptible and have growth inhibition properties about 10 fold less than average. Although (2*S*, 3*S*)-3 and

(2*R*, 3*R*)-**3** show excellent growth inhibition in leukaemia cell lines, this does not translate to the total growth inhibition with much higher concentrations needed to achieve total growth inhibition. These compounds have high total growth inhibition activity in the otherwise non-susceptible melanoma and non-small cell lung cancer cell lines.

The (2*S*, 3*R*)-**3** and (2*R*, 3*S*)-**3** also possess a similar activity profile, with (2*S*, 3*R*)-**3** showing a greater activity in leukaemia cell lines whereas (2*R*, 3*S*)-**3** show a preference for renal cancer cell lines. Interestingly the breast cancer cell line, NCI/ADR-RES, which is adriamycin resistant shows high sensitivity to the four diastereoisomers.

2.2.8 Discussion

Azinomycin metabolite analogues which do not contain the epoxide functionality do not possess cytotoxic activity. Therefore it is likely that these compounds exert their biological effect through covalently modifying their biological target DNA. Gates et al showed that this DNA adduct formation occurs through an attack of the electrophilic epoxide ring by the N-7 of guanine.⁷² The formation of the N-7 ammonium ion makes the guanine more acidic and therefore shifts the equilibrium in favour of the enol tautomer. Guanine, in this tautomeric form, can form anomalous base pairs with thymine and one major mutagenic effect of alkylating agents is suggested to involve subsequent transitions from guanine-cytosine to guanine-thymine base pairs (**Figure 2.21**).¹⁰²

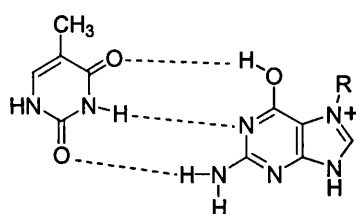


Figure 2.21 Anomalous base pairing of guanine with thymine

Depurination of the DNA, with ring opening of the imidazole moiety, can also occur, resulting in strand scission owing to concomitant ring opening of the sugar phosphate backbone of DNA (**Figure 2.22**). Strand scission also occurs as a result of

endonuclease activity when the cell attempts to repair the segment of DNA containing the drug adducts. The preceding reaction to these cytotoxic lesions is the alkylation of DNA by the reactive epoxide moiety. We therefore hypothesised that any change associated with the epoxide will affect the reactivity and consequently the cytotoxicity of the alkylating compounds. The four diastereoisomers are chemically similar differing only in their geometric 3D structure. The tables showing the IC_{50} , TGI and LC_{50} (Appendix 1) indeed confirm that stereochemistry is vital for the reactivity/cytotoxicity of the azinomycin analogue **3** and indicates some level of chiral recognition in their interaction with DNA their biological target. The four diastereoisomers tested in the NCI's 60 cell line panel were found to be active in a variety of cells with varying degrees of potency. When the IC_{50} s were compared for the various compounds, an interesting pattern was revealed (**Figure 2.23**).

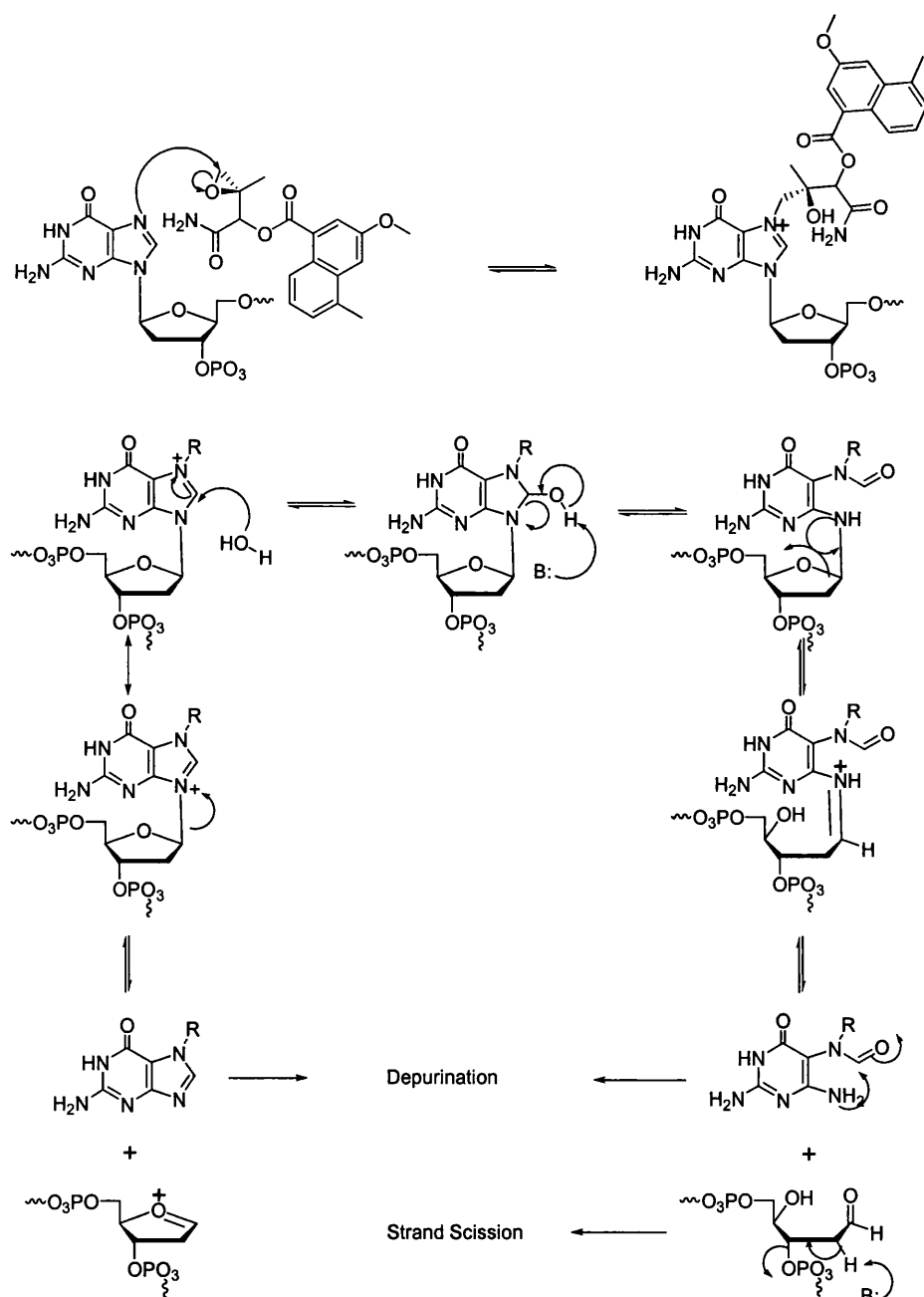


Figure 2.22 Proposed mechanism of action of the azinomycin metabolite. R = azinomycin analogue

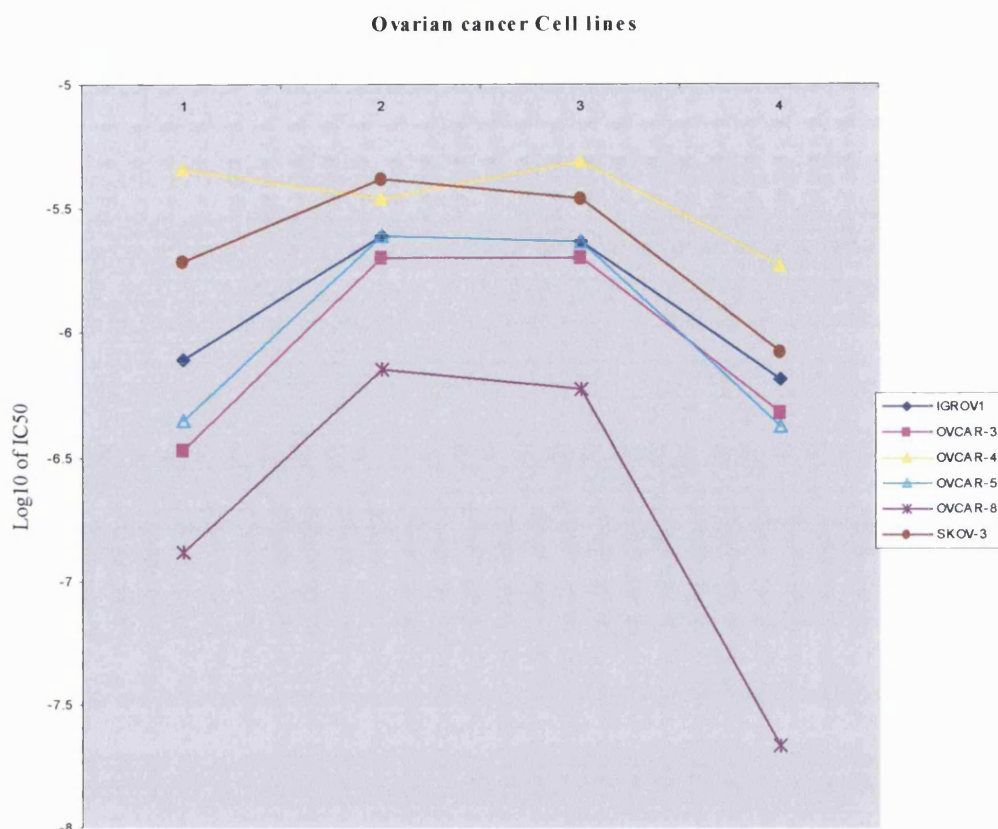


Figure 2.23 Graphs of the IC_{50} of (2*S*, 3*S*)-**3** [1], (2*S*, 3*R*)-**3** [2], (2*R*, 3*S*)-**3** [3], and (2*R*, 3*R*)-**3** [4] in the ovarian cell lines (IGROV1, OVCAR-3, OVCAR-4, OVCAR-5, OVCAR-8 and SKOV-3).

The natural product with the (2*S*, 3*S*) stereochemistry was found to be more potent than the corresponding unnatural (2*S*, 3*R*) stereoisomer. Interestingly, the (2*S*, 3*R*) isomer has similar activity to the (2*R*, 3*S*), which implies that any change in stereochemistry from the natural isomer diminishes the antitumour activity of the azinomycins. The computer modelled energy minimised structures of the (2*S*, 3*S*) and (2*S*, 3*R*) stereoisomers (**Figure 2.24**), reveals that the reactive epoxide of each isomer has a different 3D orientation. This could confer differential reactivity towards their biological target DNA. This data also suggests that intercalation may precede the alkylation process as the molecule will have less degrees of freedom when bonding by intercalation and as such its 3D orientation becomes crucial for alignment with and covalently binding to the adjacent N-7 of guanine.

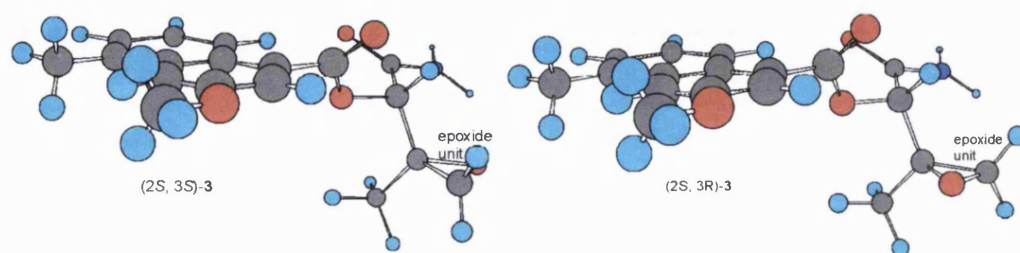


Figure 2.24 Computer modelled energy minimised structures of (2*S*, 3*S*)-**3** and (2*S*, 3*R*)-**3**

The (2*R*, 3*R*) stereoisomer, which constitutes a change at both carbons, has similar biological activity to its natural enantiomer and a change in stereochemistry at the epoxide leads to a similar decrease in activity. The mean graphs for (2*S*, 3*S*)-**3**, (2*S*, 3*R*)-**3**, (2*R*, 3*R*)-**3** and (2*R*, 3*S*)-**3** show above average growth inhibition in selected leukaemia, non-small cell lung cancer, colon and CNS cancer cell lines. The diastereoisomers have different tumour growth inhibition patterns, which is attributed to the only viable parameter, the stereochemistry and consequent orientation of the compounds.

2.2.9 Conclusions

Synthesis of the four diastereoisomer analogues of azinomycins was achieved by Sharpless asymmetric dihydroxylation. It involved epoxidation of the allyl alcohol intermediate using mCPBA to give a 33:67 mixture of the diastereoisomers as identified by ^1H NMR spectroscopy. Column chromatography was used to isolate the stereoisomeric moieties, which were then coupled to the naphthoate chromophore.

Compounds, which did not contain the epoxide functionality, did not unwind DNA whereas the epoxy amides were potent DNA unwinding agents, which implies that the azinomycin metabolite was a DNA intercalator. The DNA unwinding by **3** and its stereoisomers is inhibited by ethidium bromide, suggesting that this process is reversible and that association of the planar naphthoate chromophore with DNA is in equilibrium with the free drug and free DNA. This equilibrium may account for the lack of unwinding activity observed for the non-alkylating analogues as DNA alkylation will work to shift the equilibrium towards DNA association. The unwinding process is also sensitive to changes in stereochemistry and the (2*S*, 3*S*), (2*R*, 3*R*) compounds are more potent unwinders than those with the (2*S*, 3*R*), (2*R*, 3*S*) conformation. Depending on the dynamics of the intercalation process, DNA

intercalation may precede alkylation or vice versa. The results obtained so far from our DNA unwinding assay support the former since the chromophore must have an intrinsic affinity to DNA in order to intercalate rather than remaining unassimilated. Although the epoxide functionality is vital for DNA alkylation and intercalation, the ester analogues containing this group do not possess any DNA unwinding ability and suggest a role of the primary amide as hydrogen bond donor.

The cytotoxicity data shows that the stereochemistry of the epoxide is relevant to the biological activity of the compounds. The (2*S*, 3*S*) and its unnatural enantiomer (2*R*, 3*R*) have similar potency in the NCI 60 cell line screen, a change in stereochemistry at one stereocentre (i.e. either at C2 to give (2*R*, 3*S*) or C3 to give (2*S*, 3*R*) results in a ten fold decrease in cytotoxicity. This result correlates with the DNA unwinding assay results, which also show similar relationship between stereochemistry and activity in vitro. A previous investigation into the sequence selectivity of the naturally occurring azinomycin analogue (2*S*, 3*S*)-**3** suggests that this compound alkylates DNA non-selectively at all guanines and in the absence of DNA sequencing data for the unnatural stereoisomers, it is not clear whether these compounds [(2*S*, 3*R*)-**3**, (2*R*, 3*R*)-**3**, (2*R*, 3*S*)-**3**], will share the same behaviour.

Preliminary experiments in collaboration with Dr. Bailly (INSERM, Lille) using ³²P-end labelled DNA sequences suggest that (2*S*, 3*S*)-**3** and (2*R*, 3*R*)-**3** do exhibit slightly different sequence selectivities and has also demonstrated that the azinomycin analogues based on **3** do not inhibit topoisomerase in vitro.

Chapter 3

Design and Synthesis of DNA Crosslinking Analogues of the Azinomycins

3.0 Introduction

DNA replication is achieved by DNA polymerases, which utilise single stranded DNA as a template for the synthesis of the complementary strand.^{103,104,105} DNA polymerases add deoxyribonucleotides to the 3'-hydroxy terminus of a pre-existing DNA chain or primer only if the base on the incoming nucleotide is complementary to the base on the template strand. The process is therefore dictated by Watson-Crick base pairing^{103,104} and leads to new strands capable of annealing with the original template. As DNA replication is semiconservative, it is crucial that there is progressive separation of the parental helix to facilitate the synthesis of the two daughter strands.¹⁰⁶ Parental strand separation occurs at a point referred to as the replication fork. The blockage of this replication fork halts DNA replication and prevents DNA parent strand separation and consequently cell division.^{107,108} This can constitute a lethal event and can trigger apoptosis leading ultimately to death of the cell in question. DNA interstrand cross-linking agents (ISCs) block the replication fork and halt replication, thus inflicting a catastrophic event on the cell.¹⁰⁸ DNA ISCs therefore comprise an extremely important class of agents for the treatment of cancer.¹⁰¹ Several clinical drugs used for the treatment of cancer are known to induce inter strand cross-link (ISC) formation. This group of drugs fall into five classes namely, nitrogen mustards, aziridines, alkanesulfonates, nitrosoureas and platinum compounds. The nitrogen mustards, developed from mustard gas used in the first world war, constitute the earliest and perhaps most extensively studied of the DNA interstrand cross-linking agents.¹⁰⁷ Independent of their long history, mechlorethamine and chlorambucil (**Figure 3.1**) are amongst the most widely employed clinical anticancer agents in use today.¹⁰¹ Together with the other mustard based compounds (**Figure 3.1**), their high cytotoxic potency is attributed to their ability to induce DNA interstrand cross-links.

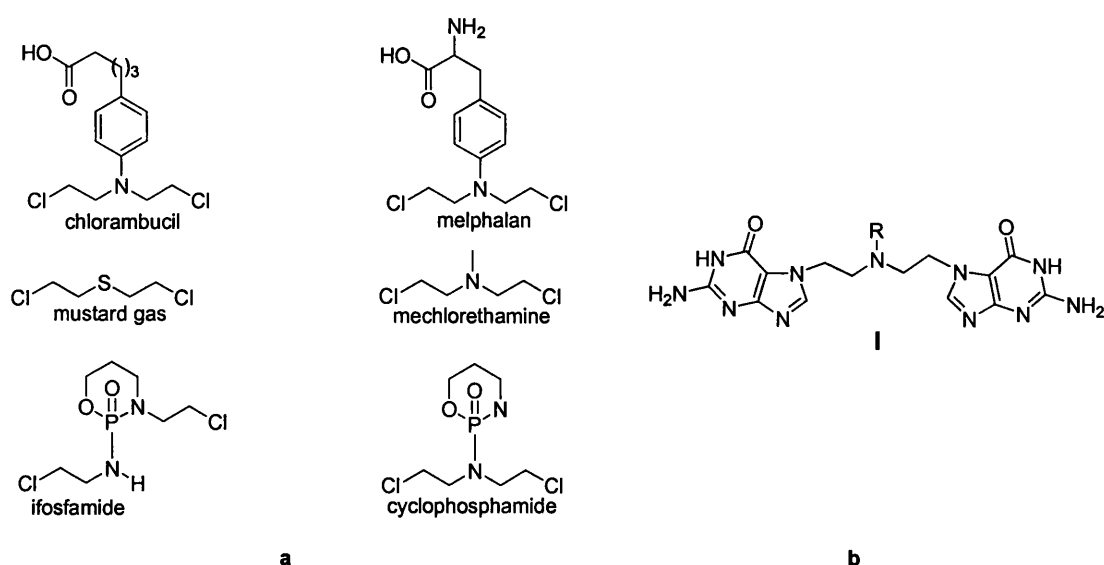
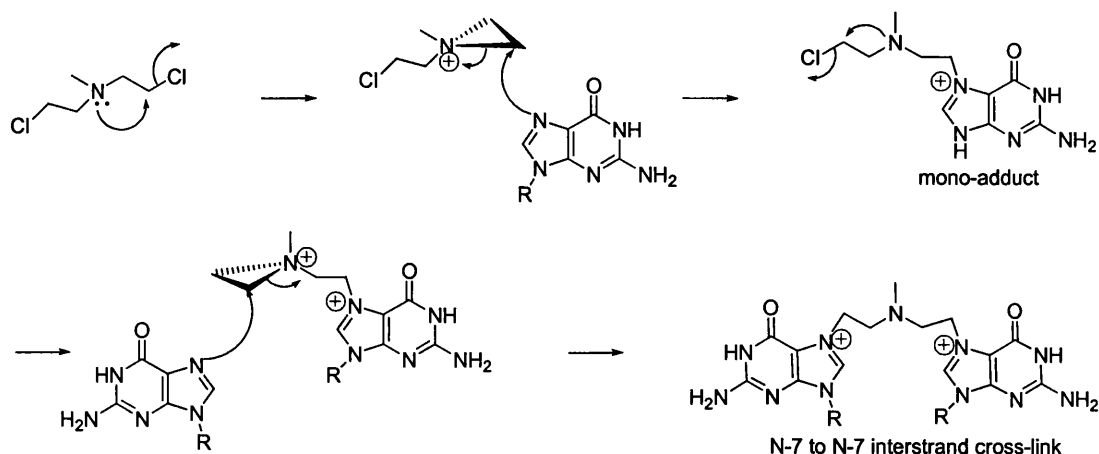


Figure 3.1 a) Structures of mustard gas, and some nitrogen mustards in clinical use. b) example of a bischloroethyl mediated cross-link of guanine.

In 1961 Lawley and Brookes¹⁰⁹ first reacted mechlorethamine with guanosine monophosphate and isolated a product in which two guanine residues were bridged via their respective N⁷ atoms (see figure 3.1b). Comparison of the R_F of this lesion to the ones obtained from acid hydrolysates of mechlorethamine treated RNA and DNA, showed that these also produce the same lesion as mechlorethamine treated guanosine monophosphate.¹¹⁰ From these experiments, the guanine residue bridge lesion **I** in Figure 3.1 was postulated to result from bisalkylation at the sequence 5'-GC-3'. However, 30 years later, two laboratories independently demonstrated that, in vitro, the distal guanosines of 5'-GNC-3' are crosslinked much more efficiently than 5'-GC-3'.^{111,112} Whether **I** arose from intrastrand, interstrand or even interhelical crosslinks was not directly demonstrated until Rink et al.¹¹³ used a 1:1 molar mixture of two DNA duplexes which differed in length, one 12 base pairs (GGGCCC-12) and the other 20 (GGGCCC-20) to show that the interstrand cross-link resulted from an intrahelical reaction. This reaction was within a single helix linking the two strands, rather than an interhelical reaction linking two helices to one another or a reaction joining non-associated single strands. The cross-linking reaction is thought to progress via the mechanism outlined in Scheme 3.1.



Scheme 3.1 Proposed mechanism of DNA-DNA interstrand cross-linking by mechlorethamine

At neutral pH, the lone pair on the nitrogen displaces one of the chloride atoms and cyclises to form an aziridinium ion intermediate, which is reactive to guanine N-7 to form a monoadduct. The aziridinium ion formation is then repeated at the second arm, which is subsequently attacked by guanine N-7 on the DNA strand complementary to the monoalkylated strand to yield a covalently cross-linked double helix.

Another class of compounds that can induce ISC formation are the aziridines. Mitomycin C, which was isolated from a streptomyces species^{114,115} has similar antitumour potency to the azinomycins, which were also extracted from a streptomyces species. Both types of compound exert their cytotoxic potency by covalently cross-linking DNA. However, Mitomycin C has no effect on purified DNA *in vitro* unless a cell extract is added.^{116,71} This is because chemical or enzymatic reduction of the Mitomycin quinone group must precede DNA alkylation.¹¹⁷ In contrast the azinomycins do not need to be activated prior to DNA adduct formation. Azinomycin B was first shown to cross-link DNA by Terawaki and Greenberg.^{118,119} Lown *et al* used an ethidium fluorescence assay to study the reactions of azinomycin B with DNA.³¹

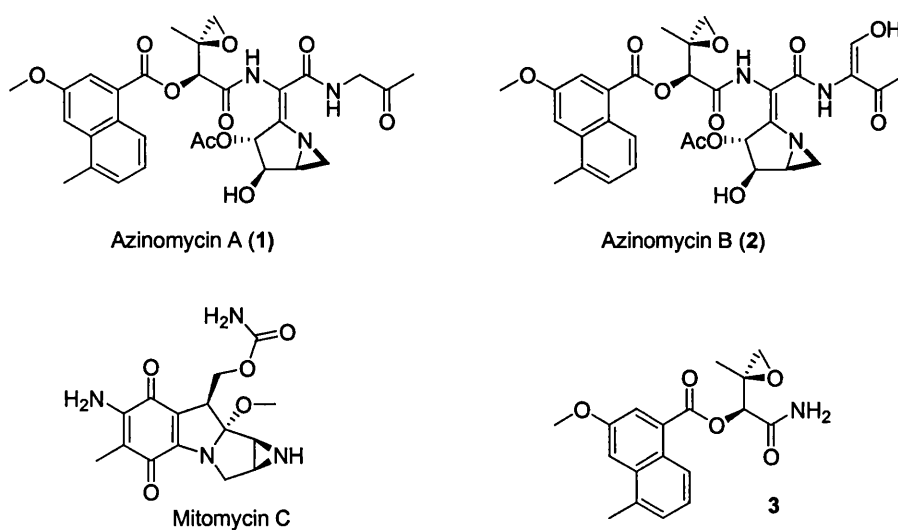
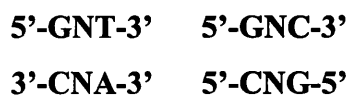


Figure 3.2 Structures of azinomycin A and B, analogue 3 and mitomycin C.

The ratio of EtBr fluorescence before and after heating gave the extent of covalent cross-linking of the DNA since cross-linked DNA provided a nucleation site for DNA renaturation and hence EtBr/DNA association fluorescence. They also found that lower pH favours DNA cross-linking by azinomycin B. Due to the production of lactic acid, the tumour cell environment is characterised by a lower pH than normal cells and this effect may contribute to the selectivity of the tumour agent.^{120,121} Although the early studies in the azinomycin/carzinophilin area outlined their general interaction with DNA, they did not address base specificity in the alkylation reaction. Armstrong et al¹²² addressed this issue by demonstrating that bifunctional alkylation by azinomycin B caused interstrand cross-links between guanine and purine residues two bases removed in duplex DNA fragments containing the sequences:-



This study used synthetic oligonucleotide segments containing inosine and 7-deazaguanine at the target alkylation site of a duplex with one long and a complementary short strand. The duplex DNA, ³²P-end labelled at the 5' terminus of the long or the short strand was incubated with azinomycin B. Denaturing polyacrylamide gel electrophoresis (PAGE) was used to reveal bands of higher molecular weight (lower gel mobility), which were identified as cross-linked DNA.

The sequence specificity was elucidated by cutting out bands corresponding to cross-linked material and isolating the drug/DNA adduct by electroelution. Piperidine treatment of the adduct and PAGE analysis then revealed that cross-linked material 5'- end-labelled on the shorter strand gave rise to a major break at the guanine at position 12 (G₁₂) when compared to a Maxam and Gilbert G-specific lane. Likewise, cross-linked material 5'- end-labelled on the longer strand gave cleavage at the A₁₇ residue, corresponding to two base pair bis-alkylation between G and A residues in the sequence 5'-GNT.¹²² These findings were significant but the detailed chemistry of the cross-linking reaction was not addressed. Fujiwara et al investigated DNA alkylation by using HPLC to monitor the reaction between self complementary oligonucleotide d(TAGCTA)₂ and azinomycin B.⁷¹ In this study, it was demonstrated that the alkylation step occurred between the aziridine moiety and the adenine N-7 and that the highly efficient second arm cross-linking proceeded between the epoxide moiety and guanine N-7. Figure 3.3 shows the HPLC profile of the reaction mixture after 20 h indicating the formation of major product and minor product eluted at 16 and 27 min which were revealed to correspond to cross-linked adduct (**3a**) and monoalkylated adduct (**2a**) by ion spray MS of the HPLC peaks.⁷¹

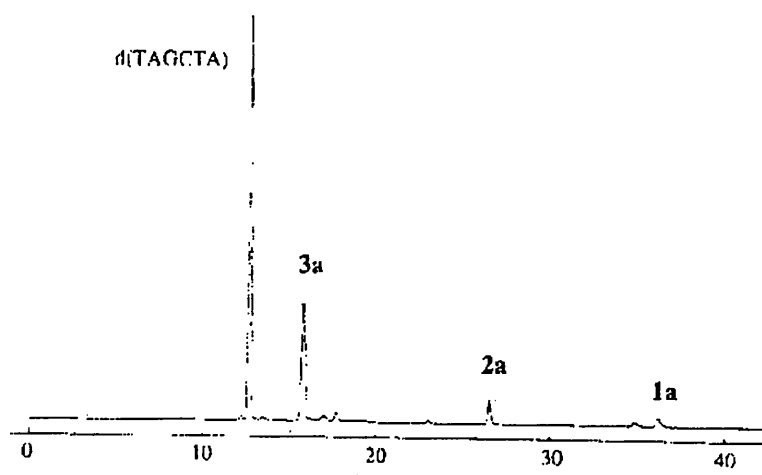


Figure 3.3 HPLC profile of azinomycin cross-linking reaction⁷¹

The azinomycins are relatively unstable and this has somewhat hampered investigations into their mode of action. In the total synthesis of azinomycin A, the product was not isolated, instead complete synthesis was inferred from NMR studies

on the deprotected product generated in situ. This indicates that the natural products are not likely to be sufficiently robust as therapeutic agents. More clinically amenable analogues are required. Several groups have previously reported analogues that are closely related to the natural products but only Shipman et al have demonstrated the ability of selected analogues to cross-link DNA. Interestingly, Shipman and co-workers synthesised a simplified analogue of azinomycin A (**1**) which effectively crosslinked DNA. In a study of the biological activity of **1** in cell culture, it was discovered that a non-crosslinking analogue **3** has similar, if not superior antitumour activity. The potent activity of **3**, raises the question as to whether crosslinking by this group of compounds is actually required for antitumour activity.

In this chapter, azinomycin analogues incorporating a sterically constrained mustard moiety are investigated for their DNA cross-linking potential. This functionality is anticipated to diminish the reactivity on the chloroethyl alkylating moiety compared with the more traditional chloroethyl nitrogen mustards. This is because the lone pair on the nitrogen is more hindered to nucleophilic attack and hence aziridinium ion formation. This biological diminished reactivity is useful as it could minimise unwanted alkylation of other components. It may also make these compounds potential prodrug candidates through N-oxide formation (see chapter 4).

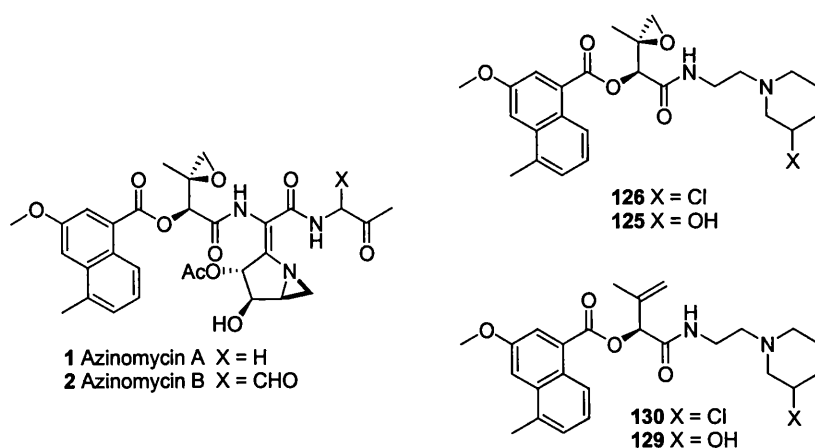
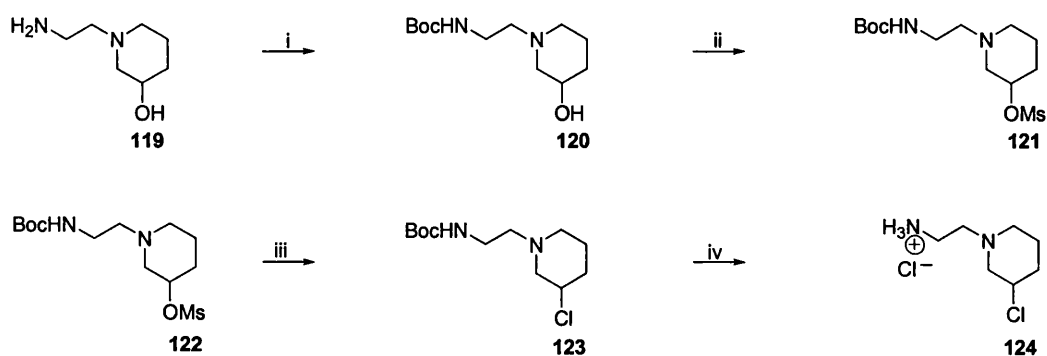


Figure 3.4 Structures of the azinomycins and the piperidine based analogues

3.1 Chemistry Results

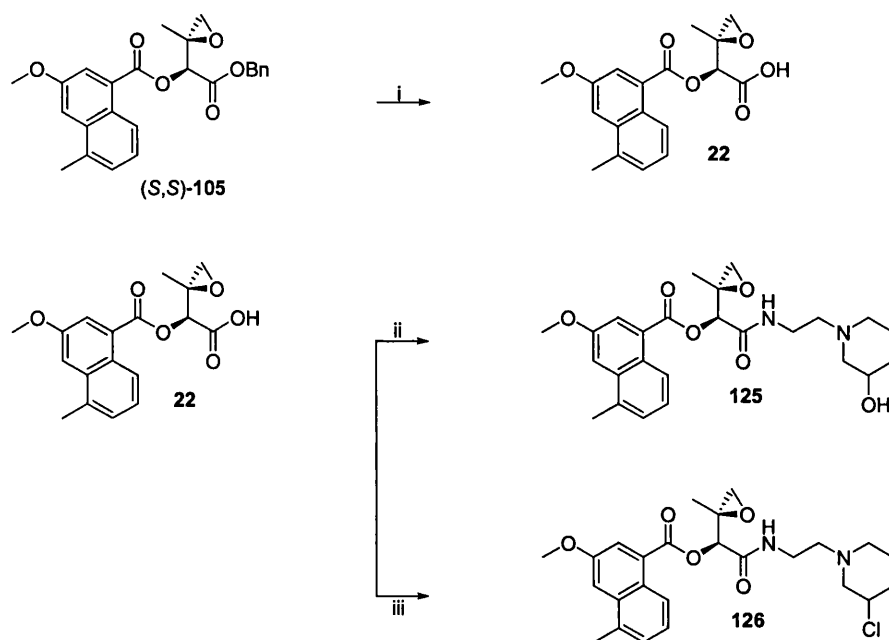
The 2-chloropiperidine **124** was synthesised from 1-(2-aminoethyl)-piperidin-3-ol **119** following Boc-protection of the primary amine. This was achieved by stirring the diamino alcohol **119** in CH₃OH for 5 min after which Boc₂O (dissolved in CH₃OH) was added dropwise over 20 min and the reaction mixture stirred at 45 °C for 20 h. It was concentrated in vacuo, dissolved in EtOAc and washed with H₂O to afford **120** as a straw coloured oil in 95 % yield [FAB MS *m/z* 225 (M+H), 245].



Scheme 3.2 Synthesis of mustard side chain. *Reagents and Conditions:* (i) Et₃N, Boc₂O, CH₃OH, 45 °C, 20 h, 95 %. (ii) Et₃N, MsCl, anhyd. CH₂Cl₂, N₂, 0 °C, 1 h, 71 %. (iii) TBAC, anhyd. DMF 90 °C, 30 min, 92 %. (iv) 2.5 M HCl/EtOAc, 1 h.

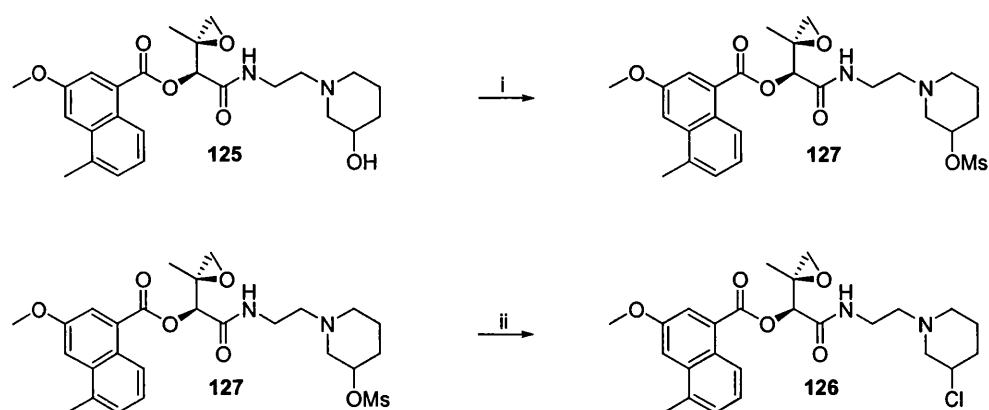
The Boc-protected amine **120** was then converted to the mesylate **121** by stirring in anhyd. CH₂Cl₂, with Et₃N and adding MsCl dropwise at 0 °C. After 1 h the reaction was quenched with ice cold NaHCO₃ in brine and extracted with cold CH₂Cl₂ to give **121** the precursor to the Boc protected 2-chloropiperidine derivative in 71 % yield. The product that resulted from this reaction was unstable and all attempts at isolating this compound failed due to the susceptibility of the mesylate group to nucleophilic attack by the lone pair on the nitrogen. Therefore, the mesylate was immediately transformed into the Boc-protected mustard. This was achieved by heating **121** in anhyd. DMF to 90 °C in the presence of TBAC for 30 min after which the DMF was removed in vacuo and the reaction residue redissolved in CH₂Cl₂ and washed with cold NaHCO₃ to give the Boc-protected mustard **123** in 92 % yield. Prior to coupling to the carboxylic acid functionality of the left hand portion of the azinomycins, the Boc-protected amine was deprotected by stirring in dry 2.5 M HCl in EtOAc for an hour. EtOAc was then removed by evaporation to give the chloride salt of the amine.

The benzyloxy ester (*S,S*)-**105** was synthesised using a stereoselective method (see chapter 2) and then converted to the free epoxy carboxylic acid in Scheme 3.2 by hydrogenolysis using Pd-C in CH₃OH under hydrogen atmosphere.



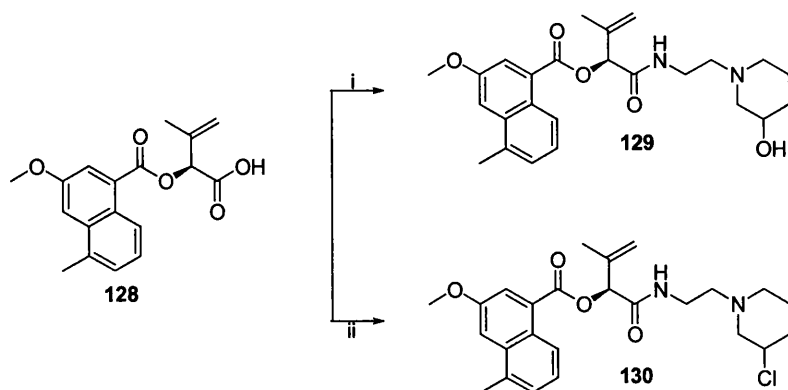
Scheme 3.3 Synthesis of **125** and **126**. *Reagents and Conditions:* (i) H₂, Pd-C, MeOH. (ii) **119**, Et₃N, PyBOP, HOBT. (iii) **124**, Et₃N, PyBOP, HOBT.

To prepare the piperidine alcohol analogue **125**, the freshly prepared epoxy carboxylic acid was dissolved in dry DMF, stirred at 0 °C and was successively treated with 1-(2-aminoethyl)-piperidin-3-ol **119**, Et₃N and PyBOP. The reaction mixture was then warmed to RT and stirred for 18 h after which toluene was added and the resulting solution successively washed with NaHCO₃ and brine. Column chromatography (10 – 20 % CH₃OH/CH₂Cl₂) provided **125** in 49 % yield. The same method was employed to synthesise **126** using freshly deprotected **124**. The yield of **126** was 67 %. NMR confirmed the structures.



Scheme 3.4 Attempted synthesis of mustard analogues. Reagents and conditions: (i) Et_3N , MsCl . (ii) TBAC , DMF , 90°C .

An alternative route for the synthesis of the prototype compound **126** (**Scheme 3.4**) was briefly explored but was abandoned due to very low yields brought about by nucleophilic attack at the epoxide moiety by the chloride on treatment with TBAC .



Scheme 3.5 Synthesis of **129** and **130**. Reagents and Conditions: (i) **119**, Et_3N , PyBOP , HOBt . (ii) **124**, Et_3N , PyBOP , HOBt .

To synthesise the non-alkylating analogue **129**, compound **128** (see chapter 4) the carboxylic acid intermediate was coupled with hydroxypiperidine **119** in 66 % yield using PyBOP methodology. A similar method was used to synthesise the alkylating analogue using the mustard and alkene carboxylic acid to give **130** (59 % yield).

3.2.1 DNA Interstrand Cross-linking

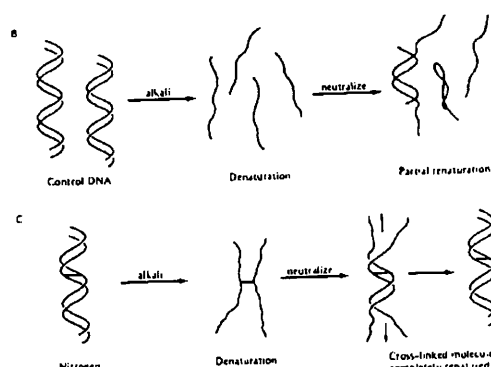


Figure 3.5 Schematic presentation of the response to denaturation and renaturation of crosslinked DNA⁵

A structural requirement of double stranded DNA is the formation of Watson-Crick hydrogen bonding between the DNA base pairs. This hydrogen bonding holds the two complementary strands together but can be disrupted through heat or alkali treatment leading to single stranded DNA. However when alkali denatured DNA is neutralised or when heat denatured DNA is cooled, only partial renaturation takes place because of the random nature of complementary strand annealing. However, DNA, chemically cross-linked is unable to be fully denatured by alkali or heat. Hence when neutralised or cooled, complete renaturation of the DNA takes place because the complementary DNA strands are able to reassume the correct hydrogen bonding sequence (**Figure 3.5**).⁵

3.2.2 Agarose Gel DNA Cross-linking Assay

Plasmid DNA pUC 18 was linearised by digestion with Hind III. The linear DNA was then dephosphorylated with BAP and ³²P-radiolabelled on the 5'-end. The DNA was then purified by EtOH precipitation to remove unincorporated γ -³²P ATP and the DNA resuspended in sterile double distilled H₂O. To each reaction sample was added ³²P-end labelled DNA and drug at the appropriate concentration. Following incubation at 37 °C for the required time, the reaction was terminated by the addition of Stop Solution Buffer. The DNA-drug adduct was EtOH precipitated and dried by lyophilisation. Each dried DNA sample including an untreated DNA single strand as a control was denatured by resuspending in alkali denaturing buffer. The double

stranded control DNA was then dissolved in sucrose loading buffer and the samples loaded and electrophoresed on a 20 cm long 0.8 % horizontal agarose gel submerged in $1 \times$ TAE buffer at 40 V for 16 h. Gels were then dried and autoradiographed.¹²³

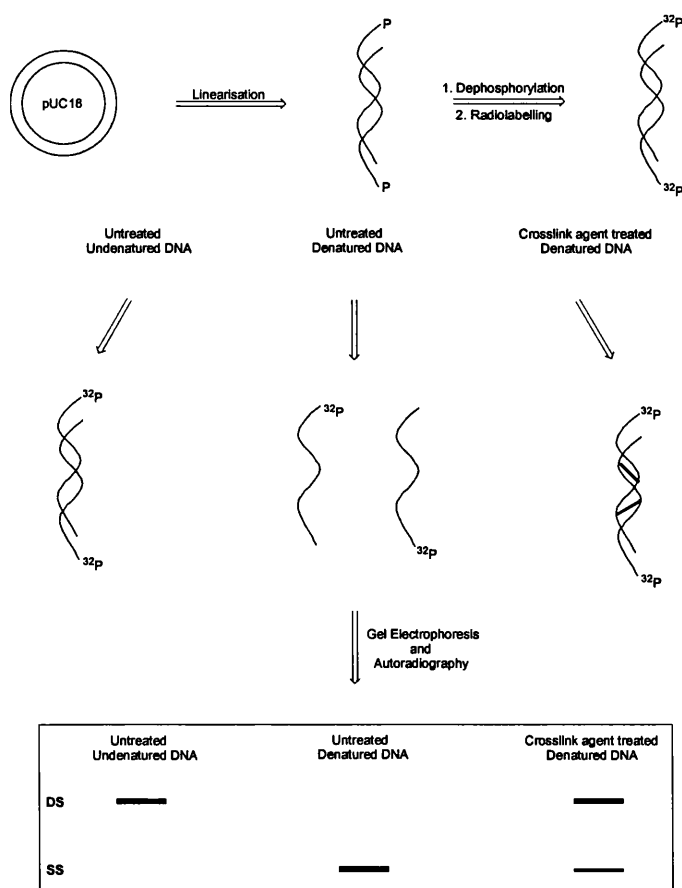


Figure 3.6 Summary of crosslink assay showing the manipulations involved.

3.2.3 Results of DNA Cross-linking with azinomycin derivatives.

Hind III mediated linearized double-stranded pUC18 DNA in the native form electrophoreses as a single band on a neutral agarose gel. Upon denaturation by alkali, there is complete separation of the two DNA strands and upon electrophoreses in a neutral agarose gel, single stranded DNA molecules are more mobile than double stranded DNA. However interstrand cross-linking of DNA prevents the complete separation of double helix such that the cross-linked DNA has the same electrophoretic mobility as native double stranded DNA. The extent of cross-linking can therefore be determined by measuring the relative DNA intensity in the gel.



Figure 3.7 Structures of azinomycin derivatives used to explore DNA cross-linking.

Compounds **125-130** (Figure 3.7) were investigated for their ability to covalently crosslink duplex plasmid DNA. Compound **129** did not crosslink DNA even at high concentrations. (100 μ M). Figure 3.8 shows that drug treated DNA migrated as that for the single strand DNA consistent with no crosslinking activity. This is consistent with the lack of alkylating epoxide or mustard functionalities.

Figure 3.8 shows that **129** does not cross-link DNA even at 100 μM .

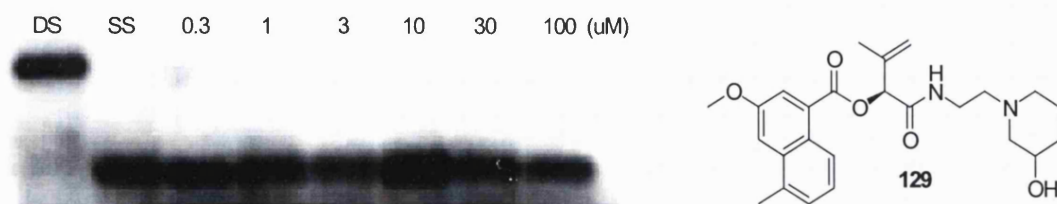


Figure 3.8 Effect of **129** on DNA cross-linking.

DS = double strand DNA, SS = single strand DNA. [For experimental details see]

Figure 3.9 shows that the mono-alkylators **130** and **125** did not cross-link DNA even at concentration up to 3 μM . The drug treated DNA had the same mobility as single stranded DNA after denaturation. At higher concentration DNA degradation is evident.

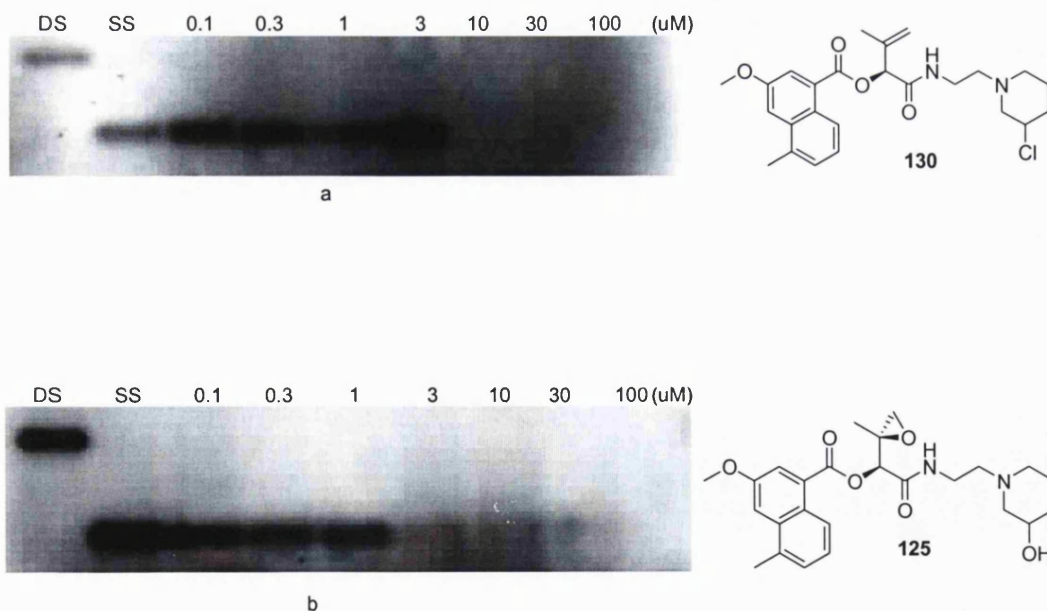


Figure 3.9 (a) Effect of **130** on DNA cross-linking. (b) Effect of **125** on DNA cross-linking.

DS = double strand DNA, SS = single strand DNA.

Since the DNA is visualised through the single ^{32}P end labelling, any DNA cleaving activity causing fragmentation of the DNA results in the different smaller fragments of DNA, which run off the gel causing the single strand band to disappear. In Figure 3.9, gel a the band for single stranded DNA disappears at concentrations $\geq 10\ \mu\text{M}$ and corresponds to compound **129** whereas in gel b the single stranded DNA band disappears at concentrations $\geq 1\ \mu\text{M}$. Although the exact mechanism responsible for the diminishing single strand bands at higher concentrations cannot be unambiguously determined at this point, DNA strand cleavage is a plausible route and the concentration dependence suggests that **125** is a more efficient DNA alkylator and perhaps a more potent antitumour agent than **130**.

Compound **126** which consists of both the epoxide and mustard functionality was tested at concentrations between 0.1 and 50 μM at 1 h, 2 h and 3 h intervals. The autoradiograph and the concentration-response curve shows that **126** can imitate the natural product and crosslinks linear double stranded plasmid pUC18 DNA after one hour incubation (Figure 3.10). Crosslink formation starts at concentrations as low as 0.1 μM and reaches 100 % crosslinking at $\sim 10\ \mu\text{M}$. After incubation for an hour the CR_{50} was determined to be 3.1 μM .

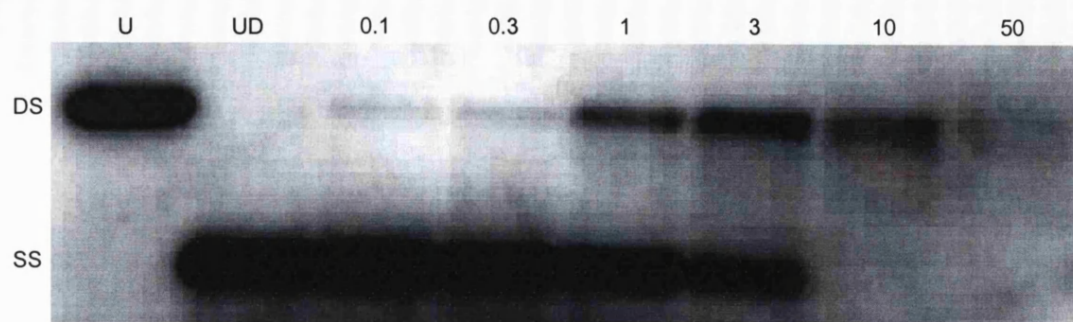
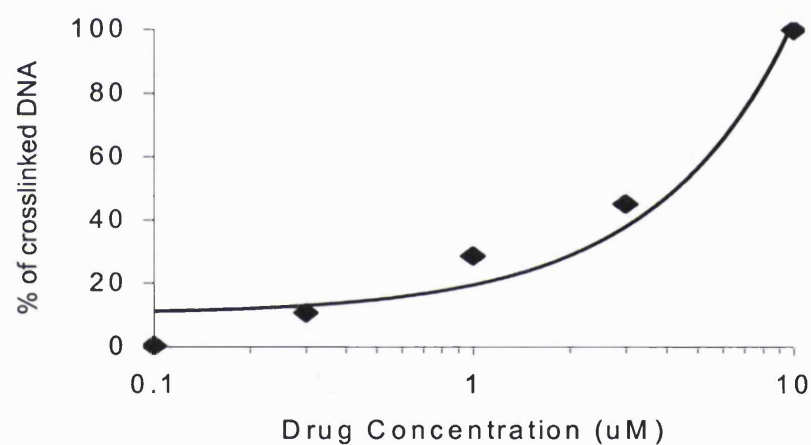
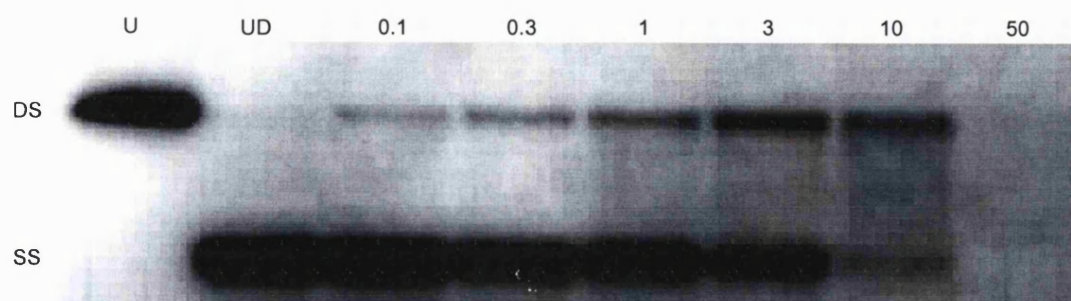
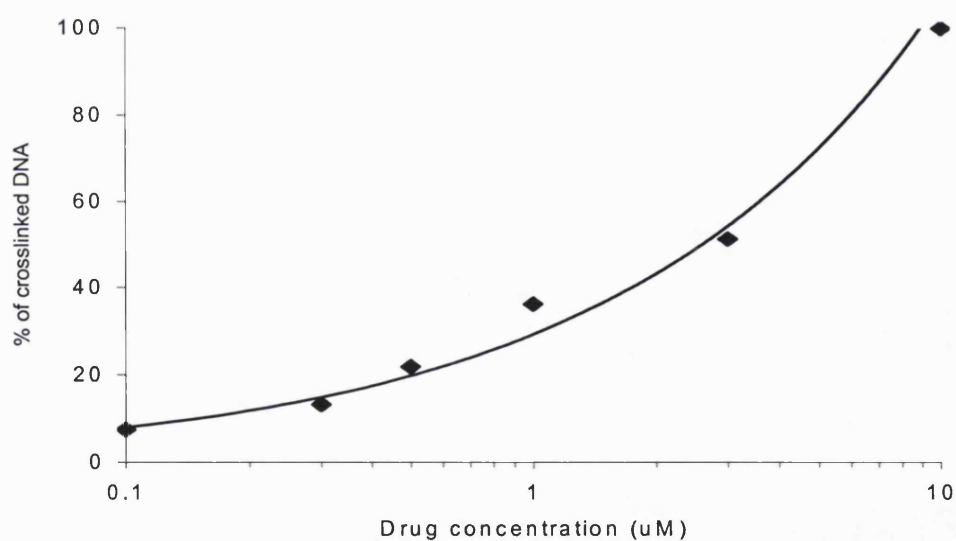
**a****b**

Figure 3.10 (a) Effect of 126 on DNA crosslinking after 1 h incubation with pUC18 plasmid DNA (b) The percentage crosslinked (double stranded) DNA. Determined from the autoradiograph by densitometry. DS = double stranded DNA, SS = single stranded DNA, U = untreated nondenatured DNA, UD = untreated denatured DNA. [CR₅₀ is the percentage at which 50 % of duplex DNA is crosslinked]

Crosslink formation progressed steadily over time and after 2 h the CR_{50} was reduced from 3.1 μM to 2.7 μM (**Figure 3.11**). After 3 h the CR_{50} was 2.2 μM .

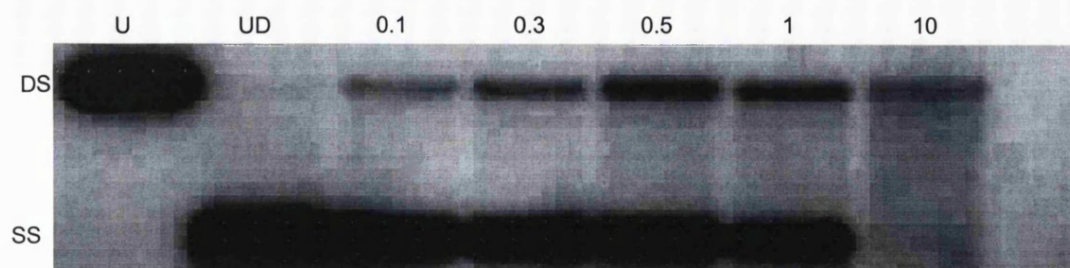


a

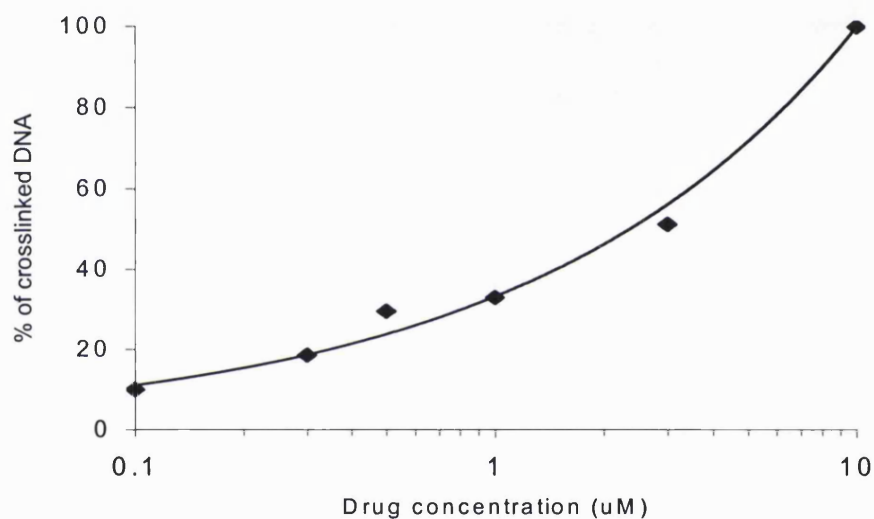


b

Figure 3.11 (a) Effect of **126** on DNA crosslinking after 2 h incubation with pUC18 plasmid DNA (b) The percentage crosslinked (double stranded) DNA. Determined from the autoradiograph by densitometry. DS = double stranded DNA, SS = single stranded DNA, U = untreated nondenatured DNA, UD = untreated denatured DNA. [CR_{50} is the percentage at which 50 % of duplex DNA is crosslinked]



a



b

Figure 3.12 (a) Effect of 126 on DNA crosslinking after 3 h incubation with pUC18 plasmid DNA (b) The percentage crosslinked (double stranded) DNA. Determined from the autoradiograph by densitometry. DS = double stranded DNA, SS = single stranded DNA, U = untreated nondenatured DNA, UD = untreated denatured DNA. [CR₅₀ is the percentage at which 50 % of duplex DNA is crosslinked]

3.2.4 Effect of Piperidine Based Analogues on Unwinding of Supercoiled Plasmid DNA

Piperidine analogue **129** which contains the alkenyl and hydroxy functionalities respectively in place of the epoxide and chloroethyl functionality did not unwind DNA (**Figure 3.13**). Subsequently the ability of the mono-alkylators **125** and **130** to unwind supercoiled DNA was examined, as an indicator of intercalative activity as previously discussed in chapter two. The results did not show clearly that these agents intercalate. Figure 3.14c, d shows that **130** and **125** initiate a change in the electrophoretic mobility of supercoiled DNA at a drug/bp ratio of 0.1. However at higher concentration, DNA degradation by **125** and **130** is evident. This could be due to the presence of the piperidine group which could attack and ring open the alkylated guanine and thus facilitate DNA cleavage.

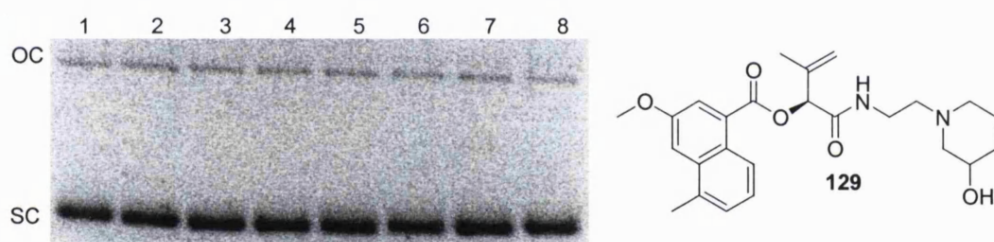


Figure 3.13 Effect of **129** on the electrophoretic mobility of ϕ X174 plasmid DNA. Lane 1 DNA only, lanes 2-8 10^{-3} , 10^{-2} , 10^{-1} , 1, 10, 20, 30 drug/bp ratio. DNA ($3.84 \mu\text{M}$). SC = Supercoiled DNA, OC = Open Circular DNA.

The unwinding results for the monoalkylators and the crosslinker are presented in Figure 3.14. Although the unwinding result for the mono-alkylators are equivocal, the crosslinking compound presents a pattern of interaction which resembles that for compounds such as the nonalkylating AQ4, which have been unambiguously shown to be potent DNA intercalators. It therefore appears that the crosslinking event positions the chromophore to successfully intercalate into the DNA. It is interesting though that the mono-alkylators should show such different interaction profile.

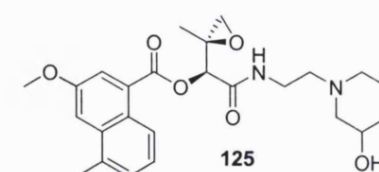
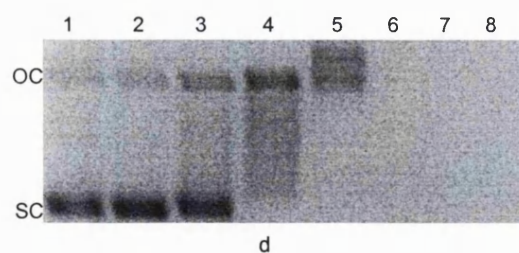
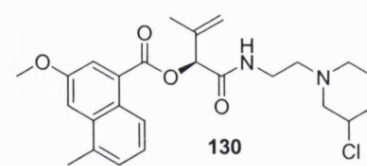
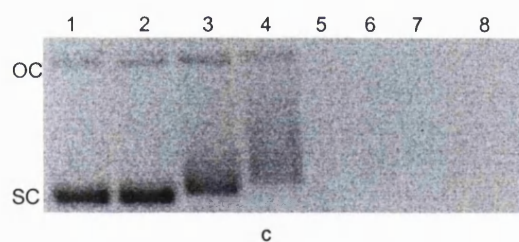
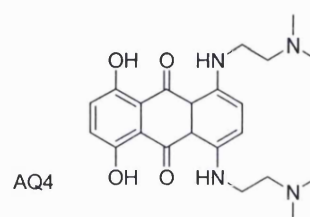
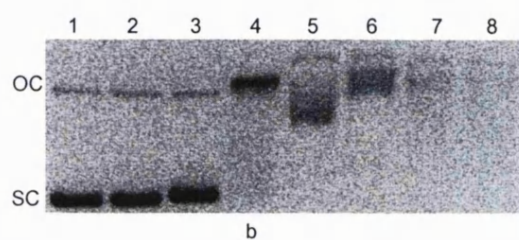
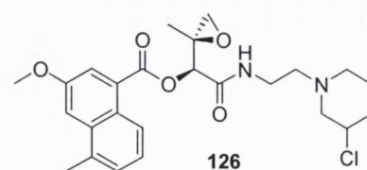
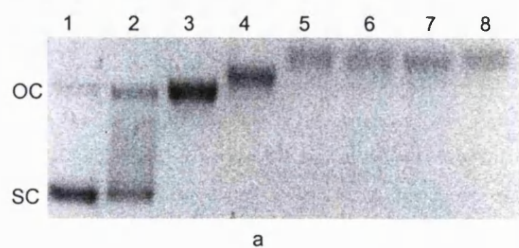


Figure 3.14 Effect of **125**, **130**, **126** and **AQ4** on the electrophoretic mobility of ϕ X174 plasmid DNA. Lane 1 DNA only, lanes 2-8 10^{-3} , 10^{-2} , 10^{-1} , 10^0 , 10, 20, 30 drug/bp ratio. Except for AQ4 which is 10^{-4} , 10^{-3} , 10^{-2} , 10^{-1} , 1, 10, 20. DNA ($3.84 \mu\text{M}$). SC = Supercoiled DNA, OC = Open Circular DNA.

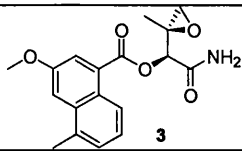
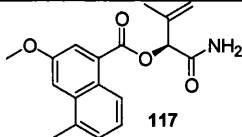
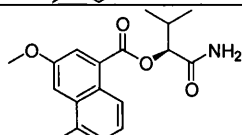
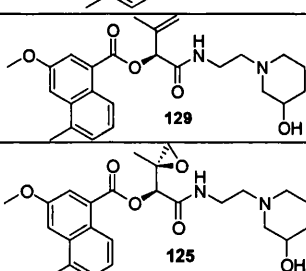
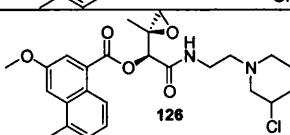
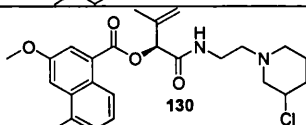
Compound	Alkylator	Unwinding
 3	+	+
 117	-	-
 129	-	-
 125	+	(+)
 126	++	(+)
 130	+	(+)

Table 3.1 Table showing mode of interaction of selected compounds

3.2.5 Cytotoxicity Studies of Piperidine Based Analogues

Cytotoxicity studies using the U2OS osteosarcoma cell line showed that compounds **125**, **126** and **130** all had effective cytotoxicity at about 40 μM . However, compound **129**, which has no alkylation functionality and which was not shown to interact with DNA was not cytotoxic. Compounds with alkylating potential were submitted to the NCI 60 cell line screen and results obtained together with those obtained for compound **3** are shown in table 3.2. This shows that (2*S*, 3*S*)-**3** is more potent than the piperidine analogues. All three inhibited cancer cell growth in vitro in all the 60 human cancer cell lines. The epoxy piperidine mono-alkylator **125** was most promising and with an average IC_{50} of 2.1 μM its potency surpassed that of the crosslinking analogue **126** and the mustard mono-alkylator **130** which had $\text{IC}_{50\text{s}}$ of 12.3 μM and 5.1 μM respectively. These values, which are in the low μM range, are consistent with the cytotoxic potential of these agents. The IC_{50} values match the tumour growth inhibition and, overall the epoxy monoalkylator **125** showed cell growth inhibition profile superior to both the cross-linker **126** and the mono-alkylator **130**. Interestingly, compound **126**, which cross-links duplex DNA, has less activity than **125** the monoepoxide and in most cell lines it is less active than the mustard monoalkylator.

Cell line	(2S, 3S)-3	125	126	130
leukemia				
CCRF-CEM	0.01	2.95	3.26	3.24
HL-60(TB)		2.94	6.98	12.1
K562	0.028	2.93	8.33	5.16
MOLT-4	0.01	2.15	3	3.3
RPMI-8226	0.25	2.1	4.18	3.43
SR		1.58	2.02	2.34
NSCLC				
A549/ATCC	1.41	3.05	31.1	8.26
EKVX	2.75	3.39	17.5	11.4
HOP-62	0.045	1.58	100	3.45
HOP-92	0.21	2.18	13.8	4.12
NCI-H226	1.12			
NCI-H23	0.068			
NCI-H322M	2.57	5.58	17.9	8.07
NCI-H460	0.74	2.62	13	6.26
NCI-H522	1.54	1.62	7.77	5.1
COLON				
COLO 205	0.43	2.98	13.8	6.08
HCC2998		1.61	8.25	4.27
HCT-116	0.016	1.63	100	12.8
HCT-15		0.39		0.049
HT29	0.22	3.4	11	7.26
KM12	1.48	2.67	14.5	9.3
SW-620	0.01	1.29	5.26	2.76
CNS				
SF-268	0.079	3.03	16.6	11.9
SF-295	0.44	2.26	13.1	4.35
SF-539	0.44	1.7	6.27	0.45
SNB-19	1.77	3	14.3	5.63
SNB-75	1.9	2.54		1.2
U251	0.023	1.59	7.82	2.63
MELAN				
LOX IMVI		1.4	3.62	2.84
MALME-3M	4.16	4.81	14.8	7.51
M14	0.15	1.44	100	1.75
SK-MEL-2	1.17	1.81	18.6	7.81
SK-MEL-28	1.81	4.47	11.6	8.48
SK-MEL-5	0.19	1.21	1.56	1.99
UACC-257	1.12			
UCC-62	0.15	1.66	14.7	4.41
OVAR				
IGROV1	0.78	1.78	12.1	4.21
OVCAR-3	0.34	1.86	18.6	10.2
OVCAR-4	4.57	4.74	21.5	20.9
OVCAR-5	0.45	2.76	16.1	11.1
OVCAR-8	0.13	3.59	44.5	32.9

SKOV-3	1.94	4.37	19.7	17.2
RENAL				
786-0	0.031	2.19	100	4.48
A498	2.45	0.39	17.7	0.19
ACHN	0.01	0.26	1.17	1.78
CAKI-1	0.31	2.33	10.3	5.66
RXF 393	0.6	1.77	17.5	19.1
SN12C	0.26	1.46	6.76	3.76
TK10	0.68	2.78	23.4	12.1
PROST				
PC-3	0.14	3.53	11.2	7.96
DU-145	0.32	1.66	4.49	5.15
BREAST				
MCF7	0.01	1.91	14.7	4.62
NCI/ADRRES	0.015	2.26	11.1	12.8
MDA-MB-				
231/ATCC		1.65	14	11
HS 578T	1.55	1.99	17.5	3.69
NMDA-MB-				
435	1.15	1.78	14.3	7.62
BT-549	2.29	2.37	12.5	4.55
T-47D	1.74	2.34	23	10.8
MGMID		2.08	12.3	5.12

Table 3.2 Antitumour activity (GI_{50} , μM) of compounds (2*S*, 3*S*)-3, 126, 125 and 130.

3.3 Discussion

The piperidine analogues were synthesised using a route that involved Boc-protection of the primary amine 1-(2-aminoethyl)-piperidin-3-ol. The Boc-protected amino alcohol was then transformed into the mesylate, which was chlorinated to give the Boc-protected mustard. Acid catalysed deprotection of the Boc group furnished the hydrochloric acid salt of the mustard, which was directly coupled, using PyBOP and HOBt, to the epoxy or alkenyl carboxylic acids **126** and **125**. This route was found to be more productive than an alternative route involving coupling of the alcohol before proceeding with the chlorination step. Compound **125** was similarly synthesised from the naphthalene epoxide fragment with the alcohol **119** and compound **129** and **130** from the novel naphthalene alkene carboxylic acid and either the mustard or the alcohol.

Mustard-based agents have a long history in cancer chemotherapy and they are still widely employed in the clinic. Piperidine mustards have been developed with the view of reducing the reactivity of the mustard functionality in order to minimise the non-target reactivity associated with conventional alkylating agents and thereby optimise their biological potential. Piperidine-based mustards have been employed in the synthesis of intercalator-alkylator conjugates that have broad spectrum antitumour activity.¹²⁷ The parent azinomycins being densely functionalised and unstable are unlikely therapeutic agents. In comparison the analogues described are the first to be developed as likely therapeutic candidates. The piperidine mustard moiety is more stable and more easily accessible than the densely-functionalised system of the azinomycins but positions the alkylating function relative to the epoxide in a similar fashion to the natural products. Initial computer modelling studies suggested that **126** could alkylate both through the epoxide and mustard functionality and still maintain sufficient rotational freedom to allow the chromophore to intercalate. Further, the model revealed GXC as the preferred binding site.

Preliminary cytotoxicity studies showed the propenyl hydroxy agent **129** to be inactive. Consistent with this **129** did not crosslink or unwind DNA. Similarly, the mono-alkylators (**125** and **130**) also lacked DNA crosslinking ability, although they appeared to cleave duplex DNA under the conditions of the crosslinking assay. In this respect the mono-epoxide showed 3 times higher cross-linking activity than the

mustard mono-alkylator. It is possible that the epoxide is responsible for initial DNA alkylation. In contrast the natural azinomycins alkylate initially at the aziridine moiety. The relative stability of the piperidine mustards supports this since they must undergo cyclisation to the aziridine prior to alkylation (**Figure 3.15**).

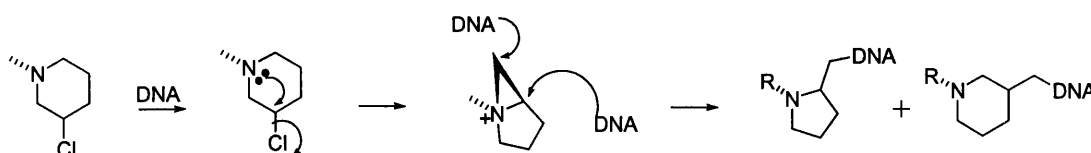


Figure 3.15 Mechanism of aziridinium ion formation. The DNA can alkylate either the primary or the tertiary carbon of the aziridinium ion to form a five or six membered ring.

The loss of DNA visualised in the gels (see figures 3.9 and 3.14) at higher concentrations of agent could be due to DNA precipitation, however this mechanism is unlikely since the substituent-dependent effect translates to their cytotoxicity, with the mono-epoxide *circa* 2.5 times more toxic. Compound **126** is a potent DNA crosslinking agent and is believed to alkylate guanines two base pairs removed from each other. This is in contrast to the natural compounds, which were shown to alkylate a GXT sequence. Recently, it was suggested that azinomycin B also alkylates a GCT.CGA and GCC.CGG sequence.⁷³ Shipman et al investigated cross-linking activity of symmetrical dimers of the azinomycins based upon the epoxide domain and found that the bisepoxide **85b** (Figure 1.11) induces total ISC's at 1 μM .⁷⁵ This group also studied the interstrand cross-linking activity of a synthetic epoxy aziridine analogue **86** and found it had a poorer cross-linking ability than the bisepoxides. The epoxy aziridine analogue produces DNA cross-link formation at 10 μM with 100% cross-link formation at 100 μM after 1.5 h.⁶⁸ The chloropiperidine epoxide analogue **126** investigated in this thesis induced DNA cross-linking at 0.1 μM and 100 % cross-linking at 3.1 μM . The piperidine epoxide is less active than the bisepoxide **85b** but is more potent than Shipman et al's aziridine epoxide. This suggests that the chloro piperidine side chain of **126** could be further optimised in order to increase the potency of this class of analogues. Also an advantage of the piperidine analogue may be its likely increased biological

robustness in vivo. Due to the need for the piperidine mustard to form the bicyclic intermediate containing a strained aziridine ring (see figure 3.25) the aziridine moiety is likely to be less reactive towards DNA. Therefore the likely sequence of reaction is the epoxide forming the first covalent attachment with DNA followed by the less reactive mustard forming the cross-link (see figure 3.16).

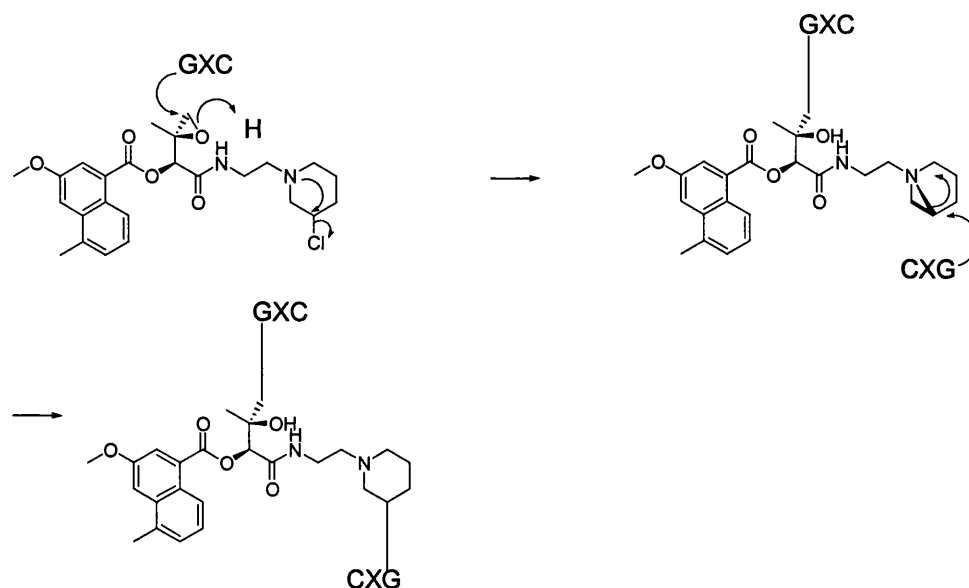


Figure 3.16 Proposed mechanism of interstrand crosslink formation by the piperidine analogue

The cytotoxicity data for the three new agents and the monoalkylator **3** is shown in Table 1. The piperidine analogues demonstrated a decrease in cytotoxic activity compared to the natural product **3**. One possibility is that because the piperidine nitrogen is protonated at physiological pH it could impair cell uptake leading to low intracellular drug availability.

DNA crosslinking inhibits DNA replication^{107, 108} and constitutes a lethal assault on cell division and growth. Generally, it is considered that crosslinking agents have higher cytotoxicity than monoalkylators, although there are notable exceptions such as the duocarmycins. In this study, monoalkylators displayed more potent cytotoxicity in vitro than the crosslinking analogue **126**. This findings are consistent with previous studies⁷⁸ and suggest that monoalkylators have intrinsic activity separate to the cross-linking agents.

3.4 Conclusion

The objective of this study was to investigate the effect of crosslinking on biological activity using compounds that are modelled upon the natural product azinomycins. This was achieved through the design and synthesis of structural analogues that incorporate a structurally constrained nitrogen mustard in place of the aziridine. From the results it can be concluded that the crosslinking agent binds to and crosslinks duplex DNA. In vitro this activity appears to be associated with a loss of biological activity. Clearly the mono-epoxides are the most active agents and require further evaluation. The cross-linking piperidine compounds also warrant further evaluation since they are significantly active in vitro and may demonstrate biological robustness in vivo.

Chapter 4

Development of a prodrug based on the azinomycins

4.0 Introduction

Prodrugs are inactive when administered until they are metabolised to an active drug. Cancer cells are biochemically very similar to normal body cells and therefore cancer chemotherapeutic drugs, which are administered to patients in their active form, may kill both healthy as well as cancerous cells alike. This can give rise to severe side effects including secondary tumours. It is therefore desirable to target cancer chemotherapeutic agents to the cancer cells in order to minimise the severe side effects suffered by patients. The azinomycins derive their biological activity, in part, from their high reactivity with nucleophiles. Azinomycins are especially labile in acidic media^{20, 24} and their ability to DNA interstrand cross-link is pH dependent with more rapid cross-link formation at lower pH. Due to the high reactivity of both the epoxide and aziridine functionalities, azinomycin B is likely to react with non-target biological nucleophiles, which could lead to side effects. It is therefore necessary to seek ways to deactivate the reactive groups on the molecule, employing mechanisms that will reactivate the molecules, preferably when in close proximity to the tumour mass. The parent azinomycins, with their instability and poor solubility, do not make for a good lead compound. The low molecular weight azinomycin analogue **3**, has similar biological activity to the more structurally complex azinomycins A and B. It is also more biologically robust and therefore makes a good lead compound. This chapter describes for the first time, an attempt to develop a prodrug strategy for the azinomycin antitumour antibiotics.

4.01 Design of a prototype bioreductive prodrug based upon the azinomycin metabolite.

Cells in solid tumours several cell diameters (~100 μm) from blood vessels develop tissue hypoxia (low oxygen), which results from an inadequate supply of oxygen that compromises oxidative biological functions.¹²⁴ The high metabolic demand of cells close to the blood supply contribute to this phenomenon in more distant cells.¹²⁵ Tumour hypoxia has been considered a therapeutic problem because it renders solid tumours more resistant to radiation therapy, a process that is dependent on molecular oxygen. Traditional cancer chemotherapeutic agents may also be less effective if they cannot reach the hypoxic cells due to poor blood supply. The concept of

hypoxia has created much interest in the development of hypoxia-selective cytotoxins capable of being activated by enzymatic reduction (bioreductive drugs) to exploit this feature of tumour cells.¹²⁶

Many DNA intercalating agents with chemotherapeutic value possess, in addition to a planar chromophore, basic functionalities, often in the form of alkyl-amino side chains. Compounds in this class include the anthraquinones, anthrapyrazoles, anthracenes and acridines. Agents based on these chromophores have been shown to possess potent cytotoxicity against proliferating cells, and generally their mechanism of activity is thought to be through a combination of DNA binding and inhibition of topoisomerase II, an enzyme which is crucial to processing DNA prior to cell division. The basic side chains are ionised at physiological pH and interaction of the planar chromophore of these compounds with DNA is facilitated by electrostatic interactions of the basic moieties with the sugar phosphates that are in close proximity to the intercalation site. It was hypothesised by Patterson (1997) that the use of a amine side chain moiety with a masked amine would reduce their ability to electrostatically interact with the DNA duplex and should destabilise the intercalation process, hence diminishing cytotoxic activity.¹²⁷ Consequently, Patterson et al. demonstrated that conversion of tertiary amines of alkyl-amino side chains to their corresponding *N*-oxides renders them less basic and electronically neutral. This resulted in diminished intercalation of DNA interacting chromophores such as anthrapyrazole di-*N*-oxide, anthracene di-*N*-oxide and anthraquinone di-*N*-oxide (**Figure 4.1**). Significantly, the *N*-oxide formation of cytotoxic agents including the anthrapyrazoles and anthracenes rendered them markedly less cytotoxic to V79 and MCF7 cells than their respective tertiary aliphatic amine parent compounds.¹²⁷

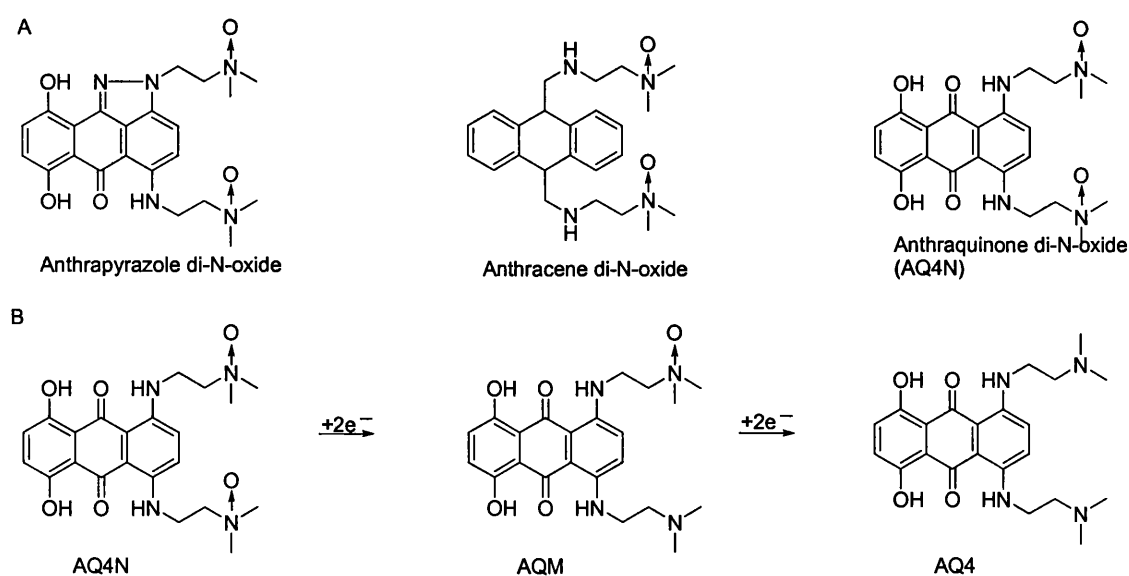


Figure 4.1 A. *N*-oxides of DNA anthraquinone intercalators. B. AQ4N and its reductive metabolites

AQ4N, an *N*-oxide of an alkylamino anthraquinone which is currently in clinical trials, has been shown to potentiate the effect of radiation treatment and enhance the antitumour effect of certain anticancer drugs such as cyclophosphamide and cisplatin.^{128,129} Reduction of *N*-oxides to their active tertiary amine parent compounds was shown to be mediated by the cytochrome P450 family of enzymes and is thought to be a four electron process.

Nitrogen mustards such as mechlorethamine, melphalan and chlorambucil are clinically relevant DNA crosslinking agents. Their mechanism of action is heavily dependent on the aziridinium ion formation through the displacement of the chloride leaving group by the lone pair on nitrogen.⁵ Oxidation of the mustard nitrogen to the *N*-oxide renders the *N*-chloroethyl group more stable because it is less likely to form ring aziridinium ion and therefore prevent it from reacting with DNA until metabolised in vivo to the amine. This approach has been employed in an attempt to develop *N*-oxide prodrugs of mechlorethamine and chlorambucil.^{130,131} However, *N*-oxide formation with traditional mustards has generated molecules that proved to be unstable due to rearrangement of the mustard functionality.¹³¹ In order to develop more stable nitrogen mustard *N*-oxides, 2,6-disubstituted *N*-methylpiperidine derivatives and their *N*-oxide analogues (Figure 4.2) have been investigated. The amine mustards were found to be equally cytotoxic in two cell lines whereas the *N*-oxide counterpart proved to be relatively non-toxic.¹³² Significantly, the *N*-oxides

were found to be biologically stable as opposed to the *N*-oxides of traditional mustards and thus presents a powerful tool for the development of mustard based bioreductive prodrugs.

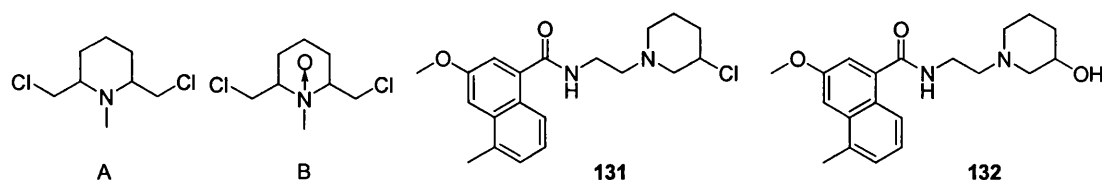
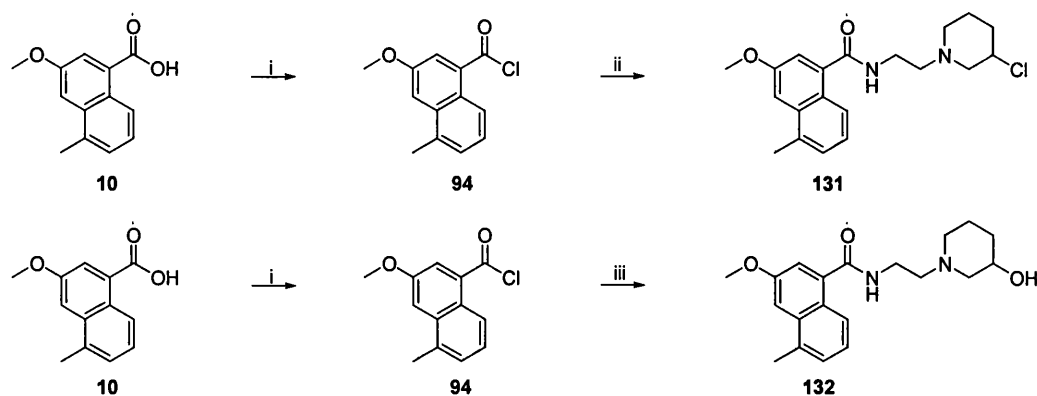


Figure 4.2 A. 2,6-disubstituted *N*-methylpiperidine derivative. B. *N*-oxide analogue. **131** azinomycin mustard, **132** hydroxyl analogue

The azinomycin metabolite **3** has greater therapeutic potential than the parent azinomycin A and B. It is considered a good lead compound for the design, synthesis and investigations of analogues that may have properties useful in the design of prodrugs. The interest in bioreductive prodrugs led to the design and synthesis of **131**, a nitrogen mustard similar to **3** in that it will covalently bind to DNA and place the chromophore in close proximity to the duplex. **131** also contains a more biologically stable amide bond between the chromophore and the alkylating group.

4.1 Chemistry Results

The compounds were synthesised using the methods described in previous chapters. The acid chloride **94** was freshly prepared from the carboxylic acid **10** by refluxing in pure, dry thionyl chloride for 2 h.



Scheme 4.1 Synthesis of piperidine analogues **131** and **132**. Reagents and conditions: (i) SOCl₂, reflux. (ii) **124**, Et₃N, DCM. (iii) **119**, Et₃N, DCM.

Excess thionyl chloride was removed in vacuo to give **94** as a yellow solid, which was used without further purification. The HCl salt of the piperidine analogue (see chapter 3) was stirred in dry CH₂Cl₂ under a nitrogen atmosphere and the acid chloride then added dropwise at 0 °C to afford, after 1 h, compound **131** in 55 % yield. The structure was confirmed by NMR, which showed the naphthoyl protons as a doublet at 8.07 ppm and a multiplex at 7.33-7.28 ppm. The NH proton appeared at 6.51 ppm and the two methyl protons as singlets at 3.95 and 2.65 ppm. The CH₂ signals appeared as triplets at 3.61 and 2.63 ppm. The piperidine ring hydrogens were all multiplets at 1.30, 1.55, 2.07, 2.21 and 2.37 ppm. Compound **132**, the hydroxy (non-alkylating) version was synthesised using the same route but employing 1-(2-aminoethyl)-piperidine-3-ol in place of **131** at the ultimate coupling to give the final product **132** (61 % yield). The structure was confirmed by NMR with the naphthoyl protons as a doublet at 8.04 ppm and a multiplet at 7.32-7.28 ppm. The NH proton appeared at 6.51 ppm and the two methyl protons gave singlets at 3.94 and 2.64 ppm. The OH gave a singlet at 3.76 ppm whereas the CH₂ signals appeared as triplets at 3.60 and 2.59 ppm. The benzoyl mono-alkylating analogue

133 (**Figure 4.4**) was also prepared from benzoyl chloride and the piperidine mustard analogue.



Scheme 4.2 Synthesis of analogue **133**. Reagents and conditions: **124**, Et₃N, DCM.

4.2 DNA Unwinding Studies of Piperidine Based analogues

Compound **131** was investigated regarding unwinding of supercoiled DNA and was shown to unwind/relax DNA in a similar fashion to the azinomycin analogue **3** (**Figure 4.3**). Complete DNA unwinding was observed at a 1:1 ratio of [drug] to [base pairs]. **131** appeared to bind reversibly to DNA as indicated by the prevention of unwinding ability in the presence of EtBr.

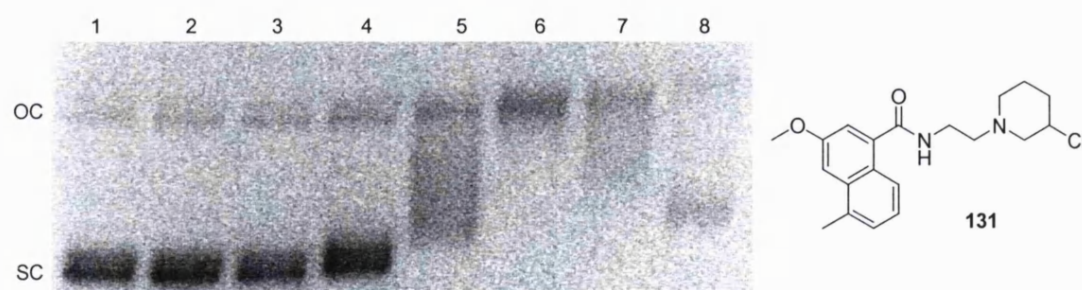


Figure 4.3 Effect of **131** on the electrophoretic mobility of ϕ F174 plasmid DNA. Lane 1 DNA only, lanes 2-8 10^{-3} , 10^{-2} , 10^{-1} , 1, 10.0, 20, 30 drug/bp ratio. DNA ($3.84 \mu\text{M}$). SC = Supercoiled DNA, OC = Open Circular DNA.

Compound **132**, the hydroxy analogue of **131** has no alkylation functionality and does not unwind the duplex even at drug base pair ratios of 30:1 (**Figure 4.4**).

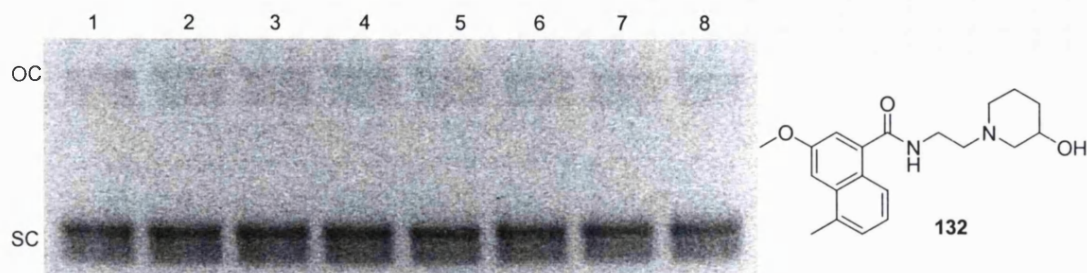


Figure 4.4 Effect of **132** on the electrophoretic mobility of $\phi F174$ plasmid DNA. Lane 1 DNA only, lanes 2-8 10^{-3} , 10^{-2} , 10^{-1} , 1, 10.0, 20, 30 drug/bp ratio. DNA ($3.84 \mu\text{M}$). SC = Supercoiled DNA, OC = Open Circular DNA.

133 was prepared as an analogue to **132** that possessed the alkylating subunit but with a benzene ring in place of the naphthoyl group in order to verify whether alkylation and subsequent interaction of the benzoyl group with the DNA will be enough to effect unwinding/relaxation. This compound showed no DNA unwinding (**Figure 4.5**). In order to assess DNA alkylation, an experiment to study nicking of the helix by **133** was also carried out. Using similar conditions to the DNA unwinding experiment, the samples were heated to 80°C for 10 min to facilitate DNA nicking. **133** failed to show DNA damage-induced DNA relaxation even at drug/basepair ratio of 30 (**Figure 4.6**). However, when unwinding reaction samples of (2*S*, 3*S*)-**3** and **131** were heat treated as for **133**, there were no bands indicating the electrophoretic mobility of DNA, perhaps due to total fragmentation of the plasmid DNA as result of DNA alkylation of several bases spanning the length of the molecule.

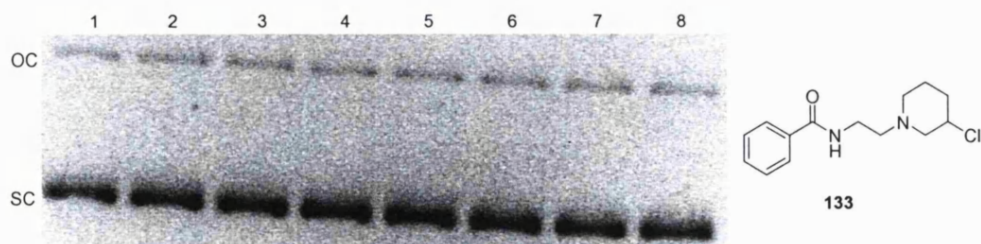


Figure 4.5 Effect of **133** on the electrophoretic mobility of $\phi F174$ plasmid DNA. Lane 1 DNA only, lanes 2-8 10^{-3} , 10^{-2} , 10^{-1} , 1, 10.0, 20, 30 drug/bp ratio. DNA ($3.84 \mu\text{M}$). SC = Supercoiled DNA, OC = Open Circular DNA.

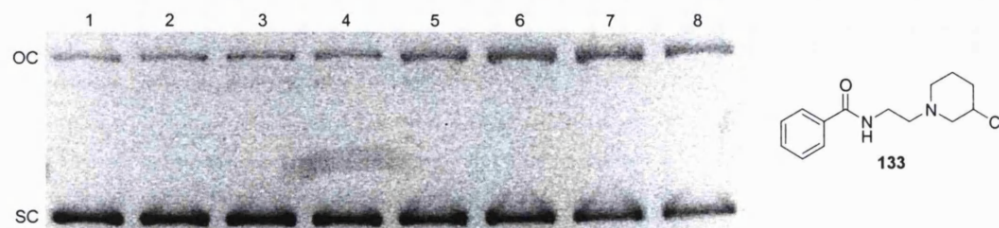
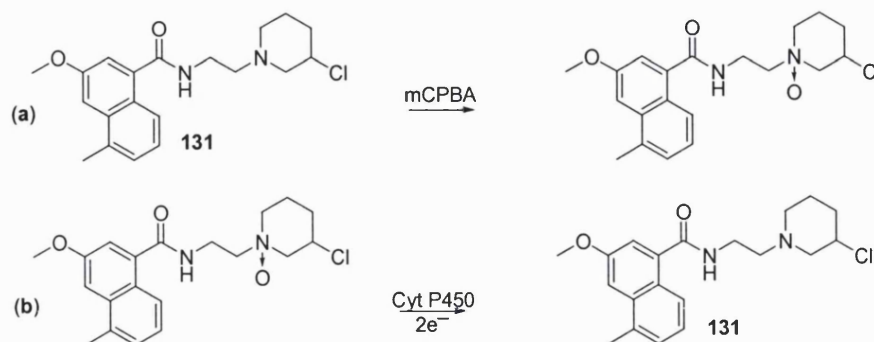


Figure 4.6 Effect of **133** on the electrophoretic mobility of ϕ F174 plasmid DNA. Lane 1 DNA only, lanes 2-8 10^{-3} , 10^{-2} , 10^{-1} , 10^0 , 10^1 , 20, 30 drug/bp ratio. DNA ($3.84 \mu\text{M}$). SC = Supercoiled DNA, OC = Open Circular DNA.

This result suggests that alkylation is necessary for DNA unwinding and also that a DNA affinic chromophore is needed for the chloro-piperidine and epoxide side chains to alkylate DNA efficiently. It has been shown that (2*S*, 3*S*)-**3** incorporating the naphthoate chromophore does have a weak affinity towards DNA. Compared to the naphthoyl-based analogue (2*S*, 3*S*)-**3**, the benzoyl-based analogue **133** appears to have an even weaker intrinsic affinity for DNA. Epoxide analogues, which are not coupled to the naphthoyl chromophore, are $10000\times$ less cytotoxic than molecules incorporating the naphthoate group.⁷²

The ability of the mustard containing chromophore to interact with DNA and elicit a similar effect to (2*S*, 3*S*)-**3** the azinomycin metabolite presents an interesting prospect. This is because the piperidine mustards can be converted to the *N*-oxide derivative (see **Scheme 4.3**). It is anticipated that these *N*-oxides will lose their ability to interact with DNA until metabolised *in vivo* in oxygen deficient cells under reducing conditions.

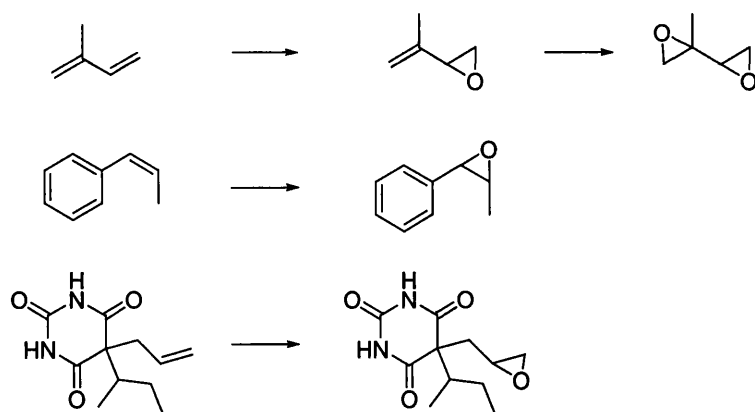


Scheme 4.3 (a) Mode of formation of *N*-oxide of **131**. (b) The proposed route of possible biotransformation to the active compound **131**.

4.3 The Bio-oxidative Prodrug Activation Pathway

The results obtained in this work lead to the conclusion that the epoxide functionality is vital to the activity of the azinomycins and the azinomycin analogues (chapter 2). Removal of this group leads to loss of cytotoxic activity in both the simple and extended analogues.

Mammals are equipped with a variety of enzyme systems that catalyse the transformation of xenobiotics to form, in general, more polar metabolites. Phase I or functionalisation reactions proceed by oxidative, reductive and hydrolytic pathways and leads to the introduction or exposure of a functional group. Phase II or conjugation reactions may modify the newly introduced functional group to form *O*- and *N*-glucuronides, sulfate esters and glutathione conjugates. The general pathway for the metabolism of an olefin function is its oxidation to an epoxide.¹³³ In animals, this transformation is catalysed by CYP-450 enzymes. Many substrates such as poly aromatic hydrocarbons (PAHs), compounds with conjugated and isolated double bonds have been shown to be metabolised by CYP-450 enzymes in vivo and in vitro (Scheme 4.4).^{133,134,135}

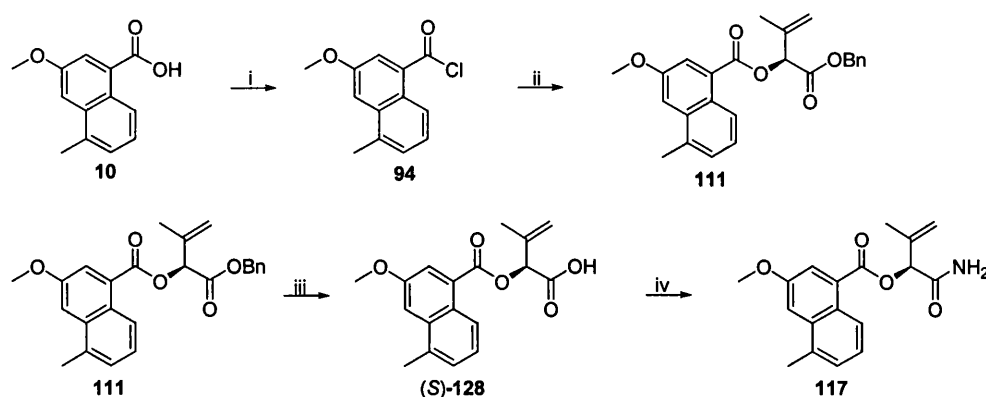


Scheme 4.4 The epoxidation of isoprene, styrene and secobarbital by cytochrome P-450

As the premier site of action of the azinomycin and its analogues is the epoxide functionality, the compounds **117** and **118** in which the epoxide is substituted with the alkene precursor, were designed and synthesised in order to investigate whether this novel analogue will benefit from the CYP-450 metabolism pathway and whether this will lead to enhanced selectivity in vivo.

4.4 Chemistry Results

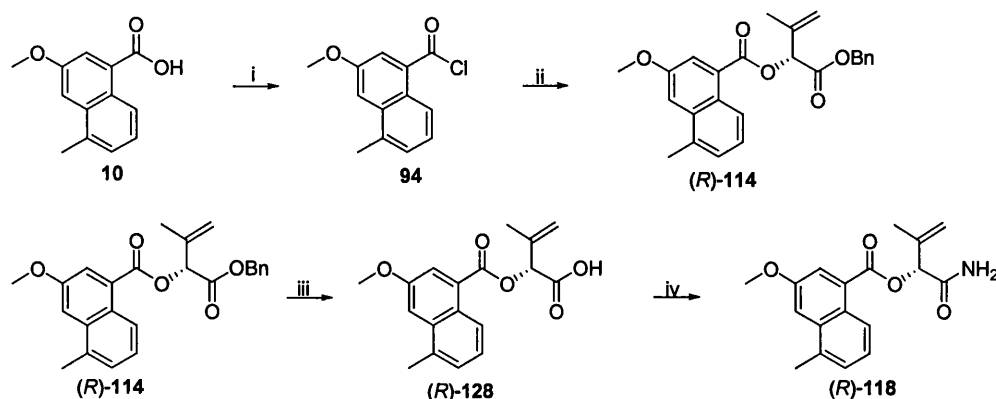
The novel alkene amides were prepared from the carboxylic acid **10** in four steps. The acid chloride **94** was coupled to the benzyl hydroxybutenoate by dropwise addition to a stirred solution of alcohol together with Et₃N in dry CH₂Cl₂ under a nitrogen atmosphere at 0 °C. After 4 h the reaction was quenched with H₂O, extracted with CH₂Cl₂ and purified to give **111** in 65 % yield. Proton NMR analysis confirmed the structure and showed the alkenyl protons as multiplets at 5.33 and 5.18 ppm. The benzyl CH₂ protons also appeared as a multiplet at 5.31 ppm, the H-2 proton was detected at 5.77 ppm and the methyl hydrogens had values of 2.68 ppm for the aromatic methyl and 3.96 ppm for the methoxy methyl.



Scheme 4.5 Synthesis of analogue 117. Reagents and conditions: (i) Thionyl chloride, reflux. (ii) (S)-**29**, Et₃N, DCM. (iii) Pd(OAc)₂, Et₃N, Et₃SiH. (iii) H₂, Pd-C, Methanol. (iv) Et₃N, PyBOP, HOBt, NH₃.

Initial steps to selectively deprotect the benzyl group using catalytic Pd-C led to concomitant reduction of the double bond to the corresponding alkane **113**. The benzyl group was selectively deprotected using catalytic Pd(OAc)₂.¹³⁶ A solution of the Pd(OAc)₂, Et₃N and Et₃SiH in dry CH₂Cl₂ was stirred at RT under N₂ for 15 min. A solution of the ester **111** in dry CH₂Cl₂ was then added dropwise. The mixture was stirred at RT overnight before quenching the reaction by the addition of NH₄Cl. After extraction with Et₂O the alkenyl carboxylic acid was recovered in 90 % yield. This acid was then treated with 35 % NH₃, Et₃N, HOBt and PyBOP to give the amide (S)-**117** in 66 % yield. NMR analysis showed the NH₂ protons as broad singlets at 6.13 and 5.65 ppm whereas the H-2 proton appeared at 5.87 ppm. The alkene methylene

protons were identified as two multiplets at 5.36 and 5.21 ppm, and the methyl groups as singlets at 3.95 (OCH₃), 2.52 (Ar-CH₃) and 1.96 ppm (CH₃). The aromatic protons on the naphthalene chromophore were at 8.65 (1H), 7.90 (1H), 7.50 (1H) and 7.36 ppm (2H). The stereoisomer, compound (*R*)-118 was synthesised using the same route but employing (*R*)-hydroxy butenoate.



Scheme 4.6 Synthesis of analogue 118. Reagents and conditions: (i) SOCl₂, reflux. (ii) (*R*)-29, Et₃N, DCM. (iii) Pd(OAc)₂, Et₃N, Et₃SiH. (iv) Et₃N, PyBOP, HOBt, NH₃.

4.5 Preliminary Biological investigations of Potential Bio-oxidative Prodrugs

Initial cytotoxicity studies in the osteosarcoma cell lines U2-OS and HoeR revealed that the alkene amide analogues 117 and 118 were not cytotoxic compounds whereas their epoxide counterparts (2*S*, 3*S*)-3, (2*S*, 3*R*)-3, (2*R*, 3*R*)-3, (2*R*, 3*S*)-3 demonstrated good activity in these cell lines (**Table 2.1**). This result is encouraging since any potential prodrug must be inactive until metabolised.

Panel/ Cell line	IC ₅₀ (nM) of compound						
	(2 <i>S</i> , 3 <i>S</i>)-3	(2 <i>S</i> , 3 <i>R</i>)-3	(2 <i>R</i> , 3 <i>R</i>)-3	(2 <i>R</i> , 3 <i>S</i>)-3	117	118	113
U2-OS	15	120	40	40	>10 000	>10 000	>10 000
HoeR	14	121	40	45	>10 000	>10 000	>10 000

Table 2.1 IC₅₀ values in U2-OS and HoeR. U2 OS is a human osteosarcoma cell line, HoeR is a Hoechst415 resistant version of U2-OS.

In figure 4.7 the result shows the alkene amide **117** with no alkylation functionality does not unwind DNA.

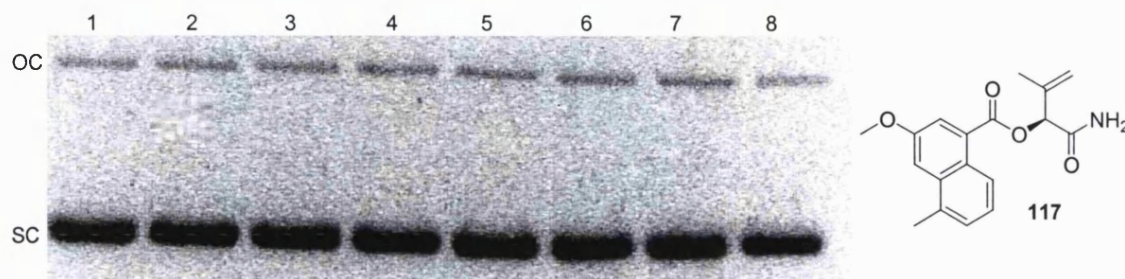


Figure 4.7 Effect of **117** on the electrophoretic mobility of $\phi F174$ plasmid DNA. Lane 1 DNA only, lanes 2-8 10^{-3} , 10^{-2} , 10^{-1} , 1, 10.0, 20, 30 drug/bp ratio. DNA ($3.84 \mu\text{M}$). SC = Supercoiled DNA, OC = Open Circular DNA.

4.5.1 Preliminary Metabolism Studies

Table 4.1 shows that **117** lacks cytotoxic activity in U2-OS and HoeR cell lines in vitro at concentrations as high as $10 \mu\text{M}$. Further studies of **117** in wild type CHO cells and CHO cells that have been transfected with CYP3A4* revealed that the prodrug **117** appears more cytotoxic in CYP3A4 CHO cells compared to wild type (absent in CYP3A4) (**Figure 4.8**). By comparison the epoxide (active) compound has high cytotoxicity in either cell line. This is an initial indicator that shows that the alkene functionality can indeed be metabolised by cytochrome P-450 enzymes to a compound, which is more cytotoxic than the parent alkene precursor.

* Cytochrome P-450 sub family 3A4

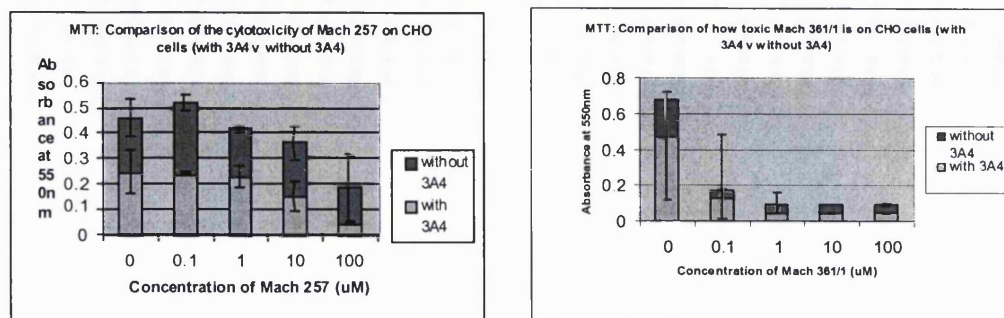


Figure 4.8 (a) Cytotoxicity of mach 257 (**117**) on CHO cells (with or without CYP3A4). (b) Cytotoxicity of mach 361/1 ((2*S*, 3*S*)-**3**) on CHO cells (with or without CYP3A4).

4.6 Discussion

The bio-reductive prodrug candidate **131** was synthesised from the reaction of naphthoate acid chloride **94** and the chloro-piperidine analogue **124**. The hydroxy (non-alkylating) analogue version of **131** (**132**) was prepared in a similar fashion from the piperidine alcohol and **94**. Compound **131** is the first candidate of a totally synthetic analogue of the azinomycin metabolite **3**. Significantly it unwinds supercoiled DNA as was observed for the natural compound. The data generally supports the principle that the azinomycins and their synthetic analogues act by alkylating and covalently modifying DNA.

The chloroalkyl analogue agents alkylate DNA through the aziridinium ion formed as a result of displacement of the chloride ion by the lone pair on nitrogen. It has been shown that *N*-oxide derivatives of tertiary amines render the lone pair unavailable for nucleophilic attack.¹²⁷ Derivatisation of the tertiary amine in the piperidine ring to the corresponding *N*-oxide should therefore prevent formation of the aziridinium ion and consequently DNA alkylation. This prospect is highly attractive since **131** has been shown to preserve the DNA affinity seen in the natural compounds. Testing of this principle awaits synthesis of the piperidino mustard *N*-oxide derivative. The closely related analogue **111** in which the naphthoyl chromophore is substituted for a benzoyl group shows no DNA unwinding and no DNA nicking when heated to 80 °C suggesting that this analogue has little affinity for DNA.

It has been shown previously that microsomal enzymes are capable of oxidising carbon-carbon double bonds to their corresponding epoxides. Compounds **117** and **118**, which are designed to be further metabolised to the active agent by

cytochrome P-450 family of enzymes, have satisfied the first criteria of a potential prodrug. This class of analogues have no cytotoxic potency and do not interact with DNA in vitro. They also are more cytotoxic in CYP 3A4 containing cells suggesting that CYP oxidation is contributing to their activity and therefore constitute a very attractive class of compounds from an anticancer prodrug development point of view.

Chapter 5

Biology and Chemistry Experimental

5.0 Experimental Details

Chemicals and Reagents

All chemicals were supplied by Aldrich, Lancaster and VWR. PyBOP and HOBt were supplied by Nova Biochem. Silica for column chromatography: particle size 35-70 μm and 20-35 μm , was supplied by VWR. Aluminium backed thin layer chromatography plates were supplied by VWR, Poole, Dorset, England.

Biochemicals

$[\gamma\text{-}^{32}\text{P}]$ ATP was purchased from Amershambiotech. T_4 polynucleotide kinase and Hind III were supplied by Promega and pUC 18 and ϕF174 plasmid DNA were supplied by Sigma.

Sample Analysis

Melting points were determined with a Stuart Scientific SMP3 Melting Point Apparatus. ^1H and ^{13}C NMR spectra were measured on a Bruker Avance AM 400 (400 MHz) spectrometer. NMR spectra were processed using a Bruker XWIN NMR 3.5 program. Elemental analysis was performed by Kersti Karu using a Carlo Erba CHN1108 Elemental Analyser. IR was recorded using a Nicolet Smart Golden Gate Spectrometer (Avatar 360 FT-IR E.S.P). Mass spectra were obtained on a ZAB-SE4F. Optical rotation was recorded using a Bellingham and Stanley ADP 220 polarimeter.

5.1 DNA Unwinding Assay

5.1.1 Preparation of Ethidium Bromide Free Electrophoresis Gel

A suspension of 1.0 g of agarose in 100 ml of 1 × TAE was heated to boiling with stirring. The clear solution was allowed to cool to approximately 80 °C. An 8-tooth comb was inserted into the gel casting rig and the hot agarose was poured into the rig. The gel was allowed to set (~ 1 h). When set, the comb was removed and the gel was placed in an electrophoresis chamber. The chamber was then filled with 1 × TAE buffer making sure the gel is completely covered and that no air bubbles are left in the wells.

5.1.2 Preparation of Electrophoresis Gel Containing Ethidium Bromide

As above except 1 × TAE buffer contains 0.5 µg/ml of ethidium bromide.

5.1.3 Protocol for DNA Unwinding Assay

Molecular weight of ϕ X174 plasmid DNA is 3.5×10^6 daltons, 5386 base pairs. Therefore 0.25 µg in 10 µl gives 3.84×10^{-4} µmoles. A 10:1 agent/basepair ratio requires a stock concentration of agent of 3.84×10^{-2} µmoles/µl (1 in 10 dilution). Appropriate dilutions were made for other ratios. Stock ϕ 174 plasmid DNA solution is 1 µg/µl).

ϕ X174 plasmid DNA (2 µg) was suspended in 54 µl of Tris-HCl buffer (pH 8.0, 50 mM) and 7 µl (0.25 µg) pipette into small clearly labelled eppendorf tubes. Each agent concentration (1 µl) and Tris-HCl buffer (2 µl) were added to each DNA solution. DMSO (1 µl) and Tris-HCl buffer (2 µl) were added to the control and the mixture incubated at 37 °C for 1 h. The incubation was stopped by the addition of 20 % glycerol in Tris-HCl loading buffer (4 µl). The total amount in each tube (14 µl) was loaded into each well and the gel electrophoresed at 50 V for 3 h.

5.1.4 Ethidium Bromide Staining of Electrophoresed Gel

The electrophoresed gel was placed in a container containing $1 \times$ TAE with ethidium bromide (50 μ l of a 10 mg/ml solution in 1 litre of TAE) and gently agitated for 1.5 h. The ethidium bromide solution was poured off and the process repeated. Water was added to the gel in the container and gently agitated for 20 min. (to wash off excess ethidium bromide). The gel was then visualised with a UV transilluminator and photographed with a digital camera.

5.2 Agarose Gel DNA Cross-linking Assay

5.2.1 Linearisation of pUC 18 plasmid DNA

A mixture of pUC 18 plasmid DNA (96 μ l, 22.752 μ g), REact 2 buffer (12 μ l), and H₂O (9 μ l) was vortexed in a sterile eppendorf tube and the restriction enzyme Hind III (3 μ l) added. The sample was then incubated at 37 °C for 1 h. For the purpose of precipitating the DNA, sodium acetate (12 μ l, 3 M), tRNA (1 μ l), glycogen (1 μ l) and 95 % ethanol (396 μ l) were added and the sample vortexed and placed on a dry ice/ethanol bath for 10 min. Following centrifugation at 13 000 rpm for 10 min., the supernatant was discarded and the pellet washed once with 70 % EtOH (200 μ l) and further centrifuged and the supernatant removed. The pellet was lyophilised and the dry DNA pellet resuspended in dH₂O (304 μ l).

5.2.2 Dephosphorylation of Linearised pUC 18 plasmid DNA

Linearised pUC 18 plasmid DNA (80 μ l), BAP buffer 10 \times (10 μ l), H₂O (8 μ l) and bacterial alkaline phosphatase (BAP) 3 μ l were mixed and the sample incubated at 65 °C for 1 h. The sample was allowed to cool to room temperature and 2 vols. (200 μ l) of phenol:chloroform:isoamyl alcohol (1:24:1) added and the mixture vortexed and centrifuged for 4 min. The aqueous layer (DNA) was removed and 1 vol. of H₂O (100 μ l) was added to the organic phase and the mixture was vortexed, spun and the aqueous layer removed. The combined aqueous layers was washed with 1 vol. of chloroform (300 μ l). After pulse spinning, the aqueous layer was removed and the volume made up to 400 μ l with dH₂O. The DNA solution was aliquoted into four

eppendorf tubes each containing 100 μ l (\sim 5 μ g). Each aliquot was precipitated with 3 M NaOAc (10 μ l) and 95 % ethanol (330 μ l). The precipitation mixture was vortexed and placed in a dry ice/ethanol bath (10 min.), spun and the supernatant removed. The DNA pellet was lyophilised and the pellet resuspended in dH₂O (10 μ l).

5.2.3 5'-End Labelling of Linearised and Dephosphorylated DNA

Forward reaction buffer 5 \times (4 μ l), γ ³²P-ATP (1 μ l), H₂O (4 μ l) and T4 polynucleotide kinase (1 μ l) were added to a sterile eppendorf containing a mixture of linearised dephosphorylated pUC 18 plasmid DNA (10 μ l, \sim 5 μ g) and the reaction mixture incubated at 37 °C for 1 h. 7.5 M NH₄OAc (20 μ l) and 95 % EtOH (120 μ l) were added. The mixture was cooled, spun, and lyophilised. The pellet was re-suspended in 0.3 M NaOAc, 10 mM EDTA (50 μ l) and 95 % ethanol (150 μ l) and the mixture cooled, spun and lyophilised after which the pellet was washed with 70 % cold ethanol (2 \times 100 μ l). Following removal of supernatant and lyophilisation the labelled DNA was re-suspended in dH₂O (40 μ l) to give a 125 ng/ μ l stock solution. 10 μ l (\sim 1000 ng) of this stock solution is further diluted to 100 μ l of which 10 μ l (\sim 100 ng) is used for each drug reaction lane.

5.2.4 Drug Treatment of Labelled DNA

To 10 μ l (\sim 100 ng) of ³²P-radiolabelled DNA was added x μ l of a drug dilution (where x is between 1-15 μ l) and y μ l of TeoA buffer to give a final volume of 50 μ l. The samples were incubated at 37 °C for the appropriate time and the reactions terminated by addition of equal volumes (50 μ l) of stop solution (0.6 M sodium acetate, 20 mM EDTA, 100 μ g/ml tRNA) and the DNA precipitated by addition of 3 volumes of 95 % ethanol. After removal of the supernatant, the DNA was dried by lyophilisation. Each dried drug treated sample and the single stranded control was initially dissolved in strand separation buffer (30 % DMSO, 1 mM EDTA, 0.04 % bromophenol, 0.04 % xylene cyanol) and heat denatured at 90 °C for 2 min, and chilled immediately in an ice-water bath prior to loading. The double strand undenatured control sample was dissolved in 10 μ l loading buffer (6 % sucrose, 0.04 % bromophenol blue) and loaded directly. The heat denaturing proved unsuccessful for this class of compounds, therefore the drug treated samples and the single strand

control were alkali denatured by adding the alkali denaturing buffer (0.25 M NaOH, 0.04 % bromophenol blue, 6 % sucrose) and the samples loaded directly. Double strand control is always dissolved in sucrose loading buffer irrespective of how denaturing is achieved. Samples were electrophoresed on 20 cm long 0.8 % horizontal agarose gels submerged in 1 × TAE buffer at 40 V for 16 h. Gels were then covered with cling film and dried for 2 h at 80 °C onto one layer of Whatman 3 MM paper and one layer of DE81 filter papers on a vacuum connected BIO-RAD gel drier. Autoradiography was performed using Kodak hyper film for 5 h at −70 °C in a cassette with an intensifying screen.

5.3 Chemistry Experimental

Benzyl 3-methyl-2-enoate [31]

A stirred solution of 3,3-dimethylacrylic acid (14 g, 0.140 mol) and tetra-*n*-butyl ammonium iodide (4.1 g, 11.7 mmol) in chloroform (100 ml) at room temperature was treated with KOH (8.51 g, 0.152 mol) in water (50 ml) followed by benzyl bromide (13.91 ml, 0.117 mol). The resulting two-phase mixture was heated at reflux for 18 h and, on cooling, water (150 ml) was added. The organic layer was separated and the aqueous layer extracted with dichloromethane (3 × 100 ml). The combined organic layers were dried (MgSO₄), filtered, and concentrated in *vacuo* to give a yellow oil. Flash chromatography (5% EtOAc-hexane) gave benzyl 3-methylbut-2-enoate as a yellow liquid (21.56 g, 81 %); IR ν_{\max} (neat)/cm⁻¹ 1717 (C=O), 1649 (olefinic C=C), 1453 (aromatic C=C); ¹H NMR, δ_{H} (500 MHz, CDCl₃) 7.37-7.31 (5H, m, ArH), 5.75(1H, s, CH), 5.15(2H, s, CO₂CH₂Ph), 2.19(3H, s, CH₃), 1.90(3H, s, CH₃); δ_{C} (100 MHz; CDCl₃) 166.68 (C-1), 157.56 (C-3), 136.80 (ArC), 128.79 (ArCH), 128.39 (ArCH), 128.29 (ArCH), 116.10 (C), 65.64 (CH₂), 27.70 (CH₃), 20.56 (CH₃) FAB MS *m/z* 190 [(M⁺), 41 %], 191 [(M + H)⁺, 70%], 213 [(M + Na)⁺, 10 %], fragments [181, 22 %], [173, 39 %]. Anal. calcd. C₁₂H₁₄O₂ C, 75.76 %; H, 7.42 %. Found: C, 75.40 %; H, 7.49 %.

(2*R*)-Benzyl 2,3-dihydroxy-3-methylbutanoate [(*R*)-32]

A solution of AD-mix- α (50 g), methane sulphonamide (3.39 g, 35.7 mmol) and NaHCO₃ (8.99 g, 0.107 mol) in *t*-BuOH (136 ml) and H₂O (136 ml) was prepared at room temperature. The reaction mixture was cooled to 0 °C. Benzyl-3-methylbut-2-enoate (6.78 g, 35.68 mmol) was added in one portion and the orange heterogeneous slurry stirred at 4 °C for 60 h. Anhydrous sodium sulphite (53.55 g, 0.425 mol) was added at 4 °C and the reaction mixture allowed to warm to room temperature and stirred for 1 h. EtOAc was added to the resulting mixture and, after separation of the layers, the aqueous phase was further extracted with EtOAc. The combined organic extracts were washed with 2M KOH, dried (MgSO₄), filtered and concentrated in *vacuo* to give a pale yellow oil. Flash chromatography (30% EtOAc-hexane) provided (2*R*)-benzyl 2,3-dihydroxy-3-methylbutanoate as a pale yellow oil (6.64 g, 83 %). $[\alpha]_{\text{D}}^{22}$ -8.5 (*c* 1.06 CH₂Cl₂), lit.⁴⁷ $[\alpha]_{\text{D}}^{22}$ -10.8 (*c* 1.0 EtOH); IR ν_{\max}

(neat)/cm⁻¹ 3331 (OH), 1606 (C=O), 1494 (aromatic C=C); ¹HNMR (CDCl₃, 500 MHz) δ 7.37-7.34 (5H, m, ArH), 5.30-5.27 (1H, d, *J* = 12.0 Hz, CO₂CH₂Ph), 5.24-5.21 (1H, d, *J* = 12.0 Hz, CO₂CH₂Ph), 4.01-3.99 (1H, d, *J* = 6.8 Hz, H-2), 3.20-3.18 [1H, br d, *J* = 6.8 Hz, C-2(OH)], 2.57 [1H, br s, C-3(OH)], 1.26 (3H, s, CH₃), 1.17 (3H, s, CH₃); δ_C(100 MHz; CDCl₃) 173.03 (C-1), 134.73 (ArC), 128.78 (ArCH), 128.78 (ArCH), 128.63 (ArCH), 72.13 (C-2), 67.74 (CH₂), 25.66(CH₃), 24.96(CH₃); FAB MS *m/z* [357 (M + Cs)⁺, 90 %], [247 (M + Na)⁺, 100 %], [225 (M + H)⁺, 31 %], fragments [207, 14 %], [181, 13 %]. Anal. Calcd. C₁₂H₁₆O₄ C, 64.27 %; H, 7.19 %. Found: C, 64.15 %; H, 7.40 %.

(2S)-Benzyl 2,3-dihydroxy-3-methylbutanoate [(S)-32]

A stirred solution of AD-mix-β (50 g), methane sulphonamide (3.39 g, 35.66 mmol) and NaHCO₃ (8.99 g, 0.107 mol) in *t*-BuOH (136 ml) and H₂O (136 ml) was prepared at room temperature. The reaction mixture was cooled to 0 °C. Benzyl-3-methylbut-2-enoate (6.78 g, 35.68 mmol) was added in one portion and the orange heterogeneous slurry stirred at 4 °C for 60 h. Anhydrous sodium sulphite was added at (53.55 g, 0.425 mmol) 4 °C and the reaction mixture allowed to warm to room temperature and stirred for 1 h. EtOAc was added to the resulting mixture and, after separation of the layers, the aqueous phase was further extracted with EtOAc. The combined organic extracts were washed with 2M KOH, dried (MgSO₄), filtered and concentrated *in vacuo* to give a pale yellow oil. Flash chromatography (30 % EtOAc-hexane) provided (2S)-benzyl 2,3-dihydroxy-3-methylbutanoate as a pale yellow oil (6.50 g, 81 %). [α]_D²² + 6.1 (*c* 1.0 CH₂Cl₂); ν_{max} (neat)/cm⁻¹ 3335 (OH), 1608 (C=O), 1492 (aromatic C=C) ¹HNMR (CDCl₃, 400 MHz) δ 7.38-7.36, (5H, m, ArH), 5.30-5.27 (1H, d, *J* = 12.0 Hz, CO₂CH₂Ph), 5.24-5.21 (1H, d, *J* = 12.0 Hz, CO₂CH₂Ph), 4.01-3.99 (1H, d, *J* = 6.8 Hz, H-2), 3.18-3.16 [1H, d, *J* = 6.8 Hz, C-2(OH)], 2.55 [1H, br s, C-3(OH)], 1.26 (3H, s, CH₃), 1.17 (3H, s, CH₃). δ_C(100 MHz; CDCl₃) 173.27 (C-1), 134.97 (ArC), 128.03 (ArCH), 128.99 (ArCH), 128.87 (ArCH), 72.37 (C-2), 67.99 (CH₂), 25.89 (CH₃), 25.21 (CH₃); FAB MS *m/z* [247 (M + Na)⁺, 95 %], [225 (M + H)⁺, 31 %], fragments [207, 15 %], [180, 21 %]. Anal. Calcd. C₁₂H₁₆O₄ C, 64.27 %; H, 7.19 %. Found: C, 64.99 %; H, 7.31 %.

(2*S*)-Benzyl 3-hydroxy-2-(methanesulfonyloxy)-3-methylbutanoate [(*S*)-90]

Methanesulfonyl chloride (2.14 ml, 27.65 mmol) was added dropwise to a stirred solution of (2*S*)-benzyl 2,3-dihydroxy-3-methylbutanoate (5.9 g, 26.34 mmol) and Et₃N (5.50 ml, 39.53 mmol) in dry CH₂Cl₂ (50 ml) at 0 °C under a nitrogen atmosphere. The reaction mixture was stirred at 4 °C for 4 h and then saturated aqueous sodium hydrogen carbonate (50 ml) was added. The organic layer was separated and aqueous layer extracted with CH₂Cl₂ (3 × 50 ml). The combined organic extracts were then dried (MgSO₄), filtered, and concentrated *in vacuo* to give a yellow oil. Flash chromatography (10 % EtOAc-CH₂Cl₂) provided (2*S*)-Benzyl 3-hydroxy-2-(methanesulfonyloxy)-3-methylbutanoate as a white crystalline solid (5.7 g, 80 %), mp 57 – 60 °C. $[\alpha]_D^{22} - 37$ (*c* 1.1 CH₂Cl₂); IR ν_{\max} (neat)/cm⁻¹ 3515 (OH), 1748 (C=O), 1489 (aromatic C=C); ¹H NMR, δ_H (400 MHz, CDCl₃) δ 7.38-7.36 (5H, m, ArH), 5.32-5.29 (1H, d, *J* = 12.0 Hz, CO₂CH₂Ph), 5.24-5.21 (1H, d, *J* = 12.0 Hz, CO₂CH₂Ph), 4.86 (1H, s, H-2), 3.05 (3H, s, OSO₂CH₃), 2.51 (1H, br s, OH), 1.31 (3H, s, CH₃), 1.30 (3H, s, CH₃). δ_C (100 MHz; CDCl₃) 167.54 (C-1), 134.46 (ArC), 128.89 (ArCH), 128.77 (ArCH), 128.65 (ArCH), 82.90 (C-2), 71.61 (C-3), 67.96 (CO₂CH₂Ph), 38.90 (OSO₂CH₃), 25.75 (CH₃), 25.65 (CH₃). FAB MS *m/z* [325 (M + Na)⁺, 76 %], [303 (M + H)⁺, 99 %], fragments [285, 34 %]. Anal. Calcd. C₁₃H₁₈O₆S C, 51.64 %; H, 6.00 %. Found: C, 51.53 %; H, 6.09 %.

(2*R*)-Benzyl 3-hydroxy-2-(methanesulfonyloxy)-3-methylbutanoate [(*R*)-90]

Prepared as for the 2(*S*) analogue using (2*R*)-benzyl 2,3-dihydroxy-3-methylbutanoate (5.8 g, 26.34 mmol). The product was a white crystalline solid and the yield was 84 %, mp 59 – 61 °C, lit. 57.5 – 59 °C.⁴⁷ $[\alpha]_D^{22} 26.2$ (*c* 1.1 CH₂Cl₂), lit. $[\alpha]_D^{22} 21.5$ (*c* 1.0 EtOH)⁴⁷; IR ν_{\max} (neat)/cm⁻¹ 3515 (OH), 1748 (C=O), 1489 (aromatic C=C); ¹H NMR (CDCl₃, 400 MHz) δ 7.38-7.35 (5H, m, ArH), 5.32-5.30 (1H, d, *J* = 12.0 Hz, CO₂CH₂Ph), 5.24-5.21 (1H, d, *J* = 12.0 Hz, CO₂CH₂Ph), 4.86 (1H, s, H-2), 3.05 (3H, s, OSO₂CH₃), 2.48 (1H, br s, OH), 1.31 (3H, s, CH₃), 1.30 (3H, s, CH₃). δ_C (100 MHz; CDCl₃) 167.55 (C-1), 134.46 (ArC), 128.89 (ArCH), 128.77 (ArCH), 128.65 (ArCH), 82.88 (C-2), 71.61 (C-3), 67.96 (CO₂CH₂Ph), 38.91 (OSO₂CH₃), 25.75 (CH₃), 25.66 (CH₃); FAB MS *m/z* [325 (M + Na)⁺, 91 %], [303 (M + H)⁺, 19 %], fragments [312, 47 %], [251, 70 %], [181, 100 %]. Anal. Calcd. C₁₃H₁₈O₆S C, 51.64 %; H, 6.00 %. Found: C, 51.60 %; H, 6.12 %.

(2S)-Benzyl 2,3-epoxy-3-methylbutanoate [(S)-91]

A stirred suspension of (2R)-benzyl 3-hydroxy-2-(methanesulfonyloxy)-3-methylbutanoate (4 g, 14.81 mmol) and anhydrous K₂CO₃ (14.04 g, 0.132 mol) in dry acetonitrile (30 ml) was heated at reflux under N₂ atmosphere for 48 h. The resulting pale yellow heterogeneous mixture was quenched with water (30 ml) and extracted with dichloromethane (3 x 50 ml). The combined organic extracts were dried (MgSO₄), filtered, and concentrated *in vacuo* to give a yellow liquid. Flash chromatography (10 % EtOAc-hexane) gave (2S)-Benzyl 2,3-epoxy-3-methylbutanoate as a colourless oil (2.62 g, 86%). [α]_D²² 2.6 (*c* 1.1 CH₂Cl₂), [α]_D²⁰ 3.54 (*c* 1.2 EtOH); IR ν_{\max} (neat)/cm⁻¹ 1749 (C=O), 1499 (aromatic C=C); ¹H NMR (CDCl₃, 400 MHz) δ 7.37-7.34 (5H, m, ArH), 5.27-5.24 (1H, d, *J* = 12.0 Hz, CO₂CH₂Ph), 5.21-5.18 (1H, d, *J* = 12.0 Hz, CO₂CH₂Ph), 3.37 (1H, s, H-2), 1.41 (3H, s, CH₃), 1.36 (3H, s, CH₃); δ_{C} (100 MHz; CDCl₃) 168.41 (C-1), 135.24 (ArC), 128.64 (ArCH), 128.56 (ArCH), 128.54 (ArCH), 67.05 (CO₂CH₂Ph), 60.36 (C-2), 59.37 (C-3), 24.28 (CH₃), 18.24 (CH₃). FABMS *m/z* [207 (M + H)⁺, 65 %], [229 (M + Na)⁺, 13 %], fragments [115, 26 %], [108, 23 %]. Anal. Calcd. C₁₂H₁₄O₃ C, 69.88 %; H, 6.84 %. Found: C, 69.91 %; H, 6.94 %.

(2R)-Benzyl 2,3-epoxy-3-methylbutanoate [(R)-91]

Prepared as for (2S)-91 using (2S)-benzyl 3-hydroxy-2-(methanesulfonyloxy)-3-methylbutanoate (5 g, 18.52 mmol). The product was a colourless oil and the yield was 92 %. [α]_D²² - 2.9 (*c* 2.1 CH₂Cl₂); IR ν_{\max} (neat)/cm⁻¹ 1749 (C=O), 1499 (aromatic C=C); ¹H NMR (CDCl₃, 400 MHz) δ_{H} 7.37-7.34 (5H, m, ArH), 5.27-5.23 (1H, d, *J* = 12.0 Hz, CO₂CH₂Ph), 5.21-5.18 (1H, d, *J* = 12.0 Hz, CO₂CH₂Ph), 3.37 (1H, s, H-2), 1.41 (3H, s, CH₃), 1.36 (3H, s, CH₃). δ_{C} (100 MHz; CDCl₃) 168.41 (C-1), 135.24 (ArC), 128.64 (ArCH), 128.56 (ArCH), 128.54 (ArCH), 67.05 (CO₂CH₂Ph), 60.36 (C-2), 59.37 (C-3), 24.28 (CH₃), 18.24 (CH₃); FABMS *m/z* [207 (M + H)⁺, 51 %], fragments [137, 25 %], [119, 19 %], [109, 14 %], [105, 24 %]. Anal. Calcd. C₁₂H₁₄O₃ C, 69.88 %; H, 6.84 %. Found: C, 69.83 %; H, 6.86 %.

(2S)-Benzyl 2-hydroxy-3-methylbut-3-enoate [(S)-29]

A stirred mixture of epoxide (2S)-**91** (2.5 g, 12.14 mmol) and (+/-)-camphor-10-sulfonic acid (0.56 g, 2.4 mmol) in dry toluene (21 ml) was heated at reflux under a N₂ atmosphere for 4 h. On cooling, the heterogeneous mixture was filtered and concentrated *in vacuo*. Flash chromatography (5 % EtOAc-hexane) gave allylic alcohol (2S)-**29** as a colourless liquid (1.98 g, 79 %). $[\alpha]_D^{22}$ 61.8 (*c* 0.8 CH₂Cl₂), lit. $[\alpha]_D^{20}$ 71.7 (*c* 1.1 EtOH)⁴⁷; IR ν_{\max} (neat)/cm⁻¹ 3456 (OH), 1735 (C=O), 1455 (aromatic C=C); ¹H NMR (CDCl₃, 400 MHz) δ 7.36-7.33, (5H, m, ArH), 5.25 (2H, s, CO₂CH₂Ph), 5.14 (1H, s, =CH₂), 5.03 (1H, s, =CH₂), 4.63-4.61 (1H, d, *J* = 5.2 Hz, H-2), 3.10-3.09 [1H, d, *J* = 6.0 Hz, C-2(OH)], 1.72 (3H, s, CH₃). δ_C (100 MHz; CDCl₃) 173.40 (C-1), 141.72 (C-3), 135.07 (ArC), 128.74 (ArCH), 128.64 (ArCH), 128.56 (ArCH), 128.22 (ArCH), 115.29 (=CH₂), 74.89 (C-2), 67.64 (CH₂), 17.74 (CH₃). FABMS *m/z* [338 (M + Cs)⁺, 32 %], [229 (M + Na)⁺, 100 %], [207 (M + H)⁺, 37 %], fragments [189, 26 %], [181, 43 %]. Anal. Calcd. C₁₂H₁₄O₃ C, 69.88 %; H, 6.84 %. Found: C, 69.41 %; H, 6.86 %.

(2R)-Benzyl 2-hydroxy-3-methylbut-3-enoate [(R)-29]

Prepared as for (2S)-**91** using epoxide (2R)-**91** (2.5 g, 12.14 mmol). This gave (R)-**29** as a liquid and the yield was 72 %. $[\alpha]_D^{22}$ -66.4 (*c* 1.0 CH₂Cl₂); IR ν_{\max} (neat)/cm⁻¹ 3456 (OH), 1735 (C=O), 1455 (aromatic C=C). ¹H NMR (CDCl₃, 400 MHz) δ 7.35-7.32, (5H, m, ArH), 5.24 (2H, s, CO₂CH₂Ph), 5.14 (1H, s, =CH₂), 5.03 (1H, s, =CH₂), 4.62 (1H, s, H-2), 3.10 [1H, br s, C-2(OH)], 1.71 (3H, s, CH₃). δ_C (100 MHz; CDCl₃) 173.40 (C-1), 141.71 (C-3), 135.06 (ArC), 128.78 (ArCH), 128.64 (ArCH), 128.56 (ArCH), 128.22 (ArCH), 115.29 (=CH₂), 74.89 (C-2), 67.64 (CH₂), 17.74 (CH₃). FAB MS *m/z* [207 (M + H)⁺, 42 %], [229 (M + Na)⁺, 100 %], [338 (M + Cs)⁺, 53 %], fragments [189, 24 %], [181, 44 %]. Anal. Calcd. C₁₂H₁₄O₃ C, 69.88 %; H, 6.84 %. Found: C, 69.75 %; H, 6.90 %.

(2R, 3R)-Benzyl 3,4-epoxy-2-hydroxy-3-methylbutanoate [(2R, 3R)-30] and (2R, 3S)-Benzyl 3,4-epoxy-2-hydroxy-3-methylbutanoate [(2R, 3S)-30]

mCPBA (2.0 g, 11.58 mmol) was dissolved in chloroform (38 ml) and the solution stirred at 0 °C. (2R)-Benzyl 2-hydroxy-3-methylbut-3-enoate (R)-**29** (1.92 g, 9.32 mmol) dissolved in chloroform (8 ml) was added to the solution at 0 °C. The mixture

was warmed to room temperature and stirred for 18 h. The reaction mixture was filtered and washed with 10 % NaHCO₃, dried with MgSO₄, filtered and concentrated in vacuo. Flash chromatography (0-40% over 1h in EtOAc-hexane) initially eluted the (2*R*, 3*R*)-Benzyl 2-hydroxy-3-methylbut-3-enoate derivative as a viscous oil (600 mg, 38 %). $[\alpha]_D^{22} - 17.9$ (*c* 1.03 CH₂Cl₂); IR ν_{\max} (neat)/cm⁻¹ 3467 (OH), 1737 (C=O), 1456 (Ar C=C); ¹H NMR δ_H (400 MHz; CDCl₃); 7.37-7.35 (5H, m, ArH), 5.31-5.28 (1H, d, *J* = 12.0 Hz, CO₂CH₂Ph), 5.23-5.23 (1H, d, *J* = 12.0 Hz, CO₂CH₂Ph), 4.05 (1H, s, H-2), 2.99-2.98 (1H, d, *J* = 4.8 Hz, H-4), 2.96 (1H, s, OH), 2.64-2.63 (1H, d, *J* = 4.8 Hz, H-4), 1.31 (3H, s, CH₃); δ_C (100 MHz; CDCl₃) 171.98 (C=O), 134.90 (ArC), 128.68 (ArCH), 128.65 (ArCH), 128.45 (ArCH), 73.91 (C-2), 67.74 (CH₂), 56.77 (C-3), 51.71 (C-4), 17.10 (CH₃). FABMS *m/z* [222 (M)⁺, 81 %], [223 (M + H)⁺, 11 %], [245 (M + Na)⁺, 32%], fragments [181, 59 %], [131, 43 %], [107, 41 %].

Further elution gave the (2*R*, 3*S*) compound as an oil (500 mg, 31 %); $[\alpha]_D^{22} - 21.3$ (*c* 1.08 CH₂Cl₂); IR ν_{\max} (neat)/cm⁻¹ 3464 (OH), 1737 (C=O), 1457 (Ar C=C); ¹H NMR δ_H (400 MHz; CDCl₃); 7.36-7.35 (5H, m, ArH), 5.34-5.31 (1H, d, *J* = 12.0 Hz, CO₂CH₂Ph), 5.27-5.24 (1H, d, *J* = 12.0 Hz, CO₂CH₂Ph), 4.01 (1H, s, H-2), 2.86 (1H, s, OH), 2.97 (1H, d, *J* = 4.8 Hz, H-4), 2.64 (1H, d, *J* = 4.5 Hz, H-4), 1.32 (3H, s, CH₃); δ_C (100 MHz; CDCl₃) 171.98 (C=O), 134.90 (ArC), 128.68 (ArCH), 128.65 (ArCH), 128.45 (ArCH), 73.91 (C-2), 67.74 (CH₂), 56.77 (C-3), 51.71 (C-4), 17.10 (CH₃). FABMS *m/z* [223 (M + H)⁺, 29 %], [245 (M + Na)⁺, 65 %], fragments [131, 35 %], [107, 51 %].

(2*S*, 3*R*)-Benzyl 3,4-epoxy-2-hydroxy-3-methylbutanoate [(2*S*, 3*R*)-30] and (2*S*, 3*S*)-Benzyl 3,4-epoxy-2-hydroxy-3-methylbutanoate [(2*S*, 3*S*)-30]

Prepared as for (2*R*, 3*R*)- and (2*R*, 3*S*)-30 using (2*S*-29). Provided (2*S*, 3*R*)-30 as a thick oil (400, 25 %). $[\alpha]_D^{22} 19.1$ (*c* 1.01 CH₂Cl₂); IR ν_{\max} (neat)/cm⁻¹ 3466 (OH), 1734 (C=O), 1458 (Ar C=C). ¹H NMR δ_H (400 MHz; CDCl₃); 7.37-7.35 (5H, m, ArH), 5.30 (1H, d, *J* = 12.3 Hz, CO₂CH₂Ph), 5.24 (1H, d, *J* = 12.3 Hz, CO₂CH₂Ph), 4.05 (1H, s, H-2), 3.06 (1H, s, OH), 2.99 (1H, d, *J* = 4.8 Hz, H-4), 2.65-2.63 (1H, d, *J* = 4.8 Hz, H-4), 1.31 (3H, s, CH₃). δ_C (100 MHz; CDCl₃) 172.1 (C=O), 134.93 (ArC), 128.76 (ArCH), 128.42 (ArCH), 73.80 (C-2), 67.75 (CH₂), 57.76 (C-3), 51.56

(C-4), 16.61 (CH₃). FABMS m/z [222 (M⁺), 80 %], [223 (M + H)⁺, 7 %], [245 (M + Na)⁺, 37 %], fragments [131, 29 %], [107, 50 %].

Further elution gave the (2*S*, 3*S*) compound as a thick oil (500 mg, 31 %). $[\alpha]_D^{22}$ 13.8 (*c* 1.1 CH₂Cl₂), lit. $[\alpha]_D^{22}$ 11.5 (*c* 1.9 EtOH); IR ν_{\max} (neat)/cm⁻¹ 3469 (OH), 1724 (C=O), 1459 (aromatic C=C). ¹H NMR δ_H (250MHz; CDCl₃); 7.37-7.35 (5H, m, ArH), 5.32(1H, d, *J* = 12.3 Hz, CO₂CH₂Ph), 5.25(1H, d, *J* = 12.3 Hz, CO₂CH₂Ph), 4.01 (1H, s, H-2), 3.05 (1H, br s, OH), 2.86-2.85 (1H, d, *J* = 4.8 Hz, H-4), 2.63 (1H, d, *J* = 4.8 Hz, H-4), 1.31 (3H, s, CH₃). δ_C (100 MHz; CDCl₃) 172.0 (C=O), 134.90 (ArC), 128.72 (ArCH), 128.40 (ArCH), 73.97 (C-2), 67.77 (CH₂), 57.73 (C-3), 51.56 (C-4), 16.64 (CH₃). FABMS m/z [222 (M⁺), 73 %], [223 (M + H)⁺, 13 %], [245 (M + Na)⁺, 44 %], fragments [131, 38 %], [107, 44 %].

1-(2-methylphenyl)-2-propanol [92]

o-Tolyl-magnesium bromide 2 M in hexane (46.5 ml, 93 mmol) was added dropwise to a stirred solution of propylene oxide (9.76 ml, 102 mmol) in dry ether (80 ml) at 0 °C under N₂ atmosphere. The mixture was stirred at RT for 18 h after which aqueous NH₄Cl (1M, 140 ml) was added. The organic layer was separated and the aqueous layer extracted with ether (3 x 100 ml). The combined organic layers were then dried (MgSO₄), filtered and concentrated in *vacuo*. Flash column chromatography (20% EtOAc-hexane) provided 1-(2-methylphenyl)-2-propanol (7.54 g, 69%). ¹H NMR (CDCl₃, 400 MHz) δ_H 7.20-7.16 (4H, m, ArH), 4.02 (1H, br s, OH), 2.83-2.71 (1H, m, CH), 2.34 (3H, s, CH₃), 1.57 (2H, d, *J* = 6.4 Hz, CH₂), 1.27 (3H, d, *J* = 6 Hz, CH₃). δ_C (100 MHz; CDCl₃) 136.65 (ArC), 133.05 (ArC), 130.59 (ArCH), 130.87 (ArCH), 127.85 (ArCH), 126.29 (ArCH), 42.97 (CH₂), 30.92 (CH), 23.01 (CH₃), 17.53 (CH₃). FABMS m/z [151 (M + H)⁺, 13 %], fragments [133, 100 %], [119, 47 %].

Chromic acid (Jones reagent) preparation

Sodium dichromate dihydrate (10 g, 34 mmol) was dissolved in H₂O (30 ml) and concentrated H₂SO₄ (7.3 ml, 0.14 mol) was slowly added. The solution was cooled in an ice bath and diluted to 50 ml with H₂O in a graduated flask.

1-(2-methylphenyl)acetone [7]

Chromic acid (30 ml, 0.67 M) was added to a stirred solution of 1-(2-methylphenyl)-2-propanol (4.39 g, 29 mmol) in ether (15 ml) at 0 °C over 5 min. The reaction was followed with TLC. Upon completion H₂O (50 ml) and ether (50 ml) were added. The organic layer was separated and the aqueous layer was extracted with ether (3 x 40 ml). The combined organic layers were dried (MgSO₄), filtered and concentrated *in vacuo*. Flash column chromatography (10 % EtOAc-hexane) provided 1-(2-methylphenyl)acetone (1.93 g, 45 %). ¹H NMR (CDCl₃, 250 MHz) δ_H 7.18-7.13 (4H, m, ArH), 3.71 (2H, s, CH₂), 2.25 (3H, s, CH₃), 2.14 (3H, s, CH₃). δ_C(100 MHz; CDCl₃) δ_C 206.38 (C=O), 136.84 (ArC), 133.16 (ArC), 130.50 (ArCH), 130.37 (ArCH), 127.40 (ArCH), 126.29 (ArCH), 49.15 (CH₂), 29.25 (CH₃), 19.61 (CH₃). FABMS *m/z* [149 (M + H)⁺, 90 %], [171 (M + Na)⁺, 11 %], fragments [135, 100 %], [119, 50 %], [105, 89 %].

Ethyl 3-hydroxy-5-methyl-1-naphthoate [9]

Ketone 7 (1.7 g, 11.5 mmol) was added to a stirred solution of NaOEt (2M, 10 ml) under N₂ atmosphere and stirred for 5 min. Diethyl oxalate (1.7 ml, 12.5 mmol) was added, the reaction mixture was stirred for 2 h and then quenched with water (10 ml) and extracted with EtOAc (3 × 30 ml). The combined organic layers were dried (MgSO₄), filtered and concentrated *in vacuo* providing the crude product (3.85 g). This was dissolved in chloroform (50 ml) and stirred at 0 °C. Concentrated sulphuric acid (10 ml) was added and the mixture was stirred at 0 °C for 2 h. The reaction mixture was carefully poured into water (100 ml) and the organic layer was separated and the aqueous layer extracted with chloroform (3 x 50 ml). The combined organic layers were dried (MgSO₄), filtered and concentrated *in vacuo*. Flash column chromatography (15% EtOAc-hexane) provided ethyl 3-hydroxy-5-methyl-1-naphthoate (1.2 g, 45 %), mp 105–112 °C. ¹H NMR (CDCl₃, 400 MHz) δ_H 8.83-8.81 (1H, m, ArH), 7.82-7.81 (1H, d, *J* = 2.8 Hz, ArH), 7.45-7.44 (1H, d, *J* = 2.4 Hz,

ArH), 7.35-7.34 (2H, m, ArH), 4.50-4.44 (2H, q, $J = 7.2$ Hz, $\text{CO}_2\text{CH}_2\text{CH}_3$), 3.97 (3H, s, OCH_3), 2.67 (3H, s, Ar- CH_3), 1.47-1.44 (3H, t, $J = 7.2$ Hz, $\text{CO}_2\text{CH}_2\text{CH}_3$). δ_{C} (100 MHz; CDCl_3) 167.45 (C=O), 155.95 (ArC), 134.35 (ArC), 133.09 (ArC), 129.92 (ArC), 127.52 (ArCH), 126.77 (ArCH), 124.77 (ArCH), 123.92 (ArCH), 121.32 (ArCH), 107.64 (ArCH), 61.20 (CH_2), 55.50 (OCH_3), 20.12 (Ar- CH_3), 14.35 (CH_3). FABMS m/z [230 (M^+), 100 %], [231 ($\text{M} + \text{H}$) $^+$, 43 %], [253 ($\text{M} + \text{Na}$) $^+$, 5 %], fragments [185, 43 %].

Ethyl 3-methoxy-5-methyl-1-naphthoate [93]

Sodium hydride (195 mg, 4.86 mmol) was added to a stirred solution of ethyl 3-hydroxy-5-methyl-1-naphthoate (860 mg, 3.74 mmol) in dry DMF (12 ml) at RT under N_2 . The mixture was stirred for 30 min and then iodomethane (0.47 ml, 7.48 mmol) was added. After stirring for a further 30 min the reaction mixture was quenched with water (12 ml) and extracted with EtOAc (3×15 ml). The combined organic extracts were washed with water (3×15 ml), dried (MgSO_4), filtered and concentrated *in vacuo*. Flash column chromatography (2 % EtOAc-hexane) gave ethyl 3-methoxy-5-methyl-1-naphthoate (830 mg, 90 %), mp 72-76 °C, lit. 74.5-77 °C⁴⁷. ^1H NMR (CDCl_3 , 400 MHz) δ_{H} 8.83-8.81 (1H, m, ArH), 7.82-7.81 (1H, d, $J = 2.8$ Hz, ArH), 7.45-7.44 (1H, d, $J = 2.4$ Hz, ArH), 7.35-7.34 (2H, m, ArH), 4.50-4.44 (2H, q, $J = 7.2$ Hz, $\text{CO}_2\text{CH}_2\text{CH}_3$), 3.97 (3H, s, OCH_3), 2.67 (3H, s, Ar- CH_3), 1.47-1.44 (3H, t, $J = 7.2$ Hz, $\text{CO}_2\text{CH}_2\text{CH}_3$). δ_{C} (100 MHz; CDCl_3) 167.45 (C=O), 155.95 (ArC), 134.35 (ArC), 133.09 (ArC), 129.92 (ArC), 127.52 (ArCH), 126.77 (ArCH), 124.77 (ArCH), 123.92 (ArCH), 121.32 (ArCH), 107.64 (ArCH), 61.20 (CH_2), 55.50 (OCH_3), 20.12 (Ar- CH_3), 14.35 (CH_3). FABMS m/z [244 (M^+), 100 %], [245 ($\text{M} + \text{H}$) $^+$, 43 %], [267 ($\text{M} + \text{Na}$) $^+$ 3 %], fragments [199, 71 %].

3-methoxy-5-methyl-1-naphthoic acid [10]

Lithium hydroxide (714 mg, 17.08 mmol) was added to a stirred solution of ethyl 3-methoxy-5-methyl-1-naphthoate (830 mg, 3.40 mmol) in THF (18 ml), CH_3OH (12 ml) and H_2O (6 ml) at RT and the reaction was stirred for 18 h. EtOAc (20 ml) was added and the organic phase separated. The aqueous layer was acidified to pH 1 with 2M aqueous HCl and extracted with EtOAc (3×15 ml). The combined organic

layers were washed with brine (20 ml), dried (MgSO₄), filtered and concentrated *in vacuo*. The resulting solid was washed with hexane (20 ml) to give the title acid (690 mg 94%) as a white crystalline solid, mp 180-182 °C (lit. 179-180 °C)⁴⁷ which was used without further purification. ¹H NMR (CDCl₃, 400 MHz) δ_H 8.83-8.81 (1H, m, ArH), 8.06-8.05 (1H, d, *J* = 2.8 Hz, ArH), 7.55-7.54 (1H, d, *J* = 2.8 Hz, ArH), 7.42-7.39 (2H, m, ArH), 3.99 (3H, s, OCH₃), 2.69 (3H, s, Ar-CH₃), 1.47-1.44 (3H, t, CO₂CH₂CH₃). δ_C(100 MHz; CDCl₃) δ_C 172.57 (C=O), 155.86 (ArC), 134.49 (ArC), 133.26 (ArC), 127.79 (ArC), 127.67 (ArCH), 127.11 (ArCH), 125.20 (ArCH), 123.99 (ArCH), 122.75 (ArCH), 109.37 (ArCH), 55.58 (OCH₃), 20.17 (Ar-CH₃). FABMS *m/z* [216 (M⁺), 99 %], [239 (M + Na)⁺, 17 %], fragments [199, 30 %], [158, 18 %].

Ethyl 3-benzyloxy-5-methyl-1-naphthoate [95]

Prepared as for **93** using benzyl bromide (0.063 ml, 0.53 mmol) and (61 mg, 0.27 mmol). The yield was 76 mg, 89 %, mp 89-92 °C. ¹H NMR (CDCl₃, 400 MHz) δ_H 8.54 (1H, d, *J* = 8, ArH), 7.78 (1H, d, *J* = 2.4 Hz, ArH), 7.62 (1H, d, *J* = 2.4 Hz, ArH), 7.55 (2H, m, ArH), 7.37 (5H, m, ArH), 4.32 (2H, q, *J* = 7.2 Hz, CO₂CH₂CH₃), 3.71 (3H, s, OCH₃), 2.62. δ_C(100 MHz; CDCl₃) 168.87 (C=O), 154.55 (ArC), 136.70 (ArC), 133.79 (ArC), 133.09 (ArC), 130.65 (ArC), 128.39 (ArC), 127.83 (ArC), 127.71 (ArC), 127.25 (ArC), 126.04 (ArC), 124.46 (ArC), 123.54 (ArC), 120.81 (ArC), 108.88 (ArC), 69.48 (CH₂), 19.57 (CH₃), 14.35 (CH₃). FABMS *m/z* [320 (M⁺), 97 %], [343 (M + Na)⁺, 13 %].

3-benzyloxy-5-methyl-1-naphthoic acid [96]

Prepared as for **10** using ethyl 3-benzyloxy-5-methyl-1-naphthoate (100 mg, 0.31 mmol). The yield was 81 mg, 89 %, mp 196-199 °C. ¹H NMR (DMSO, 400 MHz) δ_H 8.56 (1H, d, *J* = 8 Hz, ArH), 7.76 (1H, d, *J* = 2.4 Hz, ArH), 7.50 (1H, d, *J* = 2.4 Hz, ArH), 7.53 (2H, m, ArH), 7.37 (5H, m, ArH), 3.31 (1H, br s, OH), 2.64 (3H, s, ArCH₃). δ_C(100 MHz; CDCl₃) 167.79 (C=O), 155.50 (ArC), 136.78 (ArC), 133.67 (ArC), 131.11 (ArC), 130.86 (ArC), 128.31 (ArC), 127.93 (ArC), 127.74 (ArC), 127.65 (ArC), 126.08 (ArC), 125.10 (ArC), 123.54 (ArC), 120.81 (ArC), 108.88 (ArC), 69.48 (CH₃), 20.05 (CH₂). FABMS *m/z* [293 (M + H)⁺, 57 %], [316 (M + Na)⁺, 17 %].

1-Phenylpropan-2-ol [98]

Prepared as for **92** using phenyl-magnesium bromide 1 M in THF (28 ml, 28 mmol) and propylene oxide (3.9 ml, 55 mmol). The yield was 3 g, 80 %. ^1H NMR (CDCl_3 , 400 MHz) δ_{H} 7.31 (5H, m, ArH), 4.09-4.06 (1H, m, CH), 2.87-2.72 (2H, dd, $J = 4.8$ Hz, CH_2), 1.31 (3H, d, $J = 6$ Hz, CH_3). δ_{C} (100 MHz; CDCl_3) 138.51 (ArC), 129.40 (ArC), 128.57 (ArC), 126.50 (ArC), 68.88 (CH_2), 45.82 (CH), 22.81 (CH_3). FABMS m/z [137 ($\text{M} + \text{H}$) $^+$, 52 %], [159 ($\text{M} + \text{Na}$) $^+$, 5 %].

1-Phenylacetone [99]

Prepared as for **92** using 1-phenylpropan-2-ol (3 g, 22 mmol). The yield was (1.5 g, 51 %) ^1H NMR (CDCl_3 , 400 MHz) δ_{H} 7.35 (5H, m, ArH), 3.72 (2H, s, CH_2), 2.19 (3H, s, CH_3); δ_{C} (100 MHz; CDCl_3) 206.33 ($\text{C}=\text{O}$), 134.28 (ArC), 129.40 (ArC), 129.07 (ArC), 128.77 (ArC), 127.07 (ArC), 126.74 (ArC), 51.05 (CH_2), 29.24 (CH_3). FABMS m/z 134 (M^+), 36 %], 135 ($\text{M} + \text{H}$) $^+$, 83 %].

Ethyl 3-hydroxy-1-naphthoate [101]

Prepared as for **9** using 1-phenylacetone (1.1 g, 8.2 mmol). The yield was (0.8 g, 42 %). ^1H NMR (CDCl_3 , 400 MHz) δ_{H} 8.83-8.81 (1H, m, ArH), 7.80 (1H, m, $J = 2.8$ Hz, ArH), 7.83 (1H, d, $J = 2.8$ Hz, ArH), 7.71-7.69 (1H, m, ArH), 7.49-7.42 (2H, m, ArH), 7.35 (1H, d, $J = 2.8$ Hz, ArH), 5.49 (1H, br s, OH), 4.51 (2H, q, $J = 7.2$ Hz, $\text{CO}_2\text{CH}_2\text{CH}_3$), 3.97, 1.46 (3H, t, $J = 7.2$ Hz, $\text{CO}_2\text{CH}_2\text{CH}_3$). δ_{C} (100 MHz; CDCl_3) 167.30 ($\text{C}=\text{O}$), 152.02 (ArC), 135.32 (ArC), 129.24 (ArC) (ArC), 127.05 (ArC), 126.88 (ArC), 125.75 (ArC), 125.37 (ArC), 121.77 (ArC), 114.93 (ArC), 61.37 (CH_2), 14.34 61.37 (CH_3). FABMS m/z [217 ($\text{M} + \text{H}$) $^+$, 61 %], [($\text{M} + \text{Na}$) $^+$, 10 %].

Ethyl 3-methoxy-1-naphthoate [102]

Prepared as for **93** using ethyl 3-hydroxy-1-naphthoate (100 mg, 0.46 mmol). The yield was (94 mg, 84 %). ^1H NMR (CDCl_3 , 400 MHz) δ_{H} 8.80-8.77 (1H, m, ArH), 7.95 (1H, d, $J = 2.8$ Hz, ArH), 7.70-7.68 (1H, m, ArH), 7.46-7.39 (2H, m, ArH), 7.35-7.32 (1H, m, ArH), 4.52 (2H, q, $J = 7.2$ Hz, $\text{CO}_2\text{CH}_2\text{CH}_3$), 3.97 (3H, s, OCH_3), 1.48 (3H, t, $J = 7.2$ Hz, $\text{CO}_2\text{CH}_2\text{CH}_3$). δ_{C} (100 MHz; CDCl_3) 167.41 ($\text{C}=\text{O}$), 151.87 (ArC), 135.24 (ArC), 129.10 (ArC), 127.12 (ArC), 126.85 (ArC), 126.19 (ArC),

125.60 (ArC), 122.47 (ArC), 115.34 (ArC), 60.86 (CH₂), 57.82 (CH₃), 15.23 (CH₃).
FABMS *m/z* [230 (M⁺), 77 %], [253 (M + Na)⁺, 13 %]

3-methoxy-1-naphthoic acid [103]

Prepared as for **10** using ethyl 3-methoxy-1-naphthoate (89 mg, 0.39 mmol). The yield was (56 mg, 73 %). ¹H NMR (MeOD, 400 MHz) δ_H 8.83-8.81 (1H, m, ArH), 8.64 (1H, d, *J* = 8.4 Hz, ArH), 7.68 (1H, d, *J* = 2.4 Hz, ArH), 7.61 (1H, m, ArH), 7.30 (3H, m, ArH), 3.21 (1H, br s, OH). δ_C(100 MHz; MeOD) 170.79 (C=O), 155.14 (ArC), 137.17 (ArC), 130.15 (ArC), 127.97 (ArC), 127.64 (ArC), 127.45 (ArC), 126.80 (ArC), 125.44 (ArC), 123.26 (ArC), 115.25 (ArC), 15.46 (CH₃). FABMS *m/z* [203 (M + H)⁺, 89 %], [203 (M + Na)⁺, 51 %]

(2*S*, 3*R*)-Benzyl 3,4-epoxy-2-(3-methoxy-5-methyl-1-naphthoyloxy)-3-methylbutanoate [106]

A stirred solution of ethyl 3-methoxy-5-methyl-1-naphthoic acid (100 mg, 0.46 mmol) in thionyl chloride (2 ml) was heated at reflux (80 °C) for 2 h. The solution was concentrated *in vacuo* resuspended in toluene and concentrated *in vacuo* to give acyl chloride (119 mg), which was redissolved in DCM and added dropwise to a stirred solution of epoxy alcohol (2*S*, 3*R*)-**30** (108 mg, 0.49 mmol), Et₃N (0.10 ml, 0.73 mmol) in dry DCM (3 ml) at 0 °C under N₂. The reaction mixture was stirred at 0 °C for 4 h and then H₂O (15 ml) was added. The organic layer was separated and the aqueous layer extracted with DCM (3 × 10 ml). The combined organic extracts were dried (MgSO₄), filtered and concentrated *in vacuo* give brown oil. Flash chromatography (20% EtOAc-hexane) provided epoxy ester **106** as an oil (171 mg, 86%). ¹H NMR (CDCl₃, 400 MHz) δ_H 8.60-8.57 (1H, m, ArH), 7.93-7.92 (1H, d, *J* = 2.4 Hz, ArH), 7.50-7.49 (1H, d, *J* = 2.8 Hz, ArH), 7.37-7.31 (7H, m, ArH), 5.33-5.30 (1H, d, *J* = 12.0 Hz, CO₂CH₂Ph), 5.26-5.23 (1H, d, *J* = 12.4 Hz, CO₂CH₂Ph), 5.07 (1H, s, H-2), 3.97 (3H, s, OCH₃), 3.09-3.08 (1H, d, *J* = 4.8 Hz, H-4), 2.79-2.78 (1H, d, *J* = 4.8 Hz, H-4), 2.68 (3H, s, Ar-CH₃), 1.47 (3H, s, CH₃). δ_C(100 MHz; CDCl₃) 167.20 (C=O), 166.35 (C=O), 155.90 (ArC), 135.07 (ArC), 134.33 (ArC), 133.11 (ArC), 128.65 (ArCH), 128.53 (ArCH), 128.38 (ArCH), 128.25 (ArC), 127.67 (ArC), 126.86 (ArC), 125.07 (ArCH), 123.84 (ArCH), 122.02 (ArCH), 108.45 (ArCH), 76.69 (C-2), 67.54 (CO₂CH₂Ph), 55.90 (O CH₃), 55.55 (C-3), 52.16 (C-4), 20.08,

17.08. FABMS m/z 420 (M^+), 98 %], 443 ($M + Na$)⁺, 6 %], [$(M + Cs)^+$, 61 %], fragments [286, 43 %].

(2*S*, 3*S*)-Benzyl 3,4-epoxy-2-(3-methoxy-5-methyl-1-naphthoyloxy)-3-methylbutanoate [105]

Prepared as for (2*S*, 3*R*)-106 using epoxy alcohol (2*S*, 3*S*)-30 (108 mg, 0.49 mmol). The yield was (156 mg, 79%). ¹H NMR (CDCl₃, 400 MHz) δ_H 8.60-8.58 (1H, m, ArH), 7.90-7.89 (1H, d, $J = 2.8$ Hz, ArH), 7.49-7.48 (1H, d, $J = 2.0$ Hz, ArH), 7.41-7.39 (2H, m, ArH), 7.38-7.34 (5H, m, ArH), 5.36-5.33 (1H, d, $J = 12.4$ Hz, CO₂CH₂Ph), 5.31-5.28 (1H, d, $J = 12.4$ Hz, CO₂CH₂Ph), 5.25 (1H, s, H-2), 3.97 (3H, s, OCH₃), 2.99-2.98 (1H, d, $J = 4.4$ Hz, H-4), 2.71-2.70 (1H, d, $J = 4.8$ Hz, H-4), 2.68 (3H, s, Ar-CH₃), 1.47 (3H, s, CH₃). δ_C (100 MHz; CDCl₃) 167.36 (C=O), 166.04 (C=O), 155.87 (ArC), 135.08 (ArC), 134.33 (ArC), 133.14 (ArC), 128.60 (ArCH), 128.44 (ArCH), 128.30 (ArCH), 128.15 (ArC), 127.70 (ArC), 126.66 (ArC), 125.11 (ArCH), 123.77 (ArCH), 122.08 (ArCH), 108.50 (ArCH), 75.47 (C-2), 67.46 (CO₂CH₂Ph), 55.53 (O CH₃), 55.21 (C-3), 51.96 (C-4), 20.07, 17.90. FABMS m/z [420 (M^+), 49 %], [443 ($M + Na$)⁺, 8 %], fragments [289, 11%], [199, 100%]

(2*R*, 3*S*)-Benzyl 3,4-epoxy-2-(3-methoxy-5-methyl-1-naphthoyloxy)-3-methylbutanoate [107]

Prepared as for (2*S*, 3*R*)-106 using epoxy alcohol (2*R*, 3*S*)-30 (104 mg, 0.47 mmol). The yield was 160 mg, 84 %. ¹H NMR (CDCl₃, 400 MHz) δ_H 8.60-8.57 (1H, m, ArH), 7.93 (1H, d, $J = 2.4$ Hz, ArH), 7.50 (1H, d, $J = 2.8$ Hz, ArH), 7.36-7.34 (7H, m, ArH), 5.34-5.30 (1H, d, $J = 12.4$ Hz, CO₂CH₂Ph), 5.26-5.23 (1H, d, $J = 12.4$ Hz, CO₂CH₂Ph), 5.07 (1H, s, H-2), 3.97 (3H, s, OCH₃), 3.09 (1H, d, $J = 4.8$ Hz, H-4), 2.79 (1H, d, $J = 4.8$ Hz, H-4), 2.69 (3H, s, Ar-CH₃), 1.48 (3H, s, CH₃). δ_C (100 MHz; CDCl₃) 167.21 (C=O), 166.30 (C=O), 155.99 (ArC), 135.13 (ArC), 134.56 (ArC), 133.11 (ArC), 128.65 (ArCH), 128.53 (ArCH), 128.38 (ArCH), 128.25 (ArC), 127.67 (ArC), 126.86 (ArC), 125.07 (ArCH), 123.84 (ArCH), 122.02 (ArCH), 108.45 (ArCH), 76.69 (C-2), 67.54 (CO₂CH₂Ph), 55.90 (O CH₃), 55.55 (C-3), 52.16 (C-4), 20.08, 17.08. FABMS m/z [420 (M^+), 70 %], [443 ($M + Na$)⁺, 11 %], fragments [289, 15 %], [199, 100 %], [154, 45 %], [136, 21 %].

(2R, 3R)-Benzyl 3,4-epoxy-2-(3-methoxy-5-methyl-1-naphthoyloxy)-3-methylbutanoate [108]

Prepared as for (2*S*, 3*R*)-**105** using epoxy alcohol (2*R*, 3*R*)-**30** (108 mg, 0.49 mmol). The yield was 134mg, 68 %. ¹H NMR (CDCl₃, 400 MHz) δ_H 8.59-8.57 (1H, m, ArH), 7.89 (1H, d, *J* = 2.8 Hz, ArH), 7.48 (1H, d, *J* = 2.0 Hz, ArH), 7.39-7.35 (2H, m, ArH), 7.35-7.32 (5H, m, ArH), 5.33 (1H, d, *J* = 12.4 Hz, CO₂CH₂Ph), 5.28 (1H, d, *J* = 12.4 Hz, CO₂CH₂Ph), 5.25 (1H, s, H-2), 3.97 (3H, s, OCH₃), 2.98 (1H, d, *J* = 4.4 Hz, H-4), 2.70 (1H, d, *J* = 4.8 Hz, H-4), 2.68 (3H, s, Ar-CH₃), 1.47 (3H, s, CH₃). δ_C(100 MHz; CDCl₃) 167.33 (C=O), 166.15 (C=O), 155.60 (ArC), 135.08 (ArC), 134.33 (ArC), 133.14 (ArC), 128.60 (ArCH), 128.44 (ArCH), 128.30 (ArCH), 128.15 (ArC), 127.70 (ArC), 126.66 (ArC), 125.11 (ArCH), 123.77 (ArCH), 122.08 (ArCH), 108.50 (ArCH), 75.47 (C-2), 67.46 (CO₂CH₂Ph), 55.48 (O CH₃), 55.36 (C-3), 52.12 (C-4), 20.07, 17.91. [420 (M⁺), 51 %], [443 (M + Na)⁺, 15 %], fragments [289, 22 %, 199, 100 %].

(2*S*, 3*S*)-Benzyl 3,4-epoxy-2-(3-methoxy-5-methyl-1-naphthoyloxy)-3-methylbutanamide [(2*S*, 3*S*)-3**]**

10% palladium on carbon (20 mg, 15% w/w) was added to a stirred solution of epoxy ester (2*S*, 3*S*)-**105** (133 mg, 0.33 mmol) in dry CH₃OH (19 ml) and the suspension stirred under a hydrogen atmosphere for 2 h at RT. The reaction mixture was filtered through a pad of celite and the filtrate concentrated *in vacuo* to give crude carboxylic acid (100.8 mg), which was then dissolved in dry DMF (19 ml). To this stirred solution at 0 °C were successively added 35% aqueous ammonia (0.38 ml, 77 mmol), triethylamine (0.098 ml, 0.70 mmol), 1-hydroxybenzotriazole (48 mg, 0.36 mmol) and PyBOP (185.55 mg, 0.36 mmol). After the mixture had been warmed to room temperature and stirred for 18 h, toluene (10 ml) and EtOAc (20 ml) were added. The resulting solution was successively washed with 5% aq. HCl acid (20 ml), H₂O (20 ml), saturated aqueous NaHCO₃ (20 ml) and brine (20 ml). The organic layer was dried (MgSO₄), filtered and concentrated *in vacuo* to give a brown oil. Flash column chromatography (50% EtOAc-hexane) provided epoxy amide as a white crystalline solid (50.2 mg, 46%), mp 152-154 °C, lit. 148-150.5 °C, 153-154 °C. [α]_D²⁶ 41.2 (*c* 0.3 CH₂Cl₂); lit [α]_D²² 54 (*c* 0.4 MeOH). ¹H NMR (CDCl₃, 400 MHz) δ 8.63-8.62 (1H, m, ArH), 7.92 (1H, d, *J* = 2.0 Hz, ArH), 7.50-7.49 (1H, d, *J* =

2.0 Hz, ArH), 7.39-7.36 (2H, m, ArH), 6.16 (1H, br s, NH), 5.67 (1H, br s, NH), 5.22 (1H, s, H-2), 3.98 (3H, s, OCH₃), 3.03 (1H, d, *J* = 3.6 Hz, H-4), 2.80 (1H, d, *J* = 3.6 Hz, H-4), 2.68 (3H, s, Ar-CH₃), 1.57 (3H, s, CH₃). δ_{C} (100 MHz; CDCl₃) 170.79 (C=O), 167.69 (C=O), 157.99 (ArC), 136.52 (ArC), 135.35 (ArC), 130.26 (ArC), 129.94 (ArCH), 129.02 (ArCH), 127.37 (ArCH), 125.90 (ArCH), 124.23 (ArCH), 110.23 (ArCH), 78.02 (C-2), 57.95 (C-3), 57.71 (OCH₃), 55.54 (C-4), 22.24, 19.72. EIMS *m/z* [329 (M⁺), 45 %], [352, (M + Na)⁺, 53 %] fragments [216, 37 %], [199, 100 %]. TOF MS ES⁺ Found [330.1357, 100 %], [331.1455, 28 %], [332.1465, 5 %]. C₁₈H₂₀NO₅ 330.1342, 331.1375, 332.1400. Anal. Calcd. C₁₈H₁₉NO₅ C, 65.64 %; H, 5.81 %; 4.25 %. Found: C, 65.74 %; H, 5.82 %; N, 4.21 %.

(2*S*, 3*R*)-Benzyl-3,4-epoxy-2-(3-methoxy-5-methyl-1-naphthoyloxy)-3-methylbutanamide [(2*S*, 3*R*)-3]

Prepared as for (2*S*, 3*S*)-3 using epoxy ester (2*S*, 3*R*)-105 (132 mg, 0.33 mmol). The yield was 67 mg, 62%. $[\alpha]_{\text{D}}^{26}$ 30.1 (*c* 0.3 CH₂Cl₂); ¹H NMR δ (CDCl₃, 400 MHz) 8.62 (1H, m, ArH), 7.90-7.89 (1H, d, *J* = 2.4 Hz, ArH), 7.51 (1H, d, *J* = 2.0 Hz, ArH), 7.40-7.37 (2H, m, ArH), 6.15 (1H, br s, NH), 5.66 (1H, br s, NH), 5.32 (1H, s, H-2), 3.99 (3H, s, OCH₃), 3.14-3.13 (1H, d, *J* = 3.6 Hz, H-4), 2.84-2.83 (1H, d, *J* = 3.6 Hz, H-4), 2.69 (3H, s, Ar-CH₃), 1.57 (3H, s, CH₃). δ_{C} (400 MHz; CDCl₃) 169.07 (C=O), 165.26 (C=O), 155.79 (ArC), 134.43 (ArC), 133.31 (ArC), 127.93 (ArC), 127.72 (ArCH), 126.90 (ArCH), 125.41 (ArCH), 123.65 (ArCH), 122.13 (ArCH), 108.54 (ArCH), 56.65 (C-2), 55.58 (C-3), 53.41 (OCH₃), 52.61 (C-4), 20.11, 17.47. FABMS *m/z* [329 (M⁺), 50 %], [330 (M + H)⁺, 34 %], [352 (M + Na)⁺, 36 %], fragments [216, 23 %], [199, 100, %]. TOF MS ES⁺ Found: [330.1333, 100 %], [331.1602, 47 %] and [332.1728, 9 %]. C₁₈H₂₀NO₅ requires 330.1342, 331.1375, 332.1400. Anal. Calcd. C₁₈H₁₉NO₅ C, 65.64 %; H, 5.81 %; 4.25 %. Found: C, 65.27 %; H, 5.84 %; N, 4.27 %.

(2*R*, 3*S*)-Benzyl-3,4-epoxy-2-(3-methoxy-5-methyl-1-naphthoyloxy)-3-methylbutanamide [(2*R*, 3*S*)-3]

Prepared as for (2*S*, 3*S*)-3 using epoxy ester (2*R*, 3*S*)-30 (112 mg, 0.27 mmol). The yield was 36 mg, 41%. $[\alpha]_{\text{D}}^{26}$ -34.7 (*c* 0.3 CH₂Cl₂); ¹H NMR (CDCl₃, 400 MHz) δ_{H} 8.64-8.62 (1H, m, ArH), 7.90-7.89 (1H, d, *J* = 2.4 Hz, ArH), 7.51 (1H, d, *J* = 2.4 Hz,

ArH), 7.40-7.37 (2H, m, ArH), 6.15 (1H, br s, NH), 5.67 (1H, br s, NH), 5.32 (1H, s, H-2), 3.99 (3H, s, OCH₃), 3.14-3.13 (1H, d, $J = 4.4$ Hz, H-4), 2.84-2.82 (1H, d, $J = 4.4$ Hz, H-4), 2.69 (3H, s, ArH), 1.57 (3H, s, CH₃). δ_C (400 MHz; CDCl₃) 168.07 (C=O), 164.27 (C=O), 154.80 (ArC), 133.43 (ArC), 132.30 (ArC), 126.92 (ArC), 126.75 (ArCH), 125.91 (ArCH), 124.39 (ArCH), 122.66 (ArCH), 121.11 (ArCH), 107.55 (ArCH), 75.68 (C-2), 61.52 (C-3), 55.64 (OCH₃), 51.59 (C-4), 19.08, 13.20. FABMS m/z [329 (M⁺), 9 %], [352 (M + Na)⁺, 7 %] fragments [215, 99 %], [199, 48 %]. Anal. Calcd. C₁₈H₁₉NO₅ C, 65.64 %; H, 5.81 %; 4.25 %. Found: C, 65.31 %; H, 5.61 %; N, 4.31 %.

(2*R*, 3*R*)-Benzyl-3,4-epoxy-2-(3-methoxy-5-methyl-1-naphthoxyloxy)-3-methylbutanamide [(2*R*, 3*R*)-3]

Prepared as for (2*S*, 3*S*)-3 using epoxy ester (2*R*, 3*R*)-30 (110 mg, 0.27 mmol). The yield was 35 mg, 41 %. $[\alpha]_D^{26} -32.4$ (c 0.3 CH₂Cl₂); ¹H NMR (CDCl₃, 400MHz) δ_H 8.65-8.62 (1H, m, ArH), 7.92-7.91 (1H, d, $J = 2.8$ Hz, ArH), 7.50-7.51 (1H, d, $J = 2.4$ Hz, ArH), 7.37-7.35 (2H, m, ArH), 6.18 (1H, br s, NH), 5.81 (1H, br s, NH), 5.23 (1H, s, H-2), 3.98 (3H, s, OCH₃), 3.03 (1H, d, $J = 4.4$ Hz, H-4), 2.80-2.79 (1H, d, $J = 4.4$ Hz, H-4), 2.68 (3H, s, ArH), 1.65 (3H, s, CH₃). δ_C (400 MHz; CDCl₃) 168.07 (C=O), 164.27 (C=O), 154.80 (ArC), 133.43 (ArC), 132.30 (ArC), 126.92 (ArC), 126.75 (ArCH), 125.91 (ArCH), 124.39 (ArCH), 122.66 (ArCH), 121.11 (ArCH), 107.55 (ArCH), 75.68 (C-2), 61.52 (C-3), 55.64 (OCH₃), 51.59 (C-4), 19.08, 13.20. FABMS m/z [329 (M⁺), 41 %], [330, (M + H)⁺, 38 %], [352, (M + Na)⁺, 50 %] fragments [216, 33 %], [199, 100 %]. Anal. Calcd. C₁₈H₁₉NO₅ C, 65.64 %; H, 5.81 %; 4.25 %. Found: C, 65.58 %; H, 5.69 %; N, 4.26 %.

3-Benzoyloxy-5-methyl-naphthalene-1-carboxylic acid benzyloxycarbonyl(2-methyl-oxiranyl)-methyl ester [109]

Prepared as for 105 using epoxy alcohol and 97 (100 mg, 0.32 mmol). The yield was (125 mg, 79%). ¹H NMR (CDCl₃, 400 MHz) δ_H 8.59-8.57 (1H, m, ArH), 8.0 (1H, d, $J = 2.8$ Hz, ArH), 7.58 (1H, d, $J = 2.8$ Hz, ArH), 7.52-7.50 (2H, m, ArH), 7.44-7.32 (10H, m, ArH), 5.33-5.26 (4H, m, CO₂CH₂CH₃), 5.24 (1H, s, H-2), 3.09 (1H, d, $J = 4.4$ Hz, H-4), 2.78 (1H, d, $J = 4.4$ Hz, H-4), 2.64 (3H, s, CH₃), 1.46. δ_C (100 MHz;

CDCl₃) 167.20 (C=O), 166.30 (C=O), 154.96 (ArC), 136.48 (ArC), 135.07 (ArC), 134.28 (ArC), 133.18 (ArC), 131.92 (ArC), 128.71 (ArC), 128.65 (ArC), 128.54 (ArC), 128.38 (ArC), 128.31 (ArC), 127.72 (ArC), 127.66 (ArC), 126.99 (ArC), 125.84 (ArC), 125.20 (ArC), 123.83 (ArC), 122.38 (ArC), 110.05 (ArC), 72.09 (CH₂), 70.44 (CH₂), 67.67 (CH), 60.38 (C), 55.89 (CH₂), 52.16, 21.04, 20.05, 17.14 (CH₃), 16.98 (CH₃), 14.20. FABMS *m/z* [497 (M + H)⁺, 64 %], [519 (M + Na)⁺, 49 %], fragments [292, 70 %].

3-Methoxy-naphthalene-1-carboxylic acid benzyloxycarbonyl-(2-methyloxiranyl)-methyl ester [110]

Prepared as for **105** using epoxy alcohol and **104** (100 mg, 0.32 mmol). The yield was (125 mg, 79%). ¹H NMR (CDCl₃, 400 MHz) δ_H 8.59-8.57 (1H, m, ArH), 7.96 (1H, d, *J* = 2.6 Hz, ArH), 7.58 (1H, d, *J* = 2.5 Hz, ArH), 7.49-7.34 (8H, m, ArH), 5.33 (1H, d, *J* = 12.4 Hz, CO₂CH₂CH₃), 5.25 (1H, d, *J* = 12.4 Hz, CO₂CH₂CH₃), 5.22 (1H, s, H-2), 3.93 (3H, s, CH₃), 2.93 (1H, d, *J* = 4.4 Hz, H-4), 2.61 (1H, d, *J* = 4.4 Hz, H-4), 1.40. δ_C(100 MHz; CDCl₃) 167.31 (C=O), 166.15 (C=O), 155.87 (ArC), 135.53 (ArC), 134.28 (ArC), 134.34 (ArC), 131.92 (ArC), 128.77 (ArC), 128.55 (ArC), 128.43 (ArC), 127.85 (ArC), 127.66 (ArC), 126.93 (ArC), 125.29 (ArC), 123.80 (ArC), 122.18 (ArC), 108.76 (ArC), 73.45 (CH₂), 69.83 (CH), 60.24 (C), 55.37 (CH₂), 52.20 (CH₂), 21.19 (CH₃), FABMS *m/z* [407 (M + H)⁺, 60 %], [429 (M + Na)⁺, 17 %], fragments [201, 32 %], [107, 17 %].

(2S)-Benzyl-2-(3-methoxy-5-methyl-1-naphthoyloxy)-3-methylbut-3-enoate (111)

To a stirred solution of triethylamine (0.16 ml, 1.15 mmol), DMAP (9 mg, 0.073 mmol) and allyl alcohol (*S*)-**29** (156 mg, 0.76 mmol) in dry DCM (5 ml) at 0 °C under N₂ was added a solution of acid chloride **16** (187 mg, 0. mmol) in dry DCM (5 ml) drop wise. The reaction mixture was stirred at 0 °C for 4 h and then water (20 ml) was added. The organic layer was separated and the aqueous layer extracted with DCM (3 × 10 ml). The combined organic extracts were dried (MgSO₄), filtered and concentrated in *vacuo* to give a brown oil. Flash chromatography (10% EtOAc-hexane) provided alkene ester **111** (198 mg, 65 %). ¹H NMR (CDCl₃, 400 MHz) δ_H

8.63-8.61 (1H, m, ArH), 7.91 (1H, d, J 2.4 Hz, ArH), 7.48 (1H, s, ArH), 7.36-7.31 (7H, m, ArH), 5.77 (1H, s, H-2), 5.33 (1H, br s, =CH₂), 5.31-5.26 (2H, m, CO₂CH₂Ph), 5.18 (1H, br s, =CH₂) 3.96 (3H, s, OCH₃), 2.68 (3H, s, Ar-CH₃), 1.90 (3H, s, CH₃). δ_c (100 MHz; CDCl₃) δ_c 168.36 (C=O), 166.47 (C=O), 155.90 (ArC), 137.85 (ArC), 135.31 (ArC), 134.32 (ArC), 133.09 (ArCH), 128.69 (ArCH), 128.64 (ArCH), 128.56 (ArC), 127.63 (ArC), 126.86 (ArC), 124.99 (ArCH), 123.88 (ArCH), 121.89 (ArCH), 108.30 (ArCH), 76.70 (C-2), 67.64 (CO₂CH₂Ph), 55.52 (O CH₃), 53.42 (C-3), 52.16 (C-4), 20.09, 18.79. FABMS m/z [405 (M + H)⁺, 56 %], [428 (M + Na)⁺, 4 %], fragments [289, 26 %], [216, 9 %], [199, 100 %].

(2S)-2-(3-methoxy-5-methyl-1-naphthoyloxy)-3,3-dimethyl propanamide [113].

10% palladium on carbon (27.3 mg, 15% w/w) was added to a stirred solution of alkene ester **111** (182 mg, 0.45 mmol) in dry CH₃OH (27 ml) and the suspension stirred under a hydrogen atmosphere for 2 h at room temperature. The reaction mixture was filtered through a pad of celite and the filtrate concentrated in *vacuo* to give crude carboxylic acid (123 mg, 0.39 mmol), which was then dissolved in dry DMF (12 ml). To this stirred solution at 0 °C was successively added 35% aqueous ammonia (0.05 ml), triethylamine (0.125 ml, 0.90 mmol), 1-hydroxybenzotriazole (62 mg, 0.46 mmol) and PyBOP (243 mg, 0.46 mmol). After the mixture had been warmed to RT and stirred for 18 h, toluene (10 ml) and EtOAc (20 ml) were added. The resulting solution was successively washed with 5% aq. HCl (20 ml), H₂O (20 ml), saturated aq. NaHCO₃ (20 ml) and brine (20 ml). The organic layer was dried (MgSO₄), filtered and concentrated in *vacuo* to give a brown oil. Flash column chromatography (50% EtOAc-hexane) provided alkane amide **113** (52 mg, 42%). ¹H NMR (CDCl₃, 400MHz) δ 8.63 (1H, s, ArH), 7.88 (1H, d, J = 2.4 Hz, ArH), 7.70 (1H, d, J = 2.0 Hz, ArH), 7.36-7.32 (2H, m, ArH), 6.11 (1H, br s, NH), 6.02 (1H, br s, NH), 5.42 (1H, d, J = 4.0 Hz, H-2), 3.94 (3H, s, OCH₃), 2.51 (3H, s, Ar-CH₃), 2.50-2.46 (1H, m, H-4) 1.15 (3H, d, J = 7.2 Hz, CH₃), 1.13 (3H, d J = 7.2 Hz, CH₃). δ_c (100 MHz; CDCl₃) 171.78 (C=O), 165.86 (C=O), 1134.47 (ArC), 133.29 (ArC), 128.37 (ArC), 127.90 (ArC), 126.94 (ArCH), 125.31 (ArCH), 123.72 (ArCH), 121.78 (ArCH), 108.22 (ArCH), 76.69 (C-2), 55.55 (C-3), 30.87 (OCH₃), 20.11 (C-4), 19.00, 17.23. FABMS m/z [315 (M⁺), 44 %], [316 (M + H)⁺, 21 %], [338 (M +

Na)⁺, 9 %], fragments [216, 15 %], [199, 99 %]. Anal. Calcd. C₁₈H₂₁NO₄ C, 68.55 %; H, 6.71 %; 4.44 %. Found: C, 68.54 %; H, 6.52 %; N, 4.33 %.

(2*R*)-Benzyl-2-(3-methoxy-5-methyl-1-naphthoyloxy)-3-methylbut-3-enoate

[114]

Prepared as for **111** using allyl alcohol (*R*)-**29** (89 mg, 0.43 mmol). The yield was 120 mg, 69 %. ¹H NMR (CDCl₃, 400 MHz) δ_H 8.63-8.60 (1H, m, ArH), 7.91 (1H, d, *J* = 2.4 Hz, ArH), 7.48 (1H, m, ArH), 7.36-7.31 (7H, m, ArH), 5.78 (1H, s, H-2), 5.33 (1H, br s, =CH₂), 5.30-5.23 (2H, m, CO₂CH₂Ph), 5.18 (1H, br s, =CH₂) 3.97 (3H, s, OCH₃), 2.68 (3H, s, Ar-CH₃), 1.90 (3H, s, CH₃). δ_C(100 MHz; CDCl₃) δ_C 168.36 (C=O), 166.47 (C=O), 155.90 (ArC), 137.85 (ArC), 134.32 (ArC), 133.09 (ArC), 128.69 (ArCH), 128.56 (ArCH), 128.36 (ArCH), 128.16 (ArC), 127.63 (ArC), 126.86 (ArC), 124.99 (ArCH), 123.88 (ArCH), 121.89 (ArCH), 108.30 (ArCH), 76.70 (C-2), 67.26 (CO₂CH₂Ph), 55.52 (O CH₃), 53.42 (C-3), 52.16 (C-4), 20.09, 18.80. FAB MS *m/z* [404 (M⁺), 55 %], fragments [199, 80 %], [91, 99 %].

(2*R*)-2-(3-methoxy-5-methyl-1-naphthoyloxy)-3,3-dimethyl propanamide [116]

Prepared as for (2*S*)-**113** using alkene ester (*R*)-**114** (100 mg, 0.25 mmol). The yield was 51 mg, 65 %. ¹H NMR (CDCl₃, 400MHz) δ 8.63 (1H, s, ArH), 7.89 (1H, d, *J* = 2.4 Hz, ArH), 7.71 (1H, d, *J* = 2.0 Hz, ArH), 7.37-7.34 (2H, m, ArH), 6.07 (1H, br s, NH), 5.75 (1H, br s, NH), 5.43 (1H, d, *J* = 4.0 Hz, H-2), 3.95 (3H, s, OCH₃), 2.52 (3H, s, Ar-CH₃), 2.50-2.47 (1H, m, H-4) 1.15 (3H, d, *J* = 6.8 Hz, CH₃), 1.13 (3H, d, *J* = 7.2 Hz, CH₃). δ_C(100 MHz; CDCl₃) 172.04 (C=O), 165.66 (C=O), 155.25 (ArC), 135.67 (ArC), 133.48 (ArC), 129.26 (ArC), 127.32 (ArC), 126.63 (ArC), 124.60 (ArC), 122.92 (ArC), 111.81 (ArC), 78.30 (CH), 55.58 (CH₃), 30.88 (CH), 22.03 (CH₃), 19.05 (CH₃), 17.21 (CH₃). FAB MS *m/z* [315 (M⁺), 51 %], [316 (M + H)⁺, 14 %], [338 (M + Na)⁺, 9 %], fragments [216, 17 %], [199, 100 %]. Anal. Calcd. C₁₈H₂₁NO₄ C, 68.55 %; H, 6.71 %; 4.44 %. Found: C, 68.32 %; H, 6.65 %; N, 4.54 %.

3-Methoxy-5-methyl-naphthalene-1-carboxylic acid 1-carbamoyl-2-methyl-allyl ester [118]

A solution of Pd(OAc)₂ (3 mg, 0.013 mmol), Et₃SiH (0.082 ml, 0.51 mmol) and Et₃N (0.036 ml, 0.25 mmol) in dry CH₂Cl₂ (1 ml) was stirred at 23 °C under N₂ for 15 min. A solution of ester **114** (103 mg, 0.256 mmol) in 2 ml dry DCM was added dropwise. The mixture was stirred at RT overnight before quenching by the addition of sat. aq. NH₄Cl (5 ml). The organic layer was separated and the aqueous layer was extracted with Et₂O (3 x 5 ml) and the combined organic extracts were washed with brine (10 ml), dried (MgSO₄), filtered through a pad of celite and concentrated in *vacuo* to give a yellow oil (82 mg, 0.26 mmol) which was then dissolved in dry DMF (16 ml). To this stirred solution at 0 °C was successively added 35% aqueous ammonia (0.04 ml, 0.73 mmol), Et₃N (0.083 ml, 0.60 mmol), HOBt (42 mg, 0.31 mmol) and PyBOP (163 mg, 0.31 mmol). After the mixture had been warmed to room temperature and stirred for 18 h, toluene (10 ml) and EtOAc (16 ml) were added. The resulting solution was successively washed with 5 % HCl (16 ml), H₂O (16 ml), saturated aq. NaHCO₃ (16 ml) and brine (16 ml). The organic layer was dried (MgSO₄), filtered and concentrated in *vacuo* to give a brown oil. Flash column chromatography (50 % EtOAc-hexane) provided alkene amide as white crystalline solid (54 mg, 66 %), mp 190-193 °C. ¹H NMR (CDCl₃, 400 MHz) δ_H 8.63-8.59 (1H, m, ArH), 7.89-1.86 (1H, d, m, ArH), 7.70-7.68 (1H, m, ArH), 7.37-7.34 (7H, m, ArH), 6.13 (1H, br s, NH), 5.87 (1H, s, H-2), 5.65 (1H, br s, NH), 5.36 (1H, br s, =CH₂), 5.21 (1H, br s, =CH₂), 3.95 (3H, s, OCH₃), 2.52 (3H, s, Ar-CH₃), 1.96 (3H, s, CH₃). δ_C(100 MHz; CDCl₃) δ_C 170.17 (C=O), 165.07 (C=O), 155.31 (ArC), 139.18 (ArC), 135.58 (=CH₂), 133.46 (ArC), 129.22 (ArCH), 127.27 (ArCH), 127.10 (ArCH), 126.81 (ArC), 124.58 (ArC), 122.89 (ArC), 117.23 (=CH₂), 111.79 (ArCH), 78.34 (C-2), 76.69 (C-3), 55.58 (OCH₃), 53.42 (C-3), 52.16 (C-4), 20.09, 18.80. FABMS *m/z* 313 (M⁺, 16 %), [336 (M + Na)⁺, 14 %], fragments [216, 15 %], [199, 100 %]. Anal. Calcd. C₁₈H₂₁NO₄ C, 68.99 %; H, 6.11 %; 4.47 %. Found: C, 68.72 %; H, 6.09 %; N, 4.50 %.

3-Methoxy-5-methyl-naphthalene-1-carboxylic acid 1-carbamoyl-2-methyl-allyl ester [117]

Prepared as for **118** using ester **111** (119 mg, 0.30 mmol). The yield was 50 mg, 63 %. ¹H NMR (CDCl₃, 400 MHz) δ_H 8.64 (1H, m, ArH), 7.86 (1H, m, ArH), 7.71 (1H, m, ArH), 7.36-7.33 (7H, m, ArH), 6.14 (1H, br s, NH), 5.87 (1H, s, H-2), 5.75 (1H,

br s, NH), 5.37 (1H, br s, =CH₂), 5.21 (1H, br s, =CH₂), 3.95 (3H, s, OCH₃), 2.52 (3H, s, Ar-CH₃), 1.96 (3H, s, CH₃). δ_C (400 MHz; CDCl₃) δ_C 170.25 (C=O), 165.09 (C=O), 155.31 (ArC), 139.18 (C=), 135.58 (ArC), 133.46 (ArC), 129.22 (ArCH), 127.27 (ArCH), 127.10 (ArCH), 126.80 (ArC), 124.58 (ArC), 122.89 (ArC), 117.23 (=CH₂), 108.75 (ArCH), 76.70 (C-2), 55.57 (C-3), 55.50 (OCH₃), 30.87 (C-3), 21.97, 21.78, 19.02, 18.58, 17.22. FABMS m/z 313 (M⁺), 17 %], [336 (M + Na)⁺, 15 %], fragments [216, 15 %], [199, 100 %]. Anal. Calcd. C₁₈H₂₁NO₄ C, 68.99 %; H, 6.11 %; 4.47 %. Found: C, 68.76 %; H, 6.05 %; N, 4.44 %.

2-(3-Chloro-piperidin-1-yl)-ethyl-ammonium chloride [124]

124 was prepared in 4 steps involving;

- (i) Synthesis of *N*-[2-(3-Hydroxy-piperidin-1-yl)-ethyl]-2,2-dimethyl propionamide [120]
- (ii) Synthesis of methanesulfonic acid 1-[2-(2,2-dimethyl-propionylamino)-ethyl]-piperidin-3-yl ester [121]
- (iii) Synthesis of *N*-[2-(3-Chloro-piperidin-1-yl)-ethyl]-2,2-dimethyl propionamide [123]
- (iv) Boc deprotection of [123] to give [124]

(i) 1-(2-Aminoethyl)-piperidin-3-ol (990 mg, 6.87 mmol) and Et₃N (1.15 ml, 8.24 mmol) were stirred in CH₃OH (10 ml) for 5 min. and BOC₂O (1.8 g, 8.24 mmol) dissolved in CH₃OH (5 ml) was added dropwise over 15-20 min. The reaction mixture was stirred at 45 °C for 20 h. The reaction mixture was concentrated in *vacuo* and the oily product diluted with EtOAc (40) ml and washed with H₂O (2 x 20 ml) and brine (20 ml). The organic phase was dried (MgSO₄), filtered and concentrated in *vacuo* to give **120** as a straw coloured oil (1.60 g, 95 %), which needed no further purification. FAB MS, m/z [(M + H)⁺ 245, 100 %], [(M + Na)⁺ 267, 6 %], fragments [187, 67 %].

(ii) MsCl (0.7 ml, 9.03 mmol) was added dropwise to a stirred solution of **120** (1.5 g, 6.15 mmol) and Et₃N (1.3 ml, 9.32 mmol) in anhyd. CH₂Cl₂ (10 ml) at 0 °C

under N₂. The reaction was further stirred at 0 °C for 1 h. Cold CH₂Cl₂ (50 ml) was added and the reaction quenched by washing with cold NaHCO₃/brine (2 x 20 ml) respectively. The organic phase was dried, filtered and concentrated in *vacuo* to afford **121** as a brown liquid (1.4 g, 71 %). FAB MS, *m/z* [(M + H)⁺ 323, 11 %], fragments [243, 51 %], [187, 43 %].

(iii) TBAC (2.17 g, 7.8 mmol) was added to a stirred solution of **121** (1.05 g, 3.26 mmol) in anhyd. DMF (5 ml). The reaction was heated at 90 °C for 30 min. and the DMF was removed in *vacuo*. The product was dissolved in CH₂Cl₂ (50 ml) and washed with cold NaHCO₃ (50 ml) and cold brine (50 ml). The organic phase was dried (MgSO₄), filtered and concentrated in *vacuo* to yield **123** as a yellowish liquid (786 mg, 92 %). FAB MS, *m/z* [(M(³⁷Cl) + H)⁺ 263, 77 %], [(M(³⁷Cl) + H)⁺ 265, 23 %], fragments [259, 90 %], [261, 19 %], [203, 71 %].

(iv) **123** (750 mg, 2.87 mmol) was stirred in 2.5 M HCl in EtOAc for an hour. EtOAc was then removed by rotary evaporation to give the di HCl salt (422 mg, 90 %). The chlorinated piperidine analogue was used as the chloride salt. FAB MS, *m/z* [(M(³⁵Cl) + 2H)⁺ 164, 35 %], [(M(³⁷Cl) + H)⁺ 166, 9 %], fragments [159, 100 %], [161, 37 %], [142, 31 %], [129, 56 %], [97, 95 %].

3-Methoxy-5-methyl-naphthalene-1-carboxylic acid [2-(3-chloro-piperidine-1-yl)-ethyl]-amide [131]

Prepared as for **132** using 2-(3-Chloro-piperidin-1-yl)-ethyl-ammonium chloride (45 mg, 0.28 mmol). The yield was 50 mg, 58 %. ¹H NMR (CDCl₃, 400 MHz) δ_H 8.07 (1H, d, *J* = 8 Hz, ArH), 7.33-7.27 (4H, m, ArH), 6.56 (1H, br s, NH), 3.94 (3H, s, OCH₃), 3.62-3.60 (2H, m, CH₂), 2.65 (3H, s, ArCH₃), 2.67-2.62 (2H, m, CH₂), 2.41-2.37 (1H, m, CH), 1.85-1.79 (2H, m, CH₂), 1.61-1.55 (2H, m, CH₂), 1.29-1.30 (2H, m, CH₂). δ_C(100 MHz; CDCl₃) 169.21 (C=O), 156.37 (ArC), 136.89 (ArC), 134.24 (ArC), 133.15 (ArC), 127.63 (ArC), 125.62 (ArC), 124.21 (ArC), 123.53 (ArC), 117.04 (ArC), 105.05 (ArC), 61.01 (CH₃), 56.18 (CH₂), 55.83 (CH₂), 52.73 (CH₂), 50.80 (CH₂), 36.60 (CH), 34.43 (CH₂), 24.25 (CH₂), 19.93 (CH₃). FAB MS, *m/z* [(M(³⁵Cl) + H)⁺ 361, 79 %], [(M(³⁷Cl) + H)⁺ 363, 21 %], fragments [187, 81 %].

3-Methoxy-5-methyl-naphthalene-1-carboxylic acid [2-(3-hydroxy-piperidine-1-yl)-ethyl]-amide [132]

1-(2-Aminoethyl)-piperidin-3-ol (31 mg, 0.22 mmol) was stirred in anhyd. CH₂Cl₂ (5 ml). The acid chloride **16** was dissolved in anhyd. CH₂Cl₂ (3 ml) and added dropwise to the amine solution at °C and the reaction mixture stirred for 3 h. The reaction was quenched with NaHCO₃ (5 ml). The organic phase was separated and the aqueous phase extracted with CH₂Cl₂ (3 x 7 ml). The combined organic solutions were dried (MgSO₄), filtered and concentrated in *vacuo*. Flash chromatography (5 % CH₃OH/CH₂Cl₂) yielded the title compound as a reddish brown oil (60 mg, 58 %). ¹H NMR (CDCl₃, 400 MHz) δ_H 8.04 (1H, d, *J* = 8 Hz, ArH), 7.32-7.28 (4H, m, ArH), 6.51 (1H, br s, NH), 3.94 (3H, s, OCH₃), 3.76 (1H, br s, OH), 3.62-3.58 (2H, q, *J* = 5.6 Hz, CH₂), 2.64 (3H, s, ArCH₃), 2.61-2.58 (2H, t, *J* = 6.0 Hz, CH₂), 2.41 (1H, m, CH), 1.78-1.75 (2H, m, CH₂), 1.66-1.63 (2H, m, CH₂), 1.51-1.47 (2H, m, CH₂). δ_C (100 MHz; CDCl₃) 169.32 (C=O), 156.36 (ArC), 136.91 (ArC), 134.23 (ArC), 133.17 (ArC), 127.63 (ArC), 125.58 (ArC), 124.23 (ArC), 123.44 (ArC), 117.02 (ArC), 104.99 (ArC), 66.35 (CH), 60.32 (CH₂), 56.91 (CH₃), 55.46 (CH₂), 53.50 (CH₂), 50.77 (CH₂), 36.74 (CH₂), 31.94 (CH₂), 21.92 (CH₂), 19.92 (CH₃). FAB MS, *m/z* [(*M* + H)⁺ 343, 38 %], [(*M* + Na)⁺ 365, 14 %].

(*S*)-2-([2-(3-chloropiperidine-1-yl)ethyl]amino)-1-[(2*S*)-2-methyloxirane-2-yl]-2-oxoethyl 3-methoxy-5-methyl-1-naphthoate [126]

The epoxy ester (2*S*, 3*S*)-**30** (72 mg, 0.17 mmol) was stirred in anhyd. CH₃OH (10 ml), 10 % Pd-C (11 mg) was then added and the suspension stirred under H₂ for 2 h at RT. The reaction mixture was filtered through a pad of celite and the filtrate concentrated in *vacuo* to give crude carboxylic acid **22** as a colourless oil (49 mg). This was then dissolved in dry DMF (9 ml) and to this stirred solution at 0 °C was successively added 2-(3-Chloro-piperidin-1-yl)-ethyl-ammonium chloride **124** (0.06 ml, 0.37 mmol), Et₃N (0.052 ml, 0.37 mmol), HOBt (27 mg, 0.20 mmol) and PyBOP (93 mg, 0.18 mmol). After the mixture had been warmed to room temperature and stirred for 18 h, toluene (10 ml) and EtOAc (16 ml) were added. The resulting solution was successively washed with 5 % aq. HCl (16 ml), H₂O (16 ml), saturated aq. NaHCO₃ (16 ml) and brine (16 ml). The organic layer was dried (MgSO₄), filtered and concentrated in *vacuo* to give a brown oil. Flash column chromatography (10-20 % CH₃OH/CH₂Cl₂) provided the title compound as a yellowish-brown oil (47 mg, 67 %). ¹H NMR (CDCl₃, 400 MHz) δ 8.54 (1H, m, ArH), 7.91-7.87 (1H, m,

ArH), 7.58-7.56 (1H, m, ArH), 7.36-7.31 (2H, m, ArH), 3.97 (1H, s, H-2), 3.37-3.34 (2H, m, -CH₂-), 3.33 (3H, s, OCH₃), 3.28 (2H, q, *J* = 1.6 Hz, NCH₂-), 3.21 (2H, t, *J* = 3.6 Hz, -CH₂N), 3.11 (1H, d, *J* = 4.4 Hz, H-4), 2.98 (1H, d, *J* = 4.8 Hz, H-4), 2.67 (3H, s, Ar-CH₃), 2.53-2.50 (2H, m, -CH₂-), 2.20-2.17 (1H, m, -CHCl), 1.67-1.59 (4H, m, -CH₂CH₂-), 1.48 (3H, s, CH₃). δ_C(100 MHz; CDCl₃) 169.23 (C=O), 166.42 (C=O), 157.51 (ArC), 135.82 (ArC), 128.83 (ArC), 126.11 (ArC), 124.77 (ArCH), 109.32 (ArCH), 79.78, 77.57, 59.61, 56.81, 53.65, 37.44, 24.83, 20.75, 20.14, 18.42, 17.55, 13.95. FABMS *m/z* [M(³⁵Cl)⁺ 474, 50 %], [M(³⁷Cl)⁺ 476, 15 %], fragments [242, 100 %]. Anal. Calcd. C₂₅H₃₁ClN₂O₅ C, 63.22 %; H, 6.58 %; N, 5.90 %. Found: C, 63.30 %; H, 6.51 %; N, 5.98 %.

(*S*)-1-([2-(3-hydroxypiperidine-1-yl)ethyl]amino}carbonyl)-2-methylprop-2-en-1-yl 3-methoxy-5-methyl-1-naphthoate [129]

Prepared as for **126** using alkene ester (*S*)-**111** (111 mg, 0.27 mmol) and 1-(2-aminoethyl)-piperidin-3-ol **119** (0.052 g, 0.32 mmol). The yield was 38 mg, 66 %. ¹H NMR (CDCl₃, 400 MHz) δ 8.57 (1H, d, *J* = 8.4 Hz, ArH), 7.90 (1H, d, *J* = 2.4 Hz, ArH), 7.57 (1H, d, *J* = 2.4 Hz, ArH), 7.38-7.30 (2H, m, ArH), 5.71 (1H, s, H-2), 5.34 (1H, br. NH), 5.19-5.17 (2H, m, =CH₂), 3.99 (3H, s, OCH₃), 3.69 (1H, br s, OH), 3.44 (2H, t, *J* = 6.4 Hz, -NCH₂-), 2.96-2.89 (1H, m, CH), 3.68 (3H, s, CH₃), 2.78-2.71 (2H, m, -CH₂CH₂-), 2.68 (3H, s, Ar-CH₃), 2.35-2.29 (2H, m, CH₂), 1.92 (3H, s, CH₃), 1.81-1.75 (2H, m, -CH₂-), 1.54-1.46 (1H, m, -CHCl-), 1.38-1.29 (2H, m, -CH₂-). δ_C(400 MHz; CDCl₃) 169.78 (C=O), 168.52 (C=O), 157.53 (ArC), 140.81 (=CH₂), 135.82 (ArC), 134.74(ArC), 129.99 (ArC), 128.06 (ArC), 125.98 (ArCH), 124.77 (ArCH), 123.08 (ArC), 117.36 (=CH₂), 109.09, 79.41, 58.03, 57.99, 56.12, 54.39, 27.43, 20.13, 18.92. FABMS *m/z* [(M + H)⁺ 441, 10 %], fragments [258, 100 %], [199, 12 %], [187, 96 %]. TOF MS ES⁺ Found 441.2368, 442.0954, 443.3098. C₂₅H₃₃N₂O₆ requires 441.2390, 442.2422, 443.2450. Anal. Calcd. C₂₅H₃₂N₂O₅ C, 68.16 %; H, 7.32 %; N, 6.36 %. Found: C, 68.24 %; H, 7.29 %; N, 6.33 %.

(*S*)-1-([2-(3-chloropiperidine-1-yl)ethyl]amino}carbonyl)-2-methylprop-2-en-1-yl 3-methoxy-5-methyl-1-naphthoate [130]

Prepared as for **126** using alkene ester (*S*)-**111** (100 mg, 0.25 mmol) and 2-(3-Chloro-piperidin-1-yl)-ethyl-ammonium chloride **124** (0.029 g, 0.21 mmol). The yield was 33 mg, 59 %. ¹H NMR (CDCl₃, 400 MHz) δ 8.58-54 (1H, m, ArH), 7.88 (1H, d, *J* = 2.4 Hz, ArH), 7.57-7.50 (1H, m, ArH), 7.37-7.28 (2H, m, ArH), 5.68 (1H, s, H-2), 5.69 (1H, br. s, NH), 5.33-5.29 (1H, m, =CH₂), 5.21-5.15 (1H, m, =CH₂), 3.97 (3H, s, OCH₃), 3.95-3.91 (2H, m, -NCH₂-), 3.53-3.46 (2H, m, CH₂N-), 3.32 (3H, s, CH₃), 3.15-3.10 (4H, m, -CH₂CH₂-), 2.67 (3H, s, Ar-CH₃), 2.65-2.60 (2H, m, -CH₂-), 2.09-2.04 (2H, m, -CHCl-), 1.89-1.84 (2H, m, -CH₂-), 1.82 (3H, s, CH₃), 1.31-1.26 (3H, m, -CHCl). δ_C(400 MHz; CDCl₃) 169.21 (C=O), 167.10 (C=O), 157.34 (ArC), 139.56 (=CH₂), 136.98 (ArC), 135.56 (ArC), 133.63 (ArC), 128.63 (ArC), 125.87 (ArCH), 124.03 (ArCH), 122.21 (ArC), 116.95 (=CH₂), 80.33, 77.47, 67.86, 56.13, 53.09, 33.77, 28.78, 24.00, 20.13, 19.42, 17.21. FABMS *m/z* [(M(³⁵Cl) + H)⁺ 460, 93 %], [(M(³⁷Cl) + 2)⁺ 462, 31 %], fragments [424, 33 %], [307, 45 %], [286, 61 %], [258, 100 %]. Anal. Calcd. C₂₅H₃₁N₂O₄ C, 65.42 %; H, 6.81 %; N, 6.10 %. Found: C, 65.80 %; H, 6.76 %; N, 6.13 %.

(*S*)-1-([2-(3-hydroxypiperidine-1-yl)ethyl]amino)-1-[(2*S*)-2-methyloxirane-2-yl]-2-oxoethyl 3-methoxy-5-methyl-1-naphthoate [125]

Prepared as for **126** using epoxy ester (2*S*, 3*S*)-**30** (89 mg, 0.17 mmol) and 1-(2-Aminoethyl)-piperidin-3-ol **119** (0.02 g, 0.14 mmol). The yield was 25 mg, 60 %. ¹H NMR (CDCl₃, 400 MHz) δ 8.56 (1H, t, *J* = 7.6 Hz, ArH), 7.92 (1H, dd, *J* = 2.4 Hz, ArH), 7.59-7.57 (1H, m, ArH), 7.36-7.30 (2H, m, ArH), 5.02 (1H, s, H-4), 3.99 (3H, s, OCH₃), 3.92 (1H, s, H-2), 3.66-2.55 (2H, m, -NCH₂-), 3.44-3.37 (2H, m, CH₂N-), 3.35 (3H, s, CH₃), 3.13 (1H, d, *J* = 4.4 Hz, H-4), 3.02 (1H, d, *J* = 4.8 Hz, H-4), 2.84 (2H, m, -CH₂-), 2.68 (3H, s, Ar-CH₃), 2.65-2.61 (1H, m, -CH-), 2.54-2.49 (2H, m, -CH₂-), 2.09-1.99 (2H, m, -CH₂-), 1.51 (3H, s, CH₃), 1.31-1.22 (3H, m, -CH₂-). δ_C(400 MHz; CDCl₃) 169.39 (C=O), 166.32 (C=O), 157.51 (ArC), 135.80 (ArC), 134.74 (ArC), 129.72 (ArC), 128.64 (ArC), 126.04 (ArCH), 124.78 (ArCH), 123.21 (ArC), 109.25 (ArCH), 79.83, 77.58, 67.86, 56.13, 53.09, 33.77, 30.22, 24.00, 20.13, 18.30, 17.55. FABMS *m/z* [(M + H)⁺ 457, 97 %], fragments [258, 74 %], [187, 67 %]. TOF MS ES⁺ Found [457.2369, 100 %], [458.2410, 29 %], [459.2476, 8 %]. C₂₅H₃₃N₂O₆ requires 457.2339, 458.2371, and 459.239. Anal. Calcd. C₂₅H₃₂N₂O₆ C, 65.77 %; H, 7.07 %; N, 6.14 %. Found: C, 65.72 %; H, 7.01 %; N, 6.19 %.

***N*-[2-(3-Chloro-piperidin-1-yl)-ethyl]-benzamide [133].**

Synthesised as for 132 using benzoyl chloride (0.08 ml, 0.91 mmol) and 2-(3-Chloro-piperidin-1-yl)-ethyl-ammonium chloride [124] (115 mg, 0.71 mmol). This gave 133 as a brown oil and the yield was 51 mg, 27 %. ^1H NMR (CDCl_3 , 400 MHz) δ_{H} 7.42-7.41 (2H, m, ArH), 7.23-7.20 (1H, m, ArH), 7.14-7.11 (2H, m, ArH), 5.29 (1H, br s, NH), 4.21-4.15 (1H, m, CH), 2.83-2.79 (2H, m, CH_2), 2.22 (2H, t, $J = 8$ Hz, CH_2), 2.06 (2H, t, $J = 8$ Hz, CH_2), 1.98-1.95 (2H, m, CH_2), 1.61-1.59 (1H, m, CH_2), 1.44-1.36 (2H, m, CH_2). δ_{C} (100 MHz; CDCl_3) 174.11 (C=O), 136.92 (ArC), 131.59 (ArC), 128.97 (ArC), 128.03 (ArC), 61.63 (CH_2), 56.86 (CH_3), 55.51 (CH_2), 52.55 (CH_2), 44.56 (CH), 34.87 (CH_2), 24.73 (CH_2). FAB MS, m/z [$(\text{M}^{35}\text{Cl}) + \text{H}$] $^+$ 267, 71 %, [$(\text{M}^{37}\text{Cl}) + \text{H}$] $^+$ 269, 18 %, fragments [232, 43 %], [126, 23 %].

References

1. Pierce G.B. Letters Illustrating Clinical Aspects of Cancer. In *The biological basis of cancer*, edited by McKinnell R.G; Parchment R.E; Perantoni A.O; Pierce G.B.
2. Rang H.P; Dale M.M; Ritter J..M. Cancer Chemotherapy. In *Pharmacology*, Churchill and Livingston, London, **1996**, 696-717.
3. King R.J.B *Cancer Biology*. Harlow, Pearson Education. **2000**
4. The Cancer Research Campaign. *About Cancer*, available from: <http://www.cancerresearchuk.org/aboutcancer/statistics/incidence> [accessed 23rd December 2003]
5. Pratt W.B; Ruddon R.W; Ensminger W.D; Maybaum J. *The Anticancer Drugs*, Oxford University Press, **1994**.
6. Oliverio V.T; Zubrod C.G. Clinical pharmacology of the effective antitumour drugs. *Ann. Rev. Pharmacol.* **1965**, 5, 335.
7. Foley G.E; Friedman O.M; and Drolet B.P; Studies on the mechanism of action of cytoxan: Evidence of activation *in vivo* and *in vitro*. *Cancer Res.* **1961**, 21, 57.
8. Connors T.A; Cox P.J; Farmer P.B; Foster A.B and Jarman M. Some studies of the active intermediates formed in the macrosomal metabolism of cyclophosphamide and isophosphamide. *Biochem. Pharmacol.* **1974**, 23, 115.
9. Struck R.F; Kirk M.C; Mellet L.B; El Dareer S; Hill D.L. Urinary metabolite of the antitumour agent cyclophosphamide. *Mol. Pharmacol.* **1971**, 7, 519.
10. Searcey M. Duocarmycins – Natures Prodrugs? *Curr. Pharm. Des.* **2002**, 8, 1375-1389.
11. Li L.H; Swenson D.H; Schpok S.L.F; Kuentzel S.L; Dayton B.D; Krueger W.C. *Cancer Res.* **1982**, 42, 999.
12. Patterson L.H; McKeown S.R; AQ4N: a new approach to hypoxia-activated cancer chemotherapy. *Br. J. Cancer* **2000**, 83, 1589-1593.
13. Lissauer, II. Zwei falle von leucaemie. *Berl. Klin. Wochenschr.* **1865**, 40, 403.
14. Mann J. Natural products in cancer chemotherapy: past, present and future. *Nat. Rev. Cancer* **2002**, 2, 143-148.
15. Fahy J. Modifications of the vinca alkaloids have major implications for tubulin interacting activities. *Curr. Pharmaceut. Design* **2001**, 7, 1181-1197.

16. Zubrod C.G. Origins and development of chemotherapy research at the National Cancer Institute. *Cancer Treat. Rep.* **1984**, 68, 9-19.
17. Boger D.L; Cai H. Bleomycin: Synthetic and mechanistic studies. *Angew. Chem. Int. Ed.* **1999**, 38, 448-476.
18. Sinha B.K; Politi P.M. Anthracyclins. *Cancer chemother. Biol. Response Modif.* **1990**, 11, 45-57.
19. Hodgkinson T.J; Shipman M. Chemical synthesis and mode of action of the azinomycins. *Tetrahedron* **2001**, 57, 4467-4488.
20. Nagaoka K; Matsumoto M; Oono J; Yokoi K; Ishizeki S and Nakashima K. Azinomycins A and B, New Antitumour Antibiotics. I. Producing Organism, Fermentation, Isolation and Characterisation. *J. Antibiot.* **1986**, 39, 1527-1532.
21. Ishizeki S; Ohtsuka M; Irinoda K; Kukita K-I; Nagaoka K and Nakashima K. Azinomycins A and B, New Antitumour Antibiotics. III. Antitumour Activity. *J. Antibiot.* **1987**, 40, 60-65.
22. Yokoi K; Nagaoka K. and Nakashima K. Azinomycins A and B, New Antitumour Antibiotics. II. Chemical Structure. *Chem. Pharm. Bull.* **1986**, 34, 4554-4561.
23. Armstrong RW; Moran E.J; Chun K.O; England P. Synthetic Studies Towards Carzinophilin: Synthesis and Ammonium Hydroxide-Induced Rearrangement of the Epoxy-Acid Fragment. *Tetrahedron Lett.* **1990**, 31, 2669-2672.
24. Hata T; Koga F; Sano Y; Kanamori K; Matsumae A; Sugawara R; Hoshi T. & Shima T. Carzinophilin, a new tumour inhibitory substance produced by streptomycetes, I. *J. Antibiot., ser A* **1954**, 7, 107-112.
25. Onda M; Konda Y; Noguchi Y; Omura S. and Hata T. Revised Structure for the Naphthalenecarboxylic Acid from Carzinophilin. *J. Antibiot.* **1969**, 22, 42-44.
26. Onda M; Konda Y; Omura S and Hata T. Structure of Carzinophilin. II. A New Amino Acid and Its Derivative from Carzinophilin. *Chem. Pharm. Bull.* **1971**, 19, 2013-2019.
27. Hanstock C. C; and Lown J. W. Structure and Function of the Antitumour Antibiotic Carzinophilin A: The First Natural Intercalative Bisalkylator. *J. Am. Chem. Soc.* **1982**, 104, 3213-3214.

28. Omura S; Konda Y; Hatano A; Hata T. and Onda M Structure of Carzinophilin. IV. Structure Elucidation by Nuclear Magnetic Spectroscopy. (2) *Chem. Pharm. Bull.* **1984**, 32, 2995-3002.
29. Shibuya M. Synthetic Studies on Carzinophilin A. Synthesis of the Optically active C.1-C.18 Segment. *Tetrahedron Lett.* **1983**, 24, 1175-1178.
30. Shimada N; Uekusa M; Denda T; Ishii Y; Iizuka T; Sato Y; Hatori T; Fukui M & Sudo M. Clinical Studies of Carzinophilin, an Antitumour Substance. *J. Antibiot., ser A* **1954**, 8, 67-76.
31. Majumdar K. C. and Lown J. W. Studies Related to Antitumour Antibiotics. Reactions of Carzinophilin with DNA Assayed by Ethidium Fluorescence. *Can. J. Biochem.* **1977**, 55, 630-635.
32. Hashimoto M and Terashima S. A Stereoselective Synthesis of 4-*O*-methyl-13-desacetyl-12,13-di-*O*-benzylcarzinophilin. *Heterocycles* **1998**, 47, 59-64.
33. Hashimoto M; Matsumoto M; Yamada K. and Terashima S. Synthesis, Chemical Property, and Cytotoxicity of the Carzinophilin Congeners Carrying a 2-(1-Acylamino-1-alkoxycarbonyl)methylidene-1-azabicyclo-[3.1.0]hexane System. *Tetrahedron Lett.* **1994**, 35, 2207-2210.
34. Coleman R.S. Issues of Orthogonality and Stability: Synthesis of the Densely Functionalised Heterocyclic Ring System of the Antitumour Agents Azinomycins A and B. *Synlett* **1998**, 1031-1039.
35. Coleman R.S; Kong J-S; Richardson T.E. Synthesis of Naturally Occurring Antitumour Agents: Stereocontrolled Synthesis of the Azabicyclic Ring System of the Azinomycins. *J. Am. Chem. Soc.* **1999**, 121, 9088-9095.
36. Argoudelis A.D; Reusser F; Whally H.A. Baczynskyj L. Mizesak S.A. and Wnuk R.J. Antibiotics Produced by Streptomyces Ficellus. I. Ficellomycin. *J. Antibiot.* **1976**, 29, 1001-1006.
37. Kuo M-S; Yurek D.A. and Mizesak S.A. Structure Elucidation of Ficellomycin. *J. Antibiot.* **1989**, 42, 357-360.
38. Coleman R.S; Li J. and Navarro A. Total Synthesis of Azinomycin A. *Angew. Chem. Int. Ed.* **2001**, 40, 1736-1739.
39. Shibuya M. and Terauchi H. Synthetic Studies Towards Azinomycin A and B. Synthesis and Absolute Stereochemistry of the Minor Component Isolated from Azinomycins Producing Strain. *Tetrahedron Lett.* **1987**, 28, 2619-2622.

40. Shibuya M; Yamada T. and Ando K. Synthetic Approach towards Azinomycins. *Heterocycles* **1989**, 29, 2209-2218.
41. Shishido K; Shibuya M; Omodani T. Simple and Efficient Access to the Left-hand Segment of Azinomycins. *J. Chem. Soc. Perkin Trans. 1* **1992**, 2053-2054.
42. Schreiber S.L; Schreiber T.S; Smith D.B. Reactions That Proceed with a Combination of Enantiotopic Group and Diastereotopic Face Selectivity Can Deliver Products with Very High Enantiomeric Excess: Experimental Support of a Mathematical Model. *J. Am. Chem. Soc.* **1987**, 109, 1525-1529.
43. Konda Y; Machida T; Sasaki T; Takeda K; Takayanagi H; Harigaya K. Convenient Synthesis of the Epoxy Fragment of Azinomycin B. *Chem. Pharm. Bull.* **1994**, 42, 285-288.
44. Coleman R.S; McKinley J.D. A Correction of Three Reports on the Synthesis of the Epoxide Fragment of the Azinomycins. *Tetrahedron Lett.* **1998**, 39, 3433-3434.
45. Coleman R.S; Sarko C.R; Gittinger J.P. Efficient Stereoselective Synthesis of the Epoxyacid Fragment of the Azinomycins. *Tetrahedron Lett.* **1997**, 38, 5917-5920.
46. Shipman M.J; Bryant H.J; Dardonville C.Y; Hodgkinson T.J; Slavin A.M.Z. Asymmetric Synthesis of the Epoxide Portion of the Azinomycins. *Synlett* **1996**, 973-974.
47. Shipman M.J; Helen J; Bryant H.J; Dardonville C.Y; Hodgkinson T.J; Hursthouse M.B; Malik K.M.A. Asymmetric Synthesis of the Left Hand Portion of the Azinomycins. *J. Chem. Soc. Perkin Trans. 1* **1998**, 1249-1255.
48. Armstrong R.W; Moran E.J. Highly Convergent Approach to the Synthesis of the Epoxy-amide of the Azinomycins. *Tetrahedron Lett.* **1991**, 32, 3807-3810
49. Armstrong R.W; Kim S.W; Bauer S.M. Multicomponent Solution Phase Synthesis of Dehydroamino Acid Derivatives Based on the Passerini Reaction. *Tetrahedron Lett.* **1998**, 39, 7031-7034.
50. Armstrong R.W; Combs A.P; Tempest P.A; Brown S.D; Keating S.D. Multiple-Component Condensation Strategies for Combinatorial Library Synthesis. *Acc. Chem. Res.* **1996**, 29, 123-131.

51. Armstrong R.W. Tellev E.J; Moran E.J. Stereoselective synthesis of (E)- and (Z)-1-azabicyclo[3.1.0]hex-2-ylidene dehydroamino acid derivatives. *J. Org. Chem.* **1992**, 57, 2208-2211.
52. Armstrong R.W; Tellev J.E; Moran E.J. Mono-Osmylation of Dehydroamino Acid Dienes: Synthesis of Dehydroamino Acids Related to the Azinomycins. *Tetrahedron Lett.* **1996**, 37, 447-450.
53. Moran E.J; Tellev J.E; Zhao Z; Armstrong R.W. Dehydroamino acid derivatives from _D-Arabinose and _L-Serine: Synthesis of models for the azinomycin antitumour antibiotics. *J. Org. Chem.* **1993**, 58, 7848-7859.
54. Armstrong R.W; Moran E.J. Stereoselective synthesis of a 1-azabicyclo[3.1.0]hex-2-ylidene dehydroamino acid derivative related to the azinomycin antitumour antibiotics. *J. Am. Chem. Soc.*, **1992**, 114, 371-372.
55. Coleman R.S; Dong Y; Carpenter A.J. A Convenient Synthesis of Terminally Differentiated, Selectively Protected Six-Carbon Synthons from D-Glucose. *J. Org. Chem.* **1992**, 57, 3732-3735.
56. Coleman R.S; Carpenter A.J. Synthesis of the aziridino[1,2-a]pyrrolidine substructure of the antitumour agents azinomycin A and B. *J. Org. Chem.* **1992**, 57, 5813-5815.
57. Coleman R.S; Carpenter A.J. The Development of Strategies for Construction of the Azirdine Core of the Antitumour Agents Azinomycins A and B. *Tetrahedron* **1997**, 53, 16313-16326.
58. Coleman R.S; Kong J-S. Stereocontrolled Synthesis of the Fully Elaborate Aziridine Core of the Azinomycins. *J. Am. Chem. Soc.* **1998**, 120, 3538-3539.
59. Coleman R.S; Richardson T.E; Carpenter A.J. Synthesis of the azabicyclic core of the azinomycins: Introduction of differentiated *trans*-diol by crotylstannane addition to serinal. *J. Org. Chem.* **1998**, 63, 5738-5739.
60. Coleman R.S; Carpenter A.J. Stereoselective Bromination of Dehydroamino Acids with Controllable Retention or Inversion of Olefin Configuration. *J. Org. Chem.* **1993**, 58, 4452-4461.
61. Terashima S; Hashimoto M; Yamada K. Synthesis, Chemical Reactivity and Cytotoxicity of 2-Bis(alkyloxycarbonyl)methylidene-1-azabicyclo[3.1.0]hexane Systems Related to Antitumour Antibiotics Carzinophilin A. *Chem. Lett.* **1992**, 975-978.

62. Hashimoto M; Terashima S.A. Stereoselective Synthesis of a Novel Model Compound of Carzinophilin Carrying the C6-C13 Unit with Correct Stereochemistry. *Chem. Lett.* **1994**, 1001-1002.
63. Terashima S; Hashimoto M. The Novel Synthesis of the C1-C17 Fragment of Carzinophilin. *Tetrahedron Lett.* **1994**, 35, 9409-9412.
64. Terashima S; Hashimoto M; Matsumoto M. Synthetic Studies of Carzenophilin. Part 1: Synthesis of 2-methylidene-1-azabicyclo[3.1.0] hexane Systems Related to Carzinophilin. *Tetrahedron* **2003**, 59, 3019-3040.
65. Shipman M; Hodgkinson T.J. Practical Assymmetric Synthesis of Both Enantiomers of 6-(Hydroxymethyl)piperidine-2-one. *Synthesis* **1998**, 1141-1144.
66. Shipman M; Hodgkinson T.J; Kelland L.R; Vile J. Synthesis and Reactivity of Some Chiral, Nonracemic 1-Azabicyclo[4.1.0]heptanes Related to the Azinomycins. *Tetrahedron* **1998**, 6029-6034.
67. Konda Y; Sato T; Tsushima K; Dodo M; Kusunoki A; Sakayanagi M; Sato N; Tekada K; Harigaya Y. An efficient Synthesis of (Pyrrolidin-2-ylidene)Glycinate Using Intramolecular 1,3-Dipolar Cycloadditions of Azide and Olefin. *Tetrahedron* **1999**, 55, 12723-12740.
68. Shipman M; Hartley J.A; Hazrati A; Kelland L.R; Khanim R; Suzenet F; Wlaker L.F. A Synthetic Azinomycin Analogue with Demonstrated DNA Cross-Linking Activity: Insights into the Mechanism of Action of this Class of Antitumour Agent. *Angew. Chem. Int. Ed.* **2000**, 39, 3467-3470.
69. Coleman R.S; Alcaro S. Molecular Modelling of the Antitumour Agents Azinomycins A and B: Force-Field Parametrization and DNA Cross-linking-Based Filtering. *J. Org. Chem.* **1998**, 63, 4620-4625.
70. Coleman R.S; Alcaro S. A Molecular Model for DNA Cross-Linking by the Azinomycin Agent Azinomycin B. *J. Med. Chem.* **2000**, 43, 2783-2788.
71. Saito I; Fujiwara T. Highly Efficient DNA Interstrand Cross-Linking Induced by an Antitumour Antibiotic, Carzinophilin. *Tetrahedron Lett.* **1999**, 40, 315-318.
72. Gates K.S; Zang H. DNA Binding and Alkylation by the "Left Half" of Azinomycin B. *Biochemistry* **2000**, 39, 14968-14975.
73. Coleman R.S; Perez R.J; Burk C.H; Navarro A. Studies on the Mechanism of Action of Azinomycin B: Definition of Regioselectivity and Sequence

Selectivity of DNA Cross-Link Formation and Clarification of the Role of the Central Naphthoate. *J. Am. Chem. Soc.* **2002**, 124, 13008-13017.

74. Shipman M; Hodgkinson T.J; Kelland L.R; Suzenet F. Chemical Synthesis and Cytotoxicity of Some Azinomycin Analogues Devoid of the 1-Azabicyclo[3.1.0]hexane Subunit. *Bioorg. Med. Chem. Lett.* **2000**, 10, 239-241.
75. Shipman M; Hodgkinson T.J; Kelland L.R; Suzenet F; Hartley J.A; Hazrati A; Khanim R. Synthesis, Cytotoxicity and DNA Cross-linking Activity of Symmetrical Dimers Based Upon the Epoxide Domain of the Azinomycins. *Chem. Comm.* **2000**, 2325-2326.
76. Shipman M; Goujon J-Y. Concise Route to α -Acylamino- β -Keto Amides: Application to the Synthesis of a Simplified Azinomycin A Analogue. *Tetrahedron Lett.* **2002**, 43, 9573-9576.
77. Terashima S; Hashimoto M; Sugiura M. Synthetic Studies of Carzinophilin. Part 3: Synthetic Approach Toward Carzinophilin and Successful Synthesis of 13-O-desacetyl-12,13-di-O-methyl carzinophilin. *Tetrahedron* **2003**, 59, 3063-3087.
78. Terashima S; Hashimoto M; Matsumoto M; Yamada K. Synthetic Studies of Carzinophilin. Part 4: Chemical and Biological Properties of Carzinophilin Analogues. *Tetrahedron* **2003**, 59, 3089-3097.
79. Boger D.L; Johnson D.S; Wrasidlo W. Induction of Endonucleolytic DNA Fragmentation and Apoptosis by the Duocarmycins. *Bioorg. Med. Chem. Lett.* **1994**, 4, 631-636.
80. Boger D.L; Bollinger B; Johnson D.S. Examination of the Role of the Duocarmycin SA Methoxy Substituents: Identification of the Minimum, Fully Potent DNA Binding Subunit. *Bioorg. Med. Chem. Lett.* **1996**, 6, 2207.
81. Boger D.L; Santillan A; Searcey M; Brunette S.R; Wolkenberg S.E; Hedrick M.P; Jin Q. 1,2,8,8a-Tetrahydrocyclopropa[c]pyrrolo[3,2-e]indol-4(5H)-one, the Parent Alkylation Subunit of CC-1065 and the Duocarmycins: Implications for the DNA Alkylation Catalysis. *J. Org. Chem.* **2000**, 65, 4101-4111.
82. Casely-Hayford M.A. and Searcey M. Azinomycins. Discovery, Synthesis, and DNA Binding Studies. In *DNA and RNA Binders, From Small Molecules to Drugs*. Edited by Demeunynck C.B; Wilson W.D. 2, **2003**, 676-696.

83. Jacobsen E.N; Marko I; Mungall W.S; Schroder G. and Sharpless K.B. Asymetric Dihydroxylation via Ligand-Accelerated Catalysis *J. Am. Chem. Soc.*, **1988**, 110, 1968-1970
84. Goodman M; Shao H. An Enantioselective Synthesis of *allo*-Threonines and β -Hydroxyvalines *J. Org. Chem.* **1996**, 61, 2582-2583
85. Kolb H.C; VanNieuwenhze M.S and Sharpless K.B. Catalytic Asymetric Dihydroxylation *Chem. Rev.* **1994**, 94, 2483-2547
86. Wladman H. "Enantioselective *cis*-Dihydroxylation": In *Organic Synthesis Highlights II*. VCH, Edited by Wladmann H. **1995**, 9-18
87. Shinzer D. "The Sharpless Epoxidation": In *Organic Synthesis Highlights II*. VCH, Edited by Wladmann H. **1995**, 3-8
88. Furnings B.S; Hannaford A.J; Rogers V; Smith P.W.G; Tatchell A.R. *Vogels Textbook of Practical Organic Chemistry*. Harlow : Longman Scientific & Technical, **1989**.
89. Ksander G.M; McMurry J.E. and Johnson M. A Method for the Synthesis of Unsaturated Carbonyl Compounds *J. Org. Chem.* **1977**, 42, 1180-1185
90. Gao X; Stassinopoulos A; Gu J; Goldberg I.H. NMR Studies of the Post-Activated Neocarzinostatin Chromophore-DNA Complex. Conformational Changes Induced in Drug and DNA. *Bioorg. Med. Chem.* **1995**, 3, 795-809.
91. Lerman S. Structural Considerations in the Interaction of DNA and Acridines. *J. Mol. Biol.* **1961**, 3, 18-30.
92. Neidle S. *Nucleic Acid Structure and Recognition*. Oxford University Press. **2002**
93. Waring M. Variation of the Supercoils in Closed Circular DNA by binding of Antibiotics and Drugs: Evidence for Molecular Models Involving Intercalation. *J. Mol. Biol.* **1970**, 54, 247-279.
94. Muller W; Crothers D.M. Studies of the Binding of Actinomycin and Related Compounds to DNA. *J. Mol. Biol.* **1968**, 35, 251-290.
95. Sengupta S.K. Inhibitors of DNA-Transcribing Enzymes. In *Cancer Chemotherapeutic agents*. ACS Washington DC, **1995**, 261-292.
96. Brennan T.F; Sengupta S.K. DNA Binding of 7-Bulky-Substituted Actinomycin Analogues. *J. Med. Chem.* **1983**, 26, 448-451.
97. Suh D; Chaires J.B. Criteria for the Mode of Binding of DNA Binding Agents. *Bioorg. Med. Chem.* **1995**, 3, 723-728.

98. Lepecq J.B; Paoletti C. A Fluorescent Complex Between Ethidium Bromide and Nucleic Acids. Physical-Chemical Characterization *J. Mol. Biol.* **1967**, 27, 87-106.
99. Muller M. and Crothers D..M. Studies of the Binding of Actinomycin and Related Compounds to DNA. *J. Mol. Biol.* **1968**, 35, 251-290.
100. Waring M.J; Wakelin L.P.G. Echinomycin: A Bifunctional Intercalating Antibiotic. *Nature* **1974**, 252, 653-657.
101. Rajski S.R; Williams R.M. DNA Cross-linking Agents as Antitumour Drugs. *Chem. Rev.* **1999**, 98, 2723-2795.
102. Krieg D.R; Ethyl Methanesulfonate-induced Reversion of Bacteriophage T4rII Mutants. *Genetics* **1963**, 48, 561.
103. Watson J.D; Crick F.H.G. Molecular Structure of Nucleic Acids: A Structure of Deoxyribose Nucleic Acid. *Nature* **1953**, 171, 737-734.
104. Watson J.D; Crick F.H.G. Genetic Implications of the Structure of Deoxyribonucleic Acid. *Nature* **1953**, 171, 964-967.
105. Kronberg A. DNA Replication. *J. Biol. Chem.* **1988**, 263, 1-4.
106. Meselson M; Stahl F.W. The Replication of DNA in Escherichia Coli. *Proc. Natl. Acad. Sci. USA.* **1958**, 44, 671-682.
107. Lawley P.D. Alkylation of DNA and it Aftermath. *BioEssays* **1995**, 17, 561-568.
108. Paustenbach D.J; Finley B.L; Kacew S. Biological Relevance and Consequences of Chemical- or Metal-Induced DNA Cross-Linking. *P. Soc. Exp. Biol. Med.* **1996**, 211, 211-217.
109. Lawley P.D; Brookes P. The Alkylation of Guanosine and Guanilic Acid. *J. Chem. Soc.* **1961**, 3923.
110. Lawley P.D; Brookes P. The Reaction of Mono- and Di-functional Alkylating Agents with Nucleic Acids. *Bioch. J.* **1961**, 80, 496-503.
111. Hopkins P.B; Raucher S; Millard J.T. Mechlorethamine Cross-Links Deoxyguanosine Residues at 5'GNC Sequences in Duplex DNA Fragments. *J. Am. Chem. Soc.* **1990**, 112, 2459.
112. Grueneberg D.A; Loechler E.L; Ojwang J.O. Synthesis of a Duplex Oligonucleotide Containing a Nitrogen Mustard Interstrand DNA-DNA Cross-Link. *Cancer Res.* **1989**, 49, 6529.

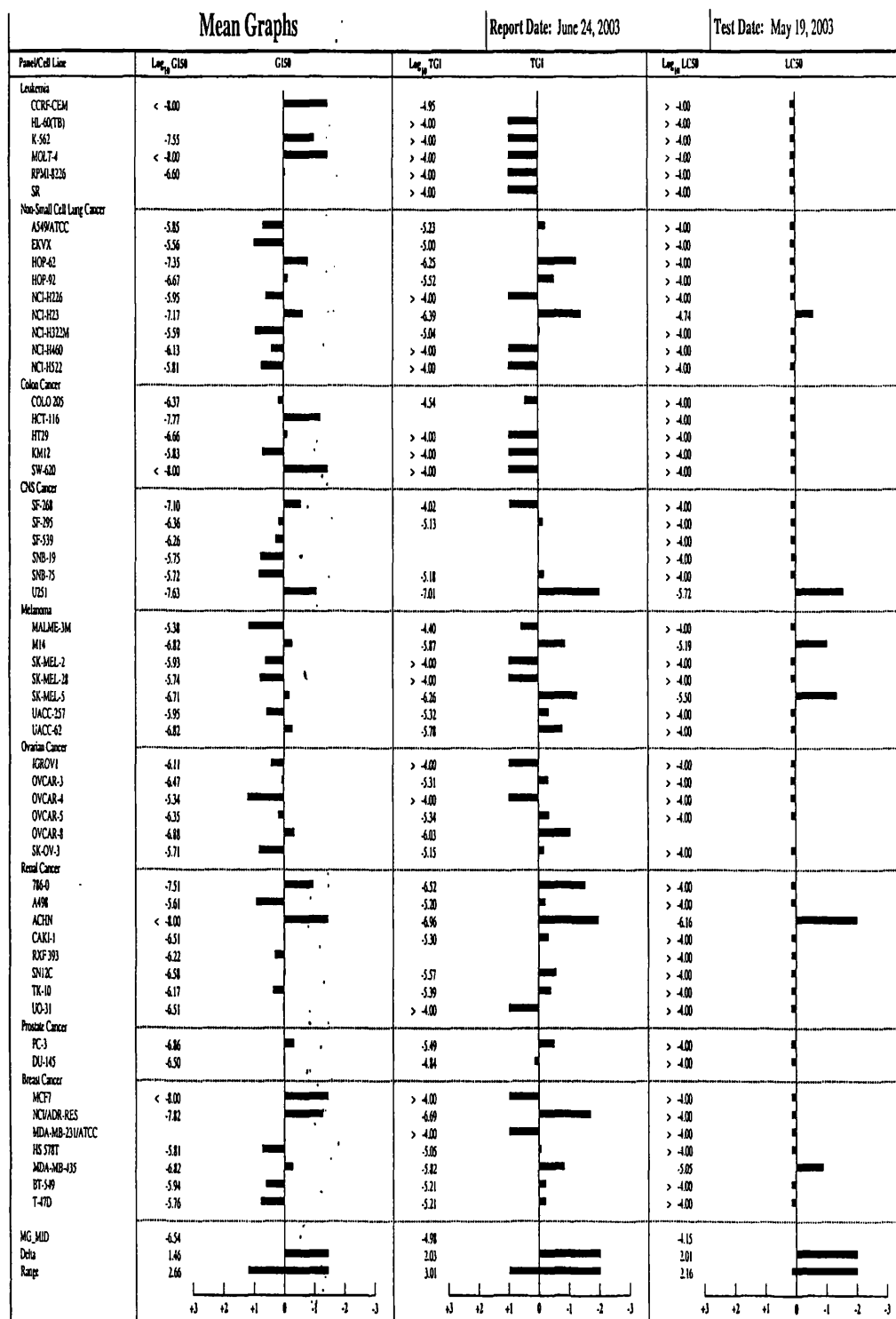
113. Rink S.M; Solomon M.S; Taylor M.J; Sharanabasava R.B; McLaughlin L.W; Hopkins P.B. Covalent Structure of a Nitrogen Mustard-Induced DNA Interstrand Cross-Link: An N-7 to N-7 Linkage of Deoxyguanosine Residues at the Duplex Sequence 5'-d(GNC). *J. Am. Chem. Soc.* **1993**, 115, 2551.
114. Hata T; Sano Y; Sugawara R; Matsumae A; Kanamori K; Shima T; Hoshi T. Mitomycin, A New Antibiotic from Streptomyces. I. *J. Antibiot. Ser A.* **1956**, 9, 141-146.
115. Hata T; Sano Y; Sugawara R. Mitomycin, A New Antibiotic from Streptomyces. II Description of the Strain. *J. Antibiot. Ser A.* **1956**, 9, 147-151.
116. Iyer V.N; Szybalski W. A Molecular Mechanism of Mitomycin Action: Linking of Complementary DNA Strands. *Proc. Natl. Acad. Sci.* **1963**, 50, 355.
117. Iyer V.N, Szybalski W. Chemical Mechanism of Activation and Cross-Linking of DNA. *Science* **1964**, 145, 55.
118. Terawaki A; Greenberg J. Inactivation of Transforming Deoxyribonucleic Acid by Carzinophilin and Mitomycin C. *Biochim. Biophys. Acta* **1966**, 119, 59-64.
119. Terawaki A; Greenberg J. Effect of Carzinophilin on Bacterial Deoxyribonucleic Acid: Formation of Inter-Strand Cross-Links in Deoxyribonucleic Acid and their Disappearance During Post-Treatment Incubation. *Nature* **1966**, 209, 481-484.
120. Ross W.C.J; Connors T.A; Mitchley B.C.V; Rosenoer V.M. *Biochem. Pharmacol.* **1970**, 13, 395-400.
121. Ross W.C.J. *Biochem. Pharmacol.* **1961**, 8, 235-240.
122. Armstrong R.W; Salvati M.E; Nguyen M. Novel Interstrand Cross-Links Induced by the Antitumour Antibiotic Carzinophilin/Azinomycin B. *J. Am. Chem. Soc.* **1992**, 114, 3144-3145.
123. Hartley J.A; Berardini M.D; Souhami R.L. An Agarose Gel Method for the Determination of DNA Interstrand Crosslinking Applicable to the Measurement of the Rate of Total and "Second-Arm" Crosslink Reactions. *Anal. Biochem.* **1991**, 193, 131-134.
124. Höckel M; Vaupel P. Tumour Hypoxia: Definitions and Current Clinical, Biological, and Molecular Aspects. *J. Natl. Cancer Inst.* **2001**, 93, 266-276.

125. Patterson L.H; Raleigh S.M. Reductive Metabolism: Its Application in Prodrug Activation in *Drug Metabolism: Towards the Next Millenium*, edited by Gooderman N, 1998, 72-79.
126. Siim B.G; Hicks K.O; Pullen S.M; Zilj P.L; Denny W.A; Wilson W.R. Comparison of Aromatic and Tertiary Amine *N*-Oxides of Acridine DNA Intercalators as Bio-reductive Drugs: Cytotoxicity, DNA Binding, Cellular Uptake, and Metabolism. *Biochem. Pharmacol.* 2000, 60, 969-978.
127. Patterson L.H; Teesdale-Spittle P; Fischer G.R. Craven M.R. Aliphatic *N*-oxides of DNA Binding Agents as Bio-reductive Drugs. *Oncol. Res.* 1994, 6, 533-538. Pors K. Synthesis and Biological Evaluation of Novel Anthraquinones with Alkylating Capability. *Thesis*, 2002.
128. Patterson L.H; Friery O.P; Gallagher R; Murray M.M; Hughes C.M; Galligan E.S; McIntyre I.A; Hirst D.G; McKeown S.R. Enhancement of the Anti-tumour Effect of Cyclophosphamide by the Bio-reductive Drugs AQ4N and Tirapazamine. *Br. J. Cancer* 2000, 82, 1469-1473.
129. Patterson L.H; Friery O.P; McKeown S.R; McIntyre I.A; Hirst D.G; Hejmadi M.V. DNA Damage following Combination of Radiation with the Bio-reductive Drug AQ4N: Possible Selective Toxicity to Oxic and Hypoxic Tumour Cells. *Br. J. Cancer* 1996, 73, 499-505.
130. Mattocks A.R; White I.N.H; Bailey E; Suzanger M; Farmer P.B; Connors T.A. Reaction of Nitromin to Nitrogen Mustard: Unscheduled DNA Synthesis in Aerobic or Anaerobic Rat Hepatocytes, JB1, BL8 and Walker Carcinoma Cell Lines. *Carcinogenesis* 1989, 10, 2113-2118.
131. Denny W.A; Tercel M; Wilson W.R. Hypoxia Selective Antitumour Agents. II. Chlorambucil *N*-oxide: A Reappraisal of its Synthesis, Stability, and Selective Toxicity for Hypoxic Cells. *J. Med. Chem.* 1995, 38, 1247-1252.
132. Henderson N.D; Workman P; Plumb J.A; Robins D.J. Synthesis and Anti-Cancer Activity of 2,6-Disubstitute *N*-Methylpiperidine Derivatives and their *N*-Oxides. *Anticancer Drug Design* 1996, 11, 421-438.
133. Ortiz De Montellano P.R. Alkenes and Alkynes. In *Bioactivation of Foreign Compounds*. Edited by Anders M.W. Academic Press 1985, 121-145
134. Golding B.T; Cottrell L; Mackay D; Zhang D; Watson W.P. Stereochemical and Kinetic Comparisons of Mono- and Diepoxide Formation in the In Vitro

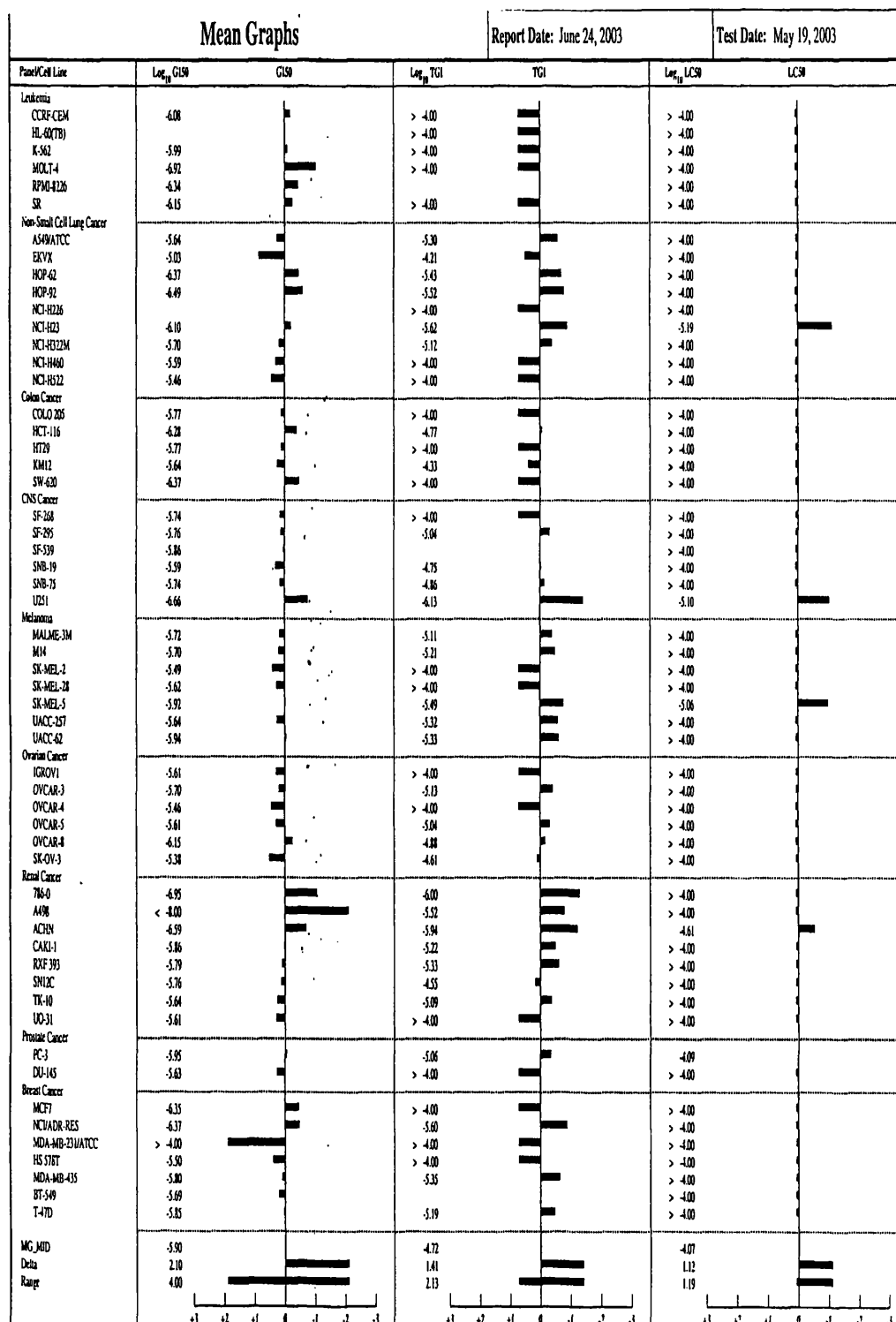
Metabolism of Isoprene by Liver Microsomes from Rats, Mice and Humans.
Chem. Res. Toxicol. **2003**, 16, 933-944.

135. Golding B.T; Cottrell L; Watson W.P; Kronberg L; Munter T. Identification of Adducts Derived from Reactions of (1-Chloroethenyl)oxirane with Nucleosides and Calf Thymus DNA. *Chem. Res. Toxicol.* **2002**, 15, 1549-1560.
136. Coleman R. S; and Shah J. A. Chemoselective Cleavage of Benzyl Ethers, Esters, and Carbamates in the Presence of Other Easily Reducible Groups. *Synthesis* **1999**, 1399-1400.

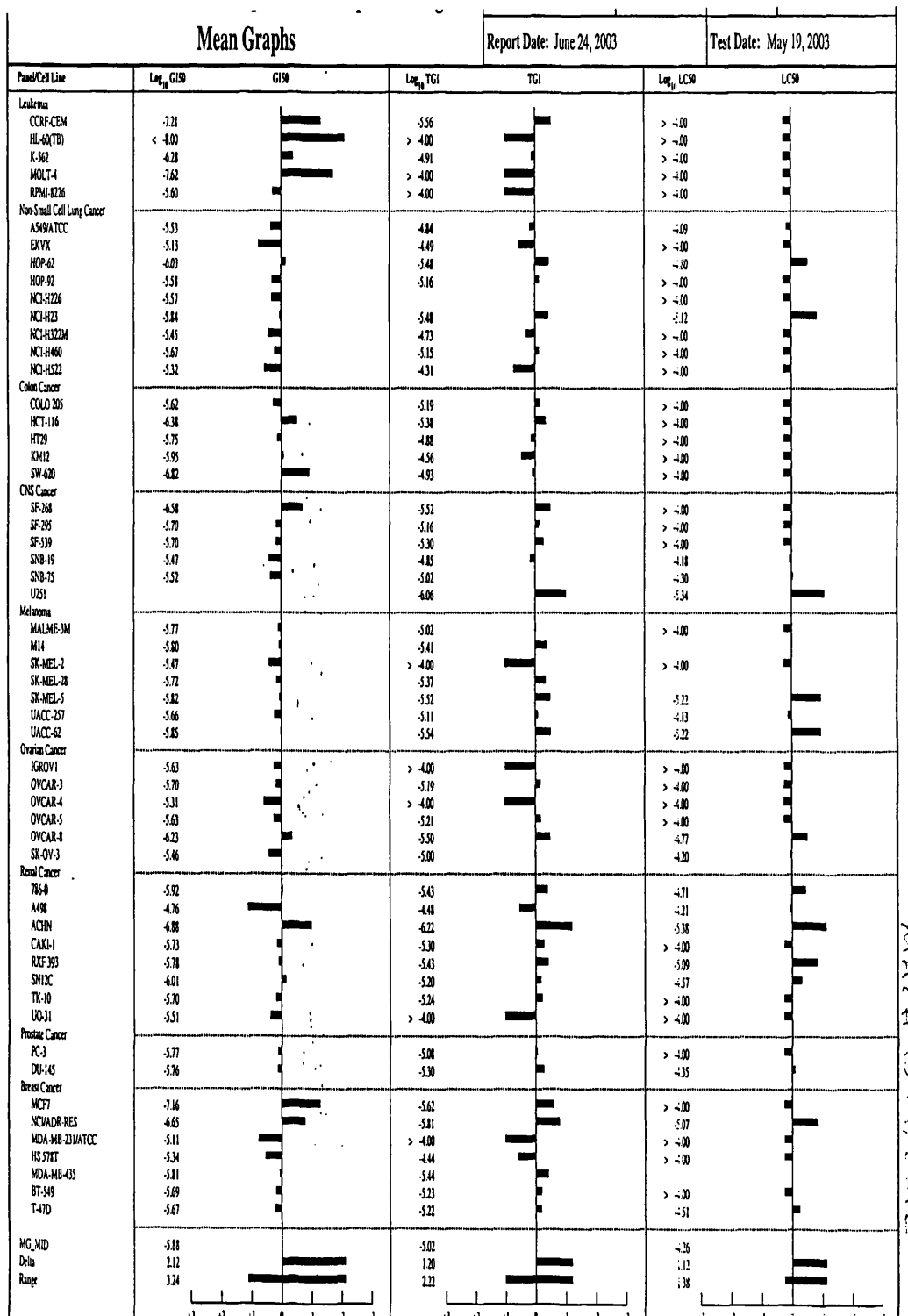
Appendix 1. Table1: Mean graph for (2S, 3S)-3



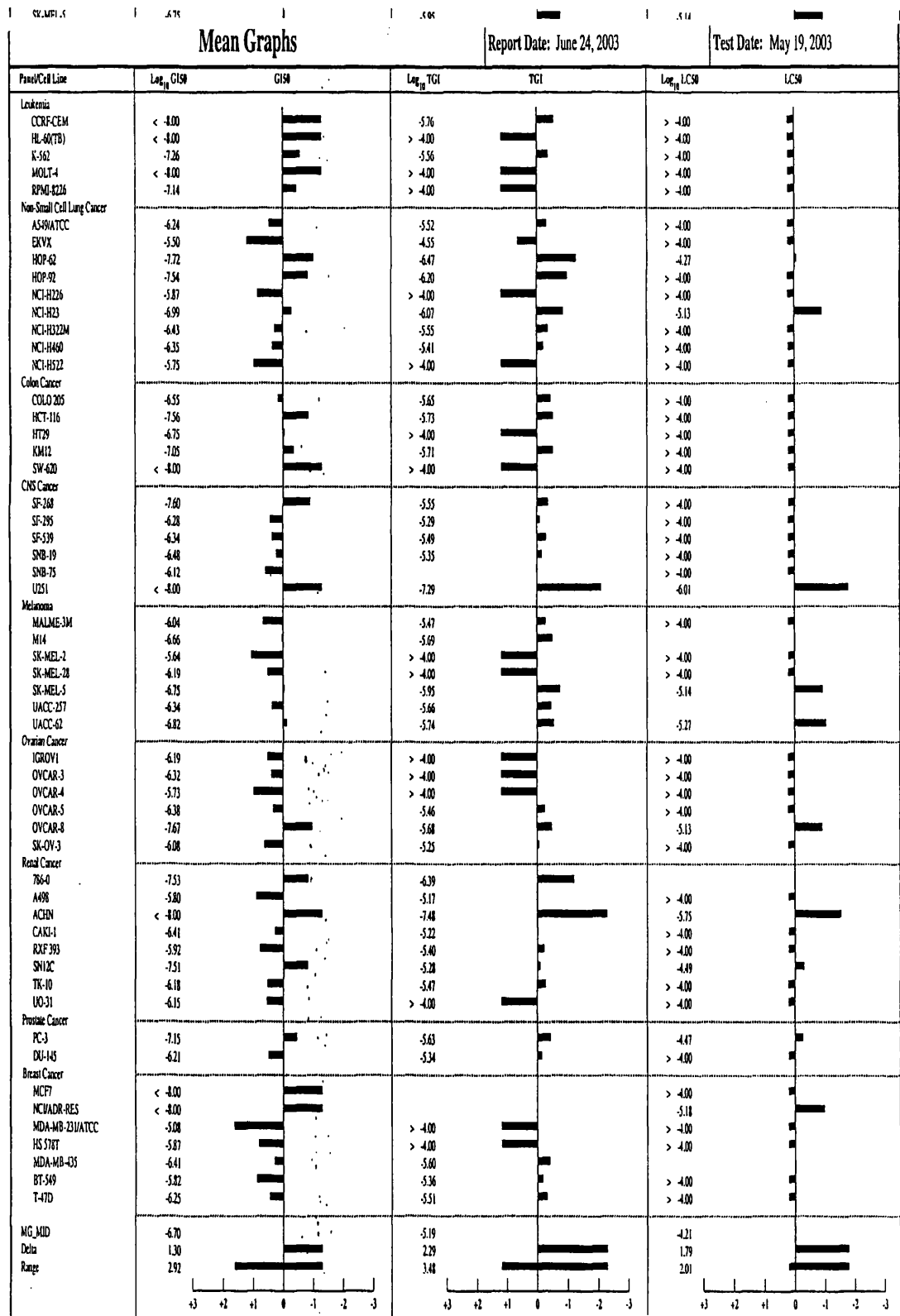
Appendix 1 Table 2. Mean graph for (2S, 3R)-3



Appendix 1 Table 3 Mean graph for (2R, 3S)-3



Appendix 1. Table 4; Mean graph for (2R, 3R)-3



Appendix 2 Buffer Solutions

3 M NaOAc

NaOAc (40.81 g)

dH₂O (100 ml)

TAE (50×)

EDTA (18.6 g)

Trizma base (121.0 g)

Glacial acetic acid (28.55 ml)

dH₂O to make up final volume of (500 ml)

0.5 M EDTA

EDTA (18.61 g)

dH₂O (80 ml)

pH 8 (with NaOH)

dH₂O to make up final volume of (100 ml)

TEoA

EDTA (200 µl, 0.5 M)

Triethanolamine (2.5 ml)

ddH₂O (80 ml)

pH 7.2 with HCl

dH₂O to make up volume of 100 ml

Strand Separation Buffer

DMSO (15 ml)

EDTA (100 µl, 0.5 M)

Bromophenol blue (0.02 g)

dH₂O to make up volume of 50 ml

Sucrose Loading Buffer

bromophenol blue (0.02 g)

sucrose (1.5 g)

dH₂O to make up volume of 25 ml

Stop Solution

3 M NaOAc (2 ml)

EDTA (0.4 ml, 0.5 M)

tRNA (100 µl)

dH₂O to make up volume of 50 ml

aliquot 500 µl in eppendorfs and store at –20 °C

Alkali Loading Buffer

bromophenol blue (4 mg)

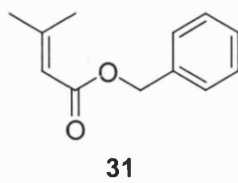
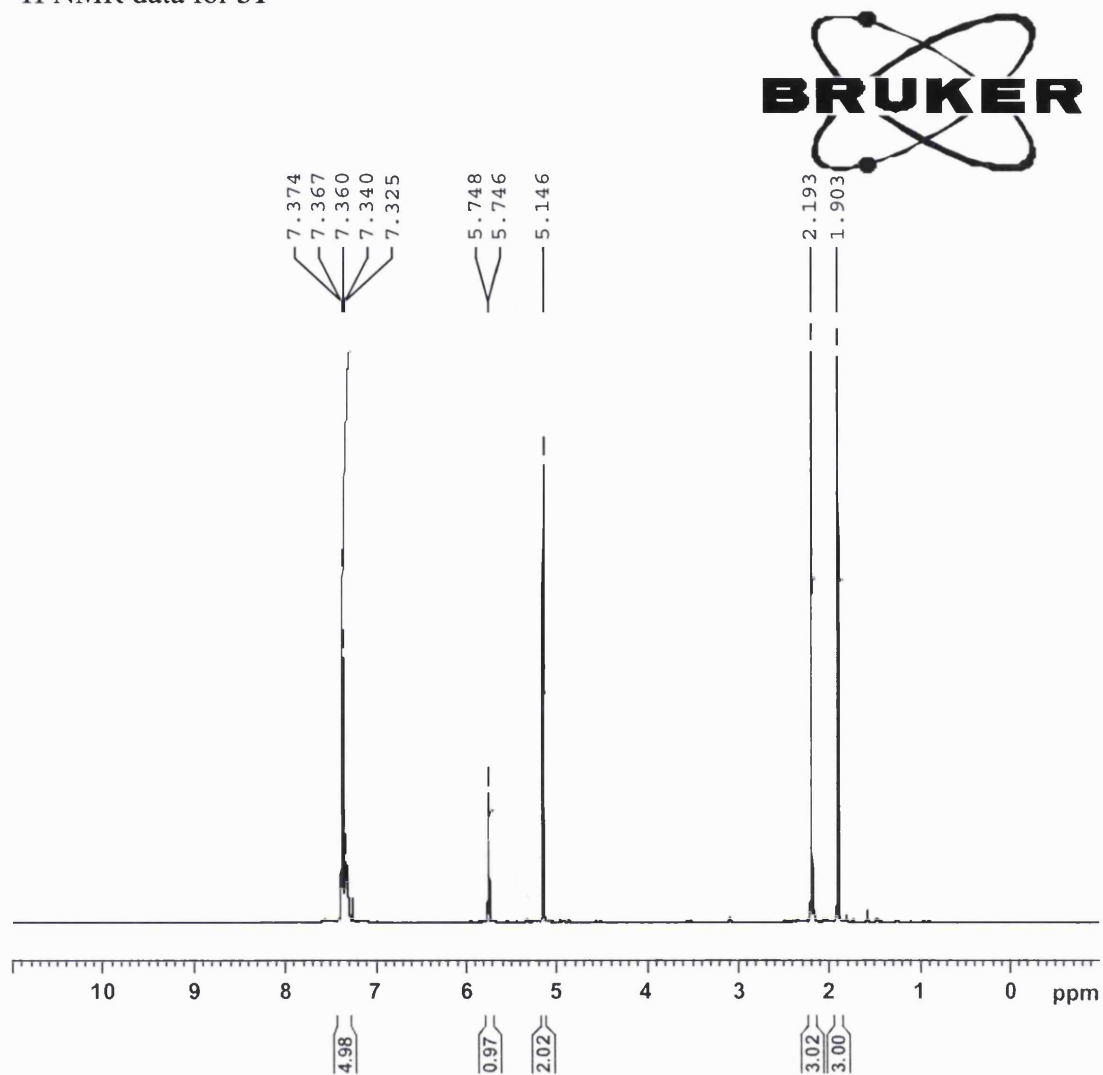
sucrose (0.6 g)

NaOH (0.04 g)

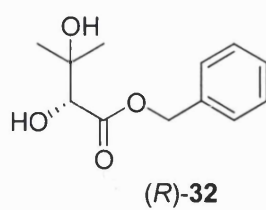
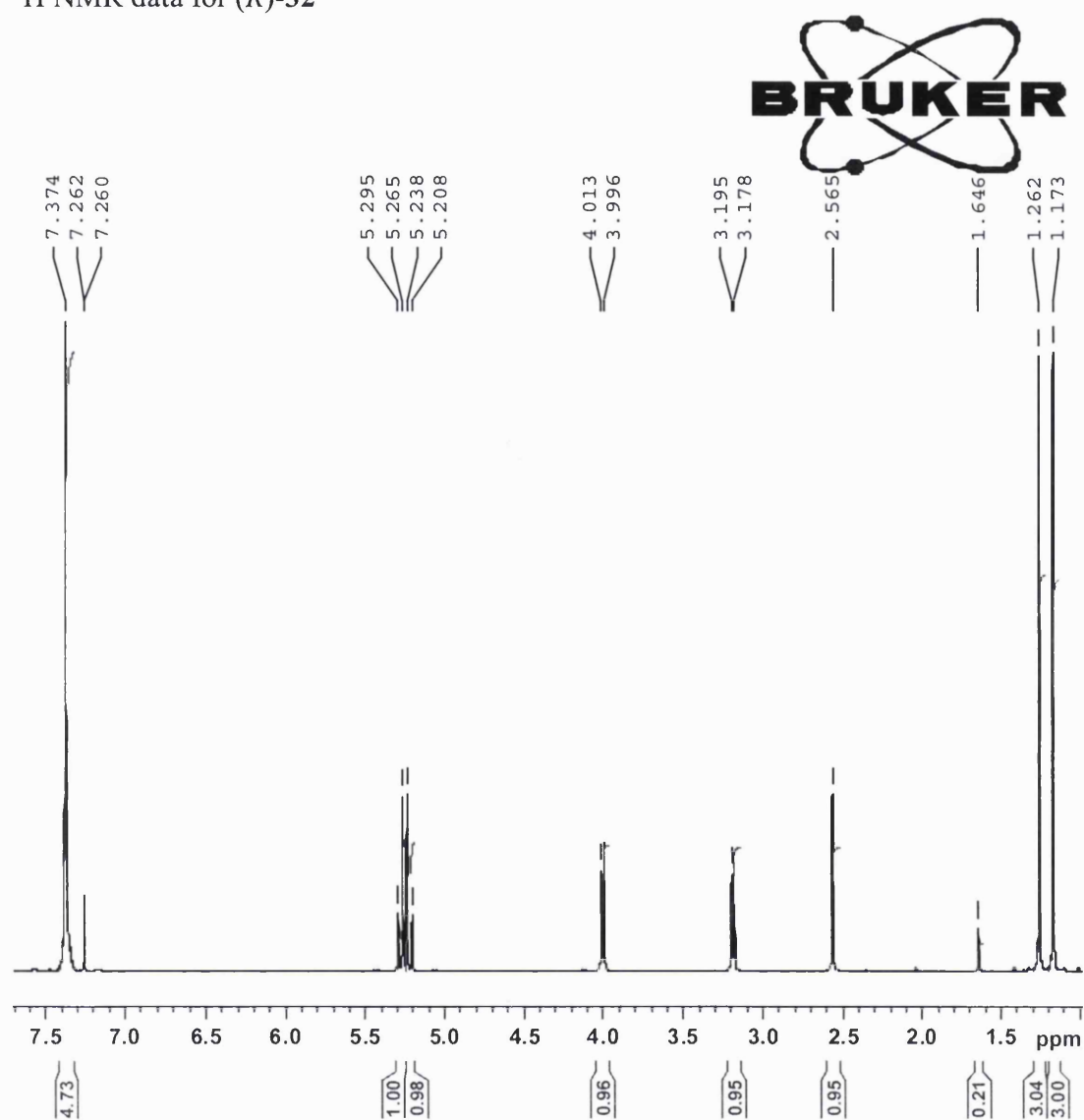
dH₂O to make up volume of 10 ml

Appendix 3 ^{13}C and ^1H NMR

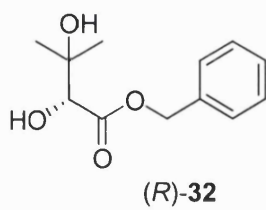
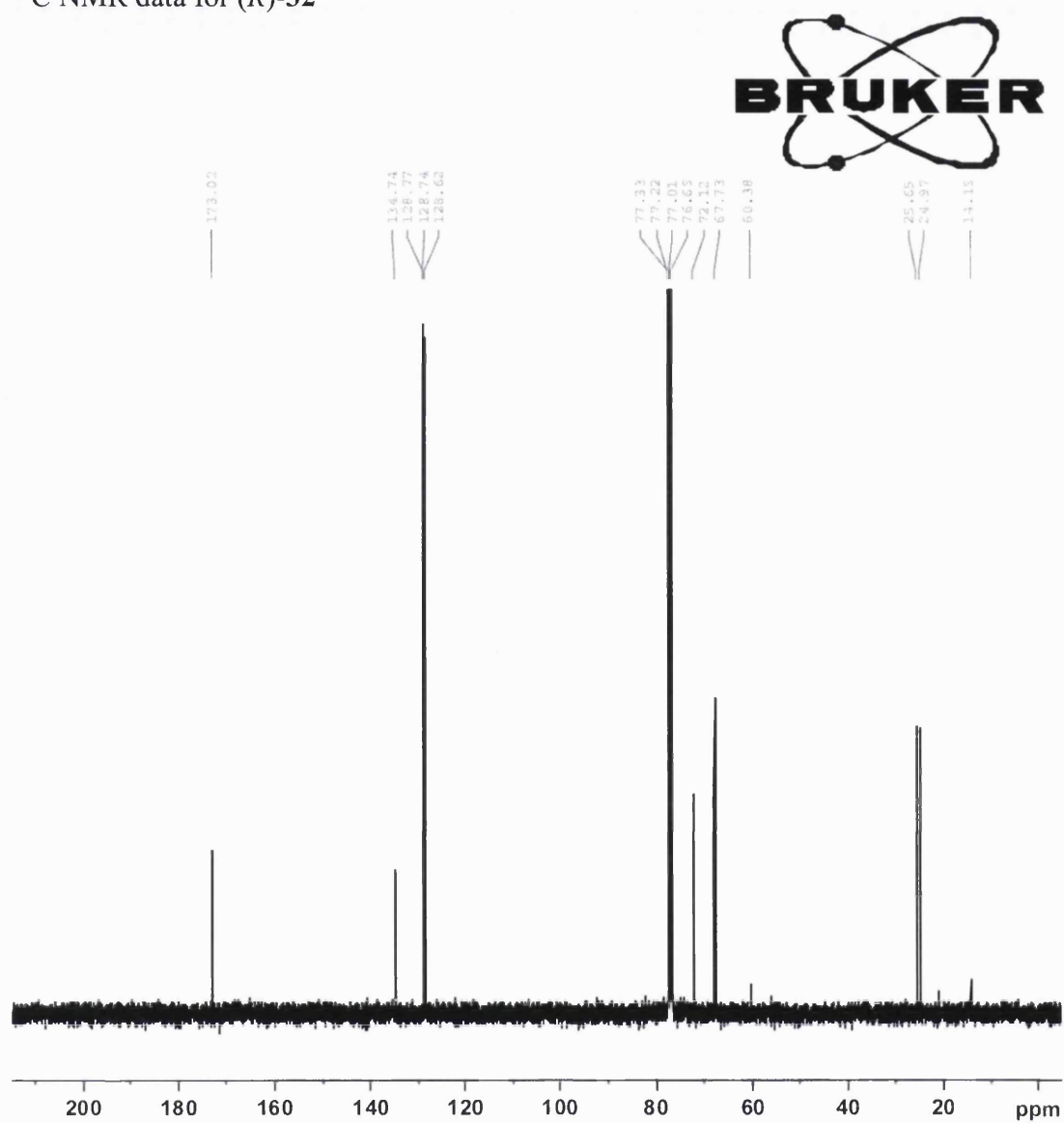
^1H NMR data for **31**



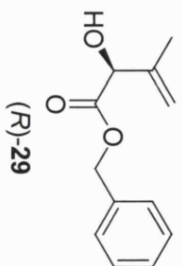
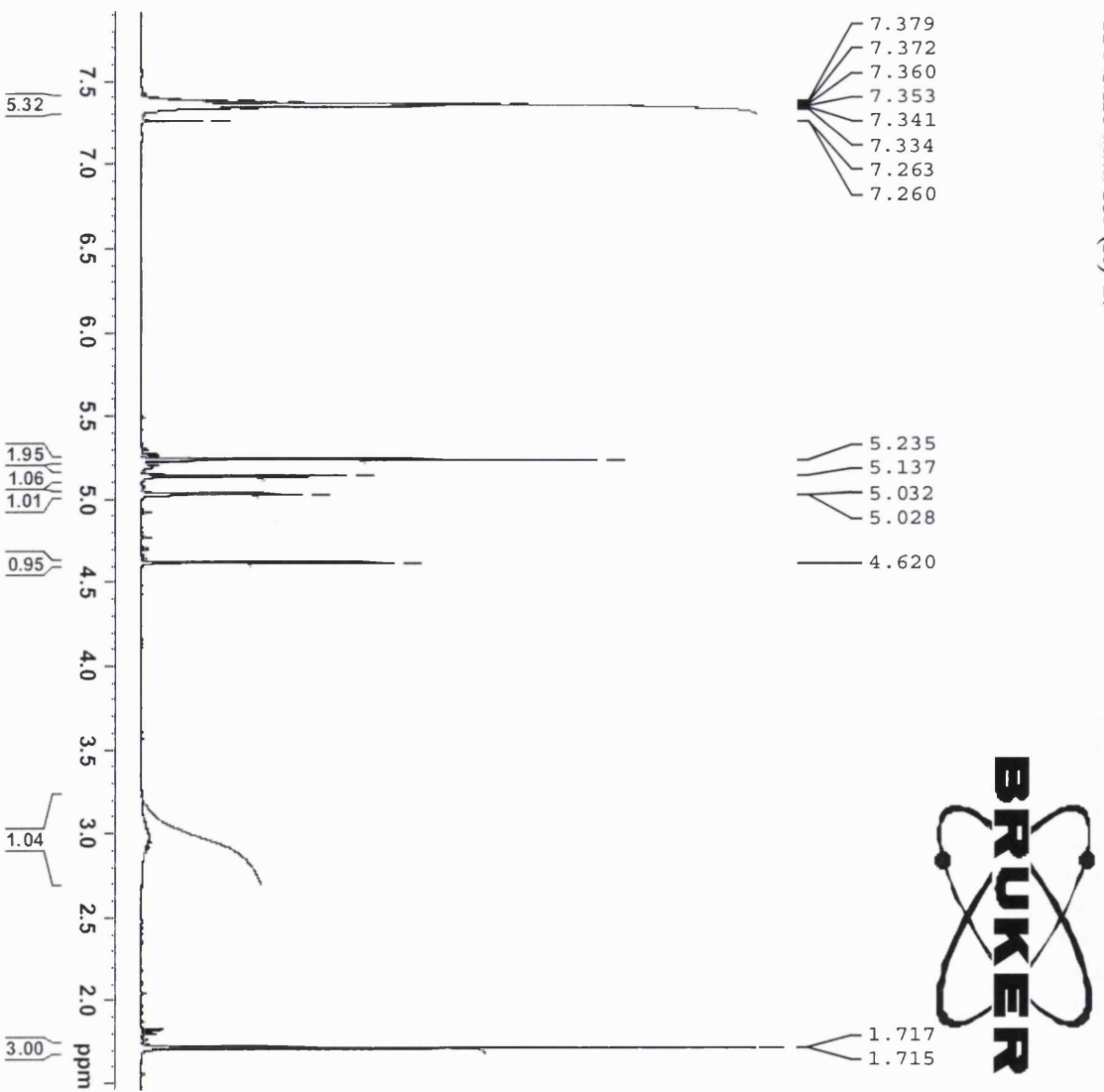
^1H NMR data for (*R*)-32



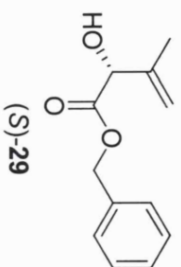
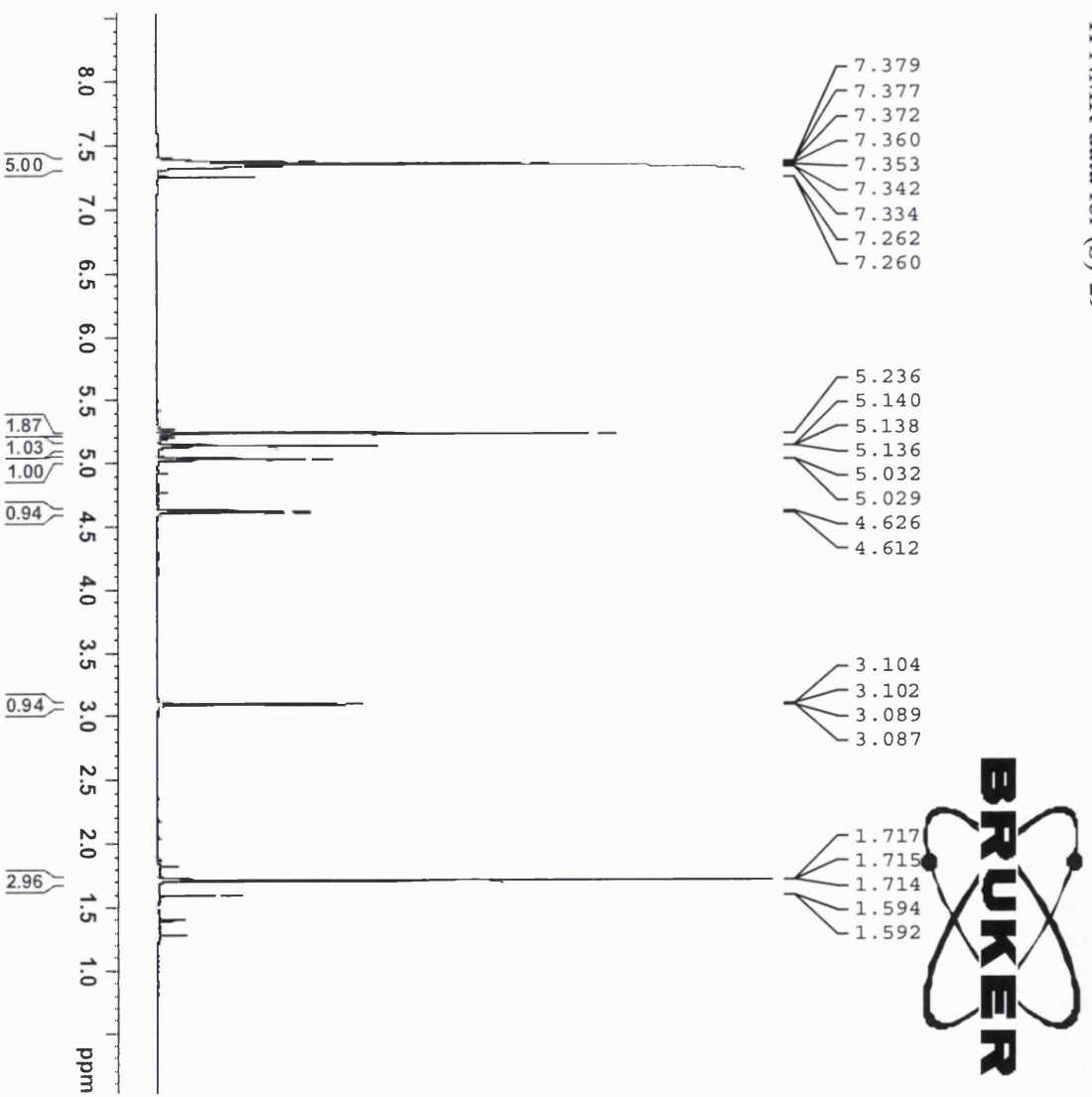
^{13}C NMR data for (*R*)-32



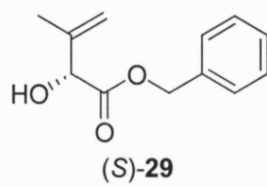
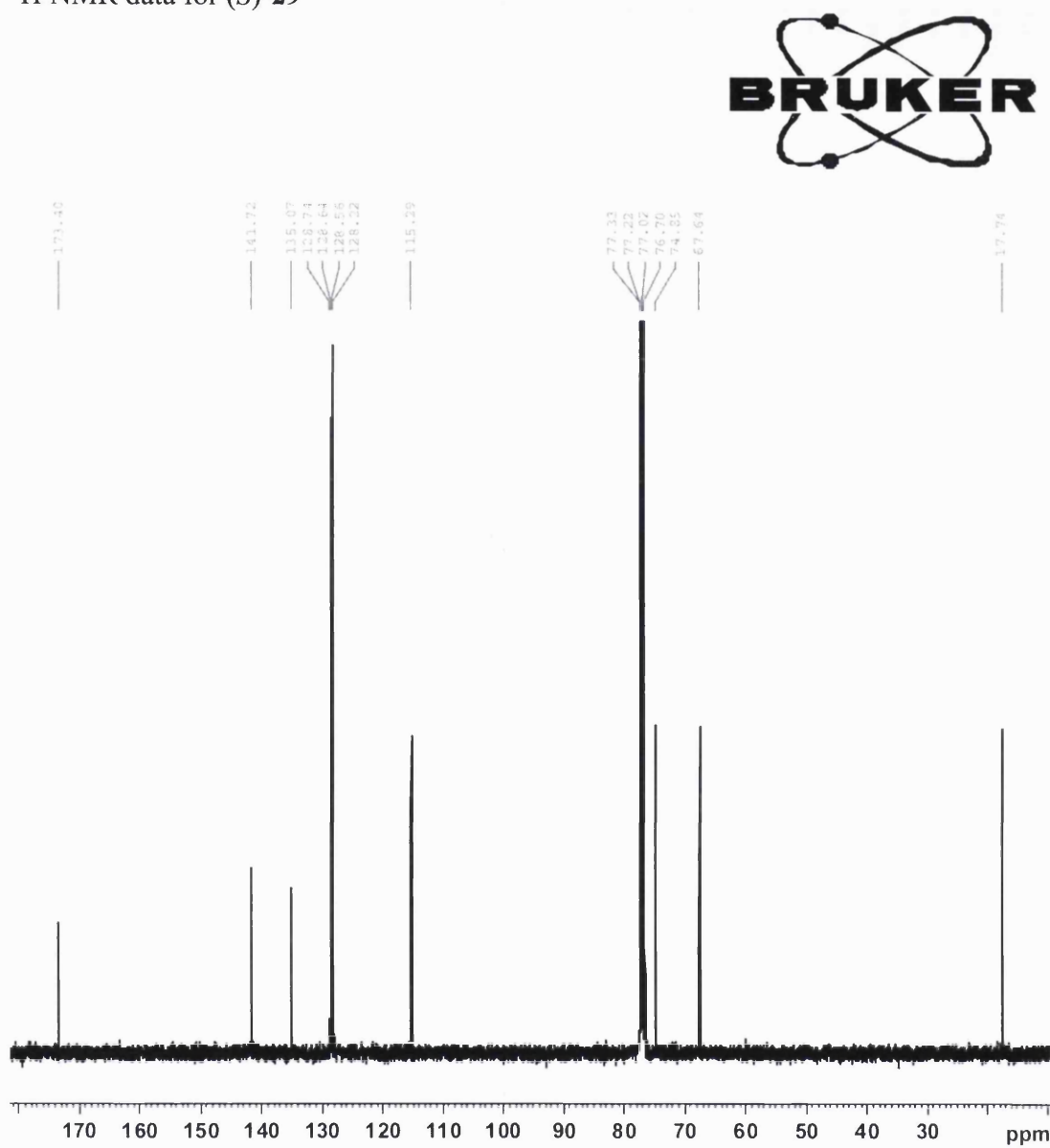
¹H NMR data for (*R*)-29



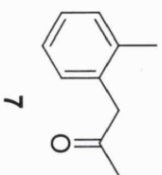
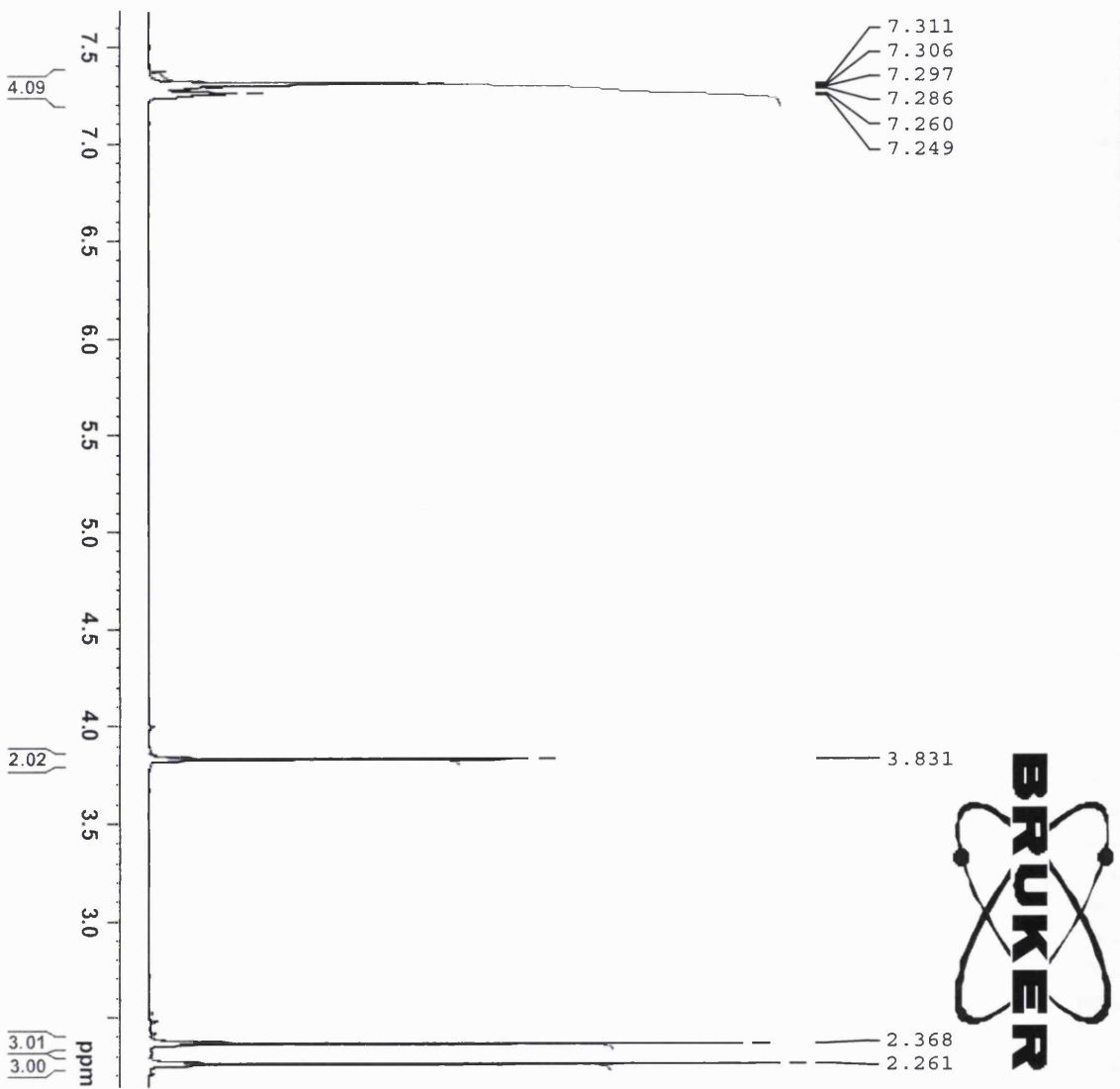
¹H NMR data for (S)-29



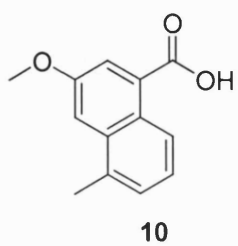
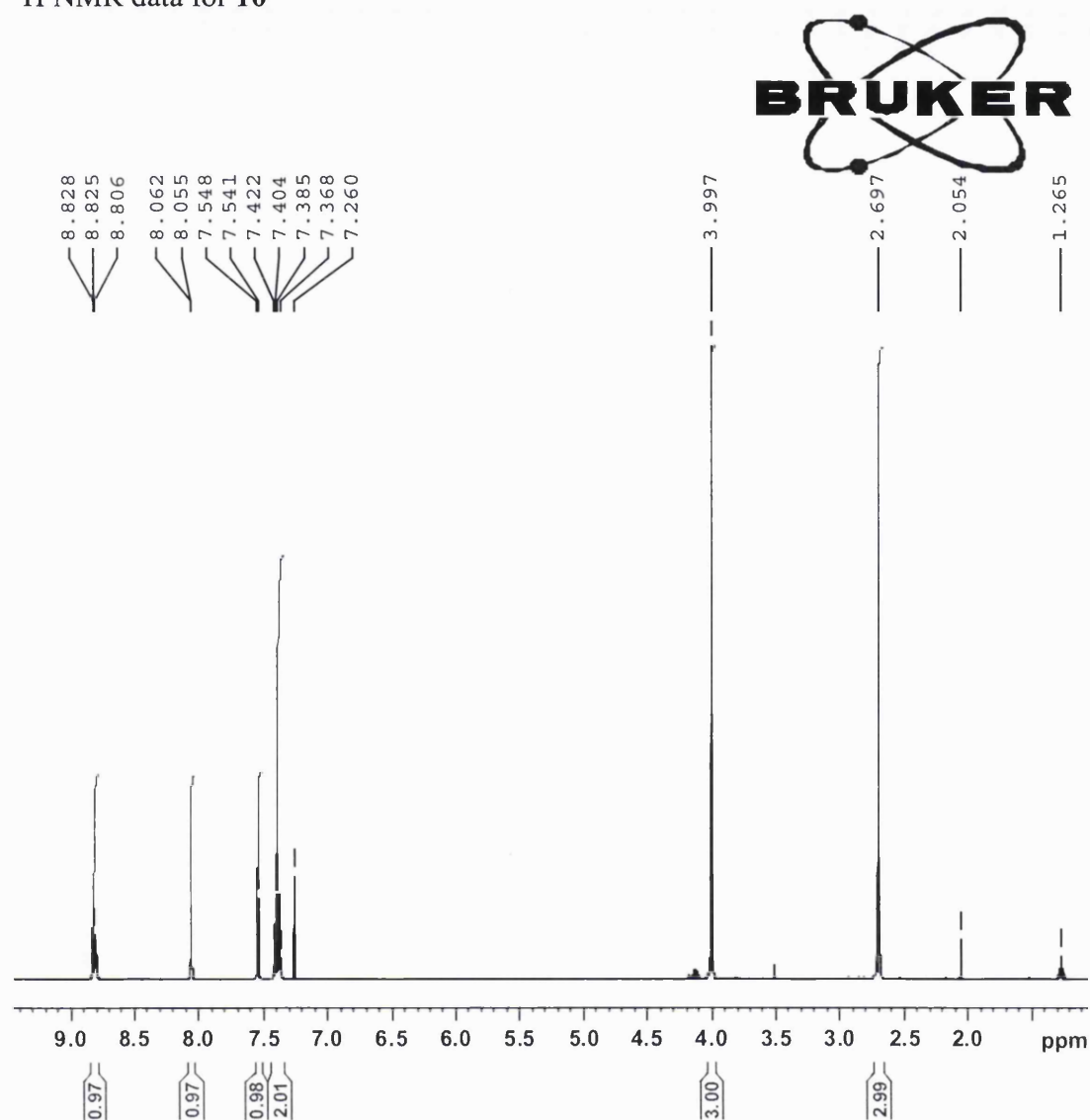
^1H NMR data for (*S*)-29



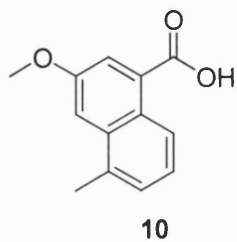
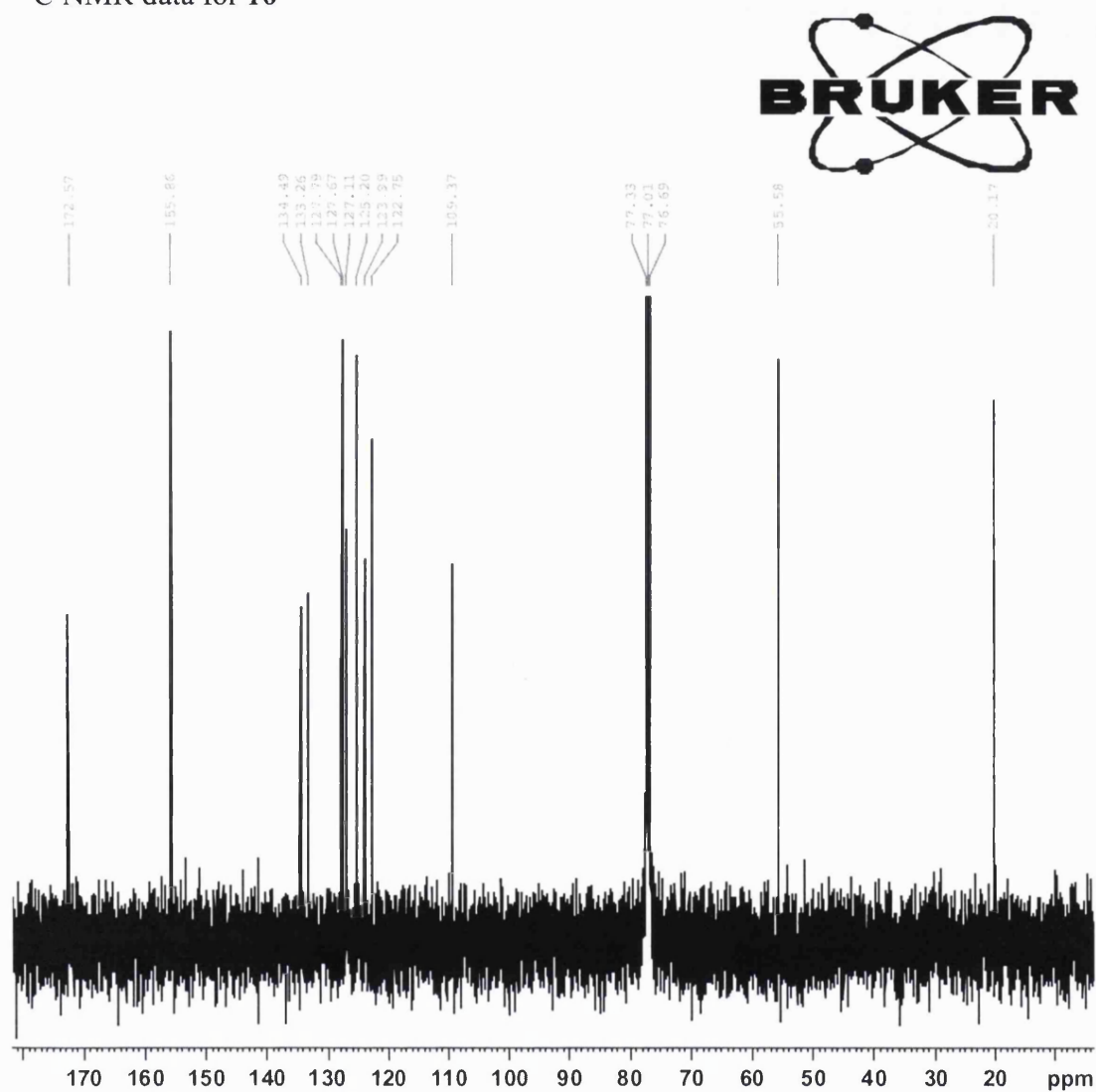
¹H NMR data for 7



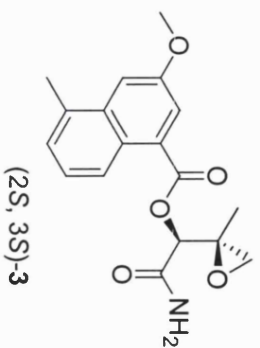
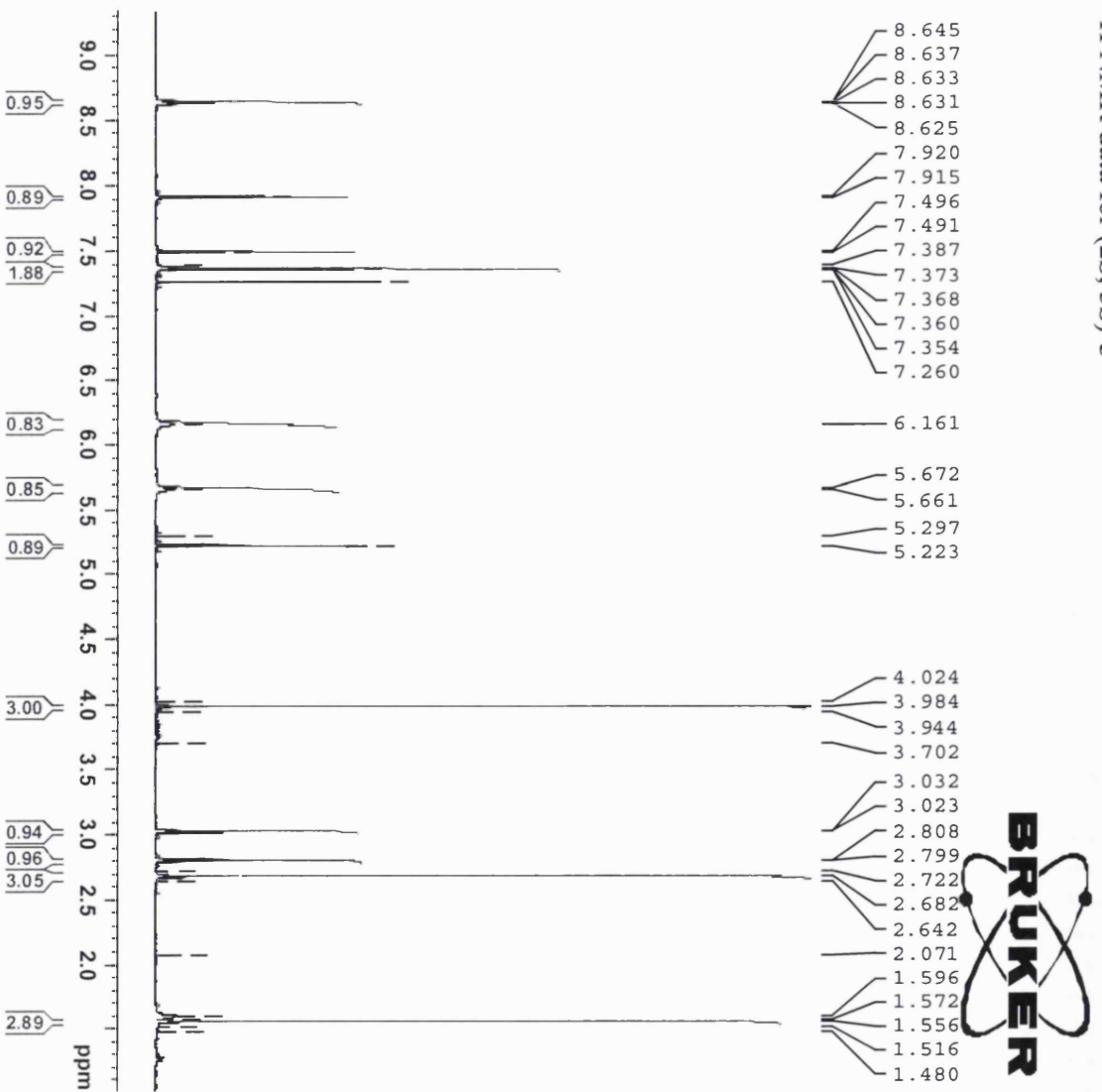
^1H NMR data for **10**



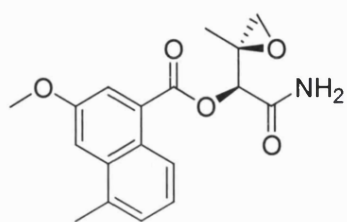
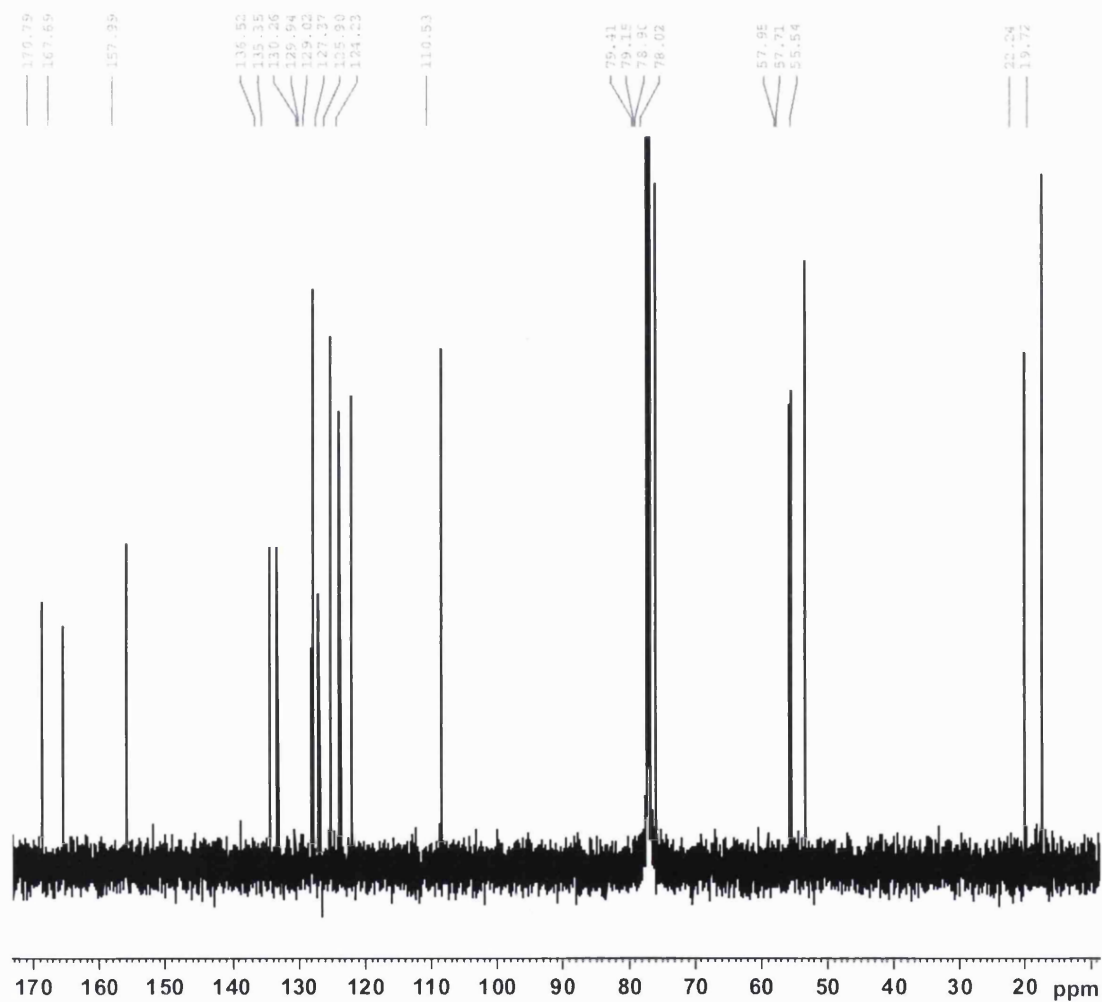
^{13}C NMR data for **10**



¹H NMR data for (2*S*, 3*S*)-3

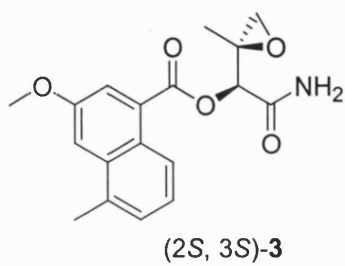
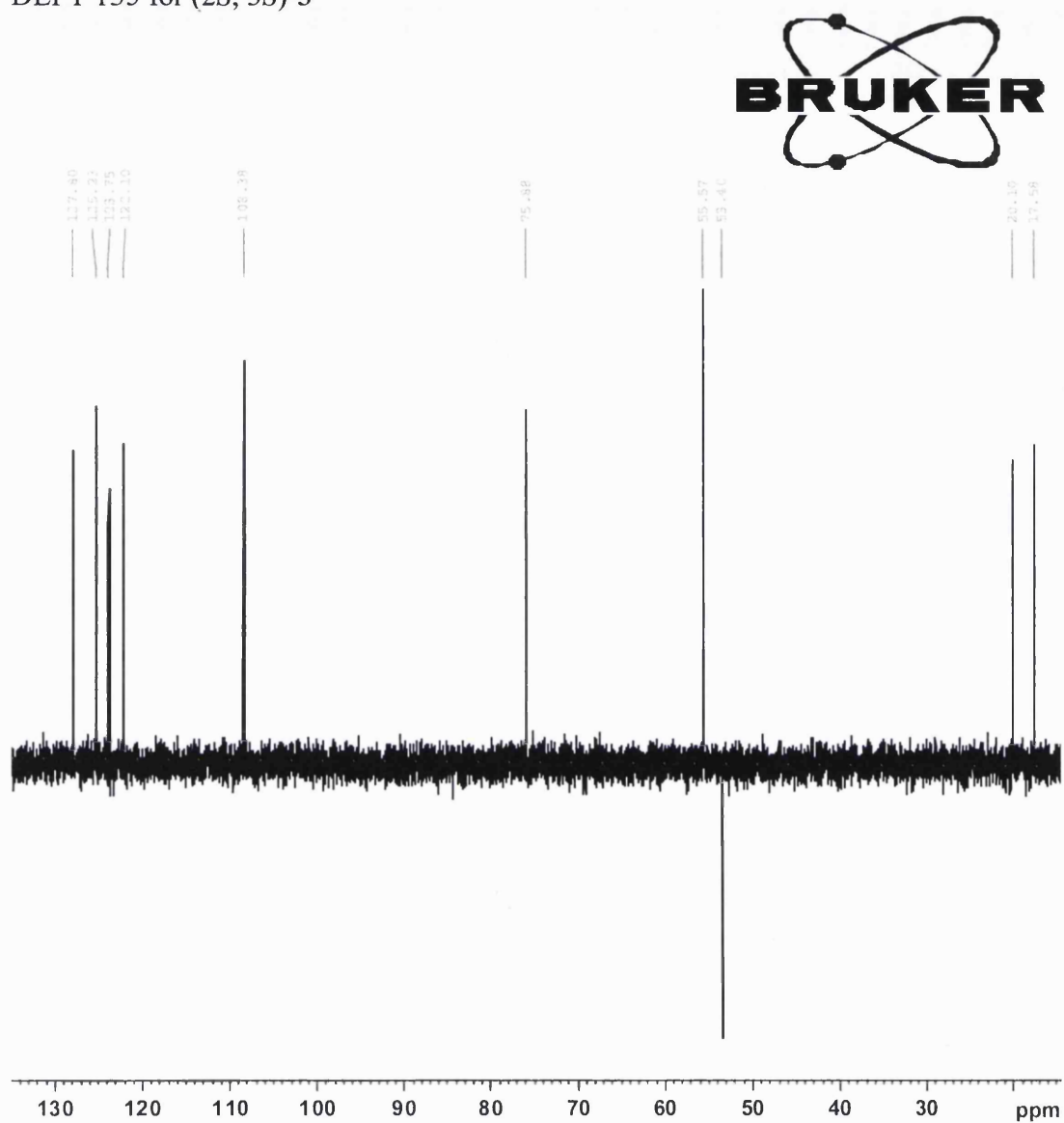


^{13}C NMR data for (2*S*, 3*S*)-3

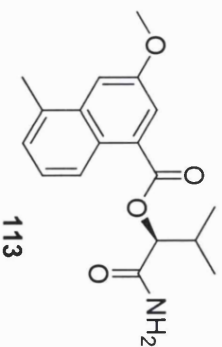
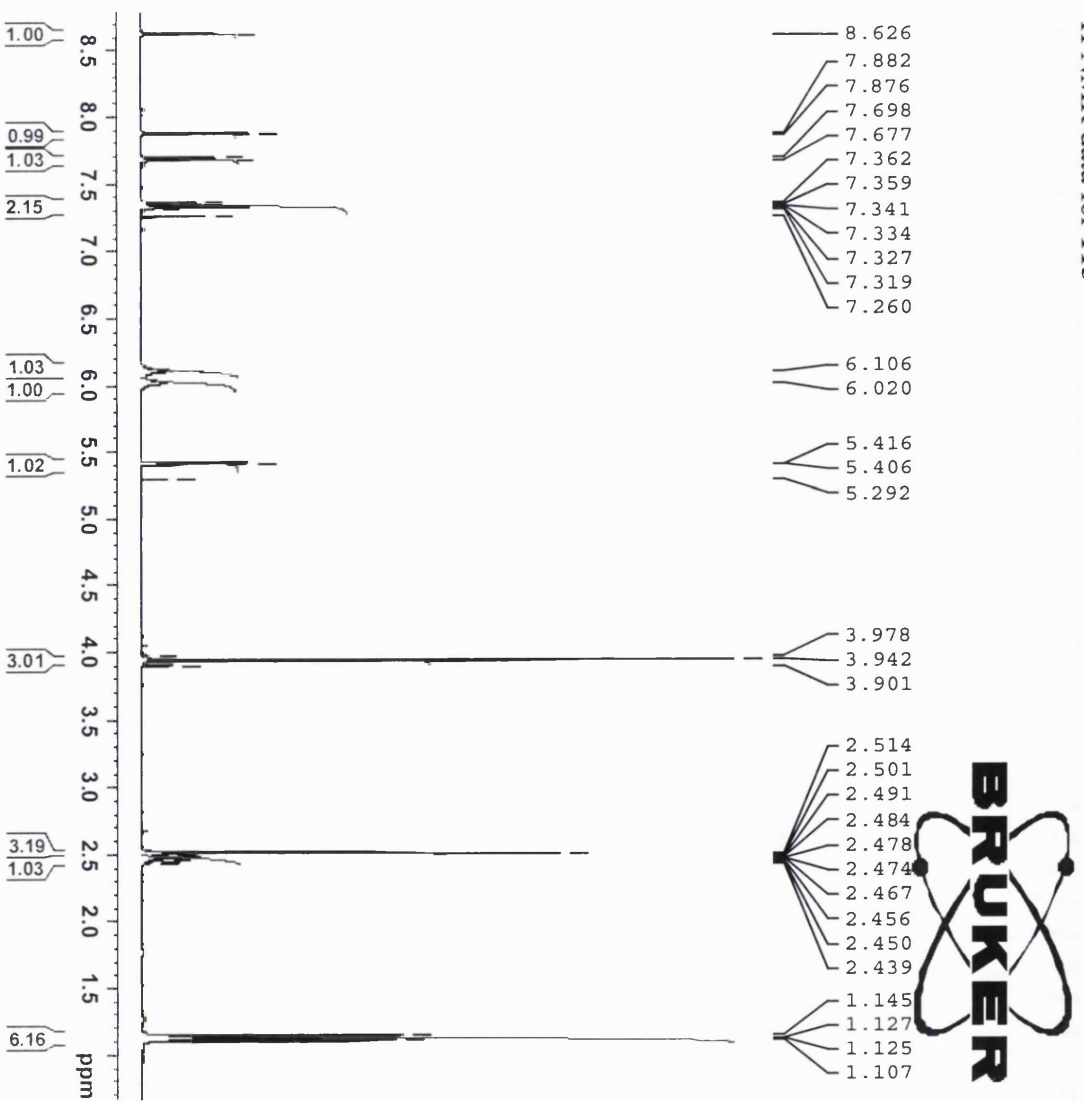


(2*S*, 3*S*)-3

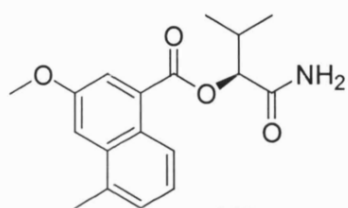
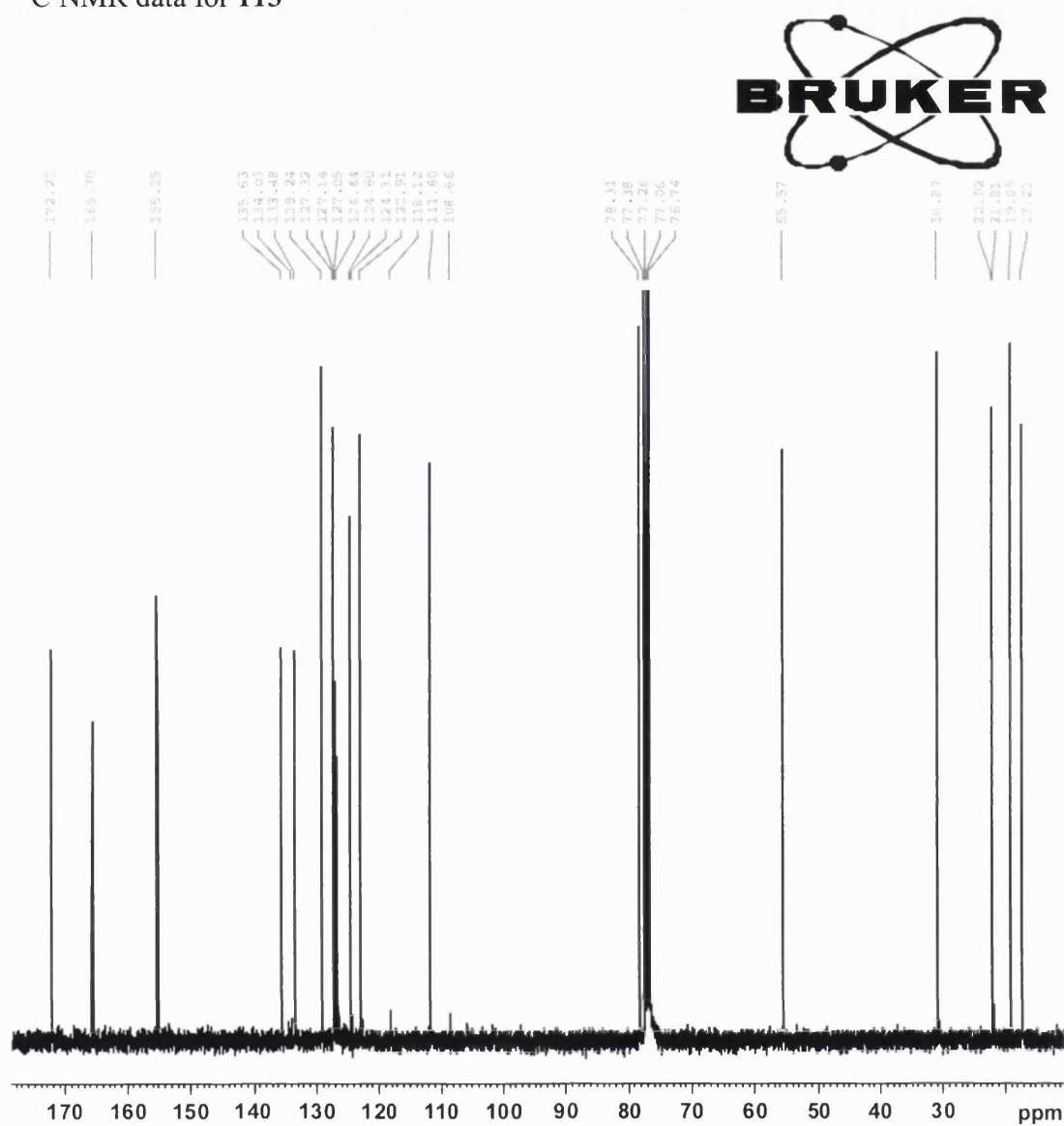
DEPT 135 for (2*S*, 3*S*)-3



¹H NMR data for 113

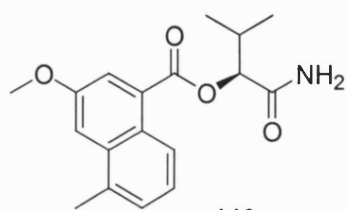
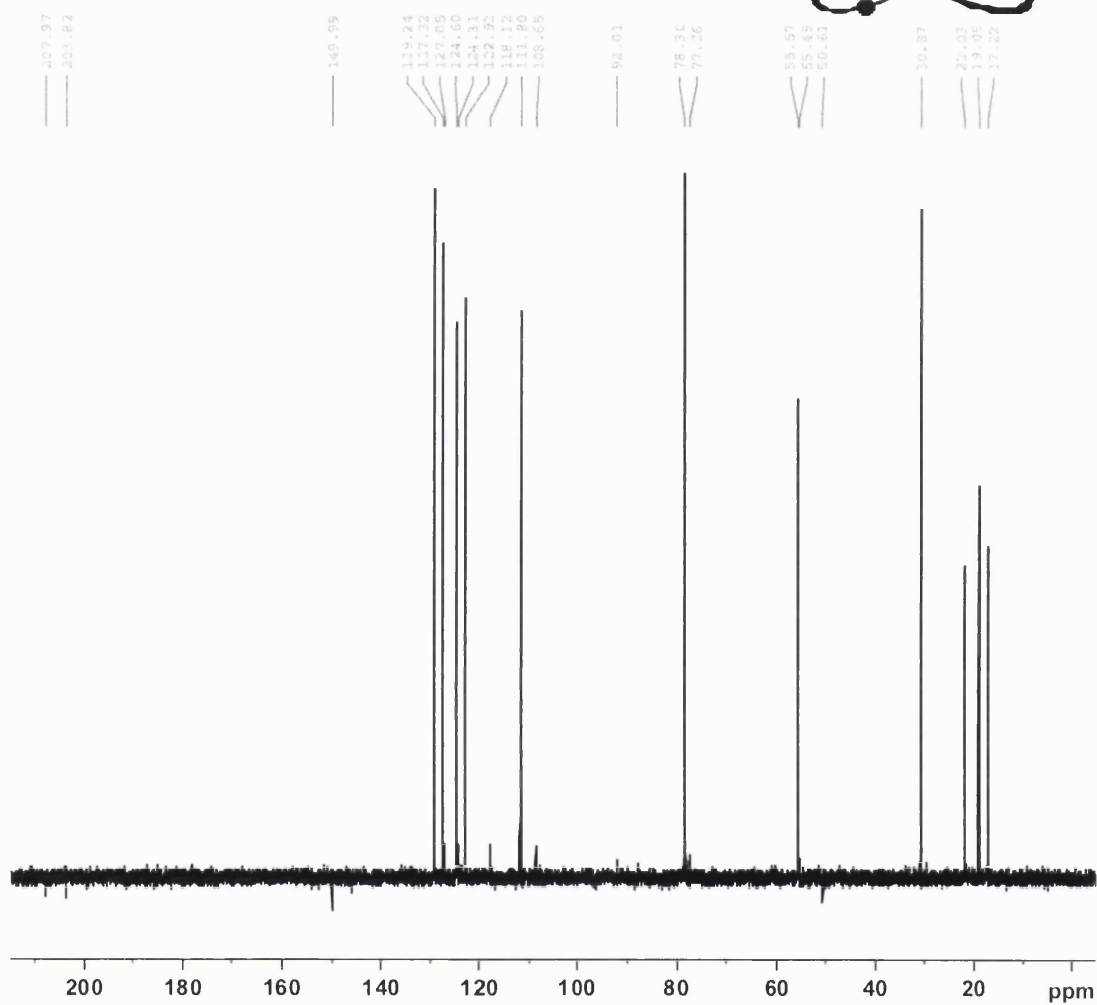
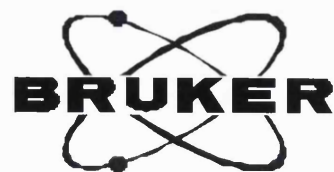


^{13}C NMR data for **113**



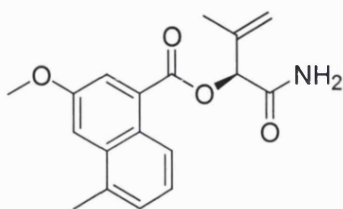
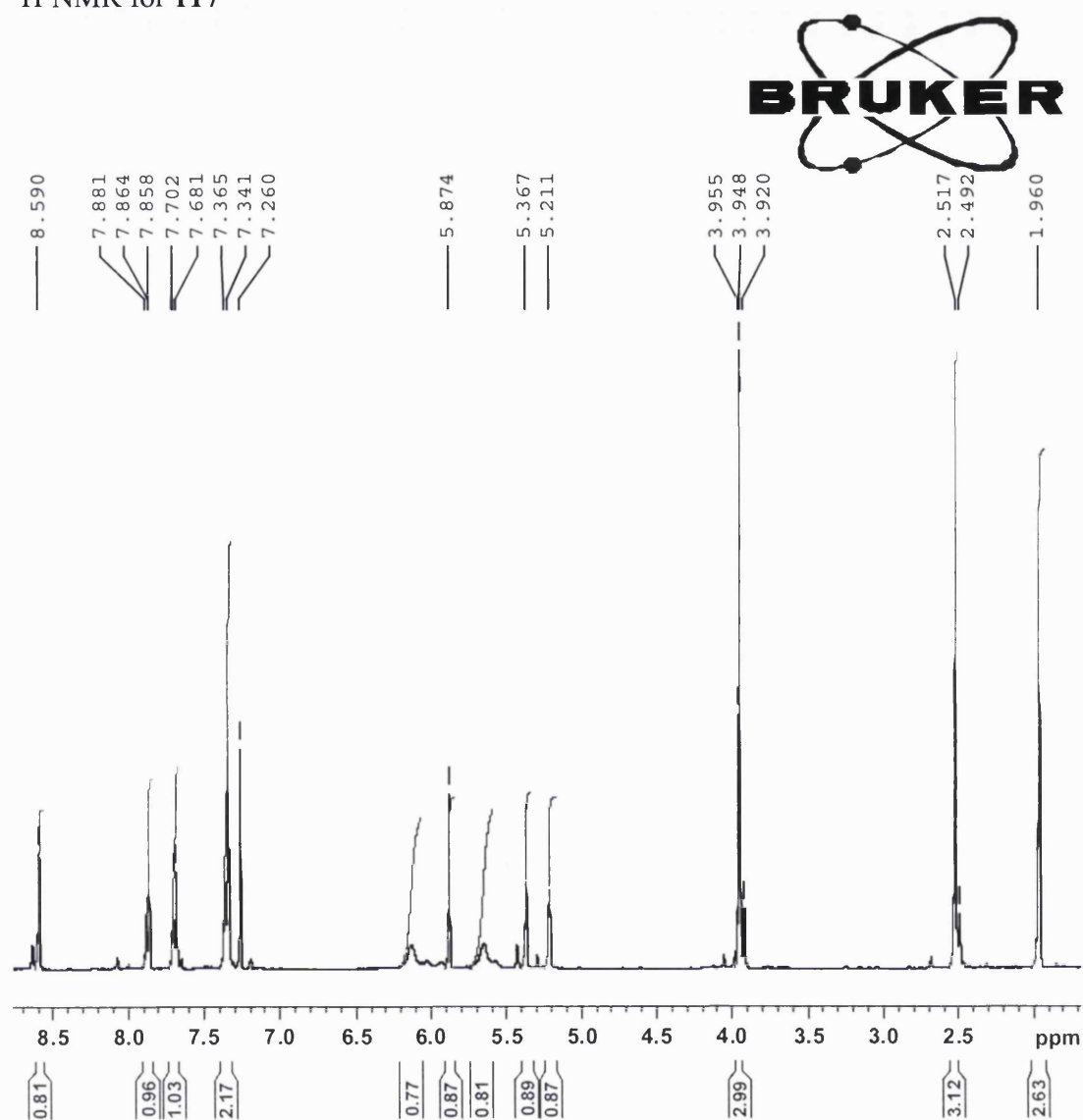
113

^{13}C DEPT135 for **113**



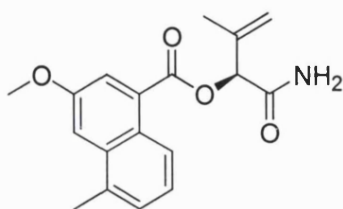
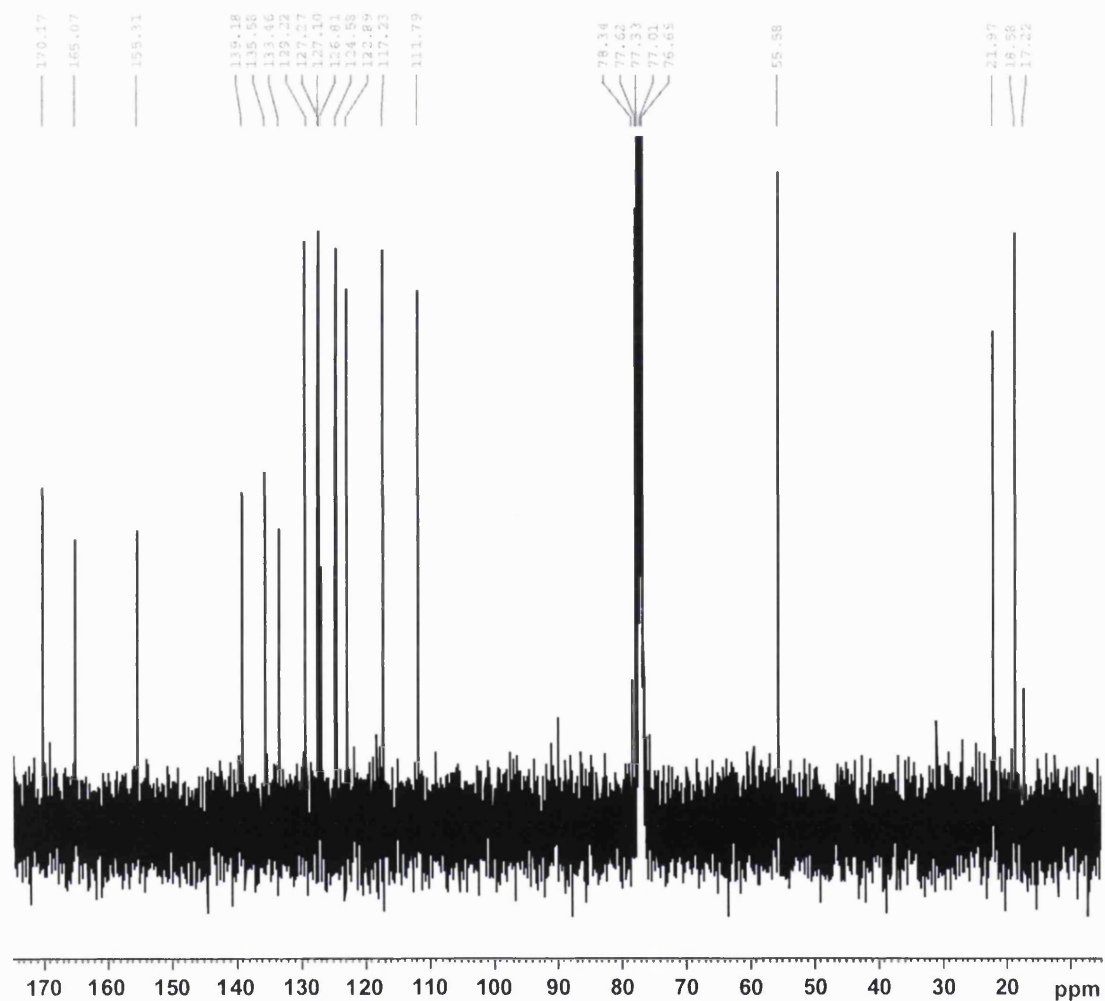
113

^1H NMR for 117



117

^1H NMR for **117**



117

